

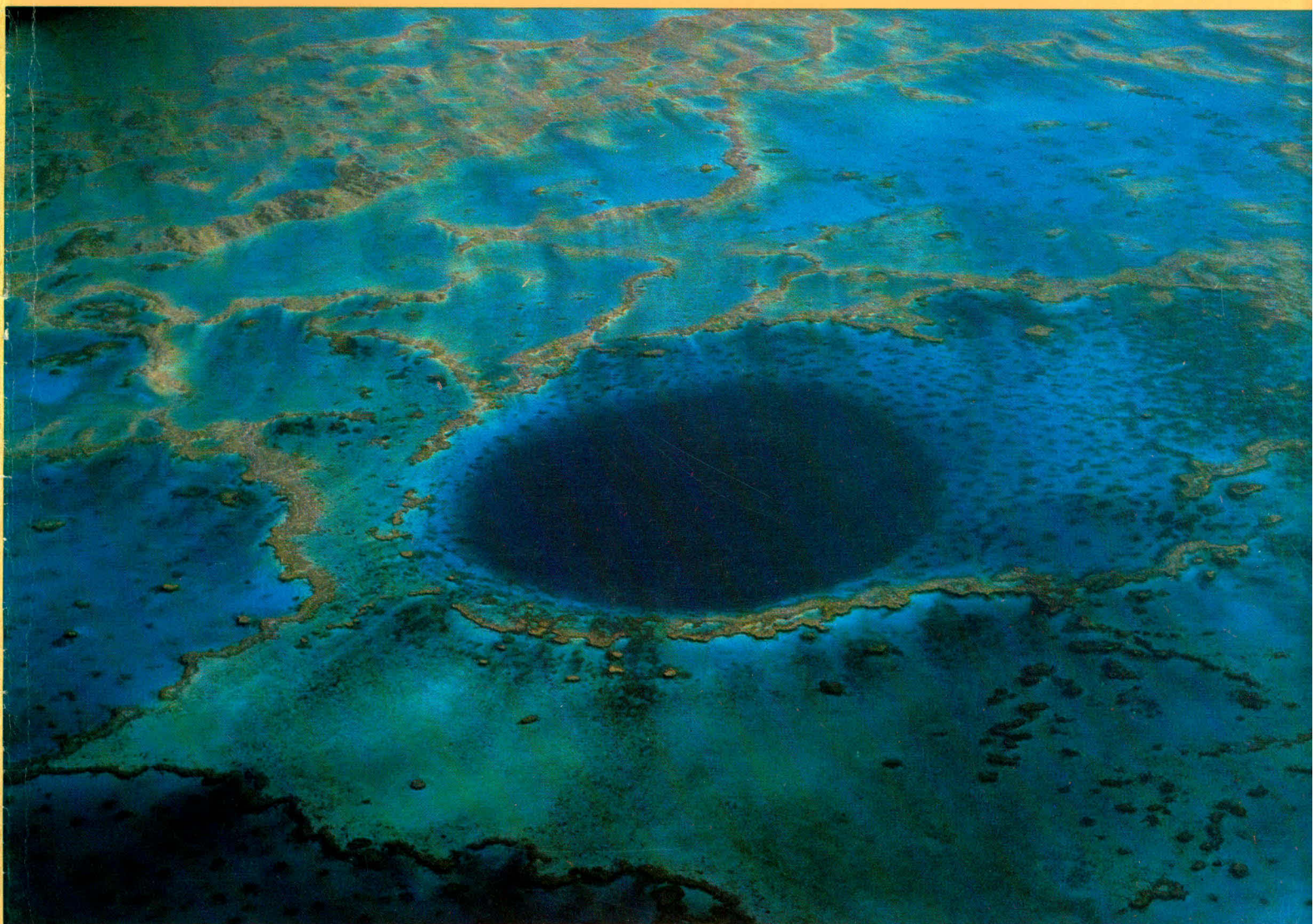
060451

BMR PUBLICATIONS COMPACTUS
(LENDING SECTION)

ø3

BMR JOURNAL of Australian Geology & Geophysics

BMR Journal of Australian Geology & Geophysics Volume 4, (2)



BMR
S55(94)
AGS.6

VOLUME 4, NUMBER 2

JUNE 1979

C3



Department of National Development, Australia

Minister: The Hon. K. E. Newman, M.P.

Secretary: A. J. Woods

Bureau of Mineral Resources, Geology and Geophysics

Acting Director: L. W. Williams

Editor, BMR Journal: J. F. Truswell

The BMR Journal of Australian Geology and Geophysics is a quarterly journal of research and related activities. Contributions are from officers of the BMR, from BMR officers working in collaboration with others, or requested work sponsored by the BMR. In addition to articles the Journal may include shorter notes and discussion of papers published in it. Discussion of papers is invited from anyone.

Annual subscription to the Journal is at the rate of \$10 (Australian). Individual numbers, if available, cost \$3. Subscriptions, etc., made payable to the Receiver of Public Moneys in Australian dollars, should be sent to the Director, Bureau of Mineral Resources, Geology & Geophysics, P.O. Box 378, Canberra, A.C.T. 2601, Australia. The Journal can also be obtained from the offices of the Department of National Development in Sydney and Melbourne.

Other matters concerning the Journal should be sent to the Director, marked for the attention of the Editor, BMR Journal.



**BMR PUBLICATIONS COMPACTUS
(LENDING SECTION)**

BMR JOURNAL of Australian Geology & Geophysics



*Volume 4, Number 2
June 1979*

AUSTRALIAN GOVERNMENT PUBLISHING SERVICE
CANBERRA 1979

Front cover:

Blue hole in the Molar Reef, Pompey Complex, Great Barrier Reef. The hole originated by collapse of the roof of a cave formed on land during a glacial, low sea-level stand. Since drowning in the Holocene transgression the hole has been modified by clastic sedimentation and reef growth (see article in this issue).

Photograph: D. Hopley, Department of Geography, James Cook University, Townsville, Qld 4811.

© Commonwealth of Australia

ISSN 0312-9608

Heavy minerals in the late Cainozoic sediments of southeastern South Australia and western Victoria

J. B. Colwell

Concentrations of heavy minerals in the prograded coastal sequence of southeastern South Australia are generally low, partly as a result of the high content of locally derived biogenic carbonate in many of the sediments. Terrigenous input to the nearshore region appears to have been relatively slight, and the operation of concentrating mechanisms minimal. The highest heavy-mineral concentrations recorded in the area (up to 1.2% total heavies) occur in a sand of probable Pliocene age underlying Quaternary beach and dune deposits. In general, the heavy-mineral suite present in the sediments consists of between 25 and 45 percent magnetite-plus-ilmenite, 5 and 20 percent leucoxene, 5 and 25 percent zircon, 5 and 30 percent tourmaline, and between 0 and 10 percent amphibole, epidote, rutile and garnet. Andalusite, sillimanite, kyanite and staurolite occur as minor components in many assemblages. Sialic igneous, reworked sedimentary, metamorphic and to a slight extent mafic igneous components are present. Probable sources include the igneous rocks of the Padthaway Ridge, metamorphic and sedimentary rocks of the Fleurieu Peninsula and Kangaroo Island, and older Tertiary sediments. Variations in the suite are defined by cluster and Q-mode factor analysis.

Higher concentrations of heavy minerals occur within the older (probably Pliocene) ridges of the western Victorian Murray Basin. These ridges which approximately parallel the southeast South Australian ridge sequence, are siliceous, and commonly contain thin bands of concentrated heavy mineral (up to 20% total heavies in the bands) in the lower part of the Parilla Sand. The suite is mineralogically mature (generally 50-70% opaque, 15-30% tourmaline, 3-5% rutile, 5-15% zircon and 1-3% others) and differs considerably from that present in the southeast South Australian sequence. The difference reflects differences in provenance of the two areas and the probable modification by intrastratal solution of the assemblages originally present in the older deposits.

Introduction

In 1974, the Bureau of Mineral Resources, in conjunction with the South Australian Geological Survey and the Department of Marine Geology in Flinders University, started a study of the stratigraphy and sedimentology of the extensive sequence of late Cainozoic sediments present in southeastern South Australia. Initial results of this study were presented by Cook & others (1977). Subsequently, additional work—mainly in the form of a continuation of the shallow stratigraphic drilling—was undertaken by BMR during early 1977 in the western Victorian part of the Murray Basin (see Colwell, 1977). This work was undertaken to investigate a possible older and more siliceous continuation to the southeast South Australian strandline sequence. Detailed sedimentological investigations were undertaken in both cases and included analyses of the heavy-mineral fraction of the sediments.

The present paper presents the results of the heavy-mineral analyses. These were undertaken to provide an indication of the region's heavy-mineral potential, and to aid the understanding of the provenance and depositional history of the sediments.

Previous investigations

The late Cainozoic sediments of southeastern South Australia have been the subject of studies by a number of workers including Crocker & Cotton (1946), Tindale (1947, 1959), Hossfeld (1950), Sprigg (1952, 1959), and Firman (1967, 1973). Little attention has, however, been paid to the heavy-mineral fraction of the sediments. The only exceptions have been reconnaissance surveys carried out by the South Australian Mines and Energy Department along several of the beaches of the modern coastline (Hillwood, 1960), and

recent investigations of certain areas by companies under exploration licence (Open File Reports, SA Dept of Mines & Energy). In general, company activity has been limited, because of disappointing initial results and the difficulties encountered in augering through the relatively well-cemented upper sediments.

The western Victorian Murray Basin late Cainozoic sediments have been described by a number of workers; principally Lawrence (1966, 1975), Lawrence & Abele (1976), and Blackburn & others (1967). Disseminated and concentrated heavy minerals have been noted in parts of the sequence by Lawrence (1966, 1975), and Macumber (1969).

Geological setting

As noted by the early workers, southeastern South Australia is characterised by late Cainozoic beach and dune strandline deposits which form a series of ridges (locally described as 'ranges') across the coastal plain (Figs. 1 and 2). These deposits, which are equivalent to the Bridgewater Formation of Boutakoff (1963), consist mainly of calcareous sand and quartzose calcarenite (skeletal carbonate, quartz and minor feldspar). Lacustrine, lagoonal and estuarine deposits, consisting of clay and marl with a small proportion of fine-grained sand, separate the ridges. The beach, dune and interdune deposits are underlain throughout much of the region by a Pliocene calcareous quartz sand. This unit does not crop out and is possibly equivalent to the Loxton Sands of Ludbrook (1961) (Cook & others, 1977). The entire sequence is underlain by the Oligocene-Miocene Gambier Limestone, which is disrupted by a major north-northwesterly-trending fault system, the Kanawinka Fault, along the region's eastern margin. Pliocene Parilla Sand of the Murray Basin

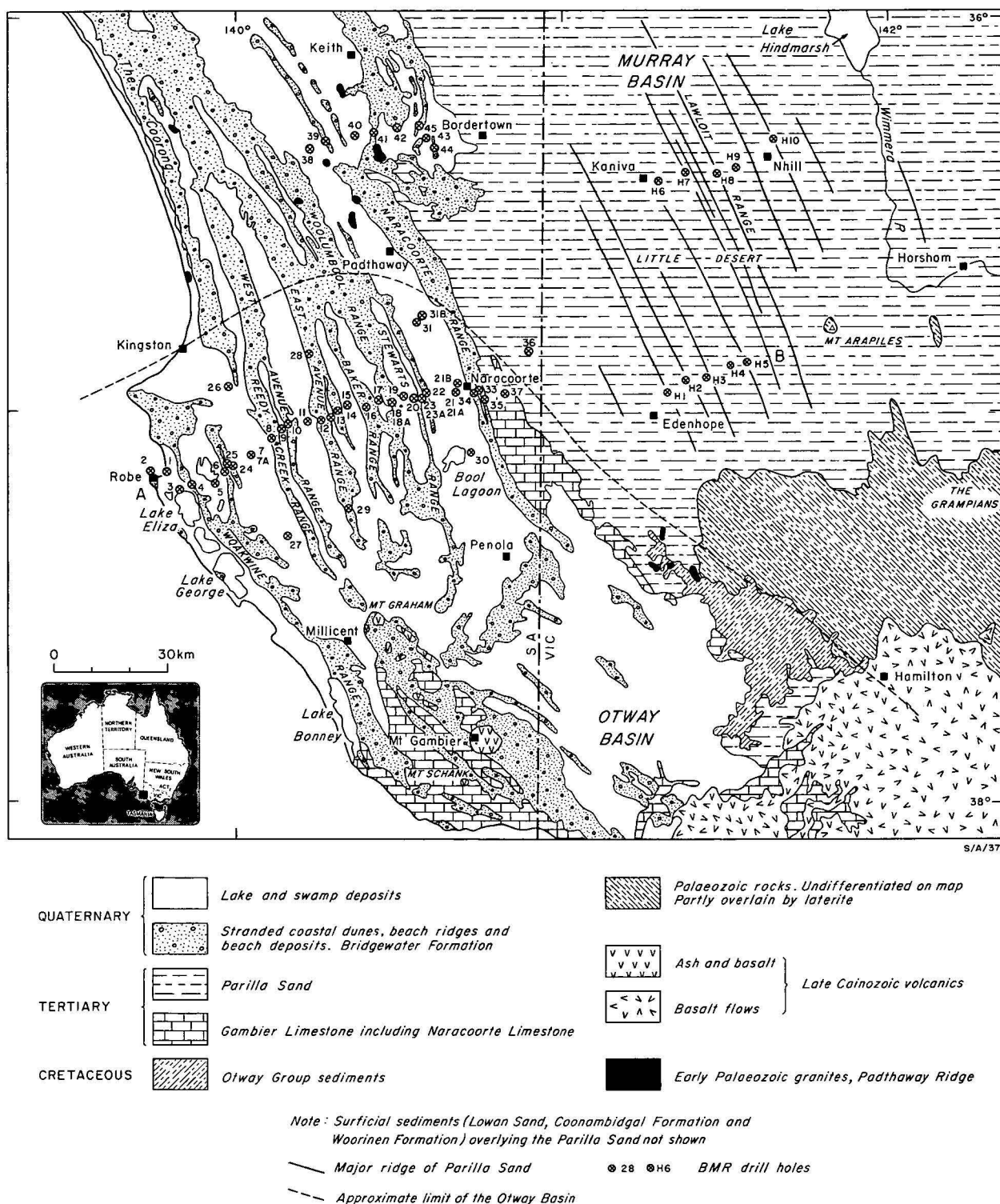


Figure 1. Geology of southeastern South Australia and western Victoria showing the location of BMR drill holes.

(Firman, 1965) extends into the region in the east and northeast (Fig. 1).

In broad terms, the beach-dune sequence gets older to the east, successive deposits of Pleistocene high sea-level stands being stranded on a coastal plain undergoing regional uplift associated with a northeasterly trending culmination through the southern part of the region (Sprigg, 1952). Precise ages are unavailable but magnetostratigraphic measurements show that the Brunhes-Matuyama polarity reversal (approximately

690 000 years BP) occurs between the East and West Naracoorte Ranges (Idnurm, *pers. comm.* in Cook & others, 1977).

In the northern part of the region, Early Palaeozoic igneous rocks of the Padthaway Ridge crop out (Fig. 1). Centres of late Cainozoic volcanism occur in the south.

To the east, in the Murray Basin, the late Cainozoic is represented by a sequence commencing with bryo-

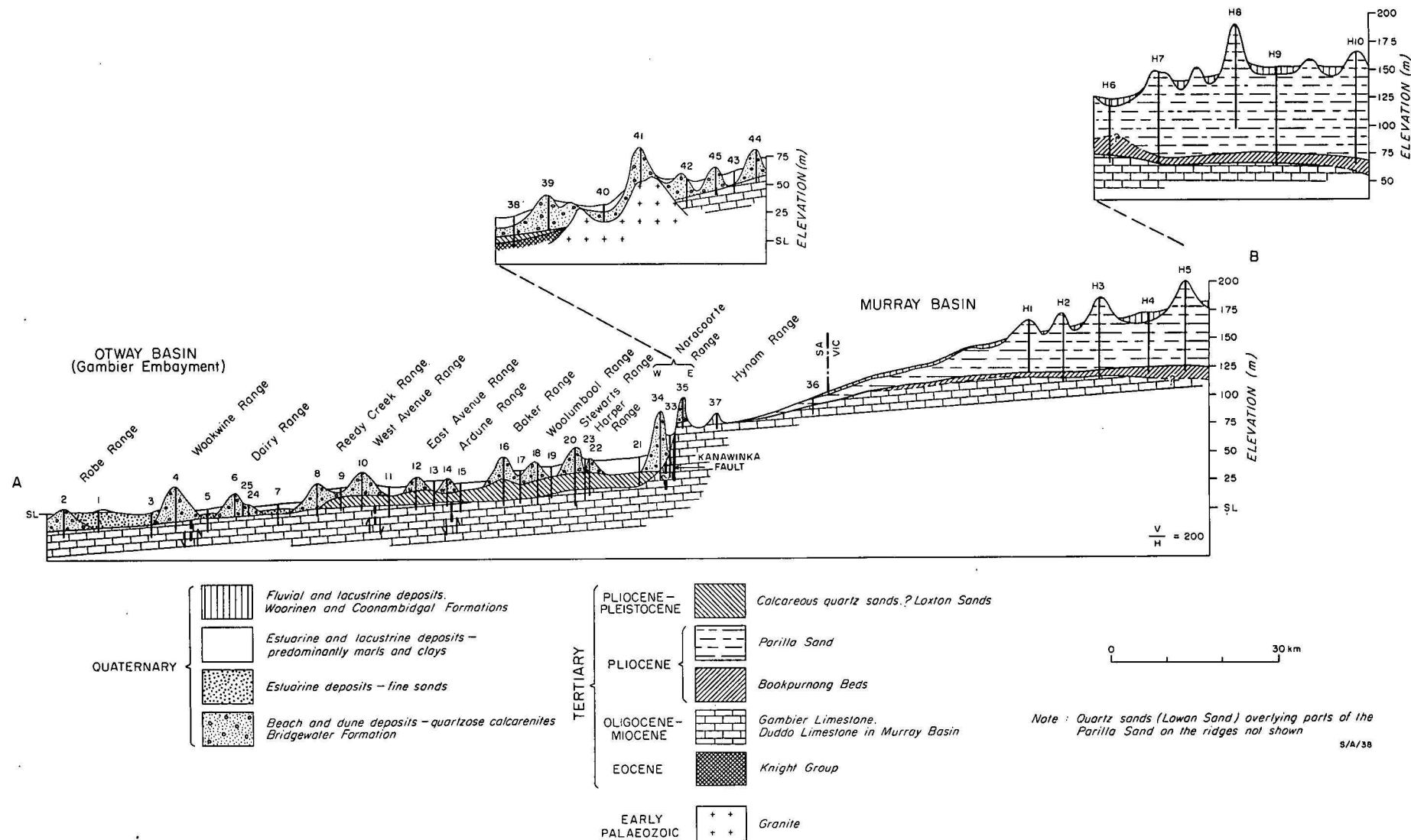


Figure 2. Sections through the Late Cainozoic sequence.

SUITE	No. of Samples	x: mean s: standard deviation	Magnetite & Ilmenite	Leucoxene	Pyrite	Zircon	Brown Tourmaline	Blue Tourmaline	Rutile	Monazite	Amphibole	Epidote	Garnet	Andalusite	Sillimanite	Kyanite	Staurolite	Others
A	20	x s	25.9 4.8	6.8 3.4	0 0	10.4 2.4	23.3 5.4	0.8 0.7	2.6 1.3	0.4 0.3	12.3 2.6	7.9 3.0	3.4 1.9	2.8 1.2	1.2 0.8	0.5 0.4	0.6 0.6	0.7 0.6
B	40	x s	28.3 6.3	7.9 4.0	0 0	9.5 4.7	32.3 6.7	0.9 0.7	3.4 1.5	0.4 0.4	3.8 2.8	3.3 1.9	5.0 3.4	2.6 1.4	0.5 0.5	0.1 0.2	0.7 0.9	0.7 0.6
C	5	x s	28.1 0.7	5.5 3.2	1.1 2.5	7.3 2.8	20.1 2.3	0.6 0.2	4.2 2.1	0.5 0.3	4.8 3.6	3.1 1.0	17.6 4.7	2.3 0.6	0.3 0.2	0 0	3.8 2.5	0.2 0.2
D	5	x s	22.6 3.5	16.7 7.2	0 0	7.0 1.3	16.6 1.3	0.9 0.2	2.3 1.1	0.2 0.2	8.8 3.0	14.8 3.8	4.4 1.2	1.1 0.9	1.1 0.1	0.7 1.0	0.5 0.4	1.1 0.4
E	1	x	15.5	15.3	0	13.6	18.8	6.3	2.1	0	3.1	11.5	6.3	3.1	2.1	1.0	0	1.0
F	60	x s	39.2 5.8	6.6 2.8	0.1 0.6	22.3 5.9	13.7 6.2	0.6 0.5	4.4 2.4	0.4 0.3	3.6 3.1	2.5 1.7	3.3 2.3	1.4 1.0	0.4 0.5	0.2 0.3	0.4 0.5	0.2 0.4
G	71	x s	45.7 8.7	7.9 3.0	0.1 0.1	13.4 3.3	10.1 3.7	0.4 0.3	2.8 1.6	0.2 0.2	8.5 5.6	4.3 2.5	3.1 1.9	1.1 0.7	0.5 0.5	0.3 0.5	0.3 0.6	0.2 0.3
H	25	x s	40.1 4.7	6.4 2.6	0.2 0.8	10.0 3.2	15.6 3.0	0.5 0.4	3.6 1.8	0.4 0.3	4.7 2.4	3.0 1.3	10.0 4.4	2.2 1.1	0.3 0.4	0.3 0.3	1.9 1.8	0.1 0.2
I	4	x s	35.0 4.6	7.2 3.3	14.0 2.6	13.1 5.4	13.6 3.4	0.2 0.3	3.7 0.8	0.1 0.1	0.9 1.3	2.1 2.1	6.6 6.2	2.0 2.3	0 0	0.4 0.2	0.2 0.3	0.4 0.3
J	32	x s	32.4 4.9	19.1 3.6	— —	16.2 3.3	17.3 3.3	0.6 0.5	3.3 1.3	0.2 0.1	1.6 1.7	3.0 2.1	3.3 2.2	0.9 0.6	0.3 0.3	0.1 0.2	0.1 0.3	0.3 0.3
K	2	x s	44.4 13.8	14.0 11.3	0 0	19.2 2.8	7.6 1.7	0.4 0.1	1.0 0.8	0 0	0.4 0.6	0.6 0.2	11.3 1.9	0.3 0.4	0 0	0.3 0.4	0.1 0.1	0 0
L	38	x s	24.0 4.1	18.9 4.0	0 0	21.7 3.3	18.8 4.2	1.4 1.0	5.1 2.9	0.1 0.2	1.8 2.8	2.5 2.2	1.4 1.4	1.7 1.1	0.5 0.8	0.4 0.4	0.1 0.3	0.8 0.6
M	4	x s	28.6 2.5	5.4 3.5	0 0	40.7 7.1	16.7 5.1	0.5 0.1	4.4 1.6	0.3 0.1	0.1 0.1	1.3 2.3	1.4 2.6	0.4 0.3	0 0	0 0	0.1 0.1	0.1 0.2
N	11	x s	28.1 8.3	17.4 5.2	0 0	8.9 3.4	10.0 1.6	0.7 0.3	2.5 1.1	0.2 0.2	15.2 5.7	8.8 3.9	1.6 0.9	1.9 1.1	1.9 0.8	0.8 0.6	0.4 0.4	0.9 0.6
O	2	x s	18.5 6.4	18.1 3.9	0 0	5.6 2.1	10.5 0.1	0.2 0.3	5.0 5.8	0.2 0.3	31.2 2.3	5.0 0.9	3.1 1.3	2.6 1.8	2.5 0.0	0.7 0.7	0.2 0.0	0 0
P	7	x s	30.5 4.8	3.3 2.3	0 0	11.7 5.6	12.0 3.7	0.8 0.5	1.7 0.7	0.3 0.1	22.8 4.7	8.6 1.1	2.0 1.7	1.4 0.5	2.3 2.0	0.7 0.5	0.5 0.4	0.7 0.6
Q	3	x s	63.4 9.7	14.0 2.5	0 0	11.9 3.7	4.4 1.7	0.1 0.1	1.1 0.2	0.1 0.1	1.1 1.4	2.3 1.0	0.7 0.5	0.4 0.2	0 0	0 0	0 0	0 0
R	1	x	18.0	10.3	0	6.1	10.4	0.4	1.1	0.7	0	6.8	44.4	0.3	0.3	0	0.7	0.3
S	2	x s	28.6 3.9	4.6 2.5	27.5 6.6	24.8 8.1	2.2 1.3	0 0	1.1 0.5	0.6 0.6	0.8 1.1	0.3 0.5	8.6 7.6	0.7 0.1	0 0	0.1 0.1	0.2 0.2	0 0
T	2	x s	10.7 1.2	1.9 2.7	55.0 0.9	12.3 5.7	9.0 3.1	0.2 0.1	0.6 0.1	0 0	6.3 2.3	0.9 0.7	1.9 0.5	0.4 0.6	0.3 0.4	0 0	0 0	0 0

Table 1. Average composition of the heavy-mineral suites in the southeast South Australian sediments.

zoan limestones of the Duddo Limestone (equivalent to the Gambier Limestone) which are dated as Early to Middle Miocene where intersected in BMR drill holes (Abele, 1977). The Duddo Limestone is overlain by clays, marls and silts of the Bookpurnong Beds (Pliocene); quartz sand and clayey sand of the Parilla Sand (Pliocene); clays and sandy clays of the Woorinen and Coonambidgal Formations (Pleistocene and Recent); and surficial quartz sand of the Lowan Sand (Pleistocene and Recent) (Lawrence, 1966, 1975; Colwell, 1977). The location of BMR drill holes (H1 to H10) and sections through the sequence are shown in Figures 1 and 2.

Of the units intersected in the Murray Basin, the Parilla Sand is of particular interest. It forms a series

of regionally prominent, subparallel, north-north-westerly trending ridges which are similar in height, form and direction of strike to the ridges of adjacent southeastern South Australia (Blackburn, 1962; Lawrence, 1966; Blackburn & others, 1967). These ridges are generally interpreted, as first suggested by Blackburn (1962), as shoreline accumulations associated with the retreat of the former Murravian Gulf from the region. They therefore represent an older (probably Pliocene), more inland and more siliceous continuation to southeast South Australia's strandline sequence. The natural division which occurs approximately along the line of the Kanawinka Fault makes necessary the separate description of the southeast South Australian and western Victorian sequences.

Field and laboratory procedures

Full details of the field and laboratory procedures used in the heavy-mineral study have been presented in unpublished reports (Colwell, 1976, 1977). A brief summary follows.

Most of the samples used in the study were selected from cores obtained by BMR in its drilling operations in the region in 1974, 1975, and 1977. Additional samples were collected from road cuttings and quarry exposures, beaches, drainage channels, and streams and creeks draining areas of Tertiary sediment to the east of the Kanawinka Fault. In all, 385 samples of the southeast South Australian sequence (mainly of the beach-dune deposits) were examined, of which 335 were examined in detail (including quantitative determinations of heavy-mineral abundance, composition of the suite, and cluster and Q-mode factor analysis of the assemblage data). In addition, 104 samples of the western Victorian Murray Basin sequence were examined.

Standard laboratory techniques were used to process the samples. Samples were oven-dried, split, weighed and leached in dilute (0.1N) HCl to remove carbonate cement and biogenic components. Percentage of carbonate was calculated by weight loss. The non-carbonate (terrigenous) residue was split to approximately 20g, weighed, and the light and heavy minerals separated in bromoform. The heavy-mineral fraction was weighed and recorded as a weight percentage of the total sediment and terrigenous fraction. In some cases the heavy-mineral fraction was treated with weak oxalic acid prior to being weighed in order to remove secondary iron-oxides and surface stains. In virtually all cases, the heavy-mineral fraction was found to lie within the 3 to 4 phi (0.125-0.062 mm) size range (very fine sand). Heavy-mineral fractions were mounted on glass slides using a 'De Pex'-based mounting medium (RI = 1.524).

Relative proportions of the different heavy minerals were determined by grain counting using a mechanical stage and 'ribbon' traverses. Grain counts were made under polarised transmitted light, to determine relative proportions of opaque and non-opaque minerals and composition of the non-opaque fraction; and in reflected light, to determine the composition of the opaque fraction. A minimum of 300 and 100 grains were counted in each sample under polarising and binocular microscopes respectively. Relative proportions of the different minerals were determined as number percentages.

The accuracy of heavy-mineral analyses based upon grain counting has been discussed by a number of workers, including Dryden (1931), Krumbein & Rasmussen (1941), Manning (1953), Galehouse (1971), Hubert (1971), and Henley (1972). These workers are generally agreed that 300-400 counts (the number used in the present study) is an optimum number with respect to accuracy and the time and effort involved in carrying out the count. Accuracy increases approximately as the square root of the number of grains counted (Dryden, 1931); a count of 300 grains yields a probable error at the 95.4 confidence level of approximately 4.5 percent for constituents in amounts of 20 percent and progressively smaller relative errors for more abundant components. Problems arising from selective size sorting have been largely overcome in the present study by the restriction in most samples of the heavy-mineral fraction to the 3 to 4 phi size range.

Heavy minerals in the southeast South Australian sediments

In general, low to very low concentrations of heavy minerals occur in the beach-dune and inter-ridge sediments of southeastern South Australia (Bridgewater Formation and younger sediments). Concentrations rarely exceed 0.5 percent by weight and commonly fall below 0.1 percent (Colwell, 1976). This partly reflects the large amount of shell and/or other carbonate material in the sediments, and partly an absence of suitable concentrating mechanisms within the depositional environments, at least in the areas sampled. In general, the beach-ridge sediments contain between 50 and 70 percent by weight carbonate with significantly higher values occurring in the more recent beach-dune deposits to the west of the Reedy Creek Range (Colwell, 1978). Few sediments contain less than 30 percent carbonate.

The highest concentrations of heavy minerals recorded in the sequence occur within the Pliocene calcareous quartz sand unit underlying part of the Quaternary beach, dune and interdune sediments. Concentrations in this unit range from 0.01 to 1.20 percent by weight and average 0.15 percent for the 74 samples examined, slightly above the average of 0.10 percent obtained for the Quaternary beach and dune deposits¹. Although in some cases the higher values reflect lower carbonate contents, in general they reflect higher concentrations of heavy minerals in the terrigenous fraction. This is most likely the result of a greater input of first-cycle terrigenous material during the Pliocene than

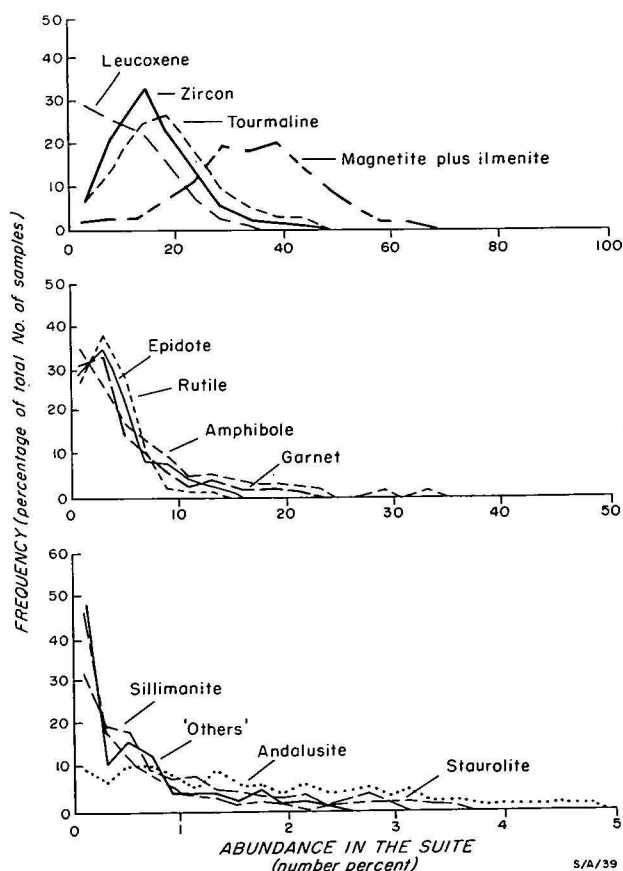


Figure 3. Frequency of abundance of the principal heavy minerals in the heavy-mineral fraction of the southeast South Australian sediments.

1. Values taken as averages over 30 cm intervals of core.

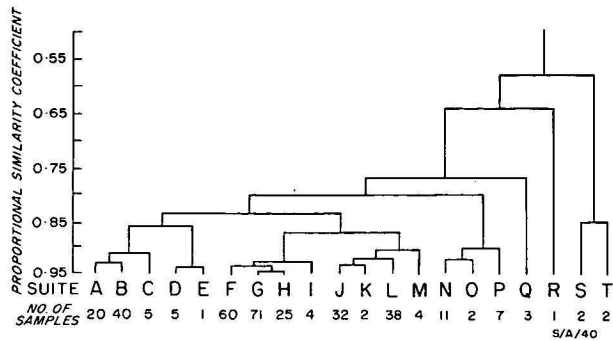


Figure 4. Q-mode cluster analysis dendrogram.

during the Quaternary—during the Quaternary terrigenous input became increasingly restricted by the prograding coastal sequence.

A broadly similar suite of heavy minerals occurs in most of the sediments throughout the region. Typically it consists of between 25 and 45 percent magnetite-plus-ilmenite, 5 and 20 percent leucoxene, 5 and 25 percent zircon, 5 and 30 percent tourmaline, and between 0 and 10 percent amphibole (mainly brownish green to blueish green hornblende), epidote, rutile and garnet (Fig. 3). Other minerals often present in the assemblage include andalusite, kyanite, sillimanite, and

staurolite (generally in amounts of one or two percent); and topaz, zoisite, apatite, monazite, pyroxene, sphene, olivine, and fluorite (in trace amounts). Framboidal pyrite occurs as a major component of the heavy-mineral fraction in several of the estuarine and lacustrine samples. Flakes of mica (mainly biotite) often occur in trace amounts, but were excluded from quantitative studies because of their range of densities similar to the density of bromoform.

In order to obtain an indication of the nature and extent of variability within the assemblage data, cluster and Q-mode factor analyses of the data were undertaken. Programs CLUSTER (Bonham-Carter, 1967) and CABFAC (Klován & Imbrie, 1971) were used—documentation of these programs and details on interpretation are given by Mayo & Long (1976).

Cluster analysis of the samples on the basis of the data array, consisting of 335 samples x 16 attributes (mineral percentages), produces the dendrogram shown in Figure 4. Twenty groups of samples are defined at a 0.95 similarity level; seven of the groups contain twenty or more samples. Each group of samples shares a relatively well-defined heavy-mineral suite, arbitrarily referred to by a letter, A to T. Compositional means and standard deviations of the suites are given in Table 1. Variations between the seven major suites in terms of mean abundance of the major mineral components

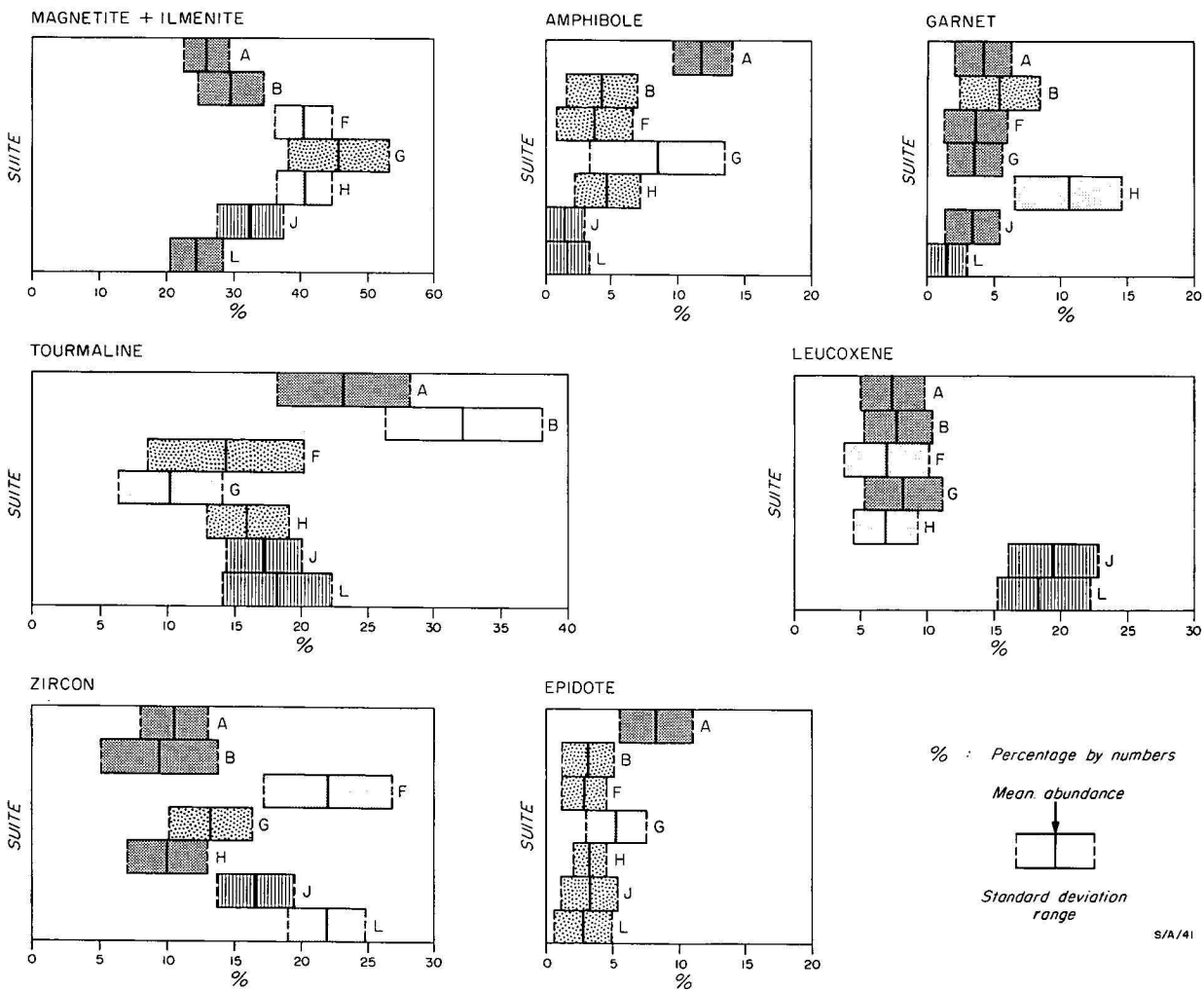
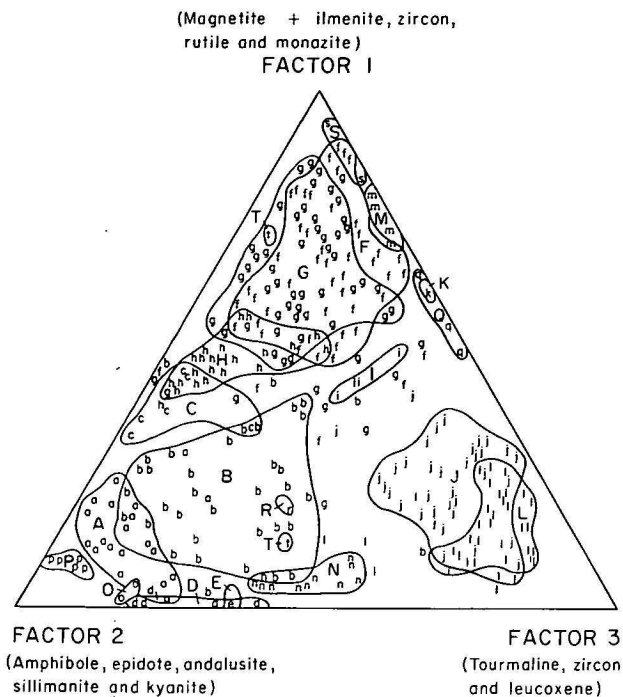


Figure 5. Variations between the principal heavy-mineral suites in terms of mean abundance of the major mineral components. For each mineral, shadings indicate those suites which differ significantly in mean abundance of the mineral. Significant differences determined using a one-sided Student's t-test at the 95% level.



335 samples plotted. Letters refer to the cluster analysis suites A-T
S/A/42

Figure 6. Triangular plot of normalised factor loadings for the three principal factors, Q-mode factor analysis. Factors 1, 2 and 3 account for approximately 80 percent of the variation in the assemblage data.

are shown in Figure 5. Q-mode factor analysis produces similar groupings (see Fig. 6) from three principal factors: Factor 1—magnetite-plus-ilmenite, zircon, rutile and monazite; Factor 2—relatively unstable (mainly first cycle) components including amphibole, epidote, andalusite, sillimanite and kyanite; and Factor

3—relatively stable and commonly multicyclic components such as tourmaline, zircon, and leucoxene.

The distribution of the suites through the sequence is shown in Figure 7. Several features stand out:

(1) Suites F and G (of similar composition) (Table 1) characterise most of the Quaternary beach-dune deposits as well as the underlying Pliocene sand unit. Their wide distribution is probably the result of the maintenance of broadly similar source areas throughout the late Cainozoic, and the erosion of the Pliocene sand unit (particularly at the western end of the section) and the subsequent incorporation of material derived from it into the overlying beach-dune deposits.

(2) Suites N, O and P, which have high contents of unstable components (mainly hornblende and epidote) are almost exclusively restricted to the Pliocene sands of the eastern part of the region, reflecting a high input of first cycle terrigenous components probably from nearby source areas such as the Padthaway Ridge.

(3) Suite B, which has a relatively high tourmaline content, occurs mainly within the beach and dune deposits of the West Naracoorte and Robe Ranges. The suite is most common in the coarser grained sediments and its distribution is probably related, at least in part, to hydraulic factors. In most samples, tourmaline grains are slightly larger than grains of the other heavy minerals, a feature reflecting differences in hydraulic size, as well as the size distribution of the minerals in the source material.

(4) Suites J, L and M which have high contents of a stable and ultrastable mineral (particularly leucoxene and zircon), are restricted to the eastern part of the region where they occur within the beach and dune deposits of the Bordertown area and Naracoorte Range, in the Parilla Sand, and in the interdune deposits adjacent to Naracoorte. Their distribution is related to provenance (a relatively high input of stable, multicyclic components from the adjacent area of Murray Basin sediments) and to the effects of intrastratal solu-

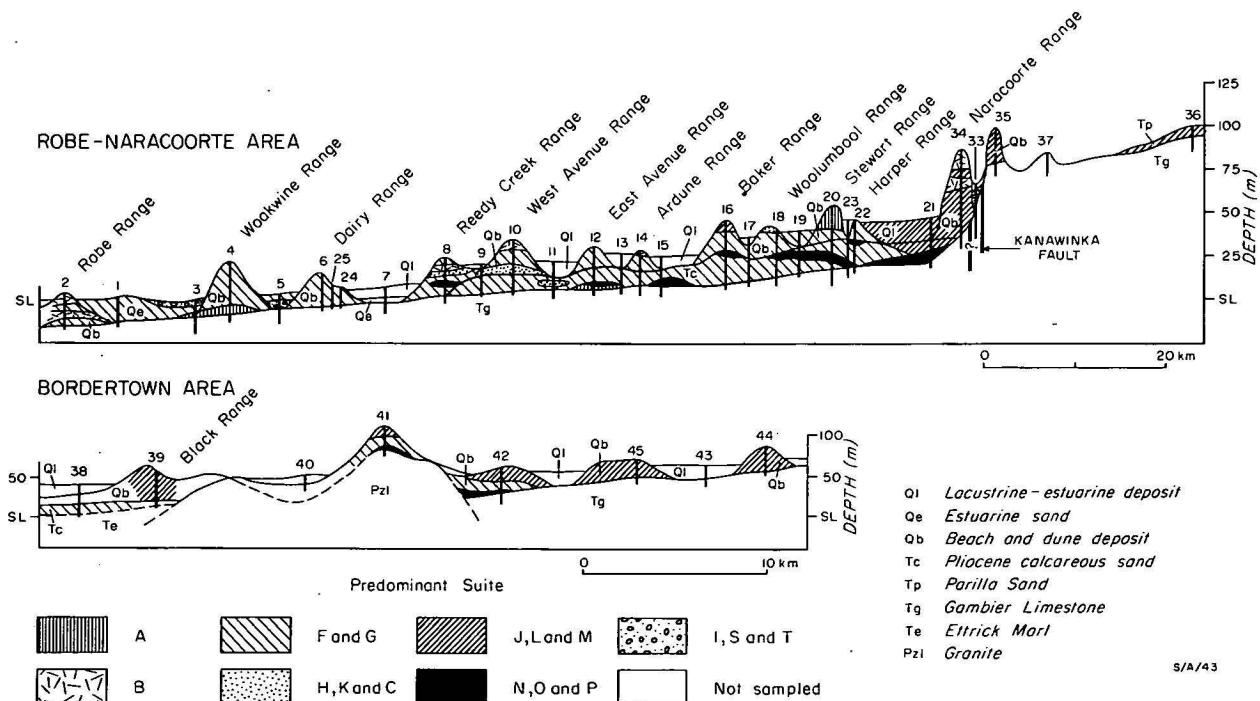


Figure 7. Distribution of the suites in the southeast South Australian sequence.

tion—removal of chemically unstable components from the older, more inland deposits.

(5) Suites I, S and T, which are characterised by framboidal pyrite, are restricted to parts of the estuarine and lacustrine deposits where their distribution is apparently controlled by the *in situ* bacterial production of the pyrite.

Heavy minerals in the western Victorian Murray Basin sediments

In contrast to the younger, calcareous sequence of southeastern South Australia, the ridge-forming sediments of the western Victorian Murray Basin (chiefly the Parilla Sand) are highly siliceous. Most of the sediments contain less than 0.5 percent of heavy mineral, although in the lower part of the Parilla Sand bands up to 4 cm thick and laminae of concentrated heavy minerals are common, generally in fine-grained quartz sands. Details of the concentrations are given in Table 2.

The heavy-mineral assemblage present remains relatively constant. In general, the sediments contain a mature suite consisting of between 50 and 70 percent opaques (leucoxene and ilmenite with lesser amounts of magnetite, hematite and limonite), 10 to 30 percent brown tourmaline, 3 to 5 percent rutile, 5 to 15 percent zircon, 0.5 to 1.5 percent blue or green tourmaline (mainly indicolite), and 0.5 to 1.0 percent andalusite (Table 3). The suites are similar to Suites J, L and M. Garnet, kyanite, staurolite, sillimanite and monazite commonly occur in trace amounts. Many of the stable and ultrastable components (particularly zircon and rutile) are well-rounded.

Compared to typical southeast South Australian assemblages, the assemblage is mature with a high proportion of stable and ultrastable, probably multicyclic, components. This difference between the two areas apparently reflects fundamental differences in provenance, the terrigenous fraction of the southeast South Australian sediments being derived principally from first or second-cycle local source areas such as the Padthaway Ridge, and the western Victorian sediments probably being mainly derived from multicyclic, distant, sources located around the margins of the basin and farther afield. The marked compositional difference which exists between the sediments of the two areas (mainly calcareous sediments in southeastern South Australia and siliceous sediments in western Victoria) probably reflects a significant age difference between the two sequences, Pliocene weathering and lateritisation of the Parilla Sand, and differences in initial sediment composition related to the presence or otherwise of major quantities of biologically-produced carbonate.

The role of intrastratal solution

Although the importance of intrastratal solution is still debated, most workers agree that it occurs at least locally (Blatt & Sutherland, 1969). In the present study, three lines of evidence suggest that solution both within the unsaturated zone and the saturated zone of what is a regionally unconfined aquifer system has occurred, significantly modifying the heavy-mineral assemblage in the older (more inland) of the beach-dune deposits. The lines of evidence are:

(1) Higher proportions of chemically stable and ultrastable minerals occur in the more inland of the

Hole	Stratigraphic unit	Heavy-mineral abundance
BMR H1	Lowan and Parilla Sands	Trace amounts. Less than 0.2 percent
H2	Lowan and Parilla Sands	Trace amounts except between 30 and 32 m where abundances (each averaged over a 30 cm interval) range from 0.7 to 1.6 percent, average 1.0 percent
H3	Parilla Sand	Trace amounts. Generally less than 0.2 percent
H4	Parilla Sand	Trace amounts
H5	Lowan Sand Parilla Sand	Trace amounts Trace amounts except in two zones (31 to 35 m and 67 to 70 m) where abundances range from 0.6 to 5.6 percent, average 2.0 percent
H6	Parilla Sand	Low (< 0.5 percent) except between 14 and 19 m where thin bands and laminae of conc. heavy mins. occur; average abundance is 1.3 percent. Individual bands (up to 3 cm thick) generally contain between 15 and 20 percent heavy mins.
H7	Parilla Sand	Low conc. (< 0.4 percent) except 60 to 64 m and 68 to 69 m where conc. range 0.1 to 12.3 percent; average 1.9 percent. Individual bands (generally 1-3 cm thick) contain up to 20 percent heavies
H8	Parilla Sand	Trace amounts
H9		Low conc. except between 58 and 61 m and 65 and 67 m where laminae of conc. heavy mins. occur and concentrations range up to 2.8 percent; average 1.2 percent
H10	Lowan and Parilla Sands	Trace amounts

Table 2. Abundance (percentage by weight) of heavy minerals in the western Victorian Murray Basin sediments.

Hole	No. of Samples	Opauques	Brown Tourmaline	Blue-green Tourmaline	Rutile	Zircon	Andalusite	Others
H2	14	72.3 (7.5)	16.5 (5.6)	0.3 (0.3)	4.2 (3.2)	5.2 (4.6)	0.4 (0.3)	0.6 (0.4)
5	10	69.1 (4.4)	18.1 (3.6)	0.8 (0.3)	3.3 (1.4)	7.1 (3.6)	0.4 (0.2)	0.5 (0.3)
6	18	51.3 (6.4)	32.2 (8.4)	1.4 (0.5)	3.5 (1.1)	5.9 (4.1)	2.4 (1.2)	0.7 (0.4)
7	39	66.4 (5.0)	13.2 (6.7)	1.0 (0.6)	3.9 (1.0)	12.6 (5.4)	1.3 (0.7)	1.0 (0.5)
9	23	70.5 (4.2)	13.0 (6.5)	1.1 (0.6)	2.6 (0.8)	9.2 (5.3)	1.4 (0.8)	0.7 (0.4)

Table 3. Average composition of the heavy-mineral fraction of the western Victorian sediments. Standard deviation values in parentheses.

beach-dune deposits than in the younger deposits closer to the coast (see Fig. 8).

(2) Many of the inland southeast South Australian beach and dune deposits (particularly those of the Bordertown area) contain sufficient hydrated secondary iron oxides (limonite, etc.) to impart a dark yellowish orange-brown colour to the sediments. This colour increases in intensity to moderate reddish brown in many of the western Victorian strandline deposits,

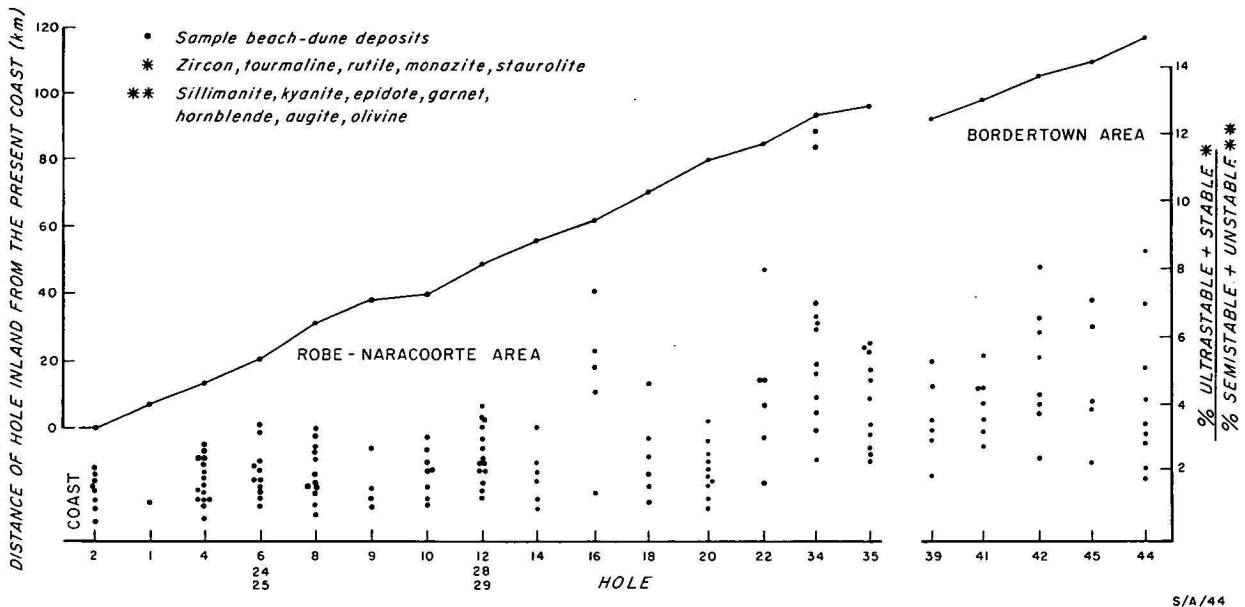


Figure 8. Plots of the ratio of the percentage of chemically ultrastable + stable/semistable + unstable minerals in the non-opaque heavy-mineral fraction of beach and dune samples.

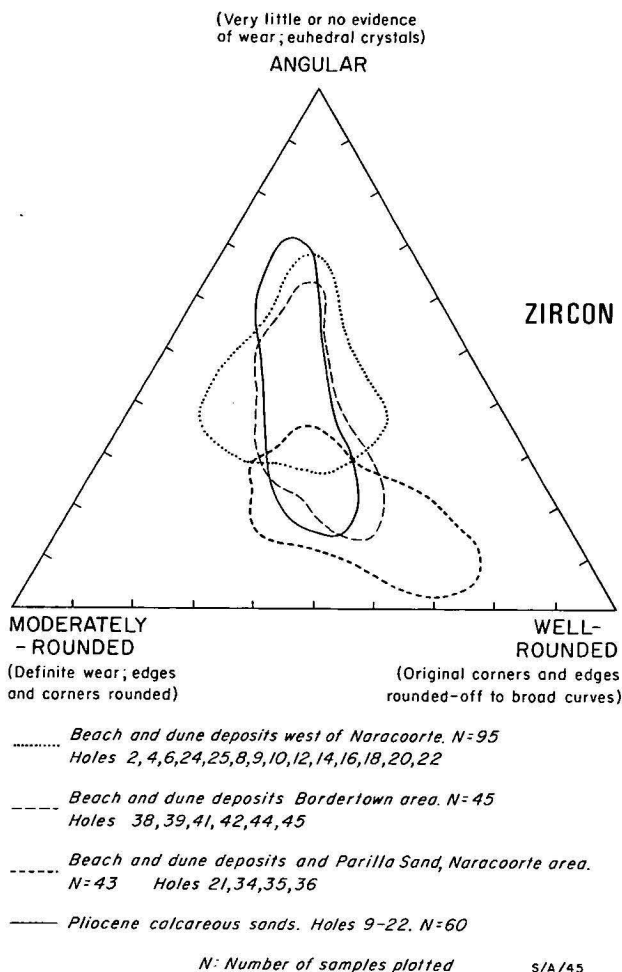


Figure 9. Field of plots of samples on the basis of the proportion of well-rounded; moderately-rounded; angular zircons in the heavy-mineral fraction.

deposits which have probably undergone Pliocene lateritisation (Lawrence, 1966). Most of the secondary iron oxides are most probably derived from iron-bearing heavy minerals such as magnetite, hornblende and biotite, and from iron-bearing clays such as illite and chlorite. In several of the Victorian ridges fossils have been completely replaced by iron-oxide casts.

(3) Grains of hornblende, epidote, augite, olivine and other chemically unstable components are commonly ragged, angular and altered, consistent with intrastatal etching and alteration.

Overall, intrastatal solution appears to have played an important, although not solitary role in increasing the maturity of the suite inland. Part of the maturity reflects a higher input of reworked multicyclic material to the eastern part of the region. This is shown by an increase in the proportion of well-rounded, stable and ultrastable components in the more inland deposits, a feature demonstrated for zircon in Figure 9. Forty zircons within the 3 to 4 phi-size fraction were examined for each sample plotted in this figure. The lower proportion of well-rounded zircons that occurs in the deposits of the Bordertown area compared to the comparable inland deposits of the Naracoorte area reflects a higher input of euhedral first-cycle zircons to the Bordertown area from the immediately adjacent granites of the Padthaway Ridge.

Provenance

Southeast South Australian sediments

A detailed analysis of the provenance of the southeast South Australian sediments has been attempted from the heavy-mineral assemblages. Overall, the nature of the suite indicates contributions from sialic igneous, reworked sedimentary, metamorphic and to a lesser extent, mafic igneous and pegmatitic sources. Sialic igneous components (zircon, brown tourmaline, hornblende, magnetite, biotite and monazite) usually form between 60 and 80 percent of the assemblage. Although most grains are angular or sub-angular and are probable

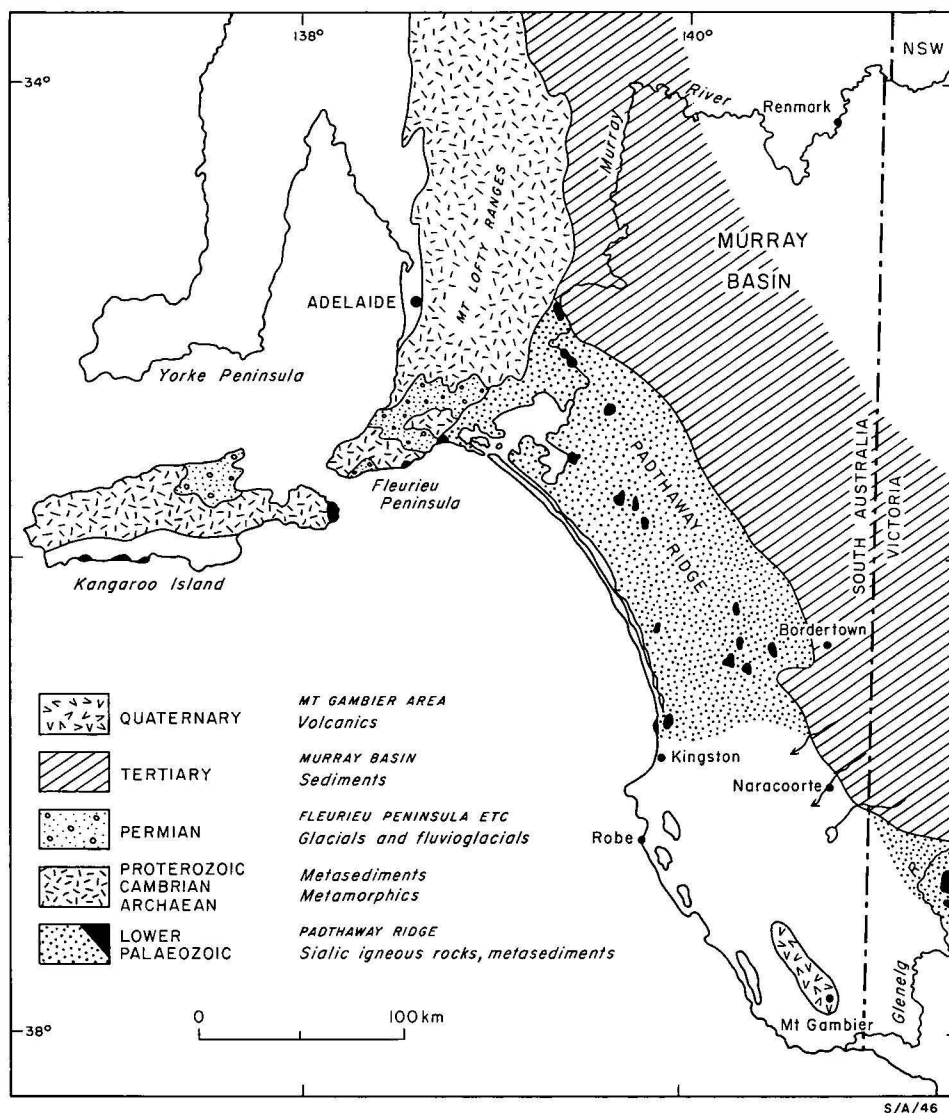


Figure 10. Suggested source areas of the terrigenous detritus present in the southeast South Australian sediments.

first-cycle components, moderately rounded grains of the stable/ultrastable minerals such as tourmaline and zircon are relatively common, particularly in the eastern part of the region, and indicate a significant contribution from pre-existing sedimentary sources. Metamorphic components (garnet, sillimanite, kyanite, staurolite, epidote and zoisite) form a minor, but significant, part of most assemblages. Mafic igneous components, other than ilmenite and leucoxene which are possibly multicyclic and originally derived from volcanics in western Victoria, are of restricted occurrence and are usually present only in trace amounts. Pegmatitic components (mainly the blue variety of tourmaline) occur in trace amounts.

The following sources for these components are suggested on the basis of the geology, geomorphology and geological history of the region (Fig. 11):

Igneous rocks of the Padthaway Ridge. These rocks crop out in the northern part of the region (Fig. 10), where they form part of the Padthaway Ridge, a basement high separating sediments of the Otway (Gambier Embayment) and Murray Basins (Rochow, 1971). They range from rhyolites and quartz keratophyres to hornblende/biotite granites and biotite adamellites

(Mawson & co-workers, 1943, 1944, 1945a, b; Rochow, 1971), and were probably emplaced during the Early Palaeozoic (Delamerian) orogenic phase of the Adelaide Geosyncline (Parkin, 1968).

Although parts of the Padthaway Ridge were covered by sediments during the early and mid-Tertiary (Firman, 1973), the topographically high areas of igneous outcrop apparently remained as exposed features subject to erosion during much of the late Cainozoic. These high areas were finally mostly covered, as shown in Figure 2, by Quaternary beach and dune deposits.

Details of the heavy minerals extracted from samples of the igneous rocks are given in Table 4. In general, magnetite, non-ferromagnetic opaques, biotite, zircon, and apatite occur in the adamellites ('Encounter Bay Granites' of Milnes & others, 1977); magnetite, biotite, hornblende, ilmenite, zircon, apatite, fluorite, and in some cases, sphene occur in the granites and microgranites ('Murray Bridge Granites'); and magnetite, non-ferromagnetic opaques, and partly chloritised groundmass components are present in the keratophyres, rhyolites and porphyries. Many of these minerals are present as major components in the heavy-mineral fraction of the late Cainozoic sediments. Sup-

Sample number*		9593			9616			9600			9615			9594			9595			9596			9599			9614			9617			9597			9613			9598			9612																																																																																																																																																																																																																																																																																																																																																																																																																																																																																																																																																																																																																																																																																																																																																										
Rock type		A			A			A			A			C			D			D			F			F			F			E			E			B			B																																																																																																																																																																																																																																																																																																																																																																																																																																																																																																																																																																																																																																																																																																																																																										
Size fraction		1	2	3	1	2	3	1	2	3	1	2	3	1	2	3	1	2	3	1	2	3	1	2	3	1	2	3	1	2	3	1	2	3	1	2	3	1	2	3																																																																																																																																																																																																																																																																																																																																																																																																																																																																																																																																																																																																																																																																																																																																																											
% Ferromagnetic		0.1	0.1	1	0	0	1	1	3	7	5	12	7	15	38	49	8	9	14	17	16	14	31	25	52	50	64	53	25	63	35	41	49	28	13	12	21	10	20	0	10	15	18																																																																																																																																																																																																																																																																																																																																																																																																																																																																																																																																																																																																																																																																																																																																																								
Ferro-magnetic	Magnetite	p	a	p			p	p	p	p	p	p		p	p	p	p	p	p	p	p	p	p	p	p	a	p	p	p	p	p	p	p	p	p	p	p	p	p	p	p	p																																																																																																																																																																																																																																																																																																																																																																																																																																																																																																																																																																																																																																																																																																																																																									
	Hematite		a											tr	tr	tr		tr	tr							a	tr	tr		c	c	c		tr		tr	tr	tr		c																																																																																																																																																																																																																																																																																																																																																																																																																																																																																																																																																																																																																																																																																																																																																											
Non-ferromagnetic minerals	Biotite	p	p	c	p	p	c	p	p	p	p	p	a				tr	p	p	c	c	c	tr		p	p	c	c	c	tr	c																																																																																																																																																																																																																																																																																																																																																																																																																																																																																																																																																																																																																																																																																																																																																																				
	Hornblende																		c	tr	tr		p	p	a							p	p	a	c	a	a																																																																																																																																																																																																																																																																																																																																																																																																																																																																																																																																																																																																																																																																																																																																																														
	Opaques	tr		c			a			c	c	c	c	c			c	a	c	c	a		tr	tr	a	c	tr	a	p	a	p		c	c	c	p	a	c	a	c	c		p	p	p																																																																																																																																																																																																																																																																																																																																																																																																																																																																																																																																																																																																																																																																																																																																																						
	Zircon		c	a			tr	a			tr	c		c	a			c	a							a			tr	a				c	c		vr	tr	a	tr	tr	a				a	c	c			p	p	p	tr																																																																																																																																																																																																																																																																																																																																																																																																																																																																																																																																																																																																																																																																																																																																													
	Tourmaline												tr							vr																																																																																																																																																																																																																																																																																																																																																																																																																																																																																																																																																																																																																																																																																																																																																																															
	Apatite		c	tr			tr	c			c	c		c	tr					tr																																																																																																																																																																																																																																																																																																																																																																																																																																																																																																																																																																																																																																																																																																																																																																															
	Allanite																																																																																																																																																																																																																																																																																																																																																																																																																																																																																																																																																																																																																																																																																																																																																																																																		</

ROCK TYPE
 A Biotite adamellites
 B Altered rhyolites and quartz keratophyres
 C Quartz porphyry
 D Hornblende-biotite granite and microgranite
 E Hornblende granite
 F Biotite granite and microgranite

SIZE FRACTION
 1 35-80 mesh
 2 80-170 mesh
 3 -170 mesh

ABUNDANCE
 p Predominant >60%
 a Abundant 20-60%
 c Common 5-20%
 tr Trace 1-5%
 vr Very rare <1%

* All numbers prefixed 7563

Sample locations given by Colwell (1976)

Table 4. Composition of the heavy-mineral fraction of the igneous rocks of the Padthaway Ridge.

ply probably took place directly and via intermediate sources such as the Pliocene calcareous quartz sands. Features of many of the minerals present in the sediments and the igneous rocks (notably zoning and inclusions in zircon, colour and pleochroism in hornblende, and inclusions in biotite) are directly comparable.

Tertiary sediments of the Murray Basin. These sediments extend into the region in the east and north-east (Fig. 10). They constitute a marine sequence of bryozoan limestones, marls and calcareous sands (Duddo Limestone and equivalents, Bookpurnong Beds, Ettrick Marl and Loxton Sand) overlain by fluvio-lacustrine and beach-dune quartz sands and sandy clays (Parilla Sand). The Pliocene Parilla Sand, which occurs on the upthrown and topographically higher eastern side of the Kanawinka Fault and over a wide area of western Victoria, is probably the most important of the units supplying heavy minerals and other terrigenous detritus to the late Cainozoic sediments to the west. This is because of its stratigraphic position at the top of the sequence, widespread distribution over the western part of the basin, and high terrigenous content. The unit contains a mature heavy-mineral suite (Suites J and L in hole 36) with a relatively high proportion of well-rounded, multicyclic components (see earlier discussion). It is suggested that heavy-minerals and other terrigenous detritus derived from this unit were supplied to the younger sediments via two major routes: (1) a westerly-flowing drainage system off the topographically high area to the east of the Kanawinka Fault—a route which became increasingly restricted with the development of beach-ridge barriers to east-west drainage on the coastal plain, and (2) the Glenelg and Murray Rivers, rivers which, as indicated by Sprigg (1952), eroded a thick sequence of Tertiary and younger sediments to well

below their modern bed levels during the late Cainozoic periods of low sea level. At present these rivers carry little sediment in their lower reaches.

Metamorphic and sedimentary rocks of the Fleurieu Peninsula, Kangaroo Island and Mount Lofty Ranges. Relatively unaltered Late Proterozoic sediments, Cambrian metasediments (Kammantoo Group) and Archaean inliers of altered gneisses and schists occur in the northern part of the region (Fig. 10) where they make up the Mount Lofty Ranges and extend through the Fleurieu Peninsula to Kangaroo Island. They form a series of metamorphic zones (Offler & Fleming, 1968) which are partly overlain by Permian glacial and fluvio-glacial deposits, as well as Tertiary and Quaternary sands (Thomson & Horwitz, 1962). The modern sediments along the coastline of these areas contain a relatively high proportion of metamorphic minerals (see Table 5), many of which were probably recycled through intermediate sources—the Tertiary sands and Permian glacials and fluvio-glacials (see Farrell, 1968). The modern Coorong Beach sediments, extending southwards from the metamorphic belt usually contain between 5 and 10 percent metamorphic minerals in their heavy-mineral fraction; values reach 40 percent at the northern end of the beach (Table 6). Similar distribution patterns probably existed in the past: most of the late Cainozoic sediments samples in the region contain, in their heavy-mineral fraction, between 10 and 15 percent metamorphic components. These components are similar to those occurring in the modern sediments.

Volcanic rocks of the Mount Gambier area. Late Tertiary and Quaternary volcanics (mainly pyroclastics) occur in the far southern part of the region (Figs. 1, 10) where they form a northwesterly-trending zone extending from Mount Schank to Mount Graham, a distance of approximately 50 km (Fig. 1). Eruption

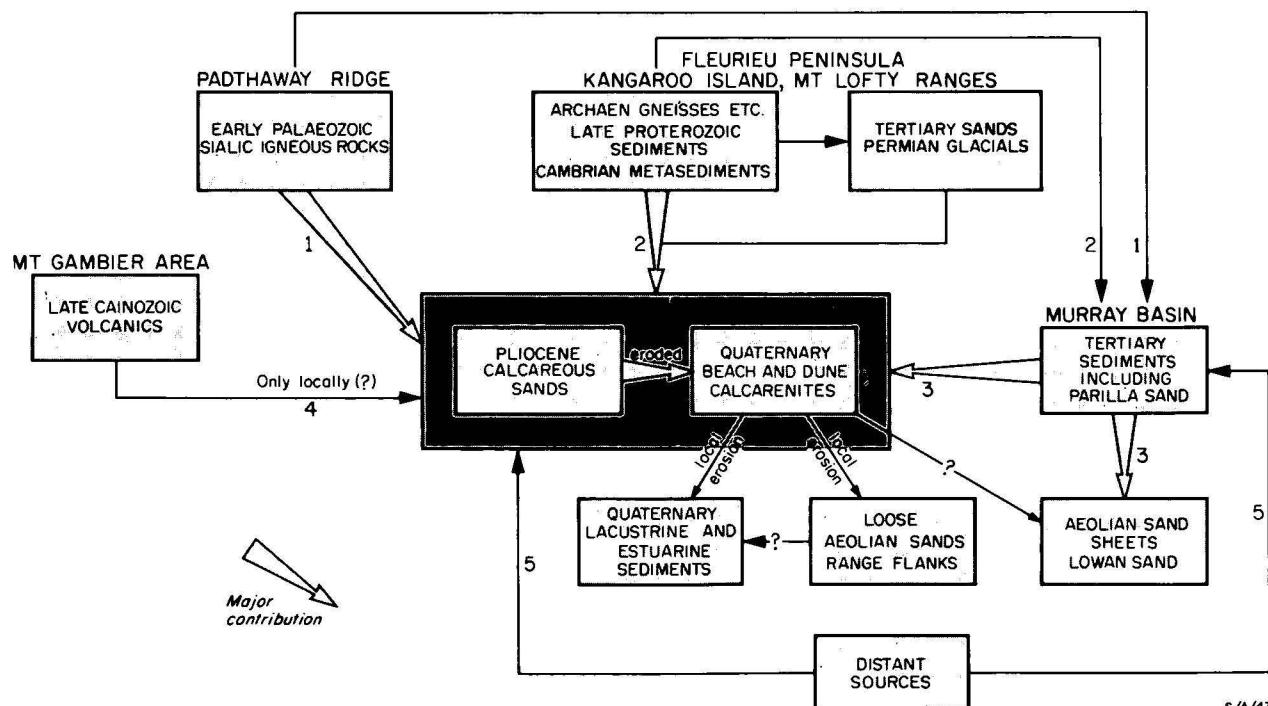


Figure 11. Summary of the suggested provenance of the terrigenous fraction of the southeast South Australian sediments. Heavy-mineral contributions are probably as follows: 1. hornblende, biotite, magnetite, ilmenite, zircon, apatite, sphene and fluorite; 2. garnet, opaques, andalusite, kyanite, staurolite, sillimanite, epidote, rutile, zircon and zoisite; 3. opaques (mainly ilmenite and leucoxene), moderately and well-rounded grains of zircon, tourmaline and rutile; 4. ilmenite, olivine, augite and apatite; and 5. rounded grains of zircon, tourmaline, rutile and other stable minerals.

occurred in two phases: the volcanics to the east of Millicent were erupted in the late Pliocene or Pleistocene, those at Mounts Gambier and Schank in a period starting in the late Pleistocene and continuing until recently (Sprigg, 1952). Subsequent to their eruption, the older deposits were modified by erosion and were largely covered by Quaternary strandline deposits. The younger deposits, on the other hand, post-date the local strandlines and therefore remained unmodified by the Quaternary high sea-levels.

Sample No.	B-8	B-9	B10	140	141
Location	Cape Jervis	Porpoise Head	Victor Harbour	Goolwa	Between Goolwa and Middleton
			percent		
<i>Opaques</i>	26.5	20.4	41.1	30.5	15.4
<i>Zircon</i>	20.5	13.7	20.3	22.7	2.2
<i>Brown tourmaline</i>	6.3	6.5	2.0	4.2	3.2
<i>Blue tourmaline</i>	0.8	0	0	0.3	0
<i>Rutile</i>	2.1	1.5	3.0	3.7	2.9
<i>Monazite</i>	0.6	0.7	0	0.4	0.5
<i>Amphibole</i>	2.4	1.8	1.6	0.7	0
<i>Garnet</i>	20.3	32.5	11.3	17.5	55.4
<i>Epidote group</i>	3.2	0	0.8	5.6	0.5
<i>Andalusite</i>	3.2	5.6	4.5	2.8	3.2
<i>Sillimanite</i>	2.1	3.6	2.2	1.4	1.8
<i>Kyanite</i>	3.8	3.6	2.6	3.1	2.8
<i>Staurolite</i>	5.4	8.9	6.6	4.5	8.3
<i>Others</i>	2.9	1.0	3.9	2.8	3.5
	100.2	99.8	99.9	100.1	99.7

Table 5. Composition of the heavy-mineral fraction of beach sands taken from the southern coastline of the Fleurieu Peninsula.

Sampling around the older volcanics, and subsequent heavy-mineral separations and thin-section studies, indicate that olivine and opaques (ilmenite and magnetite) are the principal heavy minerals associated with the volcanics; augite and apatite occur as minor ground-mass components. Except for the opaques (which are possibly derived from a variety of sources), these minerals occur in few of the late Cainozoic sediments of the region, and are almost entirely restricted to the sediments directly overlying the volcanics. This probably reflects an essentially localised contribution to the sediments from the volcanics, and also the chemical and physical instabilities of the minerals olivine and augite.

Eroded late Cainozoic sediments. Two units in the region probably acted as important intermediaries in the supply of heavy minerals and other terrigenous detritus to younger sediments. These are the Pliocene calcareous quartz sands, which appear to have undergone extensive erosion, particularly at the western end of the section (Cook & others, 1977); and those parts of the beach-dune deposits which have undergone erosion and truncation as indicated by palaeosols, intra-clasts, indurated surfaces and calcrete.

Other sources. Minor contributions have probably come from distant unidentified sources, particularly as material was probably transported over long distances by the Murray and Glenelg Rivers during periods of low sea level and higher river gradients than presently exist.

Western Victorian Murray Basin sediments

Determination of provenance of the western Victorian Murray Basin sediments is made extremely

Sample No.	Heavy minerals % by wt.	Opaques	Zircon	Tourmaline	Rutile	Monazite	Amphibole + Epidote	Metamorphic minerals*	Others	Total
						percent				
C1	0.02	54.3	8.3	12.4	0.7	0.2	18.2	5.7	0.2	100.0
C1A	0.01	55.4	7.8	15.2	1.8	0.2	15.1	4.3	0.2	100.0
C2	0.02	53.5	19.2	14.3	2.2	0	6.9	3.7	0.2	100.0
C2A	0.02	56.5	11.8	16.4	2.6	0.2	7.5	4.1	0.9	100.0
C3	0.03	50.6	5.8	22.4	1.4	0.7	12.2	6.2	0.7	100.0
C3A	0.01	43.8	7.8	28.6	2.4	0	11.0	6.1	0.4	100.1
C4	0.02	53.5	11.9	15.1	2.6	0.1	14.6	2.1	0	99.9
C4A	0.03	49.9	10.9	21.7	1.5	0.5	11.2	4.2	0	99.9
C5	0.01	38.7	24.4	21.8	1.9	1.3	8.6	2.3	0.8	99.8
C5A	0.06	54.0	12.4	16.4	3.7	0	10.2	3.1	0.2	100.0
C6	0.03	41.3	11.9	19.6	2.6	0	14.4	7.5	2.5	99.8
C6A	0.05	56.1	4.8	18.3	1.7	0.3	14.1	4.5	0	99.8
C7	0.02	51.4	3.2	16.2	1.6	0	19.4	7.2	0.8	99.9
C7A	0.04	53.3	6.3	22.7	0.2	0.4	13.4	2.9	0.8	100.0
C8	0.02	57.1	6.1	19.7	2.7	0	12.6	1.8	0	100.0
C8A	0.03	71.3	4.2	15.6	0.4	0	6.8	1.7	0	100.0
C9	0.03	51.5	9.2	18.4	0.9	0	10.1	9.7	0	99.8
C9A	0.07	69.1	9.1	12.0	1.1	0	4.3	4.3	0	99.9
C10	0.06	52.1	7.0	19.8	1.2	0	9.3	10.4	0.4	100.2
C10A	0.18	64.5	8.3	13.2	1.1	0.3	4.5	8.0	0	99.9
C11	0.11	42.9	11.8	22.6	2.0	0	12.3	8.4	0	100.0
C11A	0.06	54.5	13.0	14.8	3.0	0	9.0	5.2	0.5	100.0
C12	0.09	55.3	5.7	19.9	1.2	0	13.4	4.4	0	99.9
C12A	0.18	59.8	12.9	13.5	1.6	0	9.1	3.2	0	100.1
C13	0.78	38.0	6.0	10.8	2.2	0.5	4.0	37.7	0.7	99.9
C13A	0.35	34.1	6.2	12.7	1.4	0	4.3	40.0	1.2	99.9
C14	0.42	34.3	2.8	13.3	0.9	0.3	2.8	41.3	4.3	100.0

C1 Beach sand sample from HW mark

C1A Fore-dune sand sample

* Garnet predominant, plus staurolite, kyanite, andalusite, sillimanite

Table 6. Heavy-mineral abundance and composition of the suite in sands of the modern Coorong Beach. Sampling stations sited at approximately 15 km intervals along the length of the beach; C14 northern end.

difficult by the absence of diagnostic minerals in the heavy-mineral suite, and the presence in the suite of a relatively high proportion of stable and ultrastable, possibly multicyclic, components. Sources are probably, for the most part, distant. They cannot be identified with any certainty.

Summary and conclusions

The mainly calcareous sediments of southeastern South Australia contain low to very low concentrations of heavy minerals. This partly reflects a substantial dilution of terrigenous components by locally-derived biogenic carbonate and carbonate clays and muds. Concentrations of heavy minerals rarely exceed 0.5 percent by weight and commonly fall below 0.1 percent. No evidence exists, from the limited drilling undertaken, of enrichment of heavy minerals in particular shoreline sequences (beach and dune deposits). The highest concentrations recorded in the overall sequence (up to 1.2 percent over 0.6 m, of which approximately 20 percent consists of zircon and rutile combined) occur in an unconsolidated calcareous quartz sand unit of Pliocene age which underlies the Quaternary beach, dune, lacustrine and estuarine deposits throughout much of the region. The higher concentrations in this unit are probably related to a greater input of first-cycle terrigenous material, and to a lesser extent, to lower carbonate contents.

An inland, older, more siliceous continuation to the southeast South Australian strandline sequence occurs in the western Victorian part of the Murray Basin, and contains in the lower part of the Parilla Sand thin bands of laminae of concentrated heavy minerals. Individual bands contain up to 20 percent total heavies, substantially above the usual concentration in the unit of less than 0.5 percent.

The heavy-mineral assemblage in the southeast South Australian sediments consists of a mixture of sialic igneous (zircon, brown tourmaline, hornblende, magnetite, biotite, etc.), reworked sedimentary (well-rounded grains of the stable and ultrastable minerals), metamorphic (garnet, andalusite, sillimanite, staurolite, kyanite, etc.), mafic igneous (ilmenite) and other components. The assemblage present in the western Victorian sequence is, by comparison, relatively mature and contains a high proportion of apparently multicyclic components.

Variations in the southeast South Australian assemblage reflect the increasing age of the beach-dune deposits inland, hydraulic factors, variations in grain size, and the variable influence of source areas located in, and adjacent to, the region. Sources of the heavy minerals (and other terrigenous detritus) include the Lower Palaeozoic igneous rocks of the Padthaway Ridge (a major source of sialic igneous components), the metamorphic and other rocks of the Fleurieu Peninsula and Kangaroo Island (a major source of metamorphic components), Tertiary sediments of the Murray Basin (a major source of reworked components, particularly to the eastern part of the region), and the late Cainozoic volcanics of the Mount Gambier area (a localised contribution only). Intermediate sources (in particular the Pliocene calcareous quartz sands) have played an important role.

The proportion of unstable and semistable components in the heavy-mineral fraction decreases from the younger to older (more inland) beach-dune depo-

sits. This trend is the result of a greater contribution of multicyclic components to the eastern part of the region, and of intrastratal solution and weathering of the older deposits.

Acknowledgements

This paper represents a portion of an M.Sc. thesis submitted to the Flinders University of South Australia. An earlier and somewhat shortened version of the paper was presented at the Australasian Sedimentologists Group Meeting in Brisbane in August 1977.

I wish to thank L. Pain and D. Foulstone for assisting with the field and laboratory work, Mrs K. Long for advice on the processing of the numerical data, and Drs H. A. Jones, P. J. Cook, C. R. Lawrence and B. G. Thom for their comments on this and earlier versions of the manuscript. Figures were drawn by R. Bates and J. Mifsud of the geological drawing office, BMR.

References

- ABELE, C., 1977—Micropalaeontological report on BMR bores near Horsham, southwestern Victoria, with comments on stratigraphic nomenclature. *Geological Survey of Victoria, unpublished Report 1977/57*.
- BLACKBURN, G., 1962—Stranded coastal dunes in north-western Victoria. *Australian Journal of Science*, **24**, 388-9.
- BLACKBURN, G., BOND, R. D., & CLARKE, A. R. P., 1967—Soil development in relation to stranded beach ridges of County Lowan, Victoria. *CSIRO—Soil Publication*, **24**.
- BLATT, H., & SUTHERLAND, B., 1969—Intrastratal solution and non-opaque heavy minerals in shales. *Journal of Sedimentary Petrology*, **39**, 591-600.
- BONHAM-CARTER, G. F., 1967—FORTRAN IV program for Q-mode cluster analysis of non-quantitative data using IBM 7090/7094 computers. *Kansas Geological Survey—Computer Contribution 4*.
- BOUTAKOFF, N., 1963—The geology and geomorphology of the Portland area. *Geological Survey of Victoria—Memoir 22*.
- COLWELL, J. B., 1976—Heavy minerals in the late Cainozoic sediments of southeastern South Australia. *Bureau of Mineral Resources, Australia—Record 1976/89* (unpublished).
- COLWELL, J. B., 1977—Stratigraphic drilling of stranded beach ridges, central western Victoria, 1977. *Bureau of Mineral Resources, Australia—Record 1977/61* (unpublished).
- COLWELL, J. B., 1978—Late Cainozoic sediments of southeastern South Australia. *Bureau of Mineral Resources, Australia—Record 1978/105* (unpublished).
- COOK, P. J., COLWELL, J. B., FIRMAN, J. B., LINDSAY, J. M., SCHWEBEL, D. A., & von der BORCH, C. C., 1977—The late Cainozoic sequence of southeast South Australia and Pleistocene sea-level changes. *BMR Journal of Australian Geology and Geophysics*, **2**, 81-88.
- CROCKER, R. L., & COTTON, B. C., 1946—Raised beaches of southeast South Australia. *Transactions of the Royal Society of South Australia*, **70**, 64-72.
- DRYDEN, A. L., 1931—Accuracy in percentage representation of heavy-mineral frequencies. *Proceedings of the National Academy of Sciences*, **17**, 233-8.
- FARRELL, B. L., 1968—A beach sand study of the Fleurieu Peninsula. *B.Sc. (Hons) thesis, University of Adelaide* (unpublished).
- FIRMAN, J. B., 1965—Pinnaroo-Karoonda map sheet. *Geological Atlas of South Australia, Special Series 1:126-720, Geological Survey of South Australia*.
- FIRMAN, J. B., 1967a—Late Cainozoic stratigraphic units in South Australia. *Geological Survey of South Australia—Quarterly Notes 22*, 4-8.

- FIRMAN, J. B., 1967b—Stratigraphy of the Late Cainozoic deposits in South Australia. *Transactions of the Royal Society of South Australia*, **91**, 165-180.
- FIRMAN, J. B., 1973—Regional stratigraphy of surficial deposits in the Murray Basin and Gambier Embayment. *Geological Survey of South Australia—Report of Investigation* 39.
- GALEHOUSE, J. S., 1971—Point counting. In CARVER, R. E. (Editor), *PROCEDURES IN SEDIMENTARY PETROLOGY*. Wiley-Interscience, New York, 385-407.
- HENLEY, K. J., 1972—The quantitative evaluation of alluvial ores. *Amdel Bulletin*, **14**.
- HILLWOOD, E. R., 1960—Concentrations of heavy mineral sands on South Australian beaches. *South Australian Department of Mines—Mining Review*, **109**, 123-9.
- HOSSFELD, P. S., 1950—The Late Cainozoic history of the south-east of South Australia. *Transactions of the Royal Society of South Australia*, **73**, 232-79.
- HUBERT, J. F., 1971—Analysis of heavy-mineral assemblages. In CARVER, R. E. (Editor), *PROCEDURES IN SEDIMENTARY PETROLOGY*. Wiley-Interscience, New York, 453-78.
- KLOVAN, J. E., & IMBRIE, J., 1971—An algorithm and Fortran IV program for large-scale Q-mode factor analysis and calculation of factor scores. *Mathematical Geology*, **3**, 61-8.
- KRUMBEIN, W. C., & RASMUSSEN, W. C., 1941—The probable error of sampling beach sand for heavy mineral analysis. *Journal of Sedimentary Petrology*, **11**, 10-20.
- LAWRENCE, C. R., 1966—Cainozoic stratigraphy and structure of the Mallee region, Victoria. *Proceedings of the Royal Society of Victoria*, **79**, 517-53.
- LAWRENCE, C. R., 1975—The geology, hydrodynamics and hydrochemistry of the southern Murray Basin. *Geological Survey of Victoria—Memoir* 30.
- LAWRENCE, C. R., & ABELE, C., 1976—Murray Basin. In DOUGLAS, J. G., & FERGUSON, J. A. (Editors), *Geology of Victoria. Geological Society of Australia Special Publication* 5, 191-8.
- LUDBROOK, N. H., 1961—The stratigraphy of the Murray Basin in South Australia. *Geological Survey of South Australia—Bulletin* 36.
- MACUMBER, P. G., 1969—The inland limits of the Murranian marine transgression in Victoria. *Australian Journal of Science*, **32**, 165-6.
- MANNING, J. C., 1953—Application of statistical estimation and hypothesis testing to geologic data. *Journal of Geology*, **61**, 544-56.
- MAWSON, D., & PARKIN, L. W., 1943—Granitic rocks of south-eastern South Australia. *Transactions of the Royal Society of South Australia*, **67**, 233-43.
- MAWSON, D., & DALLWITZ, W. B., 1944—Palaeozoic igneous rocks of lower south-eastern South Australia. *Transactions of the Royal Society of South Australia*, **68**, 191-209.
- MAWSON, D., & SEGNI, E. R., 1945a—Porphyritic potash-soda microgranite of Mt Monster. *Transactions of the Royal Society of South Australia*, **69**, 217-22.
- MAWSON, D., & SEGNI, E. R., 1945b—Granites of the Tintinara district. *Transactions of the Royal Society of South Australia*, **69**, 263-76.
- MAYO, W., & LONG, K. A., 1976—Documentation of Geological Branch computer programs. *Bureau of Mineral Resources, Australia—Record* 1976/82 (unpublished).
- MILNES, A. R., COMPSTON, W., & DAILY, B., 1977—Pre- to syn-tectonic emplacement of Early Palaeozoic granites in southeastern South Australia. *Journal of the Geological Society of Australia*, **24**, 87-106.
- OFFLER, R., & FLEMING, P. D., 1968—A synthesis of folding and metamorphism in the Mt Lofty Ranges, South Australia. *Journal of the Geological Society of Australia*, **15**, 245-66.
- PARKIN, L. W. (Editor), 1969—*HANDBOOK OF SOUTH AUSTRALIAN GEOLOGY*. Geological Survey of South Australia, Adelaide.
- ROCHOW, K., 1971—The Padthaway Ridge. In WOPFNER, H., & DOUGLAS, J. G. (Editors), *The Otway Basin of south eastern Australia. Geological Surveys of South Australia and Victoria—Special Bulletin*, 325-37.
- SPRIGG, R. C., 1952—The geology of the south-east province, South Australia, with special reference to Quaternary coast-line migrations and modern beach developments. *Geological Survey of South Australia—Bulletin* 29.
- SPRIGG, R. C., 1959—Stranded sea beaches and associated sand accumulations of the upper southeast. *Transactions of the Royal Society of South Australia*, **82**, 183-93.
- THOMSON, B. P., & HORWITZ, R. C., 1962—Barker 1:250 000 Geological Sheet. *South Australian Department of Mines, Adelaide*.
- TINDALE, N. B., 1947—Subdivision of Pleistocene time in South Australia. *Record of the South Australian Museum*, **8**(4), 619-52.
- TINDALE, N. B., 1959—Pleistocene strand lines of the upper southeast of South Australia. *Transactions of the Royal Society of South Australia*, **82**, 119-20.
- WOPFNER, H., & DOUGLAS, J. G. (Editors), 1971—*The Otway Basin of southeastern Australia. Special Bulletin of the Geological Surveys of South Australia and Victoria*.

Drowned dolines — the blue holes of the Pompey Reefs, Great Barrier Reef

D. G. Backshall¹, J. Barnett¹, P. J. Davies, D. C. Duncan¹,
N. Harvey¹, D. Hopley¹, P. J. Isdale¹, J. N. Jennings²,
& R. Moss¹

Blue holes occur at Cockatoo and Molar Reefs, in the Pompey hard line reefs. These two holes are roughly circular in shape, between 240-295 m in diameter, and 30-40 m deep. They are completely (Cockatoo) or partially (Molar) rimmed by profuse living coral and surrounded by lagoonal depths of 5-10 m. The inner slopes of the Cockatoo blue hole are 60-70° down to a depth of 25 m, below which coalescing sediment fans markedly reduce this angle. At the Molar blue hole, slopes are mainly gentler (45°) and sediment fans and terraces occur below 16 m. Distinct biological/sedimentary associations occur in both holes. Seismic refraction studies across the rim of the blue holes show a shallow (8.5-11 m) pre-Holocene surface beneath the rims. The balance of evidence suggests that the blue holes represent collapsed dolines which may have taken more than one low sea-level period to form. The original surface structures have been modified by subaerial solution processes, and subsequent sediment infill and coral growth following the Holocene transgression.

Introduction

Like sapphires set in turquoise (front cover, this issue), the blue holes of coral reefs have long impressed mariners, naturalists and reef scientists. Examples of such circular, steep-sided holes in the Bahamas have caused comment since the end of the last century. Northrop (1890), and Agassiz (1894) firmly attributed them to terrestrial solution prior to substantial subsidence. However, at much the same time, Wharton (1898) vaguely linked the *Puits sans Fond* of Clipperton in the northern Pacific that had been described as 'a perfectly round hole in the lagoon which looks very much like an old crater' (J. Arundel in Wharton, 1898), with his view of the whole reef as growing on top of explosion remnants of a volcano. Volcanic rocks do project in Clipperton Rock, making Clipperton an almost-atoll (Sachet, 1962). Wharton's idea for the blue hole is somewhat far-fetched, however, and Agassiz's solution mechanism has been generally accepted for blue holes, though latterly combined with glacio-eustatism rather than with tectonic movements of reef foundations. Some recent investigators have provided powerful support for Agassiz's theory, notably Dill (1977); moreover, the origin of blue holes has become interwoven with the antecedent karst hypothesis of modern reef configuration (e.g. Purdy, 1974). Nevertheless there has been a tendency to jump to this explanation without weighing other possible modes of formation and assessing different processes subsumed within this broad standpoint.

The best Australian examples of blue holes are in the Pompey Reef Complex (Fig. 1). This is the most intricate and least known area of the Great Barrier Reef, and is composed of an inner series of linear reefs, a central series of irregular patch reefs, and an outer series of massive 'hard line' reefs. The outer reefs are up to 200 km from the mainland coast, and form a belt 140 km long and 16 km wide. Individual reefs are up to 100 km² in area.

Maxwell (1970) attributes the pattern of reefs and channels of the Pompey Complex to growth on reef-derived detritus deposited as delta sediments in a strong

tidal-current regime. He is supported in his suggestion by the strong tidal currents operative in the area today (2.5-10 kt). In contrast, however, Purdy (1974) suggested that features of Big Stephens Reef, in the Pompey Complex, were analogous to karst features. Moreover, he argued that the whole barrier platform of the Central Barrier Reef had been a large limestone drainage divide in pre-Holocene times (Purdy, 1974, p. 58). Maxwell (1976) has since disagreed with these assertions and argued that 'residual morphology of the shelf has localised reef development, but there is little evidence to suggest that it has controlled shape attributes of individual reefs' (1976, p. 79). Here we report general observations made on two of the Pompey Reefs, and detailed studies of two blue holes in them made during an expedition utilising the M.V. *James Kirby*. The hard line Pompey Reefs were visited for two weeks in October 1977, when echo-profiling, scuba exploration, sediment coring, seismic refraction, grab sampling and shallow drilling were carried out. The general description of the reefs outlined below is based on these field data, with information gained from a study of vertical air photographs (1:70 000), oblique colour photographs taken by the authors from a height of 500 m, and a series of processed colour-composite images based on LANDSAT data.

Cockatoo Reef and blue hole

Cockatoo Reef (previously unnamed, location 20°45'S, 151°02'E), one of the largest reefs of the hard line Pompey Complex, is 13.6 km long in a north-westerly direction, and 8.7 km wide (Fig. 2A). It is separated from adjacent reefs by deep channels, 93 m being recorded in the southern pass. The reef is highest next to the channels, the 350 m-wide algal rim reaching a level between mean low-water springs and mean lower water neaps. Elsewhere the reef flat is slightly lower and very sandy, with small coral heads aligned parallel to the apparent direction of tidal scour over the reef top. One prominent reef-flat ridge is continuous across the entire reef. Distinctive sediment trains lead into the intricate lagoon systems, most of which appear to have a maximum depth of 10 m. It is this mesh pattern of lagoon systems and ridges which Purdy (1974) and others have considered to be analogous to the closed depressions of Pleistocene karst topography. However, the reef cap is clearly Holocene in age, a

1. Department of Geography, James Cook University, Townsville, Qld 4811.
2. Department of Biogeography & Geomorphology, Australian National University, Canberra, ACT 2600.

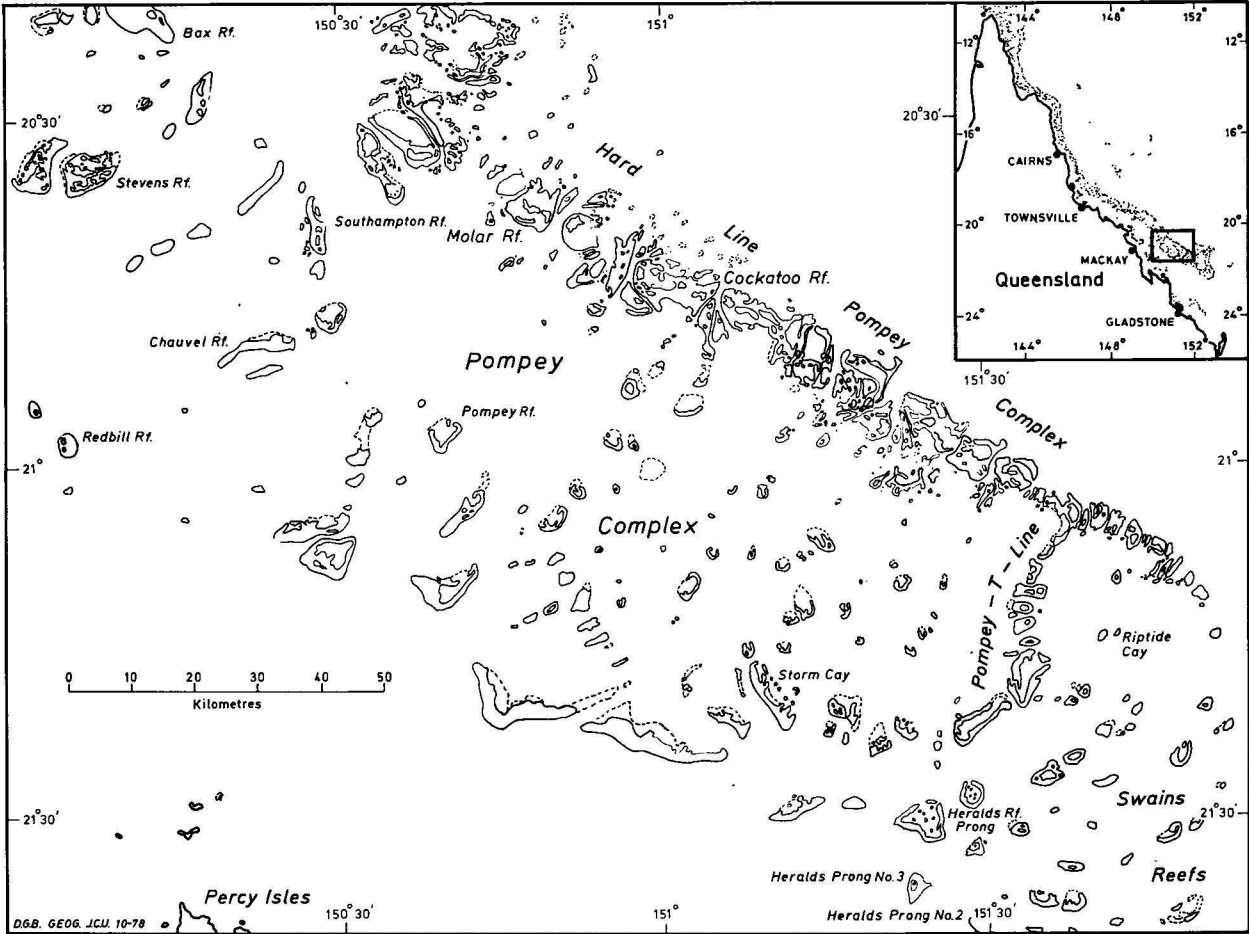


Figure 1. Location of Molar and Cockatoo Reefs in the Pompey Complex.

Code No.	Location	Depth (cm)	Material	Aragonite (percent)	Radiocarbon age (years B.P.)
GaK7270	Cockatoo Reef Algal Rim. Hole 1	15-22	<i>Acropora</i> separated from Algal Cement	98	4100 ± 100
GaK7271	Cockatoo Reef Algal Rim. Hole 1	55-70	<i>Acropora</i> separated from Algal Cement	98	3480 ± 120
GaK7269	Cockatoo Reef Algal Rim. Hole 2	12-17	<i>Acropora</i> separated from Algal Cement	98	30 ± 100
GaK7268	Molar Reef On Seismic Line C-D	65-75	<i>Acropora</i> Shingle	98	1310 ± 100
NSW259	Cockatoo Blue Hole	0-5	Coral/Algal Sediment	75	860 ± 100
NSW268	Cockatoo Blue Hole	50-60	Coral/Algal Sediment	75	1000 ± 100
NSW269	Molar Blue Hole	0-5	Coral/Algal Sediment	75	1390 ± 130

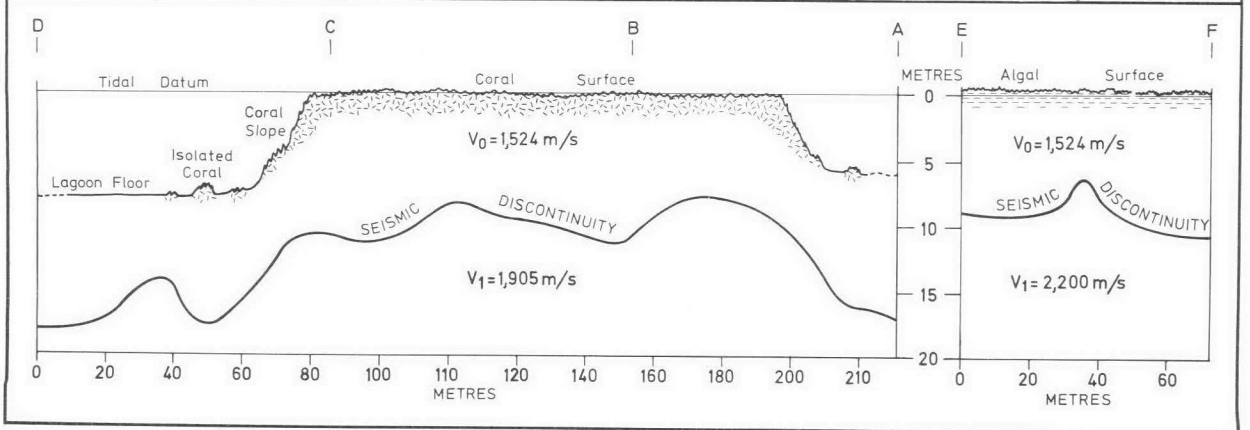
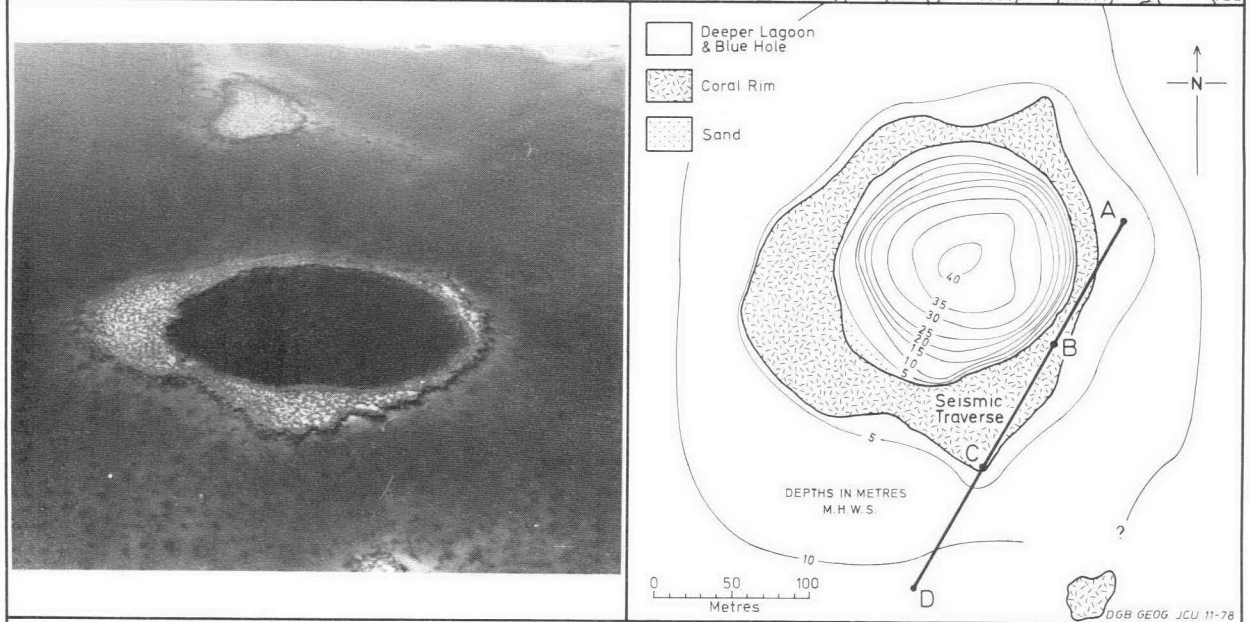
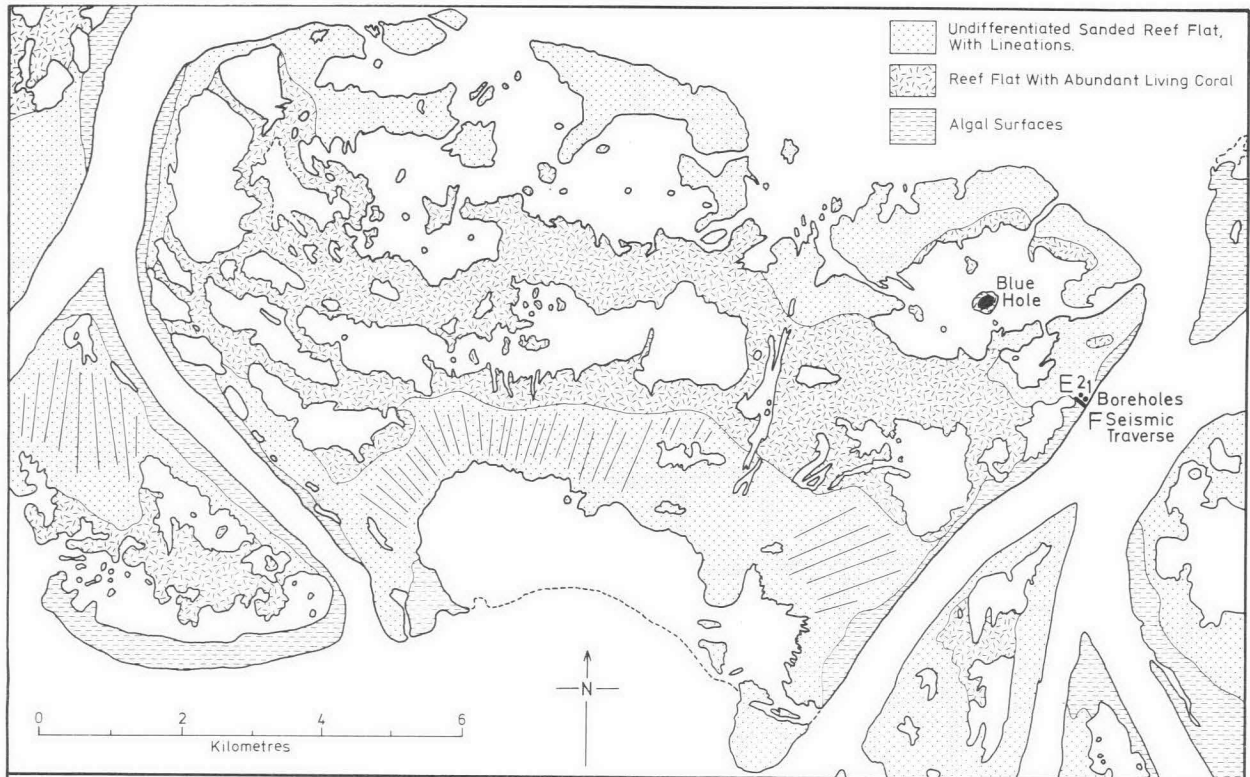
Table 1. Radiocarbon ages of rock and sediments from Cockatoo and Molar Reefs.

date of 4100 ± 100 y. BP (Table 1), being the oldest date obtained from algal-cemented *Acropora* in two drill holes into the southern algal rim.

The blue hole of this reef is centrally situated in the large lagoon at the northeastern end of the reef (Fig. 2A). The lagoon has a maximum depth of just over 10 m and is open to the ocean in three places. Its floor

is sandy, with only a few isolated coral heads. Twenty-three sediment samples from the lagoon and rim of the blue hole were dominantly fine sand (mean size 2.03 to 2.48 ϕ), only moderately sorted (SD = 1.03 to 1.53 ϕ) in the deeper lagoon, but becoming both coarser and more poorly sorted within 25 m of the living coral rim of the blue hole (mean size 1.29 to

Figure 2. A. Plan of Cockatoo Reef showing the positions of the blue hole, seismic traverses and drill holes. B. Oblique aerial photograph of Cockatoo blue hole. C. Plan of blue hole drawn from closely spaced echo profiles. The position of seismic section A-D is marked. D. Seismic sections AD and EF.



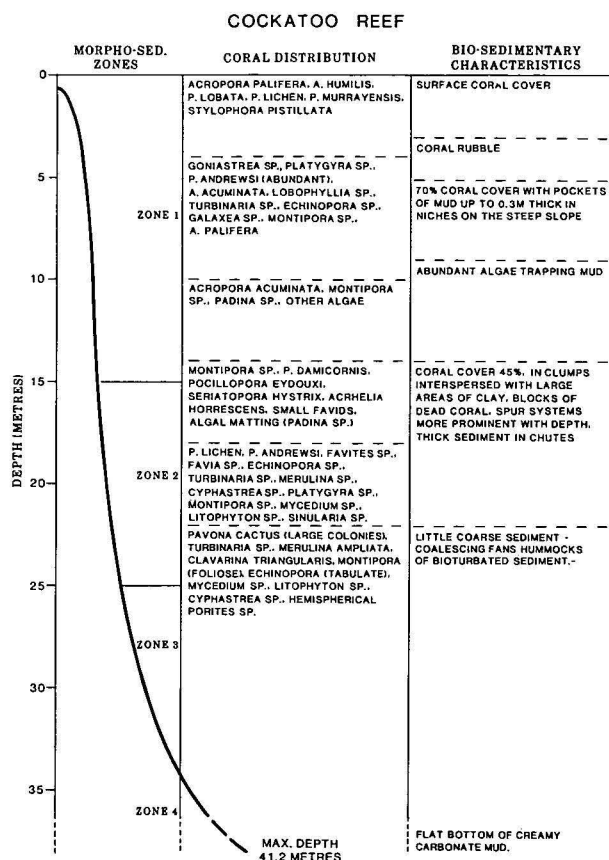


Figure 3. Bio-sedimentary characteristics of the Cockatoo blue hole. All data obtained by scuba diving.

2.21 ϕ ; SD 1.39 to 1.80 ϕ). Sediments from the rim were even coarser (mean size 0.11 to 0.64 ϕ) and also poorly sorted (SD = 1.42 to 1.51 ϕ). The sediments consisted of fragments of coral, coralline algae and molluscs, with only minor amounts of foraminifera and other calcareous organisms.

The blue hole has a rim of living coral 10 to 60 m wide. The hole (Fig. 2B) is nearly circular in plan, and has a maximum length of 240 m north-south and a width of 205 m. Echo-sounding traverses across the feature show it to be bowl-shaped and slightly asymmetrical, with the steepest side to the east, where the upper slope is 60° to 70°. Elsewhere the upper slope is between 45° and 50° (Fig. 2C).

Four morpho-sedimentary zones were recognised (Fig. 3) from scuba investigations.

Zone 1

0-15 m. This is the zone of maximum coral cover (70% down to -10 m). Abundant rubble, mainly *Acropora* sticks, occurs at near -4 m (Fig. 4A). Mud-grade sediment occurs in pockets at least 0.3 m deep; such sediment contains very little sand or silt particles. Abundant worm tubes suggest much bioturbation from 12 to 15 m. Downwards there is a decrease in coral cover to 45 percent, and soft algae, particularly *Padina*, become abundant (Fig. 4B). Fine carbonate is stabilised by these algae, even though the slope is 60-70°.

Zone 2

15-25 m. Still sloping at 60-70° (Fig. 4C), this zone is dominated by down-slope linear spurs of coral colonies separated by chutes 1.5 m wide at the top, but widening downwards to 7 m (Fig. 4D). The

coral spurs are commonly interrupted towards their ends by irregular corridors between adjacent chutes. Fans of fine sediment spill out of the deeper ends of the chutes.

Zone 3

25-35 m. The top of this zone is delineated by a gentle break of slope; the zone is marked by the almost complete absence of corals, and the presence of a very hummocky terrain. Such hummocks, up to 0.6 m high—probably the result of burrowers—are obliterating the boundaries of adjacent coalescing sediment fans. This whole slope (30°-45°) is completely built by the coalescing fans.

Zone 4

Below -35 m, the slope lessens quickly to a flat bottom composed of buff soft plastic sediment covered by algal films. There is little evidence of the burrowing activities seen in ZONE 3, but holothurians, anemones and worms are active on the bottom (Fig. 4E). The sediment has the consistency of yoghurt.

A push core was obtained in ZONE 4 sediments at a depth of -35 m, and penetrated 60 cm. The gross sedimentological features are shown in Figure 5A. No bedding is visible, the sediment being homogeneous except for the large pelecypod shell which pulled out of the core at a depth of 25 cm. Petrographic and scanning electron microscope studies of the core show the sediment to be composed of fine sand to mud, made up of degraded coral/algal fragments with abundant radiolaria, foraminifera and sponge spicules. Pellets agglutinated by organic films and algal filaments occur mainly in the lower part of the section.

Radio-carbon dating of the cores (Fig. 5A, Table 1) show no appreciable differences in age between the top and bottom. This suggests either that abundant biologic mixing of the sediment has occurred, or such mixing occurred during deposition as a result of turbulent flow down the chutes on to the floor of the blue hole. By either method, the resultant sediments are not bedded, and rates of sedimentation could not be calculated.

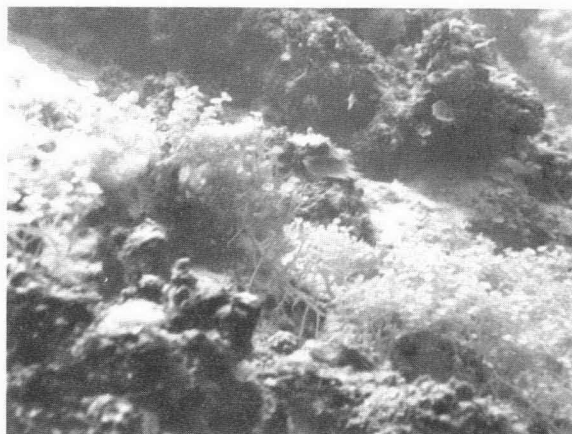
Sub-surface structure was investigated by seismic refraction profiling. Two refraction transects were completed at Cockatoo Reef, one 260 m long across the rim of the blue hole, and one 77 m long across the algal rim marking the southeastern rim of the reef (Fig. 2D). Seismic section A-D (Fig. 2D) show a seismic discontinuity at depths of 16.5 and 18 m beneath the lagoon, but rising to 9 to 11 m depth beneath the coral rim ringing the blue hole. The present surface is therefore similar in gross outline to the seismic discontinuity. Profile E-F, across the southeastern algal rim, displays the seismic discontinuity sloping from -7 m to -11 m backwards towards the lagoon. Although the profile stops before reaching the lagoon, it is pertinent that the shallowest part of the disconformity underlies the algal ridge.

Molar Reef and blue hole

Molar Reef (previously unnamed, location 20°38'S, 150°48'E) is one of the northernmost of the hard line Pompey Complex reefs (Fig. 6A). It is 7.75 km long in a northeast direction, and 7.4 km wide. Like Cockatoo and other reefs of the area it is bordered by deep channels. Algal rims are prominently developed along the margins of the channel on the southeastern side of the reef and to a lesser extent on the southwestern



Figure 4. A. *Acropora* and rubble in the top 4 m of Cockatoo blue hole.



B. *Padina* on the upper slope of Cockatoo blue hole.



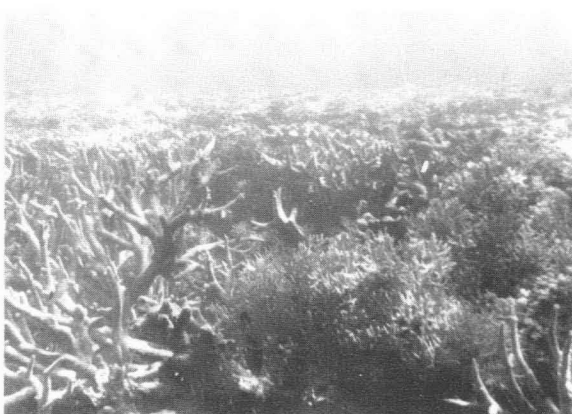
C. Steep slope with abundant coral in the depth range 15-25 m. Cockatoo blue hole.



D. Base of sediment chute bordering a coral spar, at 20 m.



E. Holothurian bioturbating sediment at a depth of 35 m; Cockatoo blue hole.



F. *Acropora* and *Seriatopora* mark inner edge of rim of Molar blue hole.

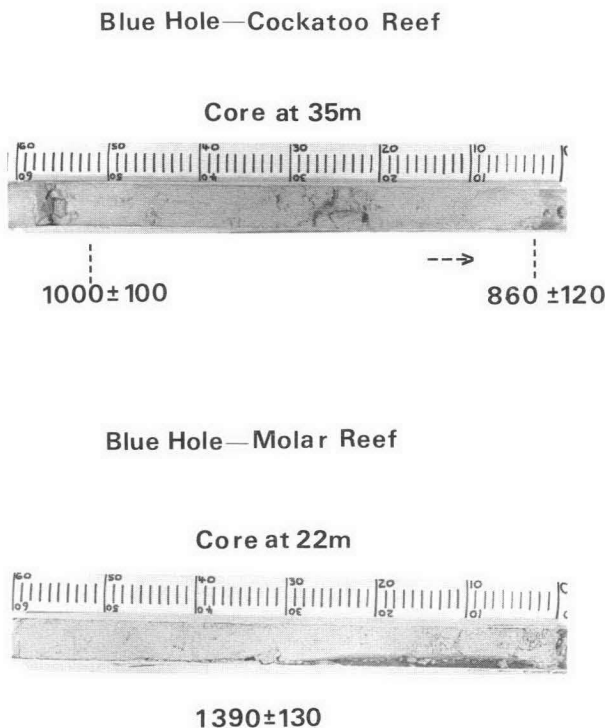


Figure 5. Push-cores, depths as shown.

and northwestern margins. A prominent feature of the reef is a central ridge separating complex lagoonal systems. The ridge rises to a level slightly above mean low water springs and has a dense cover of living corals, consisting mainly of *Pocillopora* sp., *Seriatopora* sp. and *Acropora humilis*. A shallow core 1 m into this ridge showed its upper surface to consist of similar branching corals in growth position, and probably comminuted shingle and coarse sand. Cemented shingle from a depth of 0.65 to 0.75 m produced a radiocarbon age of 1310 years \pm 100 BP (Table 1). The lagoons of the reef are sand-floored and have maximum depths of 7 m. To the southwest of the central ridge much of the reef flat consists of living corals with a strong southwesterly lineation. On the northern end of the reef is a small, deep channel branching from the main channel to the north but blocked at its eastern end. Such blind channels are common features of the hard line reefs of the Pompey Complex.

The blue hole of Molar Reef is near the centre of the reef southwest of the central ridge, and at the southern end of a small lagoon (Fig. 6A). It has a living coral rim on the southern and eastern sides but a lip of shallow (5 m) lagoon to the north and west (Fig. 6B). The rim therefore is not completely associated with the blue hole. It is larger than the blue hole on Cockatoo Reef, having an east-west length of 295 m and a width of 260 m. It is slightly asymmetric with the steeper side to the east, but has a bowl shape very similar to that of Cockatoo Reef. The shallow concave floor commences at a depth of about 25 m, with a maximum depth of 29.25 m being recorded by echo sounder, and 32.5 m by lead line (Fig. 6C).

Detailed scuba study of this hole was hampered by poor visibility below a depth of 15 m. However, five morpho-sedimentary zones were recognised (Fig. 7).

Zone 1

Surface zone of low, stunted colonies of *Acropora palifera* and *Seriatopora hystrix* forming gullies and courses floored with coral/foraminiferal sand and gravel (Fig. 4F).

Zone 2

From the surface to a depth of 3 m, a steep slope (60–70°) marks the inner edge of the rim near the blue hole. This steep slope is formed by the vertically growing surfaces of *Acropora* and *Seriatopora* (Fig. 4F).

Zone 3

From –3 to –7 m this slope is much gentler (10°–15°) and composed almost entirely of rubble mounds of *Acropora* and *Seriatopora* (Fig. 8A). There is little evidence of bioturbation, but abundant evidence of organic degradation of coral detritus by mollusc, sponge and algal borings. A coral cover of 10 percent is made up mainly by *Stylophora pistillata*, *Pocillopora damicornis*, with some *Acropora palifera*. At the base of this zone, trapping of sediment by the alga *Padina* occurs.

Zone 4

From –7 to –16 m a change in gradient to 45° occurs. The sediment is composed mainly of coral gravel decreasing downwards where sand predominates (Fig. 8B). The 45° slope is mostly bare, but scattered colonies of *Acropora palifera*, massive *Porites*, *Platygyra* and *Montastrea* break up the slope (Fig. 8C, D). The lowest level at which *Seriatopora* is found is at –13 m.

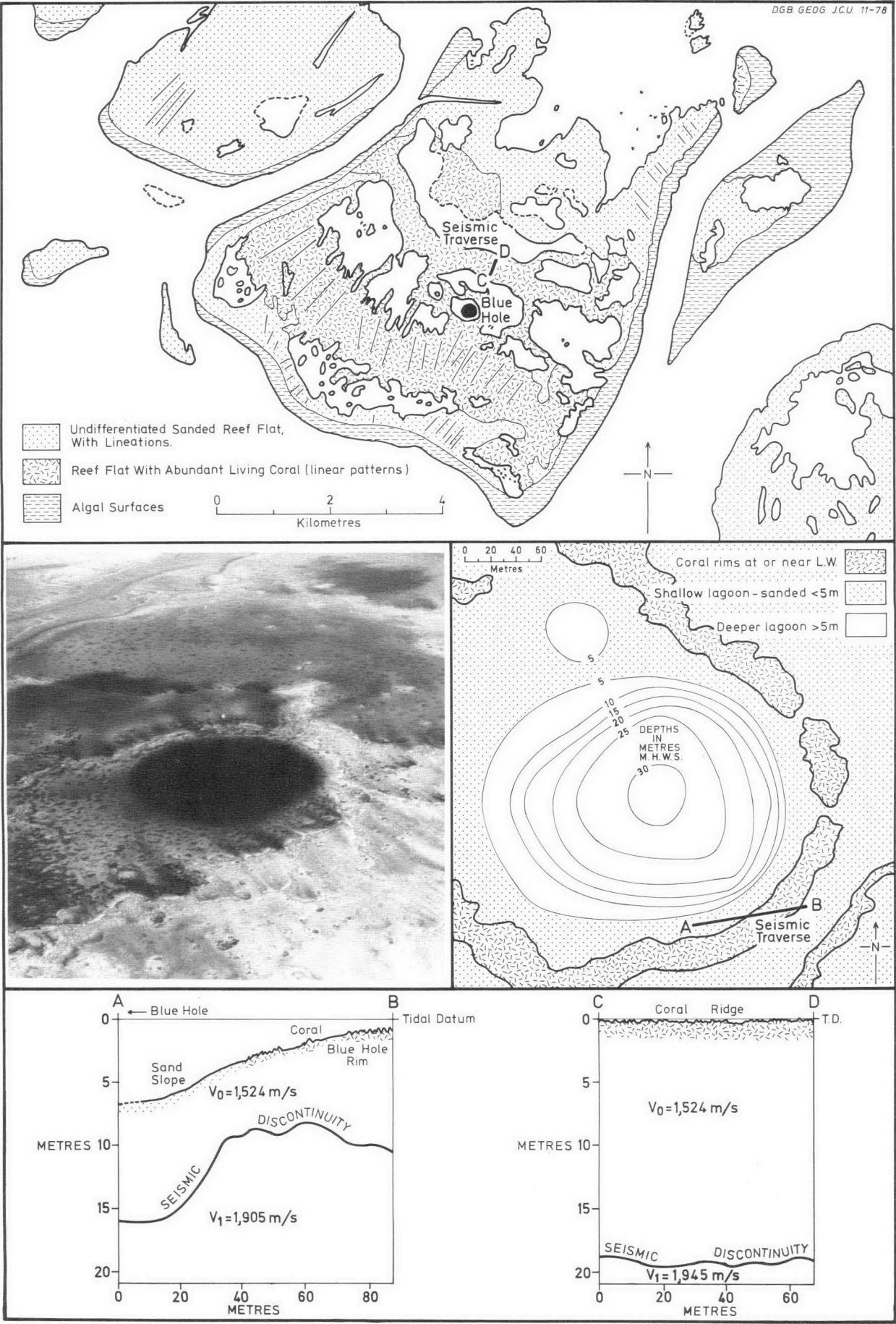
Zone 5

A marked decrease in slope below 16 m terminates in a flat plain composed of mud and admixed sand (Fig. 8E). Visibility at this depth was less than 1 m, but exploration showed the flat plain to be extensive. In fact, the divers concluded that it must represent the bottom of the blue hole. Coral cover in this zone is about 5% (Fig. 8F).

It proved impossible to take a vertical push core because gravel-sized fragments prevented penetration. A horizontal core is shown in Figure 5B. Much of the sediment is held together by organic coatings and mucus. The radiocarbon date of 1390 \pm 13 y. B.P. does not mean that sedimentation then ceased. The radiocarbon age dates the mineral components, and not the time of sedimentation.

Two refraction transects (Fig. 6D) were completed across the rim of the blue hole, and coral ridge at Molar Reef. Across the rim of the blue hole, the seismic discontinuity is highest beneath the irregular coral rim (–8.5 m) and deepest (–16 m) beneath the sand slope bordering the inner margin. The section CD across the coral ridge shows the discontinuity at a constant depth of about –20 m.

Figure 6. A. Plan of Molar Reef showing the position of the blue hole, and the position of seismic sections. B. Oblique aerial photograph of Molar blue hole. C. Plan of blue hole drawn from closely spaced echo profiles. The position of seismic section A-B is marked. D. Seismic sections A-B and C-D.



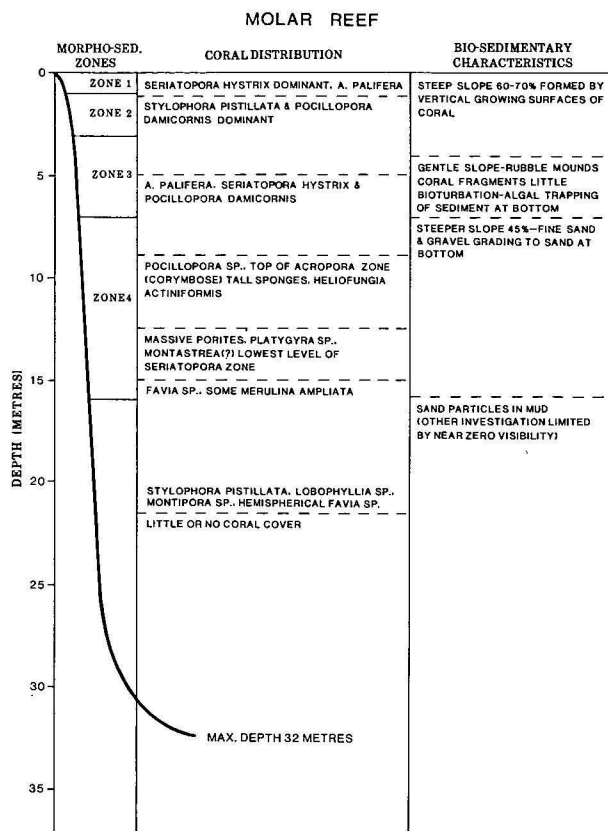


Figure 7. Bio-sedimentary characteristics of the Molar blue hole. All data obtained by scuba diving.

Discussion—origin of blue holes

Holocene coral growth and sedimentation has so obscured the nature of the pre-Holocene surface that it is necessary to consider all possible hypotheses for the formation of the blue holes. Round, closed depressions are known elsewhere to have resulted from glacial and ground ice melt processes, pseudokarst processes in basalts and laterites, volcanicity, meteorite impact, or from true karst processes. The first two groups of processes may be dismissed because of the unlikelihood of severe Pleistocene cold periods here and the absence of basalts and laterites at shallow depth beneath the reefs. Similarly a relation to constructional or destructional volcanic activity is unlikely because volcanics occur at only one locality, in the Murray Islands at the extreme northern end of the reefal province. However, a meteorite impact origin or processes of limestone karstification must be given more serious consideration.

Meteorite impact

An origin by meteorite impact cannot be ruled out on the basis of regional evidence. The dimensions of the blue holes are, for example, closely comparable to those of the Henbury craters in the Northern Territory. The fact that the blue holes' rims are capped by Holocene reef growth does not exclude an impact origin for the holes. Indeed, the rim shown by the seismic discontinuity for the Cockatoo Reef hole is typical in form for a meteorite crater. In addition, the dubious association of modern rim and blue hole at Molar Reef also does not eliminate the meteorite mechanism because rims are not necessarily formed with meteorite craters; however, it does cast some slight doubt on this interpretation. Nor is the test of presence or absence of meteoritic material critical and this cannot even be

applied because of the obscuring effect of subsequent sediment. Recourse has to be made to the less satisfactory procedure of arguing from the similarity of the cases in question to those in other areas where this mode of origin can be eliminated. Suffice it to point to the long, gently sinuous line of blue holes along the east coast of Andros Island in the Bahamas, parallel and close to the steep slope dropping to the depths of the Tongue of Ocean (Jordan, 1954; Benjamin, 1970). A meteorite shower is unlikely to produce a single chain aligned along a pre-existing topographic feature over a distance of 40 km in this way. It must be admitted, however, that blue holes need not necessarily be of the same origin everywhere; the probabilities, nevertheless, are against the Queensland blue holes being modified astroblemes.

Karst erosion

Karst remains the most likely process to have formed the Pompey blue holes. However, consideration must be given to both submarine and subaerial conditions as the necessary prerequisites for their formation.

Submarine springs are well known from many coastal karst regions, for example the Anavalos spring off the Kynourian coast of the Peloponnese in Greece, which vents onto the sea floor at a depth of -36 m (Mistardis, 1968). However, this and others like it are generally thought to have formed during a Pleistocene low sea-level period. Moreover, such springs occur in close proximity to high subaerial relief—a condition which does not occur in the Great Barrier Reef, where the blue holes are 200 km from the nearest high relief masses. A submarine vauculian spring is therefore unlikely to have brought about the formation of our blue holes. Also it is unlikely that springs have arisen as a result of leakage from a deep basement aquifer forming part of any potential offshore extension of onshore basins. We suspect that leakage from any potential basement aquifer through the thick post-basement sequence (+2000 m) would be manifested in regional features, rather than in isolated spots forming blue holes. Submarine collapse of a cave formed subaerially during periods of low sea level seems also unlikely, because submarine flooding would provide fresh support for the roof by filling the chamber with water. We conclude therefore that formation below sea level is unlikely, and are faced with the generally accepted standpoint of Agassiz for subaerial karsting as a mechanism for blue-hole formation, a conclusion supported generally by morphological comparisons between Pacific (Emery & others, 1954; Stoddart, 1969) and Atlantic (Purdy, 1974) reef features, and sinkhole plains such as those in Kentucky (Miotke, 1973); and more specifically by the distinct resemblance of the meshwork reef structure of the Molar and Cockatoo Reefs to the solution-developed ridge and corridor morphology of the Nullarbor Plain (Jennings, 1967).

Closed depressions in karst, even of the simple form comprised under the term doline, are of many types, with several processes at play (Jennings, 1971; Quinlan, 1974). We are therefore still left with several options for the formation of blue holes. Some can be set aside summarily. General knowledge of the geology of the reefs permits rejection of the origin of the blue holes as subadjacent karst dolines. An origin as dolines of the rising spring basin type (Maksimovich & Goloubeva, 1952) can be rejected because the blue holes are very much larger than known hollows of this kind, e.g. at the Blue Waterholes, Cooleman Plain, NSW



Figure 8. A. *Acropora* and *Seriatopora* rubble at depths down to 7 m in Molar blue hole.



B. Rubble with greater amounts of sand at around 12 m.



C, D. A 45° slope; *Acropora*, and massive *Porites* scattered over a rubbly/sandy bottom. About —13 m in Molar blue hole.



E. Sand/mud bottom at —20 m, with crab hole Molar blue hole.

F. Scattered interspersed corals at —20 m. Molar blue holes.

(Jennings, 1972). Subsidence dolines, i.e. the progressive removal from below of unconsolidated covering sediments down solution pipes in the reef limestone, calls for the presence of such covers elsewhere in the reefs, at least as remnants, and of this there is no evidence. The same kind of argument applies also to alluvial plain dolines. There persists the choice therefore between solution dolines and collapse dolines.

Solution and collapse dolines

The distinction between solution and collapse dolines has not been made explicitly in previous studies of reef morphology; most workers have referred to terrestrial solution in a general way and broadly to sink-holes or sinks as a single category, e.g. Emery & others (1954), Newell & Rigby (1957). The major morphological features and genetic requirements of solution

<i>Solution doline</i>		<i>Collapse doline</i>
INITIAL STAGE		
<i>Cause</i>	Solution at rock surface	Collapse of cave roof, i.e. associated solution is subsurface
<i>Shape</i>	Funnel (conical)	Box-shaped, cylindrical
<i>Sides</i>	Soil covered or partly bedrock. Tending to 20-30° uniform slopes. Sometimes steeper antidip sides	Fractured rock walls, very steep (60°) to overhanging
<i>Floor</i>	Little or no floor, soil covered	Rockfall. Central rock pile or talus slopes below walls (dependent on shape of former cave chamber). If cave chamber partly water-filled, a cenote may result
<i>Plan</i>	Circular or oval	Angular where rock strong; rounded where rock weak
<i>Relation to Caves</i>	Frequently only embryonic cave tubes below; possibly fissure or shaft to cave passage through undisturbed bedrock	Flanking cave remnants usually survive below; sometimes entrance through rockfall
<i>Occurrence</i>	Commonly in fields and associated in complex depressions. May occur singly or in chains	Isolated or several in a chain. Not in fields
LATER STAGE		
(1) <i>Removal of insolubles matching enlargement</i> Retains funnel shape. Connection with cave below more likely and more open; minor rockfall possible	(2) <i>Removal of insolubles failing to match enlargement</i> Becomes basin or dish-shaped. Parallel slope retreat accompanied by floor enlargement through soil and debris accumulation. Swamp or pond may develop. No cave connection	Become basin or dish-shaped. Slopes weather back to 20-30° and become partly or wholly soil-covered. Soil and fine debris conceal and flatten rockfall floor. Plan loses any initial angularity. Connection with cave remnants lost. No change to occurrence
Additional neighbouring dolines may develop; increasing likelihood of intersection of enlarging depressions		

Table 2. Summary of characters of solution and collapse dolines.

and collapse dolines are shown in Table 2. By applying the criteria in this table to the published accounts of modern reef morphology from many areas, solution dolines seem unquestionably the originator of modern morphology in the Bikini and Enewetak lagoons (Emery & others, 1954), on parts of the lagoon of Maroro reef of New Georgia (Stoddart, 1969) and both onshore and offshore in the Yucatan Peninsula (Purdy, 1974); however, collapse dolines seem just as surely to represent the original mechanism for the formation of Jordan's Florida Blue Holes (1954), and Stoddart's Lighthouse Reef Blue Hole off Belize (Stoddart, 1962), a conclusion supported by more recent studies (Dill, 1977). From the length, width and depth of seventeen blue holes in the Bight of Acklins in the southeast Bahamas (published in Doran, 1955), it is evident that some are collapse dolines, though others may be solution dolines.

Though the Queensland blue holes are partially infilled with recent sediments, their origin by collapse processes seems likely for the following reasons:

1. The isolation of the blue holes within the large (140 km x 85 km) Pompey Complex. Collapse dolines arise from large chambers and there are generally few in extensive systems of cave passages.
2. The slopes of the Cockatoo blue hole, generally 45-70° at the present time, are more likely to be due to collapse than to surface solution. The lesser slopes (30°-60°) of the Molar blue hole cannot be categorically attributed in this way. However, such a conclusion is strengthened when it is appreciated that the constructional modern slopes have decreased the original slope angles.
3. While the roundness in plan of the Queensland blue holes fits a solution doline mode of formation more easily, circular structures of undoubted collapse origin occur frequently, e.g. in the Gambier

Limestone of South Australia, and on the Anatolian Plateau near Konya. These examples and others like them, occur in mechanically weak, often Tertiary limestones. Moreover, initial irregularities in outline would have tended to be smoothed by Holocene sediment and reef growth in the Queensland holes.

In spite of these arguments, it should be appreciated that there is a significant difference in the relation of the two holes to their nearby rims. The Molar Reef hole lies to one side of the reef mesh defined by the rim pattern; the two features appear only accidentally associated. This suggests that the rim is based on a divide around a solution doline, within part of which a smaller collapse doline has opened up. On the other hand, the rim around the Cockatoo Reef hole is related closely to the hole and bears no relation to the large reef mesh in which both are situated. Instead this rim is suggestive of an annular solution rampart around a collapse doline such as has been described from the emerged reefs of Okinawa (Flint & others, 1963). Solution ramparts develop where scarps or cliffs promote the formation of calcrete; differential lowering occurs away from them. The rise in the seismic discontinuity over the Cockatoo Reef blue hole rim fits in with this interpretation, that such a solution rampart was produced during past sea-level lows.

The processes of subterranean solution to form a large cavern, followed by collapse, and subsequent sub-aerial solution and modification, are unlikely to have occurred over the short period of the last glacial low sea level, i.e. 100 000 y. The formation of a large cave, and ultimately a blue hole, probably occurred over several low sea-level periods, collapse occurring in the final period of karst exposure in the last glacial.

Finally, in advocating a collapse doline mode of formation for the Queensland blue holes, we are aware that two questions arise: are young Quaternary Reef

limestones strong enough to support the wide roofs required to form large dolines, and where did the water come from to form large caves? Evidence from Western Australian caves shows that Pleistocene aeolian calcarenites have sufficient strength to support wide roofs because of case hardening, and we suggest that calcretisation, almost certain to have occurred during periods of low sea levels (Harrison, 1977; Harrison & Steinen, 1978), will have added to the strength of reef limestones. Also, Maxwell's (1968, fig. 22A) map of pre-Holocene drainage on the shelf suggests that the area of the Pompey Reefs was bypassed by major streams. We are, however, uncertain how far back in the Pleistocene such a drainage pattern originated, and in any case the reef area itself is quite substantial as a catchment (12 000 km²). On balance neither the age seriously damages our advocating collapse processes seriously damages our advocating collapse processes for the formation of the blue holes.

Conclusion

Despite the interest that blue holes excite, adequate accounts of them are rare. The most notable exception is the Lighthouse Reef blue hole off Belize which has been shown to be an undoubted collapse doline, only slightly modified after submergence (Dill, 1977). The detail of the present investigation delineates two cases where sedimentation since drowning has greatly obscured their original character, thus placing them at the opposite end of the scale from the Lighthouse blue hole where the preservation of original features makes a collapse origin absolutely certain. However, we feel that the balance of evidence indicates that the Queensland blue holes have also formed by this mechanism.

The extensive blanket of sediment probably conceals, at least in the case of the Molar Reef hole, the effects of significant surface weathering of collapse doline form prior to submergence. Both Molar and Cockatoo seem likely to be older than both the Lighthouse Reef hole and certain of the Bahamas holes for which some detail is available. The likelihood that the Cockatoo Reef rim has grown on a solution rampart reinforces this inference.

A distinction has been drawn here between the blue holes and the patterns of ridge and large shallow depressions, which constitute most parts of the reefs in which they are situated. The patterns are thought to represent fields of solution dolines, but it was not our objective to muster evidence to establish this. This interpretation, however, can be said to be consistent with the antecedent karst hypothesis, whereas we believe that the blue holes provide firm evidence of substrate control of Holocene Reef growth—that substrate being formed by karst processes.

Acknowledgements

The authors wish to acknowledge encouragement and support from the Australian Institute of Marine Science and the Australian Groundwater Consultants Pty Ltd. Dr J. Veron aided in the verification of coral taxonomy. The research was substantially funded by the Australian Research Grants Committee.

References

AGASSIZ, A., 1894—A reconnaissance of the Bahamas and the elevated reefs of Cuba in the steam yacht *Wild Duck*, January to April 1893. *Harvard University Museum, Zoological Bulletin*, 26(1).

- BENJAMIN, G., 1970—Diving into the Blue Holes of the Bahamas. *National Geographic Magazine* 138, 347-63.
- DILL, R. F., 1977—The Blue Holes—geologically significant sink holes and caves off British Honduras and Andros, Bahama Islands. *Proceedings of the Third International Coral Reef Symposium, Miami*, 2, 238-42.
- DORAN, E., 1955—Land forms of the Southeast Bahamas. *University of Texas Publications* 5509, 1-38.
- EMERY, K. O., TRACEY, J. I., & LADD, H. S., 1954—Geology of Bikini and nearby atolls. *United States Geological Survey, Professional Paper* 260-A.
- FLINT, D. E., CORUNI, G., RINGS, M. G., FULLER, W. P., MACNEIL, F. S., & SAPLIS, R. A., 1963—Limestone walls of Okinawa. *Geological Society of America Bulletin*, 64, 1247-60.
- HARRISON, R. S. 1977—Caliche profiles: indicators of near-surface subaerial diagenesis, Barbados, West Indies. *Bulletin of Canadian Petroleum Geologists*, 25, 123-73.
- HARRISON, R. S., & STEINEN, R. P., 1978—Subaerial crusts, caliche profiles and breccia horizons; comparisons of some Holocene and Mississippian exposure surfaces, Barbados and Kentucky. *Geological Society of America Bulletin* 89, 385-96.
- JENNINGS, J. N., 1967—The surface and underground morphology. In DUNKLEY, J. R., & WIGLEY, T. M. L. (Editors). *Caves of the Nullarbor*, 13-31 *Speleological Research Council, Sydney*.
- JENNINGS, J. N., 1971—KARST. *Australian National University Press, Canberra*.
- JORDAN, G. F., 1954—Large sink holes in the Straits of Florida. *American Association of Petroleum Geologists Bulletin*, 38, 1810-17.
- MAKSIMOVICH, G. A., & GOLOUBEVA, L. V., 1952—Генетические типы карстовых ворохов. *Doklady Akademii Nauk SSSR*, 87, 653-655 (Types génétiques d'entonnoirs karstiques. *Translation C.E.D.P. No. 647, by S. Ketchian*).
- MAXWELL, W. G. H., 1968—ATLAS OF THE GREAT BARRIER REEF. Elsevier, Amsterdam.
- MAXWELL, W. G. H., 1970—Deltaic patterns in reefs. *Deep-Sea Research*, 17, 1005-18.
- MAXWELL, W. G. H., 1976—Book Reviews—Reefs in Space and Time. *Marine Geology*, 20, 77-84.
- MIOTKE, F. D., 1973—Der Karst in zentralen Kentucky bei Mammoth Cave. *Jahrbuch Geographisches Gesellschaft Hannover*, 360 p.
- MISTARDIS, G., 1968—Investigations upon influences of sea level fluctuations on underground karstification in some coastal regions of south Greece. *Fourth International Congress of Speleology*, 3, 335-40.
- NEWELL, N. D., & RIGBY, J. K., 1957—Geological studies on the Great Bahama Bank. *Society of Economic Palaeontologists and Mineralogists, Special Publication* 5, 15-72.
- NORTHROP, J. I., 1890—Notes on geology of Bahamas. *Transactions of the New York Academy of Science*, 10, 4-22.
- PURDY, E. G., 1974—Reef configuration. cause and effect. *Society of Economic Palaeontologists and Mineralogists, Special Publication* 18, 9-76.
- QUINLAN, J., 1972—Outline for a genetic classification of major types of sinkholes and related karst depressions. *International Geography*, 1, 58-60.
- SACHET, M. H., 1962—Geography and land ecology of Clipperton Island. *Atoll Research Bulletin* 86.
- STODDART, D. R., 1962—Three Caribbean atolls: Turneffe Islands, Lighthouse Reef and Glover's Reef, British Honduras. *Atoll Research Bulletin*, 87, 151.
- STODDART, D. R., 1969—Geomorphology of the Marora elevated barrier reef, New Georgia. *Philosophical Transactions of the Royal Society*, B255, 383-402.
- WHARTON, W. J. L., 1898—Note on Clipperton Atoll (northern Pacific). *Quarterly Journal of the Geological Society of London*, 54, 228-9.

Mineralogy and chemistry of weathered and parent sedimentary rocks in southwest Queensland

B. R. Senior

Weathered profiles and parent rocks in the Queensland part of the Eromanga Basin were investigated using geochemical and clay mineral techniques. Approximately 170 rock samples were analysed and 65 thin sections described from Winton and Eyre Formations, Morney profile, Canaway profile, Curalle silcrete profile and Haddon silcrete. Rock samples were obtained by shallow stratigraphic core-drilling and from measured outcrop sections. The results obtained show marked differences, between the parent rocks and weathered profiles, and in some instances demonstrate gradational compositional changes within profiles.

The Winton Formation contains montmorillonite with lesser amounts of kaolinite, illite, randomly interstratified clays and chlorite. Weathered profiles developed on it (Morney and Canaway profiles) contain kaolinite and lesser illite. The quartzose Eyre Formation is kaolinitic except for the upper part, in which small amounts of montmorillonite occur. Silcrete developed on this formation (Curalle silcrete profile) and subsurface silcrete (Haddon silcrete) are chemically similar and contain kaolinite, illite, and small quantities of montmorillonite.

Silica-enriched zones of all profiles examined show evidence of slight enrichment of titanium.

Introduction

The literature contains few quantitative clay mineral or geochemical data for weathered Cretaceous and Tertiary sedimentary rocks of the Eromanga and Lake Eyre Basins (Fig. 1), with the exception of chemical analyses of silcrete (*in* Langford-Smith, 1978). The analysis of relatively homogeneous rocks such as silcrete pose few sampling problems, whereas the heterogeneous materials which constitute the bulk of weathered rocks are more difficult to sample, because of poor exposure and problems of inhomogeneity. A technique is discussed later which largely overcomes the sampling problem.

Gregory & Vine (1969) reported on clay mineral and major element contents of weathered Winton and Eyre Formation rocks from a cored drillhole (BMR Canterbury 1). They found a reduction in the amount of montmorillonite upwards, and their major element analyses showed variation between interbedded rock types rather than zonation which might be expected from a weathered profile.

Dury (1969) included eight analyses of weathered rocks from widely separated localities in the Eromanga Basin and used them in his schematic chemical classification of duricrusts (Fig. 2). With one exception his weathered rocks lie within the fields determined in this paper for southwest Queensland weathered profiles.

The regional homogeneity of silcrete in southwest Queensland was determined by Senior & Senior (1972); the similarity between it and silcrete developed on a granite inlier north of Hungerford was discussed by Watts (1975), and Senior *in* Langford-Smith (1978).

Objectives of the analytical study

This study was aimed at complementing research into the origin, age, and distribution of weathering profiles, and their relation to landform evolution in southwest Queensland (Idnurm & Senior, 1978; Senior & Mabbutt, *in prep.*). The aims of the analytical work were to identify changes in the mineralogy and geochemistry of clays associated with weathering of various rock types, and to investigate the relationships between

the deeply weathered Cretaceous sedimentary rocks and silcrete beds in the overlying Tertiary quartzose rocks.

Methods

Clay and major-element analyses were undertaken on samples from measured sections and drill core. The problem of collecting representative samples for analyses from inhomogeneous weathered rocks was largely overcome by collecting regularly spaced samples from the bottom to the top of measured sections. Between 4 to 6 pieces of rock each weighing approximately 500 g, were collected from a zone about 1 m in diameter at each sample site. Samples were collected in this manner at about 3 m intervals and sealed in plastic bags. Material with surface coatings of sesquioxides was avoided by cleaning off 1 to 5 cm of the rock surface with a pick. The samples were later coarsely crushed and divided into two fractions, one for analysis and the second for reference. Other samples were collected for thin-sectioning.

Individual measured sections posed particular sampling problems, as it was not always possible to collect regularly. The effect of sampling at irregular and regularly-spaced intervals is discussed later.

Drill cores were scraped and washed to remove drilling mud and packaged in plastic tubing. The core was later slabbed, and one half of the core crushed and divided in the manner previously described.

Clay minerals were identified using X-ray diffraction. Major elements, with Zr and Ba, were determined by X-ray fluorescence. Trace elements Cr and V were identified using atomic adsorption spectroscopy. The majority of the clay and geochemical analyses were made by Dr R. N. Brown, D. C. Bowditch and P. R. Robinson of the Australian Mineral Development Laboratories (AMDEL). These analyses are contained in report Nos. AN1582/67, MP2691/74, AN2691/74, MP3716/74, AN3470/75 and AN5774/72 and are available for reference at the BMR. The geochemical work was supported by petrographic investigations; some clay and authigenic minerals in thin section which could not be identified optically were extracted and X-rayed using the powder-film method as described by Berry & Mason (1959, Appendix A).

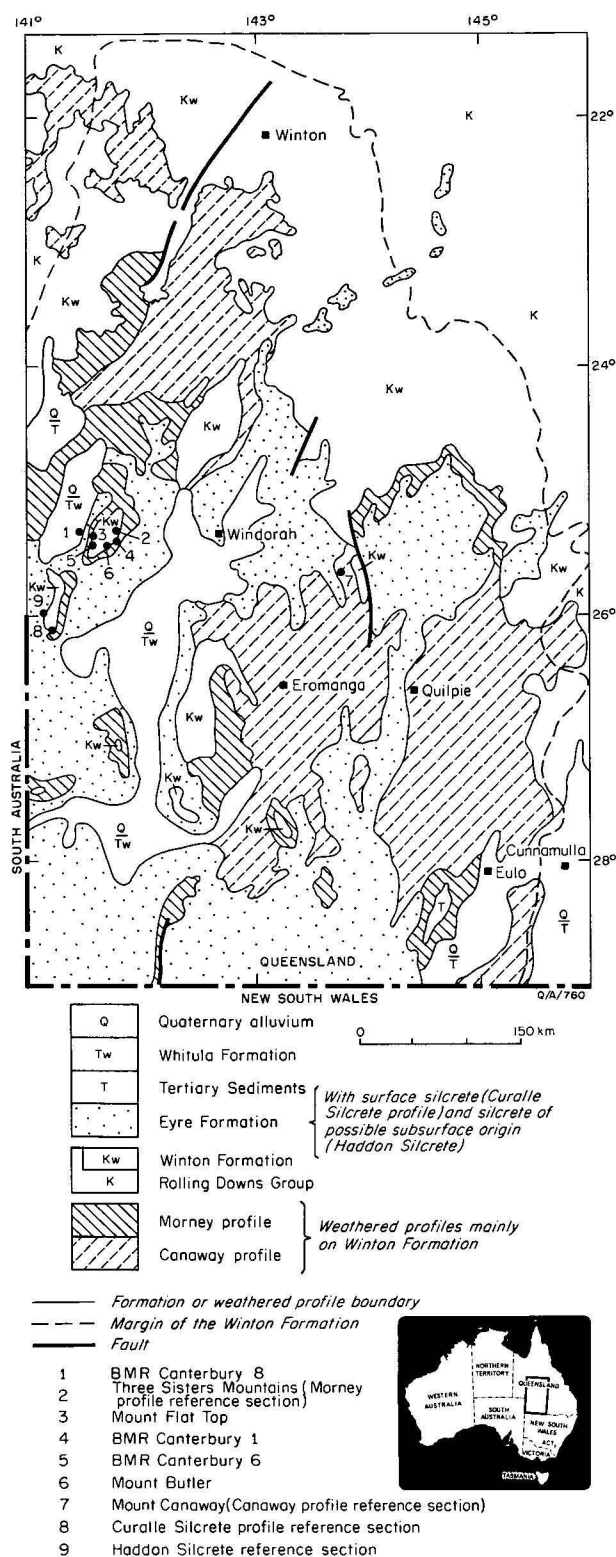


Figure 1. Generalised geological map and distribution of weathered profiles in southwest Queensland.

Examples of X-ray diffractometer traces are included in Figure 3 (Samples 26/1 and 2). Montmorillonite was identified by the change in value and position on glycolation, and in glycolated samples appear at 17.7\AA . Illite first-order reflections occur at 10.1\AA and kaolinite at 7.1\AA . Randomly interstratified clays had no well-defined peak intensities, but rather a higher intensity background at low Bragg angles.

The abundance of clay minerals were estimated by AMDEL in semiquantitative terms as follows:

Dominant. Used for the most abundant component, regardless of its probable percentage level; **Sub-dominant.** The next most abundant component(s) providing its (their) percentage level is between about 20 and 50%; **Accessory.** Components judged to be present between about 5 and 20%; **Trace.** Component judged to be below 5%.

The classification of arenites used in the petrographic descriptions is that of Packham (1954). Grainsize and class terms are those of Wentworth (1922), and roundness values were determined visually from Krumbein & Sloss (1963). Mineralogical percentages are estimates, and have probable accuracy of about 5 percent.

Most weathered rocks examined contained abundant cement and/or matrix (Table 2). The cement is expressed as a percentage where it is a precipitate filling interstices between the allogenic clastic fraction. Calcite cement is estimated separately, and appears in the composition column.

The term matrix is used for very fine clastic particles in the groundmass in which larger grains are situated. Feldspar clasts which have been altered to clay, but retain grain textural characteristics of the parent rock, appear in the rock fragment column.

An index of symbols used in the Figures is given in Table 1.

Geological framework

Winton Formation and its weathered profiles

The Winton Formation supports two weathered profiles, namely the Mornay and Canaway profiles. The profiles are defined in Senior & Mabbutt (in prep.); their distribution in the vicinity of Haddon Corner, Queensland, is shown on a geologic and geomorphic map at 1:250 000 scale (Senior, 1976).

The Mornay profile formed during a period of deep weathering, which occurred during the Maastrichtian to early Eocene (Idnurm & Senior, 1978) and consists of up to 95 m of kaolinised sediments. All well-exposed sections of this profile can be subdivided into three main zones of roughly equal thickness (Fig. 4). Above the zone of partial alteration lies a ferruginous zone where the kaolinitic rocks are cemented by iron oxides and contain dense replacement ironstones in the form of lenses, beds and concretions. This zone is overlain by a vari-coloured kaolinitised zone, which also incorporates some rock types enriched in iron oxide. The uppermost zone is pale-coloured, generally lacks iron oxides, and is mainly composed of silicified kaolinitic rocks. The zones have gradational boundaries between them. In most areas the Mornay profile is truncated by erosion; frequently it underlies quartzose rocks of Cainozoic, mixed fluvial and lacustrine rocks of the Eyre Formation. The basal part of the Eyre Formation is often conglomeratic and contains clasts from the Mornay profile.

The Canaway profile developed during a second period of weathering, which spanned the Late Oligocene and Early Miocene (Idnurm & Senior, 1978). This profile is capped by crust of kaolinitic breccia impregnated with iron oxides, grading down through a zone of mottling into kaolinitic rocks of the unaltered Mornay profile (Fig. 5); less commonly the profile grades down into weathered Winton Formation. Senior & Mabbutt (in prep.) consider that this profile demar-

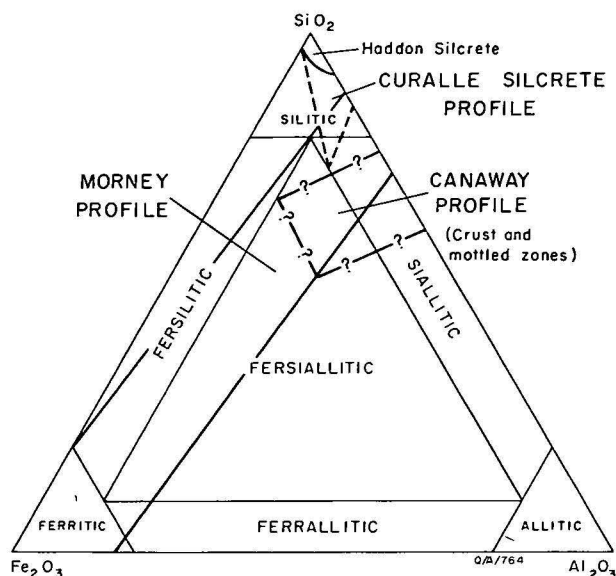


Figure 2. Ternary diagram using recalculated weight percentages of Si, Al and Fe oxides for various weathered profiles, compared with the weathered rock classification of Dury (1969).

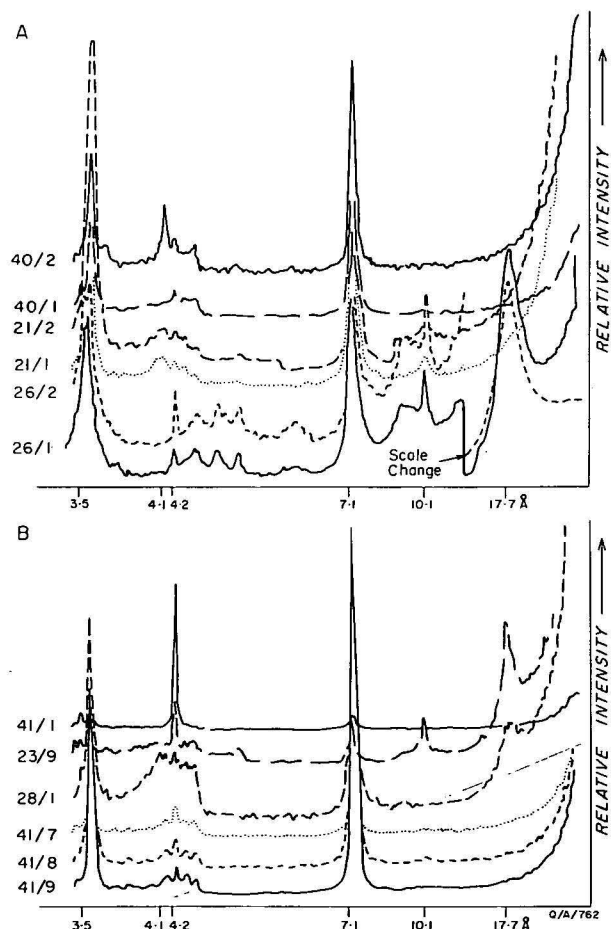


Figure 3. X-ray diffractograms of orientated clays from the Winton Formation (26/1-2), Morney profile (21/1-2), and Canaway profile (40/1-2). The diffractograms are of Mg^{++} saturated samples ($-2 \mu m$) treated with glycerol and air dried.

ates former interfluvies which remained free from burial by younger sediment cover. In such situations the Morney profile was partly eroded, prior to cementation which formed a duricrust up to 15 m thick.

Eyre Formation and its silicified parts

The Eyre Formation is distinguished by its quartzose nature—in marked contrast to the quartz-poor sedimentary rocks of the unconformably underlying Winton Formation. Textures, grain-size, and sorting of these quartzose sedimentary rocks vary, and reflect the complex fluvial and lacustrine environments in which it was deposited. Two forms of strongly silicified rocks occur in the Eyre Formation. The first is a surface-related duricrust, which consists of an upper blocky zone of columnar silcrete grading (by decreasing silicification) into a fragmental zone stained with iron oxides (Fig. 6). This disturbed zone is silicified in patches, and merges with underlying parent quartzose sandstone of the Eyre Formation. This profile was named Curalle silcrete profile by Senior & Mabbutt (in prep.), and is widespread in southwest Queensland, forming a capping to the majority of upstanding landforms. The profile has a relatively uniform thickness of about 6 m. In upwarped areas, where the parent rocks are frequently less than 6 m in thickness, the development of this profile has led to some disturbance of underlying kaolinitic rocks and to general silicification within the upper part of the underlying Morney profile.


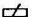






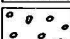



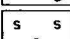



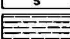


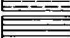



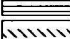







The second form of silicified rock in the Eyre Formation comprises single or multiple silcrete layers which are interbedded with unaltered quartzose sedimentary rock. This, the Haddon silcrete (Senior & Mabbutt, in prep.), has a restricted distribution and is mainly confined to the flanks of some linear cuesta-form ridges. Haddon silcrete crops out sporadically along the western limbs of the Curalle Dome, and the Morney Anticline (Fig. 7), and along the south limb of the Innamincka Dome (Senior & Senior, 1972). This silcrete does not have an underlying leached or disturbed zone, and is bounded by sharp contacts which usually accord with the bedding configuration of the enclosing strata.

Analyses of host and weathered rock units

Unweathered Winton Formation

The Winton Formation is widespread in the Eromanga Basin and occupies approximately 350 000 km² of the central axial zone of this basin in Queensland (Fig. 1). It thickens to 1100 m in the centre of the basin near Windorah township. Exon & Senior (1976) consider that it was mainly derived from an andesitic volcanic terrain. Rock types include lithofeldspathic or feldspatholithic sandstones, interbedded with siltstones, mudstones and claystones. Most rock types are poorly indurated and contain abundant montmorillonite. Concretions and platy calcareous rock types crop out, but estimates from lithological logs of drill holes show that these comprise less than 2 percent of the sequence.

Several drill holes were drilled into the Winton Formation to investigate the range of rocks and to provide cores of unweathered rock on which a comparison with the weathered profiles could be based. BMR Canterbury 6 was drilled entirely within this formation to a depth of 142 m (Fig. 8), and established the presence of interbedded feldspathic or lithic arenites, siltstones, mudstones, and claystones which are carbonaceous or

LITHOLOGY	BED THICKNESS	BEDDING STRUCTURE	
 Sandstone	 Very thick > 120 cm	 Bioturbation	 Cross stratification (group)
 Pebbly Sandstone	 Medium 5-60 cm	 Concretions ferruginous	 Scour and fill
 Conglomerate	 Thin 1-5 cm	 Slickensides	 Slumped
 Siltcrete	 Laminate < 1 cm	 Mudclast (rounded)	 Remnant bedding trace
 Siltstone	40/2 Sample number	 Mudclast (angular)	 Joints or cracks
 Mudstone	 Geochemical sample	 Parallel lamination	 Mottled
 Ferruginous layers	 Geochemical sample and thin section	 Cross stratification (solitary)	 Fe Iron mineral
 Limestone or Calcareous Sandstone			 Si Silica
 Lignite			
 Unconformity			

DRILLING DATA

Cored interval and recovery

2

CLAY MINERALOGY

Dominant

Subdominant

Accessory

Trace

>50%

20-50%

5-20%

<5%

K

M

I

R

C

K Kaolinite

M Montmorillonite

I Illite

R Randomly interstratified clays

C Chlorite

Q/A/772

Table 1. Index of symbols used on figures.

calcareous in part. Featureless wireline logs (Fig. 8) are characteristic of this formation (Senior & others, 1978) and indicate uniform composition with relatively small lithological variations.

The calcareous arenites from drill holes and outcrop were thin sectioned (Table 2): the average mineralogical composition is 11% quartz, 14% feldspar, 26% andesitic rock fragments, 5% accessories (mainly opaque iron minerals, iron pyrite, hornblende and biotite), 4% matrix and 39% calcite. The abundance of montmorillonite and lack of induration prevented the manufacture of satisfactory thin sections of the non-calcareous rock types. However, petrological examination of disaggregated arenites verified the abundance of feldspar and lithic fragments in these rocks.

Clay minerals. X-ray diffraction results show that the dominant clay mineral in the unweathered Winton Formation is montmorillonite (Table 3), which accounts for more than half of the total clay content. There are lesser amounts of illite, kaolinite, and randomly interstratified clays with no normal basal X-ray reflections. Traces or accessory amounts of chlorite were identified in 5 out of a total of 17 samples (Fig. 8, samples 26/1-3 and 26/10-11; Table 1).

In a few places, such as in the zone of partial weathering where a diffuse boundary separates weathered from unweathered rock, kaolinite is dominant (Fig. 7, Sample 28/3; Table 3, Samples 27/14 to 16). Estimates of the clay content of the Winton Formation are given in Table 3 and in Figure 8. These estimates include a small proportion of non-phyllosilicate minerals of less than 2 microns. Lutites contain 19 to 52% and the arenites 9 to 21 'clay'.

Major elements. These data are summarised in Table 4. Included are nine non-calcareous rock types, which are broadly similar in composition and, for comparison, two calcareous rock types. The latter comprise less than 2 percent of the total volume of the Winton Formation and comprise lithic or feldspatholithic sandstones and impure limestones. The arenites and lutites are not significantly different in terms of major elements at the 2 percent level, indicating that the non-calcareous rock types, regardless of grain size, are similar in composition.

Trace elements. Three samples (0044/1,2,3) from lutite beds were selected and analysed for Cr, V, Ba, and Zr from BMR Canterbury 6 (Fig. 8) drill core. These samples analysed indicate that through the ver-

tical distance of 85 m the lutites of the Winton Formation show little variation in trace element content (Table 4).

Morney profile

Clay mineralogy. The dominant clay mineral in the Morney profile is kaolinite (Tables 2 & 3). In many of the samples kaolinite was the only clay present, although traces or accessory amounts of illite may also occur. Montmorillonite occurs near the base of the profile where the degree of chemical alteration diminishes over the interface (observed in cores 24 to 29 in BMR Canterbury 1; Gregory & others, 1967) with the underlying unweathered Winton Formation (Table 3, sample 28/2). Gregory & Vine (1969) who analysed drill core from BMR Canterbury 1, noted the dominance of kaolinite in the Morney profile (their chemically weathered Winton Formation), but recorded sporadically dominant or sub-dominant montmorillonite throughout this profile. The reason for this contradiction may be due to contamination of their samples by bentonitic drilling mud.

At the Three Sisters section, traces of montmorillonite occur in the upper part of the profile; this occurrence is interpreted to be younger clay illuviated into the profile from the Eyre Formation (Fig. 4, samples 21/13-16). Apart from minor variation, the distribution of clay minerals within the profile is uniform and no changes were found corresponding to the gradational trizonal profile which is visually apparent in most field exposures.

Major elements. Evidence of zonation of major elements was obtained at the Three Sisters (Fig. 4) and Mount Flat Top sections (Fig. 9).

The Three Sisters section was sampled twice. Initially a series of sixteen samples (21/1-16) were collected at irregular intervals and the results obtained on major element analyses indicated some evidence of profile zonation, in particular a decrease in iron oxides upwards. At a later date the section was sampled in more detail to confirm and expand the results obtained (39/1-23), using methods described previously. Interbedded rock types at this site enabled an investigation of lithological effects, and alternate lutite and arenite samples were collected at regular intervals. In Figure 4 the samples with odd numbers are lutites, the even numbered samples are arenites. The cumulative percentage curves through the profile indicate that litho-

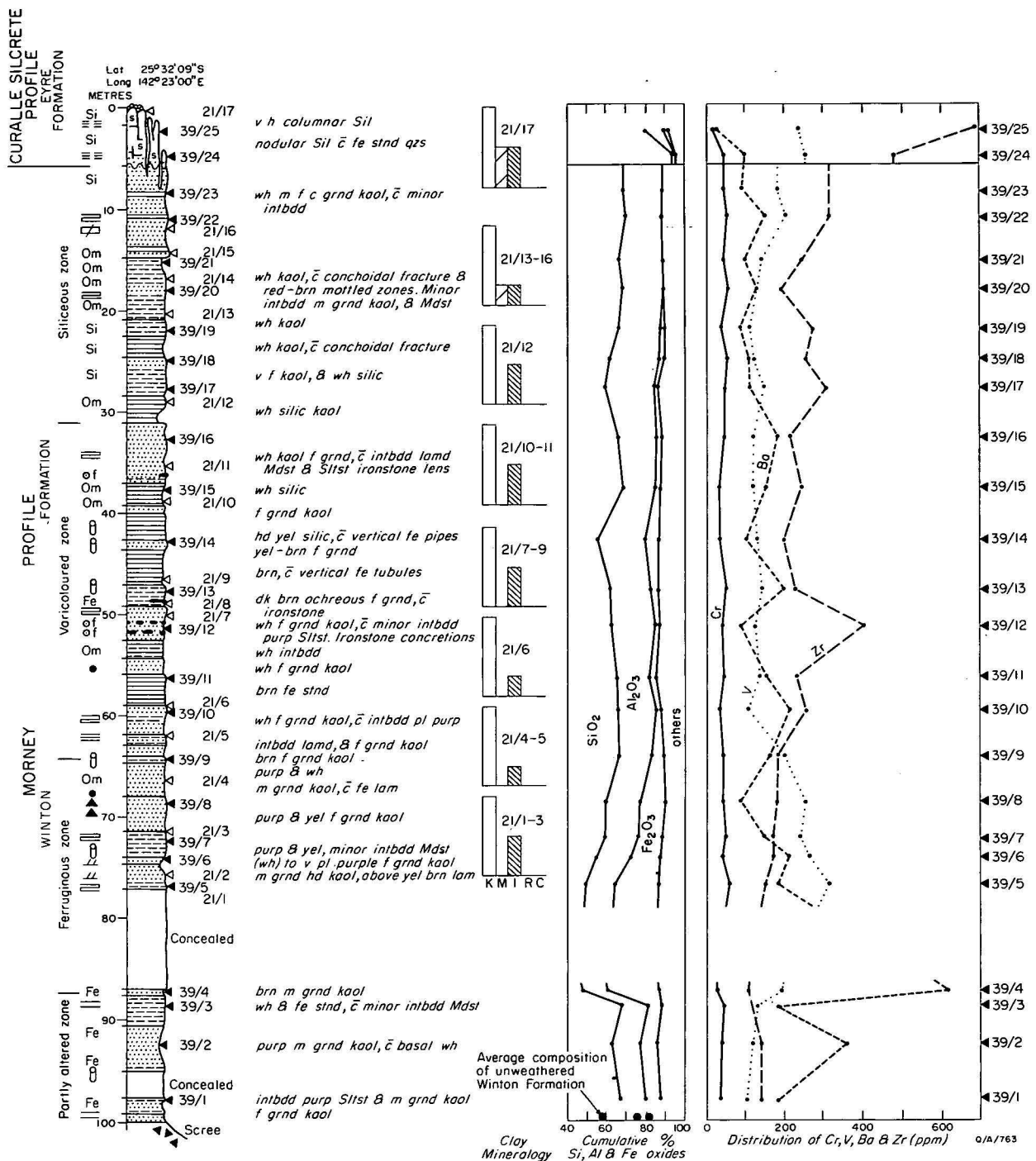


Figure 4. Reference section of the Morney profile at the Three Sisters Mountains, showing the distribution of clay minerals, major elements and trace elements.

logical effects are relatively minor, and compositional changes between the zones are gradational.

The Three Sisters reference section shows a gradual increase in silica and a small increase in alumina from about 87 m upwards. Iron oxides are abundant between 100 and 65 m, and diminish to about 1 percent or less above 20 m. The interval between 100 and 87 m does not fit with the concept of a zoned profile, and the composition within this interval is approaching that of the unweathered Winton Formation. The composition of unweathered Winton Formation (average of 9 analyses) is shown at the base for comparison (Fig. 4).

Ironstone rocks occur below 50 m and iron oxides increase with accompanying brown and purple colours towards the base of the profile. Dense brittle ironstones, which have a concretionary habit, most probably are replacing former calcareous horizons, because they occur in groups of similar size and frequency, as seen in the unweathered Winton Formation. The ironstones are composed of layered hematite and goethite, and usually contain greater than 60 percent iron oxides.

Ternary diagrams were constructed using recalculated weight percentages of Si, Al, and Fe oxides of all the profiles studied (Fig. 2). The Morney profile rock

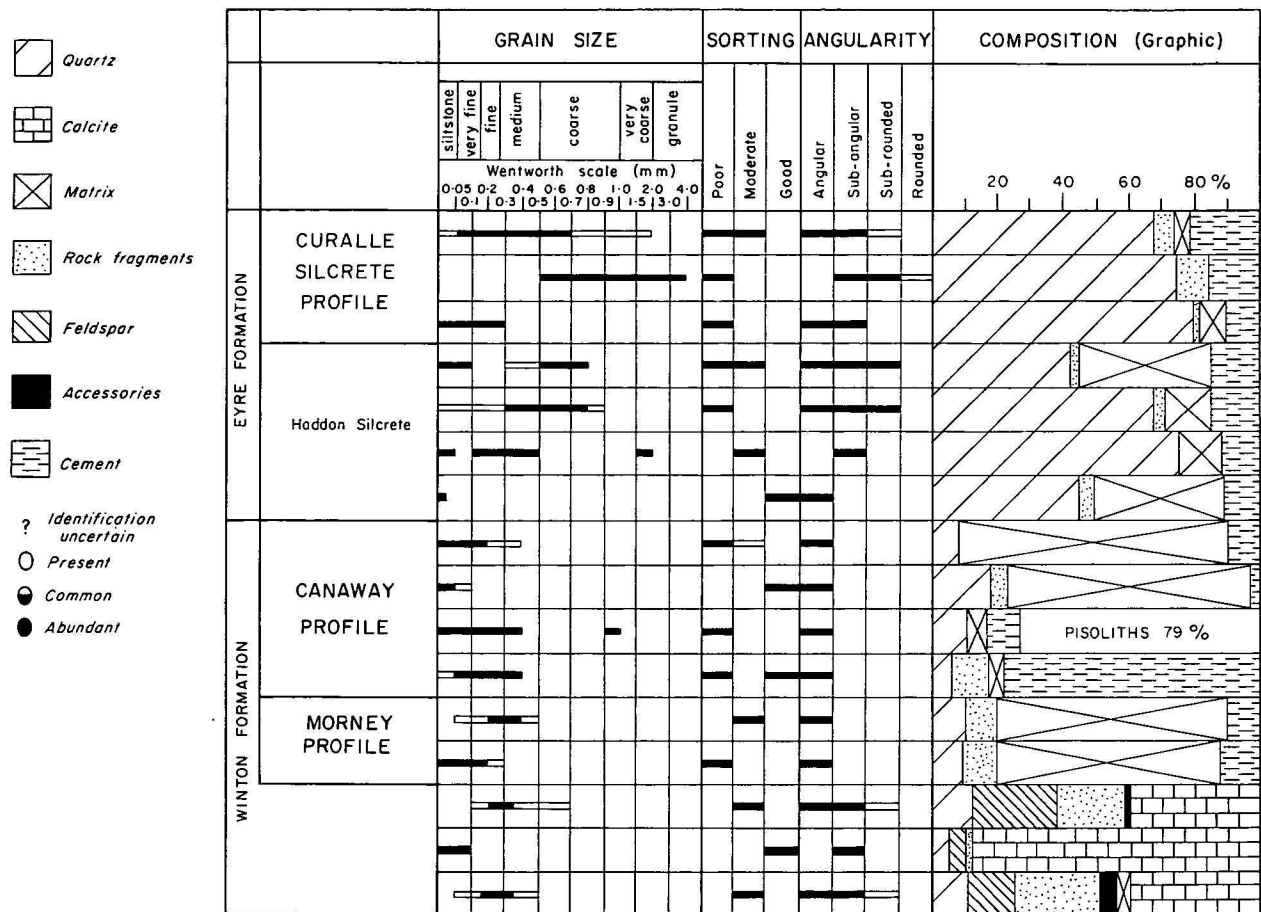


Table 2. Petrology of parent and weathered rocks (continues on facing page).

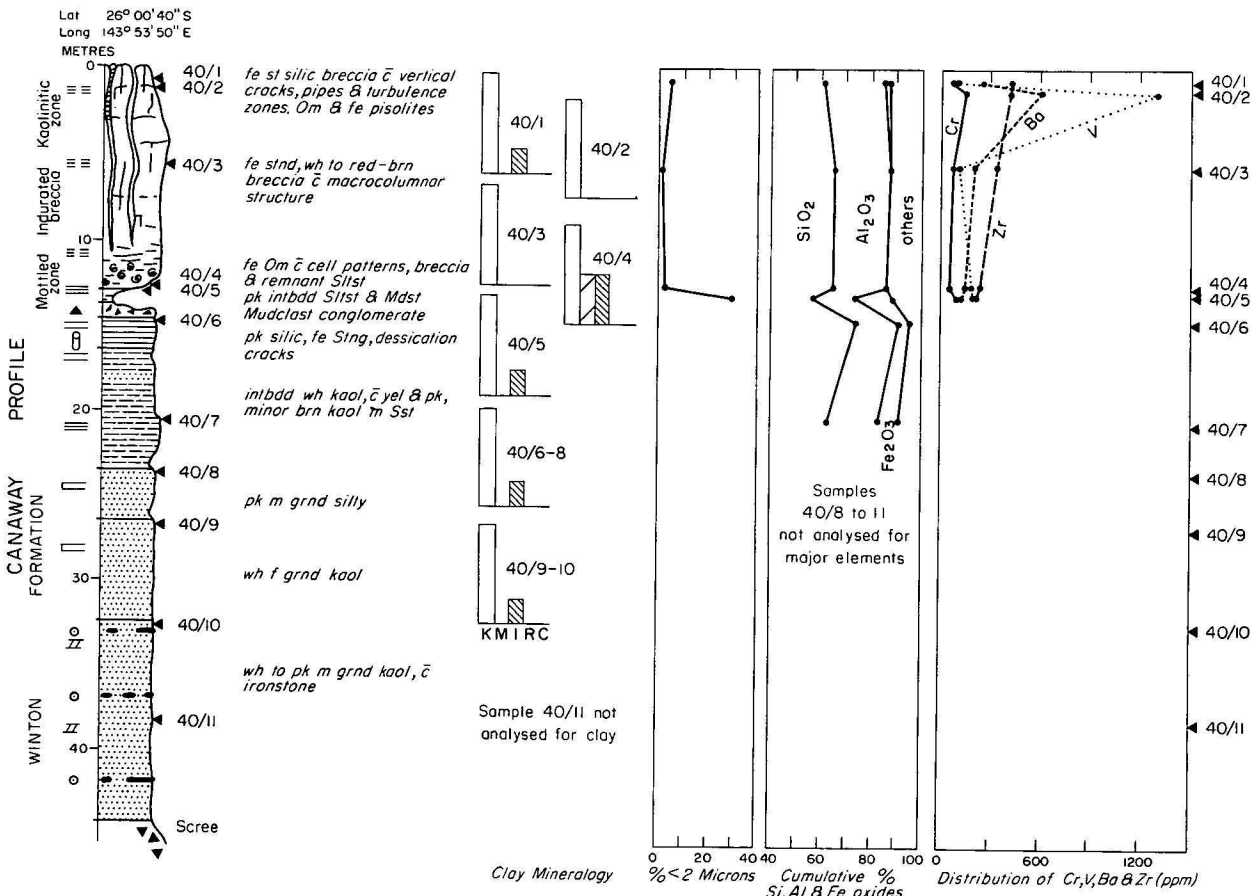
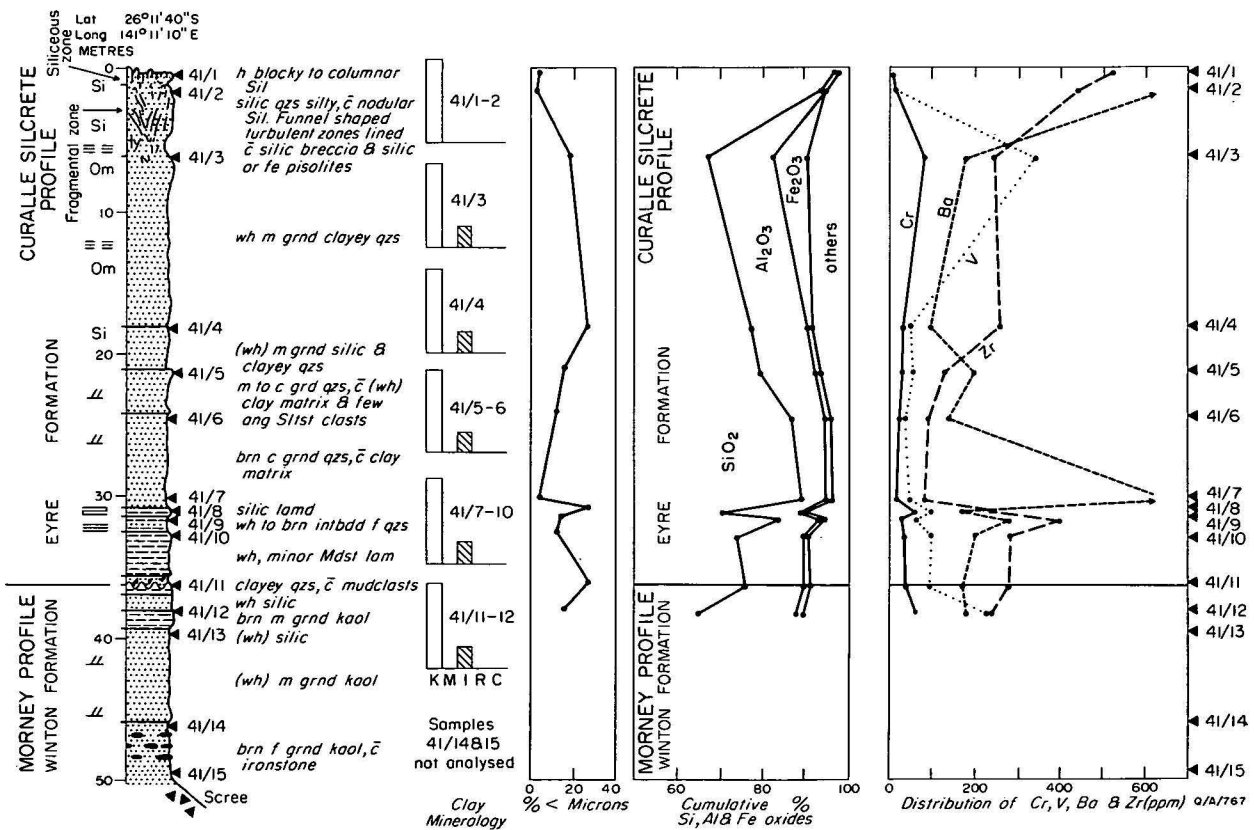


Figure 5. Reference section of the Canaway profile at Mount Canaway showing the distribution of clay minerals, major elements and four trace elements.

COMPOSITION %						FELD-SPAR	ROCK FRAGMENTS						ACCESSORIES						CEMENT				MATRIX				HEAVY MINERALS				ROCK NAMES								
Quartz	Feldspar	Rock fragments	Accessories	Matrix	Cement	Heavy minerals	Calcite	Plagioclase	Alkali	Quartz and chert	Quartzite	Schist	Sediment	Igneous	Silcrete	Muscovite	Biotite	Glauconie	Chlorite	Hornblende	Augite	Opalques	Chalcedony	Opaline silica	Titaniferous	Limonite	Quartz	Iron oxides	Chlorite	Kaolinite	Dickite	Montmorillonite	Tourmaline	Sphene	Zircon	Anatase	Monazite	(2) Number of thin sections examined	
69	6		5	20	0						●	○	●									○	●	●	○				●			?	?	○	○	?	Silicified quartzose sandstone (13)		
75	10			14	1						●		●										○	●	●	○							○		○		Silicified quartzose granule conglomerate (2)		
80	2		8	10									○											○		●								●			Ferruginous quartzose sandstone (1)		
42	3		40	15	0						○		○										○	●	○		●				●						Silicified silty-sandstone (2)		
68	0	3	0	14	15	0					○		○										○	○	○	●	●				●		○		○	○	○	Silicified quartzose sandstone (6)	
77				13	10																			○	●		○				●						Silicified concretionary sandstone (1)		
45	5		40	10							○												○	●			●				●						Silicified mudstone (2)		
8			83	9																						●		●			●				○			Kaolinitic silty-sandstone (3)	
18	5		74	3							○	○	●	○											●	○	●		●					○			Silty-ironstone (3)		
5			6	10																					●	○	●		●					○			Pisolithic ironstone (2)		
6	11		5	78											●										●	○	●		●									Concretionary ironstone (5)	
10	10		70	10							○		●										●	○	●	○	●	●	●	○					○	?		Kaolinitic sandstone (4)	
9		11	68	12							○										○	●		●			○		●	○				?				Kaolinitic silty-sandstone (3)	
12	26	20	2			0	40	●	●	○	○	?	○	●		?	●	○	○	●	○	○	○					○	?	○		●			○	○		Calcareous feldspatholithic sandstone (2)	
5	5	2				88	●	?	○	○	○	○	○					○				○		○								●						Silty or sandy-limestones (2)	
11	14	26	5	4			40	●	●	○	○		○	●			○	○	○	●	○	○						○		○		●							Calcareous lithofeldspathic sandstone (11)

QIA/TT0



types plot within a broad range in and between the ferritic and silicic zones of Dury (1969), demonstrating that a single name is unsuitable to define an entire profile.

Trace elements. Twenty-three samples were analysed for Cr, Ba, Zr, and V from the reference section of the Morney profile (Fig. 4). The curve for Cr is almost linear, and averages approximately 50 ppm through the entire Morney profile reference section. This concentration is about the same as the 55 to 65 ppm Cr determined from the parent Winton Formation. Obviously weathering had little effect on the distribution of this element.

Fluctuations in the curves of Ba, Zr, and V are apparently related to the lithologies encountered in the vertical plane of the section. However, sample 39/4 (Fig. 4) contains Ba in excess of 600 ppm, and reflects a zone of secondary enrichment. Nodules of barite crystals occur sporadically in the Morney profile (Senior, 1969). Outcrop and trace-element evidence indicates that Ba was mobilised and selectively re-deposited within the Morney profile during weathering.

The distribution of titanium oxide in the Morney profile (Fig. 10) shows a gradual increase upwards; the curve approximates the one showing the cumulative percentage diagram for silica (Fig. 4). Increasing titanium content accompanying increasing silicification is a well known phenomena in silcretes; the general abundance of amorphous and cryptocrystalline silica in the upper half of the Morney profile may be associated with slight titanium enrichment.

Canaway profile

Clay mineralogy. Kaolinite is usually dominant throughout the Canaway profile and may be accompanied by accessory or trace amounts of illite (Fig. 5). One sample (40/4, Fig. 5) from the reference section at Mount Canaway and two samples from Russell's open-cut opal mine (Table 3, 29/1-2), contain accessory or dominant montmorillonite. The presence of montmorillonite was surprising, as it is unlikely that any residual montmorillonite of the Morney profile would have survived a second phase of weathering. Possibly this clay is younger, derived by rainwash or aeolian activity, and was illuviated into the profile through the numerous joints and cracks which are abundant in the upper zone. Alternatively, the montmorillonite was introduced prior to and during weathering. The latter explanation is substantiated by field evidence, because the crustal zone has funnel-shaped structures which contain pisoliths (Table 2) and vertically aligned brecciated fragments. These structures, preserved by subsequent induration, terminate at the surface giving patterned ground features. Hallsworth & others (1955) consider that extensive seasonal drying, presence of swelling clay and high base exchange are requisites of patterned ground. Cellular patterns and slickensides within the crustal zone attest to former thrusting movements comparable to the formation of gilgai.

Major elements. Relatively few analyses were made (Fig. 5) and the results do not permit firm conclusions. The iron oxide content is low (1.2 to 1.5%), which agrees with the field evidence that the dark red-brown colour of the crustal zone is caused by films of iron oxides. However, zones of iron-oxide enrichment occur frequently in the form of irregular, diffuse or partly concretionary textured ironstones, several of

which were thin sectioned; the variation of rock types is recorded in Table 2. This material was sampled extensively by Idnurm & Senior (1978) during their palaeomagnetic study of this profile. One iron oxide enriched zone was analysed and contained 42.6 percent Fe_2O_3 , 38.7 percent SiO_2 and 14.15 percent Al_2O_3 .

Recalculated weight percentages of Canaway profile crust and mottled zone rocks partly overlap the Morney profile field on the ternary diagram (Fig. 2). However, insufficient data are available to define this profile geochemically with certainty.

Trace elements. The crustal zone is apparently enriched in Ba and Zr. Chromium is evenly distributed between 90 ppm at the base and 60 ppm at the surface (Fig. 5). The sample enriched in iron oxides (sample 40/2) is anomalously high in Cr, Ba, and V. Segregation of iron oxides appears to have been accompanied by selective enrichment of these trace elements.

Unweathered Eyre Formation

Wopfner & others (1974) reviewed the distribution of the early Tertiary quartzose sedimentary rocks of this region, and proposed the name Eyre Formation. Rock types include cross-bedded quartzose sandstone, sandy polymictic conglomerate, and sandy siltstone. Pebble clasts are most numerous at the base of the sequence, and consist of milky or grey quartz, red jasper, agate, black and red chert, and silicified wood. Considerable admixture of angular kaolinitic clasts occur above the unconformity with the underlying Morney profile (Fig. 6).

Because of variable grain-size, texture, and sorting in the Eyre Formation, few analyses were made and emphasis was placed in obtaining geochemical data for the silicified rocks (Curalle silcrete profile and Haddon silcrete) in this unit. This was done to demonstrate the nature of silicification processes which produced silcretes of uniform composition within this fine to coarse-grained quartzose arenitic sequence. For convenience analyses of the unweathered Eyre Formation are discussed with the individual silicified rocks.

Curalle silcrete profile

Clay mineralogy. Kaolinite is dominant and occurs either alone or in association with varying amounts of montmorillonite and traces of illite (Fig. 4, sample 21/17; Fig. 9, sample 23/9). The Eyre Formation has a similar assemblage, except that montmorillonite was not detected.

The silica-indurated zone of the Curalle silcrete profile, like the crustal zone of the Canaway profile, contains very low quantities of clay (average 3.2% from eight samples). The presence of minor amounts of montmorillonite in both profiles is noteworthy and strengthens the belief that both profiles developed contemporaneously (Senior & Mabbutt, in prep.).

Major elements. Analyses of silcrete from the Curalle silcrete profile are given in Table 4. The silicification process has led to an absolute enrichment of silica, which averages 96 percent. All other elements are depleted—with the exception of TiO_2 , which in most instances is present in amounts in excess of those normally found in sedimentary rocks. Silcretes with a high ignition loss (e.g. 39/25) contain more opaline silica and kaolinite.

The distribution of major elements in the reference section of the Curalle silcrete profile (Fig. 6) shows variation due to interbedded rock types. In particular the lutite bed (sample 41/8) gives a relatively low

Relative abundance of clay minerals in the Eyre Formation and its profiles

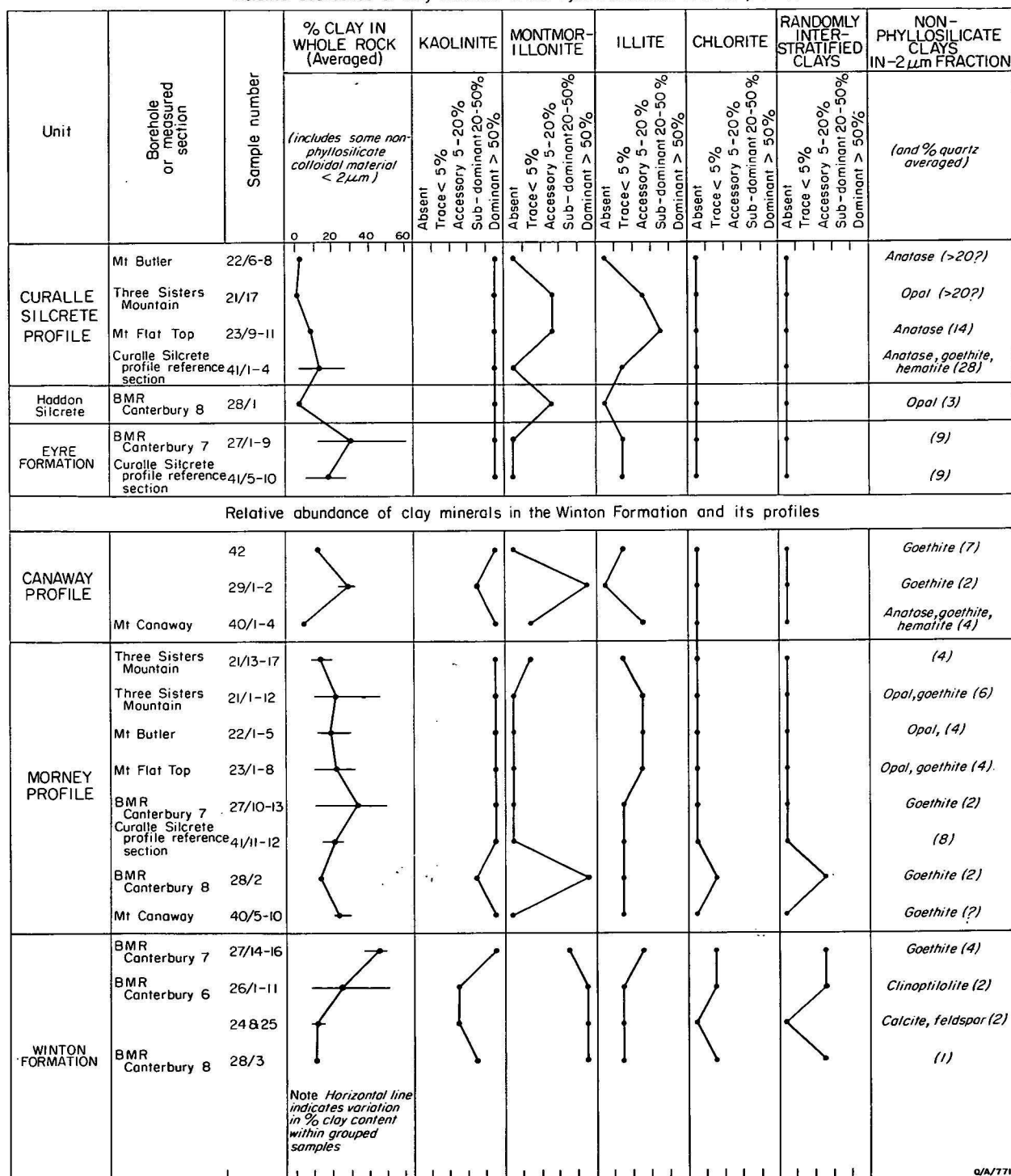


Table 3. Relative abundance of clay minerals in the Winton and Eyre Formations and their profiles.

silica value on the cumulative percentage graph. If this sample is ignored, on the basis that it is not typical of the arenitic Eyre Formation, several trends become apparent. The high alumina content at the base reflects incorporated Morney profile rock clasts and lutite material observed at and above the unconformity (Fig. 6). There is a noticeable drop in silica and an increase in iron and alumina oxides within the fragmental zone of the Curalle silcrete profile. Silica is apparently depleted below the silcrete layer; this supports the hypothesis of Stephens (1971), Smale (1973), and

Grant (1974) that silica released during weathering moves to the surface in groundwater and accumulates through evaporation. In the examples of the Three Sisters and Mount Flat Top sections (Figs. 4 & 9) the Eyre Formation is thin, the Curalle silcrete profile is superimposed on the Morney profile; silicification penetrated the unconformity between them, modifying the upper part of the older profile. In these examples the decrease in silica occurs several metres below the unconformity which separates the Winton and Eyre Formations.

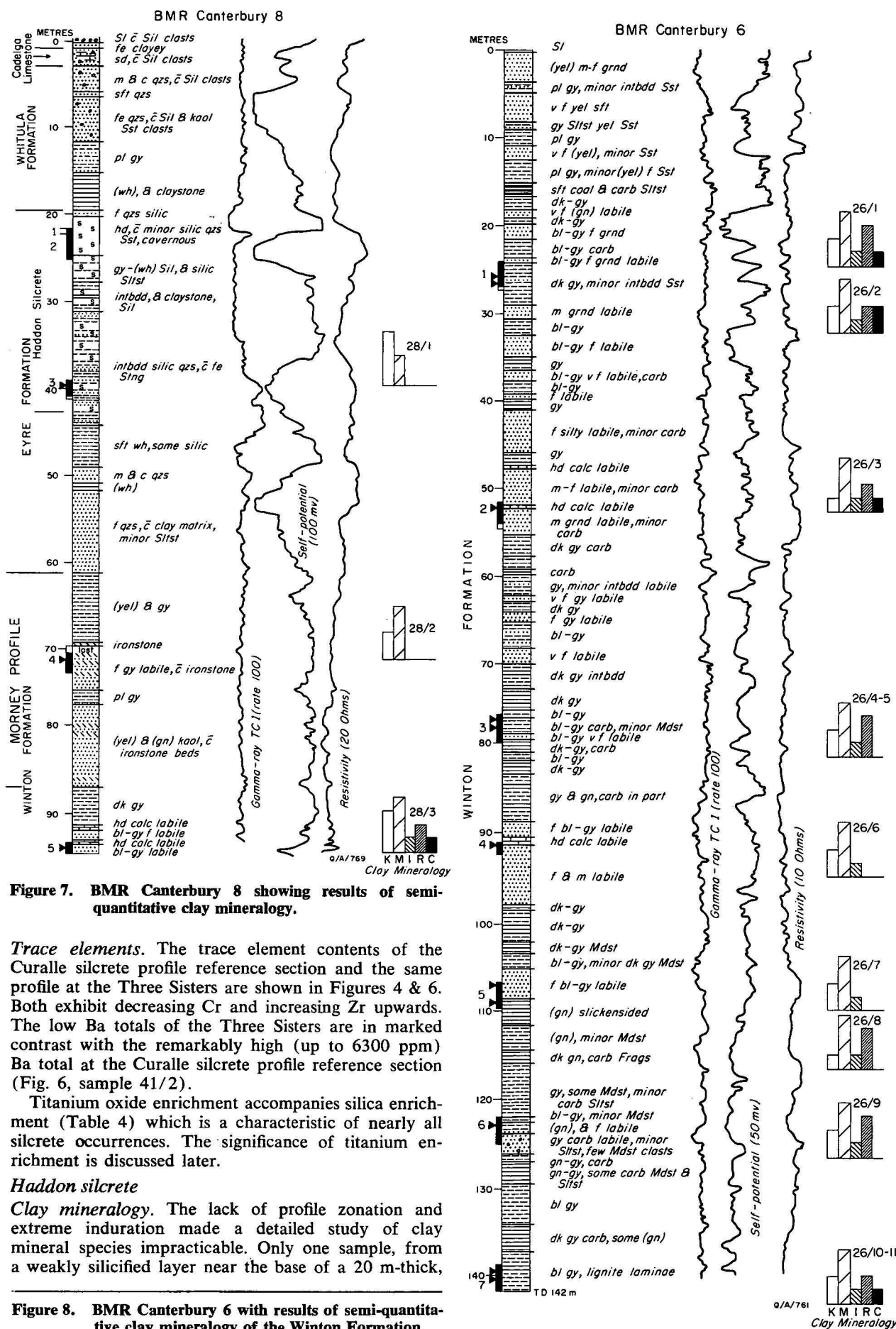


Figure 7. BMR Canterbury 8 showing results of semi-quantitative clay mineralogy.

Trace elements. The trace element contents of the Curalle silcrete profile reference section and the same profile at the Three Sisters are shown in Figures 4 & 6. Both exhibit decreasing Cr and increasing Zr upwards. The low Ba totals of the Three Sisters are in marked contrast with the remarkably high (up to 6300 ppm) Ba total at the Curalle silcrete profile reference section (Fig. 6, sample 41/2).

Titanium oxide enrichment accompanies silica enrichment (Table 4) which is a characteristic of nearly all silcrete occurrences. The significance of titanium enrichment is discussed later.

Haddon silcrete

Clay mineralogy. The lack of profile zonation and extreme induration made a detailed study of clay mineral species impracticable. Only one sample, from a weakly silicified layer near the base of a 20 m-thick,

Figure 8. BMR Canterbury 6 with results of semi-quantitative clay mineralogy of the Winton Formation.

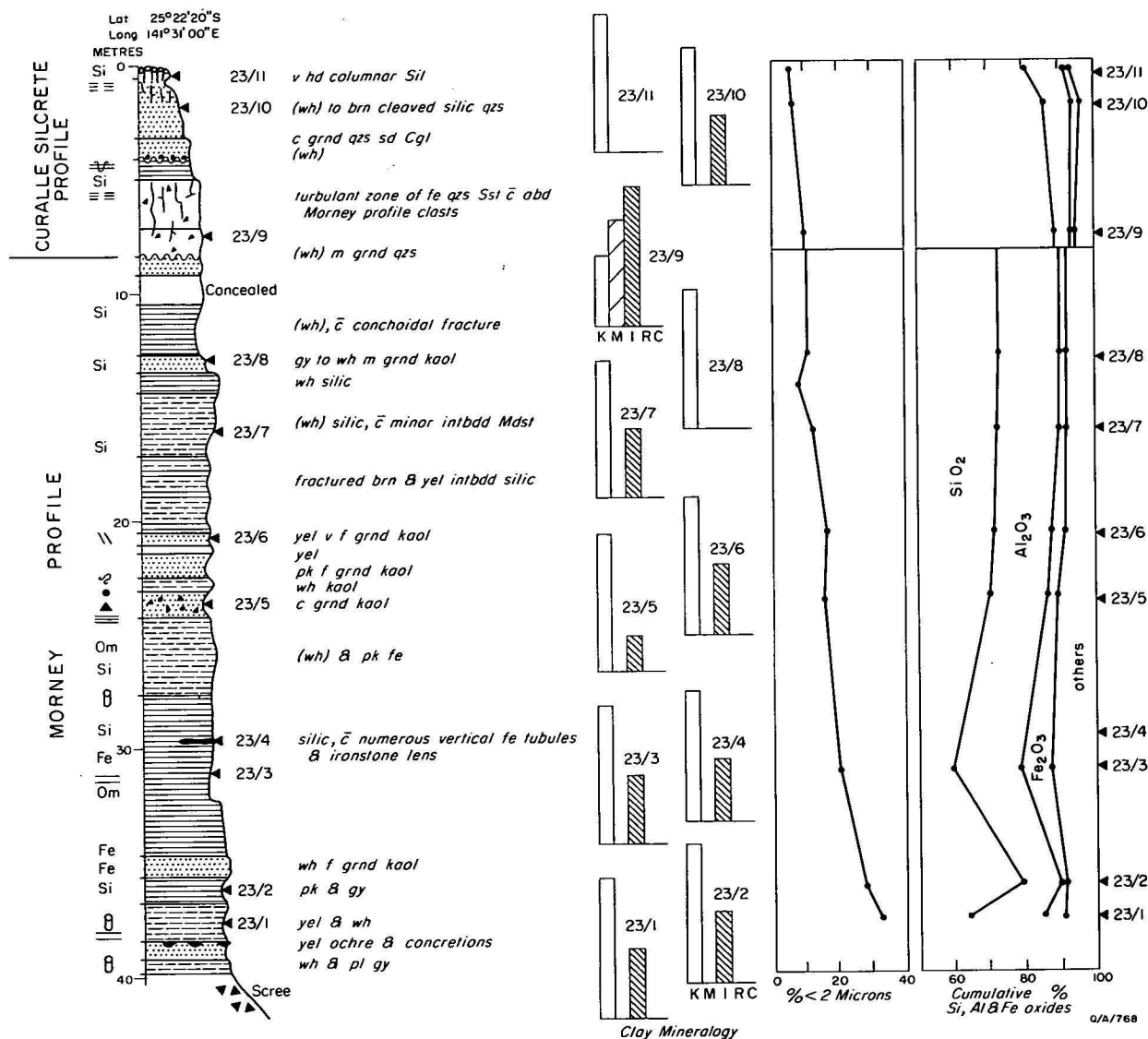


Figure 9. Morney profile and Curalle silcrete profile supplementary reference sections, showing the distribution of clay minerals and major elements.

dominantly silcrete sequence in BMR Canterbury 8 (Table 3 & Fig. 7, Sample 28/1), was analysed. The dominant clay mineral is kaolinite with accessory montmorillonite. Montmorillonite occurs as a minor clay and may have been derived by erosion of Rolling Downs Group rocks which were exposed around the northern margin of the Eromanga Basin towards the close of deposition of the parent Eyre Formation.

Major elements and titanium content of silcretes. Silcretes from the Haddon silcrete and Curalle silcrete profile are similar petrographically (Table 2), although Senior & Mabbutt (in prep.) have suggested that their mode of origin is different. Precipitation of silica in receptive strata below the land surface apparently led to similar concentrations of silica and titania to those determined for the Curalle silcrete profile (Table 4).

The relatively high titanium content in Australian silcretes was recorded by Williamson (1957), and is also a characteristic of South African silcretes (Frankel & Kent, 1938; Frankel, 1952; Mountain, 1952). Williamson (1957) suggested that titanium oxides are concentrated in syngenetic nodules or within interstices filled with microcrystalline colloform cement. Inter-

granular patches of brown to buff-coloured colloform cement were found in several thin sections examined during this study (Table 2) and some contain detrital grains of anatase. The colloform cement was X-rayed and was found to consist of microcrystalline anatase or rutile, intimately mixed with siliceous material of varying crystallinity. Anatase was detected on X-ray diffractograms of twelve silcretes from southwest Queensland (Senior & Senior, 1972) and it was also detected by AMDEL during this study at or about 3.52 Å on X-ray diffractogram traces. Hutton & others (1972) discussed the origin of silcretes which contain up to 50 percent titanium oxide in the matrix, and suggested that they formed by the leaching of silica, which led to residual surficial layers rich in titania. In the profiles discussed here there is an apparent maximum concentration of titania occurring at or near the middle of individual silcrete beds (Fig. 10). However, at several of the sites investigated maximum silica concentrations occur at or near the top of silcrete beds, and it would appear that there is a diffuse zonation of silica and titanium in southwest Queensland silcretes, although additional data are required to confirm this.

Sample No.	*24	*25	†44/1	†44/2	†44/3	Gregory & Vine (1969)	
	BMR		BMR		BMR		
	Outcrop samples		Canterbury 6		Canterbury 1		
Rock type	A	B	C	D	E	F	G
	percent						
SiO ₂	32.5	45.5	59.01	62.01	61.23	61.16	62.53
Na ₂ O	1.6	1.1	1.38	1.24	1.31	NA	NA
MgO	1.1	0.9	1.44	1.18	1.43	NA	NA
Al ₂ O ₃	11.4	11.9	19.21	18.6	18.18	18.23	17.0
P ₂ O ₅	0.1	0.1	0.21	0.04	0.03	NA	NA
K ₂ O	0.85	1.1	1.66	1.23	1.35	NA	NA
CaO	25.3	17.3	0.92	0.87	1.12	NA	NA
TiO ₂	0.30	0.4	1.09	1.08	0.99	NA	NA
MnO	1.05	0.42	0.04	0.03	0.04	NA	NA
Fe ₂ O ₃	2.4	2.8	5.59	4.39	3.9	4.05	4.35
L.O.I.	23.2	20.8	7.60	7.70	7.35	16.56*	16.12*
Total	99.95	99.32	98.16	98.39	96.94	100.00	100.00
			ppm		ppm		
Cr	—	—	55	65	55	—	—
V	—	—	150	190	160	—	—
Ba	—	—	290	320	230	—	—
Zr	—	—	230	210	190	—	—

- A Calcareous labile sandstone
B Calcareous labile sandstone
C Dark grey clayey siltstone
D Dark grey mudstone
E Dark grey carbonaceous mudstone
F Lutites (3 samples)
G Arenites (3 samples)

* For data retrieval at the BMR, the numbers 73 (year of project) 17 (geomorphology) should be used
† For data retrieval at the BMR, the numbers 75, 17 should be used
NA No analysis made
L.O.I. Loss on ignition; totals marked* include other oxides not determined by analysis

Table 4. Major element and trace element analyses of Winton Formation rocks.

Analyses carried out at the AMDEL laboratories, Adelaide

Conclusions

Although more than 170 rocks were analysed, comprising parent rocks and weathered profiles from south-west Queensland, the data are still relatively sparse and the conclusions must remain tentative. The significance of this regional overview of the clay mineralogy, and geochemistry is summarised below:

The Winton Formation contains abundant montmorillonite, with lesser illite, kaolinite, randomly interstratified clays, and chlorite. Major elements, regardless of grain size of lithological types analysed, appear evenly distributed throughout the Winton Formation.

Kaolinite, usually accompanied with lesser amounts of illite, are the diagnostic clay mineral assemblage of the Morney profile. Montmorillonite was found at the base of the profile, through the zone of partial weathering, and at the top of the profile. Younger sedimentary rocks of the Eyre Formation rest unconformably on the Morney profile and montmorillonite may have been illuviated into the top of the profile from these rocks.

The Canaway profile has a duricrust composed of kaolinitic breccia hardened with sesquioxides. The quantity of clay obtained during laboratory crushing and dispersing procedures from samples of the crustal zone was low, indicating strong grain-bonding by the sesquioxide cement. Kaolinite with minor illite are the dominant clays of the crust and mottled zones. Traces of montmorillonite and field evidence of gilgai-type

movements, attest to the former existence of more amounts of this clay.

Dominant clay minerals in the Eyre Formation are kaolinite and illite. Traces of montmorillonite were found in the upper part of the sequence and within the siliceous profiles developed in this unit. The reappearance of this clay suggests a change in provenance in the Oligocene and Miocene. At this time the Canaway and Curalle silcrete profiles were developing.

The Eyre Formation consists of quartzose arenites which support a silcrete profile (Curalle silcrete profile); in places this silcrete apparently grades laterally into multiple silcrete layers (Haddon silcrete) of probable subsurface origin. Silcretes of both types are very similar in composition, and show a tendency for the maximum TiO₂ content to occur in the central part of individual beds.

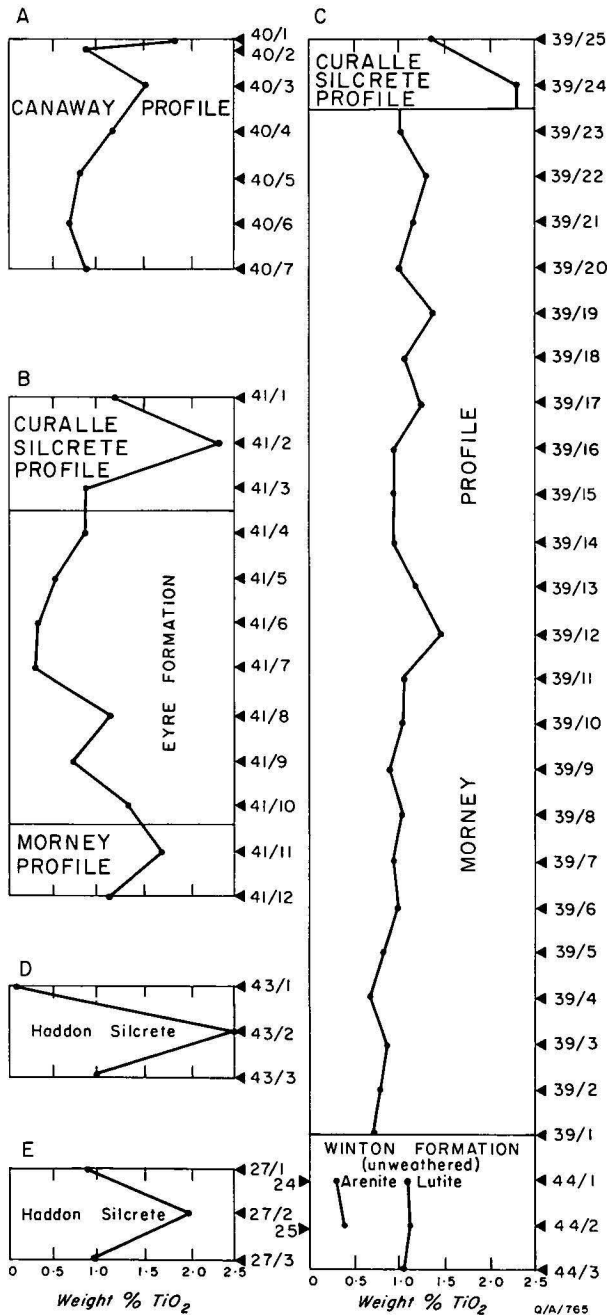


Figure 10. Comparative distribution of titanium oxide in host and weathered rocks.

Curalle silcrete profile												
	39/24	39/25	41/1	41/2	Silcrete†							
SiO ₂	96.01	79.15	96.96	95.05	96.32							
TiO ₂	2.31	1.40	1.21	2.32	1.35							
Al ₂ O ₃	.56	10.60	.83	.80	0.74							
*Fe ₂ O ₃	.08	1.96	.16	.27	0.08							
MnO	.01	.01	.01	.01	0.01							
MgO	.02	.10	.01	.01	0.23							
CaO	.05	.04	.02	.03	0.09							
Na ₂ O	.01	.02	.01	.01	0.04							
K ₂ O	.02	.18	.03	.03	0.03							
P ₂ O ₅	.03	.03	.02	.03	0.58							
L.O.I.	.32	4.55	.48	.86	2.14							
Total	99.41	98.03	99.73	99.42	100.00							

Haddon silcrete												
	43/1	43/2	43/3	1027A	1027B	1027C	0077/1	0077/2	0077/3	0079/1	0079/2	0079/3
SiO ₂	95.61	93.14	61.0	97.53	95.45	96.71	97.87	91.26	98.62	93.73	93.24	96.73
TiO ₂	.17	2.50	1.07	1.01	2.00	0.87	0.56	2.96	0.77	0.83	0.57	0.68
Al ₂ O ₃	2.29	1.10	23.19	0.38	0.64	0.38	0.48	2.00	0.16	2.15	1.71	0.68
*Fe ₂ O ₃	.21	.16	1.15	0.05	0.05	0.13	0.07	0.33	0.08	0.16	0.17	0.17
MnO	.01	.01	.01	0.01	0.04	1.01	0.00	0.00	0.00	0.00	0.00	0.00
MgO	.03	.05	.11	0.28	0.22	0.27	0.05	0.14	0.05	0.02	0.05	0.05
CaO	.04	.08	.16	0.03	0.08	0.39	0.04	0.05	0.01	0.25	0.12	0.04
Na ₂ O	.02	.05	.13	0.07	0.10	0.03	0.05	0.11	0.02	0.05	0.09	0.10
K ₂ O	.02	.04	.13	0.05	0.00	0.05	0.00	0.42	0.01	0.06	0.06	0.06
P ₂ O ₅	.01	.02	.08	0.03	0.11	0.11	0.02	0.03	0.05	1.30	2.00	0.28
L.O.I.	1.40	1.10	12.20	0.50	0.86	0.65	0.41	1.87	0.30	2.19	2.10	0.78
Total	99.74	1.30	99.18	99.41	98.71	98.81	99.55	99.17	100.07	100.83	100.10	99.57

Table 5. Major element analyses of silcrete.

† Average of 11 silcretes from southwest Queensland (Senior & Senior, 1972)

* Total iron as Fe₂O₃

Acknowledgements

The data for this paper represent part of a Ph.D. thesis completed in 1977. During the progress of this study much helpful discussion was received from the staff and students of the University of NSW and from colleagues at the BMR. I would particularly like to acknowledge the helpful criticism received from Professor J. A. Mabbutt, Dr M. J. Knight and Dr A. R. Jensen. The analytical results are mainly the work of Dr R. N. Brown, D. C. Bowditch and R. R. Robinson of the Australian Mineral Development Laboratories, Adelaide, SA. The figures were drawn by R. Bates of Geological Drawing Office, BMR. The manuscript was refereed by Dr G. E. Wilford and D. Gibson and their constructive criticisms are gratefully acknowledged.

References

- BERRY, L. G., & MASON, B., 1959—MINERALOGY. *Freeman, San Francisco*.
- DURY, G. H., 1969—Rational descriptive classification of duricrusts. *Earth Science Journal*, **3**, 77-86.
- EXON, N. F., & SENIOR, B. R., 1976—The Cretaceous geology of the Eromanga and Surat Basins in Queensland. *BMR Journal of Australian Geology & Geophysics*, **1**, 33-50.
- FRANKEL, J. J., 1952—Silcrete near Albertina, Cape Province. *South African Journal of Science*, **49**, 173-82.
- FRANKEL, J. J., & KENT, L. E., 1938—Grahamston surface quartzites (silcretes). *Transactions of the Geological Society of South Africa*, **40**, 1-42.
- GRANT, K., 1974—Laterites, ferricretes, bauxites and silcretes. *Second International Congress of Associated Engineering Geologists*, 4-31, 1-6.
- GREGORY, C. M., SENIOR, B. R., & GALLOWAY, M. C., 1967—The geology of the Connemara, Jundah, Canterbury, Windorah and Adavale 1:250 000 Sheet areas, Queensland. *Bureau of Mineral Resources, Australia Record*, **1967/16** (unpublished).
- GREGORY, C. M., & VINE, R. R., 1969—Canterbury, Qld—1:250 000 Geological Series. Bureau of Mineral Resources, Australia—*Explanatory Notes SG/54-7*.
- HALLSWORTH, E. G., ROBERTSON, G. K., & GIBBONS, F. R., 1955—Studies in pedogenesis in New South Wales, VII—The 'Gilgai' soils. *Journal of Soil Sciences*, **6**, 1-31.
- HUTTON, J. T., TWIDALE, C. R., MILNES, A. R., & ROSSER, H., 1972—Composition and genesis of silcrete skins from the Beda Valley, Southern Arcoona Plateau, South Australia. *Journal of the Geological Society of Australia*, **19**, 31-41.
- IDNURM, M., & SENIOR, B. R., 1978—Palaeomagnetic ages of Late Cretaceous and Tertiary weathered profiles in the Eromanga Basin, Queensland. *Palaeogeography, Palaeoclimatology, Palaeoecology*, **24**, 263-78.
- KRUMBEIN, W. C., & SLOSS, L. L., 1963—STRATIGRAPHY AND SEDIMENTATION. 2nd Edition, *Freeman, San Francisco*.
- LANGFORD-SMITH, T. (Editor), 1978—AUSTRALIAN SILCRETE. *University of New England Monograph Series*.
- MOUNTAIN, E. D., 1952—The origin of silcrete. *South African Journal of Science*, **48**, 201-4.
- PACKHAM, G. H., 1954—Sedimentary structures as an important feature in the classification of sandstones. *American Journal of Science*, **252**, 466-76.
- SENIOR, B. R., 1969—Jundah, Qld—1:250 000 Geological Series. Bureau of Mineral Resources, Australia—*Explanatory Notes, SG/54-4*.
- SENIOR, B. R., 1976—Geology and geomorphology of the Haddon Corner area, Qld—1:250 000 map, Preliminary edition. *Bureau of Mineral Resources, Australia*.
- SENIOR, B. R., in press—Silcrete and chemically weathered sediments in southwest Queensland. In LANGFORD-SMITH, T. (Editor) AUSTRALIAN SILCRETE. *University of New England Monograph Series*.
- SENIOR, B. R., & MABBUTT, J. A., in prep.—A proposed method of weathered rock classification, and definitions of four weathered rock units from southwest Queensland.

- SENIOR, B. R., & SENIOR, Daniele, 1972—Silcrete in south-west Queensland, in *Geological papers 1969. Bureau of Mineral Resources, Australia Bulletin*, **125**, 23-8.
- SMALE, D., 1973—Silcretes and associated silica diagenesis in southern Africa and Australia. *Journal of Sedimentary Petrology*, **43**, 1077-89.
- STEPHENS, C. G., 1971—Laterite and silcrete in Australia. *Geoderma*, **5**, 5-51.
- WATTS, S. H., 1975—An unusual occurrence of silcrete in adamellite—implications for duricrust genesis. *Search*, **6**, 434-36.
- WENTWORTH, C. K., 1922—A scale of grade and class terms for clastic sediments. *Journal of Geology*, **30**, 377-92.
- WILLIAMSON, W. O., 1957—Silicified sedimentary rocks in Australia. *American Journal of Science*, **255**, 23-42.
- WOPFNER, H., CALLEN, R. A., & HARRIS, W., 1974—The Lower Tertiary Eyre Formation of the southwestern Great Artesian Basin. *Journal of the Geological Society of Australia*, **21**, 17-51.

Source rocks and hydrocarbon potential of the Palaeozoic in the onshore Canning Basin, Western Australia

R. V. Burne, J. D. Gorter¹, & J. D. Saxby²

In the onshore Canning Basin potentially oil-bearing sediments are restricted to the Palaeozoic sequence. Analyses of organic content of the most promising source lithologies show that there is some source potential in the Ordovician of the Broome Arch and other areas, in the Devonian and Lower Carboniferous of the margins of the Fitzroy Graben and adjacent terraces, and in the Permian of the Fitzroy Graben. A review of the hydrocarbon potential of the basin suggests that there is some hope for future successful exploration, particularly in the unexplored southeast Fitzroy Graben. The data available from the scattered and often poorly sited exploration wells nevertheless indicate that because of unsuitable organic material, poor reservoir conditions, and unfavourable burial histories, the area may never become a major hydrocarbon producing province.

Introduction

The onshore area of the Canning Basin is 430 000 sq km (Figs 1, 2); it contains a sequence of dominantly Palaeozoic sedimentary rocks which attain a maximum thickness of over 9 km. The geology of the basin has been summarised by Horstman & others (1976), who have produced a generalised stratigraphical column for the area (Fig. 3).

Petroleum exploration, undertaken in the basin for the last fifty-seven years, has not revealed commercially exploitable accumulations of hydrocarbons. Some explanation for this disappointing record has been provided by analyses of levels of organic metamorphism (Hood & Castano, 1974) and thermal histories of the rocks of the basin (Burne & Kanstler, 1977). Despite the great age, slow subsidence, and low geothermal gradient of the Palaeozoic section, much of it is currently at a level of metamorphism suitable for the generation and preservation of liquid hydrocarbons.

This paper attempts to explain the poor exploration record of the basin more precisely, by examining the source rock potential of some of the Palaeozoic lithologies. This information is used to assist in delineating the areas with the greatest potential for hydrocarbon occurrence.

In this BMR-CSIRO project, JDG selected material, RVB & JDG undertook the geological interpretation, and JDS supervised the analyses and interpreted the resulting data.

Source rock analyses

Early reviews of the hydrocarbon potential of the area paid little attention to the identification of source rocks. Veevers & Wells (1961) recognised most of the then known Ordovician rocks and the Devonian and Lower Carboniferous section in the Fitzroy Graben as being possible source rocks. Koop (1966) considered that the Lower Ordovician Emmanuel Formation of the northern part of the Canning Basin could be a source lithology, and recognised good source characteristics in the Goldwyer Formation, an Ordovician black shale in the southwest, and in the Middle Devonian carbonates of the Mellinjerie Limestone. At that time geochemical data were not available to support or refute these

assessments. Indeed, as a result of the subsidised exploration for hydrocarbons in the basin there is only one record available of a geochemical assessment of source potential (Brown & Campbell, 1974). This investigation, undertaken on samples from Contention Heights 1 in the southeast of the Basin, showed low total organic carbon (TOC), generally less than 0.4 percent, for all samples except two from the Permian Poole Sandstone (now considered to be from the Noonkanbah Formation) which contain 1.3-1.55 percent organic carbon. H/C ratios of 0.70 were recorded for kerogen from the Permian Noonkanbah Formation.

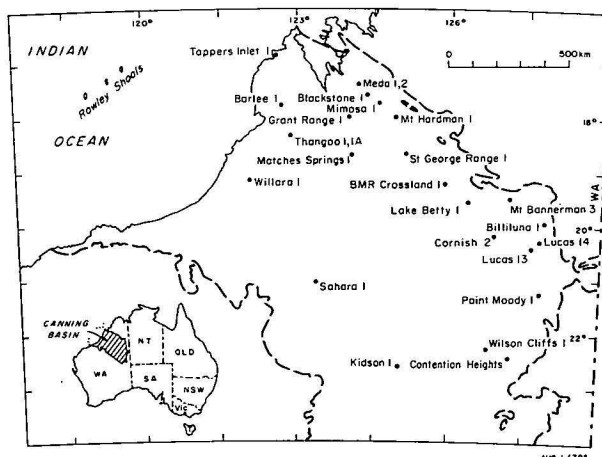


Figure 1. Location of wells referred to in text.

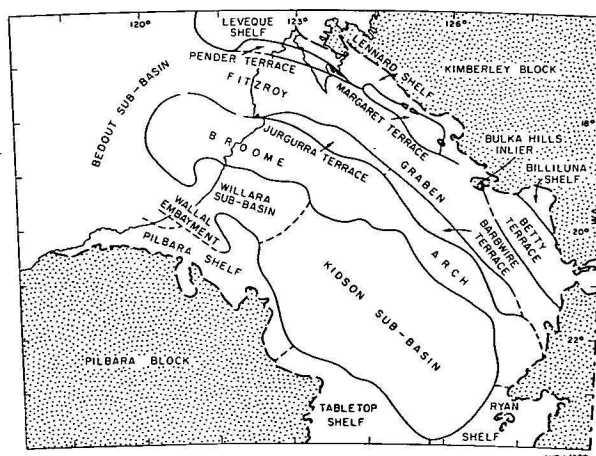


Figure 2. Structural provinces of the Canning Basin.

1. Present address: ESSO Australia Ltd, PO Box 4047, Sydney 2001.
2. Fuel Geoscience Unit, CSIRO Institute of Earth Resources, PO Box 136, North Ryde, NSW 2113.

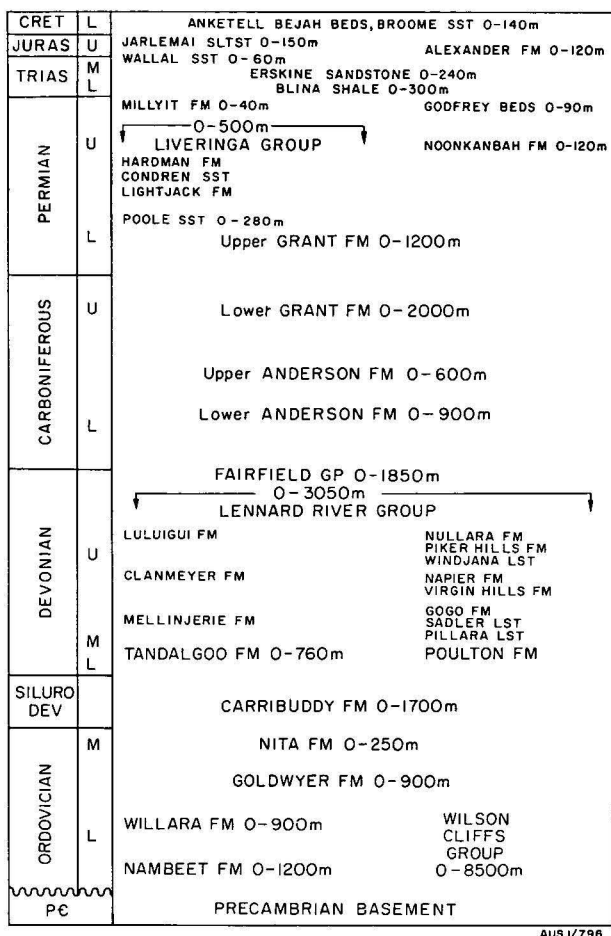


Figure 3. Generalised stratigraphical column for the on-shore Canning Basin (modified from Horstman & others, 1976).

The present study is based on data from 15 petroleum exploration wells and BMR stratigraphic holes (Fig. 1). The sampling was determined on the basis of geographical location, depth, lithology of section, and abundance of core available. Samples were taken from dark, apparently organic-rich fine-grained layers, from carbonates, and from shale partings in sandstone and limestone sections. At least 50 gm of sample was taken for analysis in each case. The analyses undertaken included total organic carbon and a determination of the amount and nature of the extractable organic matter. Vitrinite reflectance measurements were also made on the samples to augment those of Kanstler & Cook (reported in Burne & Kanstler, 1977).

Total organic carbon

Analyses were carried out using a Leco analyser on ground core samples, which had been treated with acid to remove carbonates. The results are presented in Table 1.

TOC values give an indication of the source potential of a lithology. According to Dickey & Hunt (1972) a TOC content of ≥ 0.5 percent is required to qualify a rock as having source potential, although this may be reduced to >0.2 percent for carbonates. Only eighteen of the hundred samples analysed have organic carbon values greater than 0.5 percent and fifty-five have values less than 0.2 percent.

The formations with the highest TOC are the Permian Noonkanbah Formation, the Anderson Formation

of the Upper Carboniferous, and the Ordovician in the area of Matches Springs, with the Permo-Carboniferous Grant Formation, and the Devonian Fairfield and Gogo Formations also having some potential. Low TOC values for the Devonian and Lower Carboniferous sequence are particularly disappointing, since this has traditionally been regarded as one of the most prospective sequences in the Basin. However, data recently lodged in BMR by Esso in compliance with PSSA legislation, indicates higher TOC values for this sequence than recorded here. This would seem to indicate either variable levels of organic content within the sequence and hence patchy source development, or more selective sampling of organic-rich sediment.

Extractable organic matter

Samples were crushed and extracted in a Soxhlet extractor with purified chloroform for eight hours. The solvent was then evaporated under a stream of nitrogen to give the total extract. The petroleum ether-soluble part of the extract was transferred to a 5 x 1 cm column of Florisil and eluted successively with petroleum ether to give the aliphatic fraction, with benzene to give the aromatic fraction, and with methanol to give the polar fraction. The results of these analyses are given in Table 1. The total extract should be equal to or greater than the sum of these three fractions, but in the few cases where extracts are small, discrepancies occur.

The aliphatic fraction was analysed by gas chromatography for hydrocarbons in the $n\text{-C}_{15}$ to $n\text{-C}_{35}$ boiling range (Fig. 6). In many cases the samples were too small for reliable results to be obtained.

The total extract, representing indigenous, generated, and migrated oily compounds, is at a low level in almost all samples. The aliphatic fraction from many of the extracts is almost nonexistent; this is not encouraging for exploration, since this fraction often comprises over 50 percent of crude oils, although maturation of certain types of organic matter may tend to give more than average amounts of non-aliphatics. Where chromatograms were obtained, little odd-carbon preference of normal alkanes in the high molecular weight range was observed, a fact that is consistent with an absence of immature land plant material. One exception is core 5 from BMR Crossland 1, where the unusually great amount of Permian organic matter present gives rise to a sizeable aliphatic fraction with a pronounced odd-carbon preference for n-alkanes above C₂₃. Some generation and/or migration in Ordovician, Devonian, Carboniferous and Permian rocks is probably indicated by crude oil-like distributions in Meda 1 (core 2), Grant Range 1 (cores 56 and 60), Matches Springs 1 (cores 7, 11 and 13) and Wilson Cliffs 1 (cores 15 and 20).

Prospective areas of the Canning Basin

Although source material is not abundant in the samples examined, it is worthwhile considering the relationship between the lithologies which offer the most encouraging results and areas of suitable organic metamorphism, to define the most prospective areas. The main oil-generation zone is commonly taken as covering a reflectance range of 0.7-1.3 percent, although a higher range (~ 1.0 -2.0%) can be inferred from some lines of evidence (Saxby, 1978). Thus, until the zone of generation is more precisely defined it is difficult to identify rocks that have acted as hydrocarbon sources. However, taking the extreme range of possible reflectance values for the oil generation zone of 0.7-2.0 per-

Well	Core	Depth (m)	Total extract (ppm)	Aliphatic fraction (ppm)	Aro- matic fraction (ppm)	Polar fraction (ppm)	Organic carbon (%)	Mean vitrinite reflectance (%)	Present temp. (°C)	Formation
Barlee 1	3	832.9	518	49	13	382	<0.1	0.58	53	Anderson Fm
Barlee 1	5	1089.4	299	15	8	226	<0.1	a	58	Anderson Fm
Barlee 1	8	1242.5	110	36	11	111	0.2	0.69	60	Anderson Fm
Barlee 1	10	1475.6	68	1	0	36	0.2	1.27	64	Anderson Fm
Barlee 1	12	1730.4	63	12	28	54	<0.1	0.81	68	Anderson Fm
Barlee 1	14	1984.0	333	6	6	210	<0.1	a	72	Anderson Fm
Barlee 1	16	2242.9	277	27	20	216	0.2	0.90	76	Anderson Fm
Barlee 1	18	2421.4	118	11	3	90	<0.1	1.03	79	Anderson Fm
BMR Billiluna 1	1	23.5	820	39	11	68	2.3	a	—	Noonkanbah Fm
BMR Billiluna 1	2	53.5	375	51	175	100	6.0	0.58	—	Poole Sst.
BMR Billiluna 1	3	83.3	27	0	2	4	<0.1	a	—	Grant Fm
BMR Billiluna 1	4	118.5	466	19	0	22	<0.1	a	—	Grant Fm
Blackstone 1	3	1536.2	437	81	2	316	0.2	0.48	65	Fairfield Gp
Blackstone 1	6	1690.4	436	96	40	322	0.3	0.47	66	Fairfield Gp
Blackstone 1	9	1819.3	674	133	71	302	<0.1	a	70	Nullara Lst
Blackstone 1	14	2129.3	159	22	6	136	<0.1	0.57	76	Poulton Fm
Blackstone 1	18	2368.6	107	5	4	80	<0.1	0.69	81	Nita Fm
Blackstone 1	20	2582.7	254	28	36	74	0.2	0.71	85	Goldwyer Fm
Blackstone 1	23	2834.0	170	4	0	63	<0.1	0.78	89	Goldwyer Fm
Blackstone 1	25	3008.9	255	1	1	183	<0.1	a	93	Goldwyer Fm
BMR Cornish 2	3	223.4	186	84	86	13	0.2	0.43	—	Ersine Sst
BMR Crosslands 1	3	41.9	233	9	25	150	0.3	a	—	Hardman Fm
BMR Crosslands 1	4	73.1	370	32	34	244	2.0	0.58	—	Condren Sst
BMR Crosslands 1	5	112.6	689	186	102	302	10.6	0.54	—	Condren Sst
BMR Crosslands 1	8	262.1	182	10	13	27	0.3	a	—	Lightjack Fm
Grant Range 1	26	1694.8	324	6	9	311	<0.1	1.12	58	Grant Fm
Grant Range 1	49	2224.1	4350	192	49	243	<0.1	a	68	Anderson Fm
Grant Range 1	56	2432.5	1350	760	53	292	1.0	1.54	72	Anderson Fm
Grant Range 1	60	2567.0	171	73	1	69	0.2	1.42	74	Anderson Fm
Grant Range 1	67	2777.7	564	39	17	443	<0.1	a	79	Anderson Fm
Grant Range 1	85	3711.7	174	13	7	147	0.4	1.99	96	Anderson Fm
Grant Range 1	92	3832.9	5080	23	25	2960	<0.1	2.26	98	Anderson Fm
Kidson 1	2	1554.0	51	27	15	86	<0.1	0.53	67	Grant Fm
Kidson 1	4	1791.1	79	14	11	61	<0.1	a	71	Tandagoo Fm
Kidson 1	9	2609.8	65	14	4	35	<0.1	a	85	Carribuddy Fm
Kidson 1	17	3744.0	166	69	29	130	0.2	a	104	Carribuddy Fm
Kidson 1	21	4367.6	65	36	1	30	0.2	2.16	114	Carribuddy Fm
Lake Betty 1	1	2474.3	63	18	32	52	<0.1	1.77	98	Fairfield Gp
Lake Betty 1	2	2941.7	96	5	5	83	<0.1	2.08	112	Luluigui Fm
Lake Betty 1	3	3143.3	170	7	17	165	<0.1	2.48	118	Poulton Fm
BMR Lucas 14	4	99.7	1530	85	176	135	2.1	0.54	—	Lightjack Fm
BMR Lucas 13	3	123.1	150	48	10	74	<0.7	0.60	—	Millyit Sst
BMR Lucas 13	5	186.2	35	6	0	35	<0.1	0.76	—	Godfrey Beds
Matches Springs 1	2	555.4	169	10	7	160	<0.1	a	40	Nullara Fm
Matches Springs 1	4	833.5	173	5	1	103	<0.1	a	45	Nullara Fm
Matches Springs 1	7	1221.5	151	13	6	85	<0.1	0.58	53	Gogo Fm
Matches Springs 1	9	1534.7	278	6	8	237	0.4	0.47	59	Pillara Fm
Matches Springs 1	11	1710.5	113	16	4	67	<0.1	0.61	62	Tandagoo Fm
Matches Springs 1	13	2080.1	87	11	21	33	<0.1	a	69	Nita Fm
Matches Springs 1	15	2407.6	3050	1750	592	442	1.7	a	75	Ord. Undiff.
Matches Springs 1	17	2832.5	278	89	40	169	<0.1	0.78	83	Ord. Undiff.
Meda 1	2	595.3	569	141	47	278	2.2	0.49	29	Noonkanbah Fm
Meda 1	5	1051.1	256	25	6	182	0.5	0.58	52	Grant Fm
Meda 1	8	1542.0	260	24	13	208	0.2	0.69	73	Fairfield Fm
Meda 1	12	2015.4	149	7	3	39	<0.1	a	94	Nullara Fm
Meda 1	18	2162.6	164	8	3	84	<0.1	a	101	Napier Fm
Meda 1	24	2617.6	147	6	5	132	<0.1	0.77	121	Poulton Fm
Mimosa 1	1	2426.4	811	400	100	256	0.5	0.75	88	Gogo Fm
Mimosa 1	2	3374.1	84	1	21	47	0.4	1.16	105	Gogo Fm
Mimosa 1	3	4108.1	81	0	8	49	<0.1	2.08	120	Gogo Fm
BMR Mt Bannerman 3	3	90.8	132	47	53	30	1.2	0.75	—	Grant Fm
Point Moody 1	2	278.5	221	42	25	221	2.3	0.82	54	Noonkanbah Fm
Point Moody 1	4	464.8	30	20	17	8	<0.1	0.79	56	Poole Sst
Point Moody 1	12	1212.7	256	61	40	152	0.2	1.07	60	Grant Fm
Point Moody 1	18	1647.9	112	16	10	52	<0.1	1.53	65	Grant Fm
Point Moody 1	21	1911.4	133	28	16	87	0.2	1.40	67	Grant Fm
Point Moody 1	23	2069.5	430	40	32	411	<0.1	1.54	69	Anderson Fm
Sahara 1	2	653.9	51	10	9	52	<0.1	0.74	59	Grant Fm
Sahara 1	6	1101.6	177	65	33	91	0.2	a	65	Mellinjerie Fm
Sahara 1	12	2001.1	55	23	16	67	<0.1	0.50	78	Carribuddy Fm
St George Range 1	5	740.2	223	32	7	161	<0.1	0.62	47	Grant Fm
St George Range 1	13	2503.4	677	5	8	637	1.1	1.65	76	Anderson Fm
St George Range 1	14	2594.8	210	10	1	162	<0.1	1.78	77	Anderson Fm
St George Range 1	15	2694.3	619	25	19	523	3.3	1.44	79	Anderson Fm
St George Range 1	16	2902.7	170	2	5	167	0.5	2.12	82	Fairfield Gp
St George Range 1	18	3124.6	229	1	3	202	0.2	a	85	Fairfield Gp
St George Range 1	22	3442.3	302	11	2	135	<0.1	2.45	90	Fairfield Gp
St George Range 1	24	3997.3	41	6	2	49	<0.1	2.98	100	Fairfield Gp
St George Range 1	25	4285.6	80	6	3	49	0.2	3.28	104	Fairfield Gp
Tapper's Inlet 1	2	1948.7	122	9	7	42	<0.1	a	67	Pillara Lst
Tapper's Inlet 1	3	1987.1	274	61	21	193	0.8	0.73	68	Poulton Fm

Well	Core	Depth (m)	Total extract (ppm)	Aliphatic fraction (ppm)	Aro-matic fraction (ppm)	Polar fraction (ppm)	Organic carbon (%)	Mean vitrinite reflectance (%)	Present temp. (°C)	Formation
Thangoo 1A	1	466.3	180	30	16	117	0.4	0.51	49	Grant Fm
Thangoo 1A	6	1415.8	969	574	127	46	0.9	0.78	63	Willara Fm
Thangoo 1A	7	1495.9	263	42	10	100	<0.1	0.76	64	Willara Fm
Willara 1	5	1742.3	148	1	0	73	<0.1	a	85	Nita Fm
Willara 1	7	2085.8	87	17	16	89	<0.1	0.93	86	Goldwyer Fm
Willara 1	10	2548.2	88	19	12	71	<0.1	1.96	101	Goldwyer Fm
Willara 1	13	3018.8	51	24	13	47	<0.1	2.51	116	Willara Fm
Willara 1	15	3357.5	44	20	11	15	<0.1	2.15	127	Nambeet Fm
Willara 1	17	3659.5	66	12	7	53	<0.1	2.60	136	Nambeet Fm
Willara 1	19	3900.9	95	29	18	43	<0.1	2.73	144	Nambeet Fm
Wilson Cliffs 1	2	1014.0	47	19	0	25	<0.1	0.52	43	Mellinjerie Lst
Wilson Cliffs 1	10	2212.0	102	10	12	72	<0.1	a	75	Carribuddy Fm
Wilson Cliffs 1	13	2681.2	113	33	16	77	<0.1	1.35	87	Goldwyer Fm
Wilson Cliffs 1	15	2958.9	306	91	23	225	0.2	1.94	94	Middle Ordovician
Wilson Cliffs 1	20	3282.4	222	26	10	42	<0.1	2.61	103	Nambeet Fm

a = Insufficient vitrinite for a reliable measurement

Table 1. Analytical data of Canning Basin cores.

Well	Core	Depth (m)	C	Composition (% dry, mineral-free)				Atomic Ratios		Ash
				H	N	O	S	H/C	O/C	
Meda 1	2	595.3	77.8	4.32	1.7	15.2	0.9	0.67	0.15	16.9
St George Range 1	13	2503.4	83.7	3.69	1.9	9.8	0.9	0.53	0.09	7.7
St George Range 1	15	2694.3	84.2	3.96	0.7	6.7	4.5	0.56	0.06	19.1
Point Moody 1	2	278.5	81.2	4.20	1.5	12.2	0.9	0.62	0.11	8.4
Matches Springs 1	15	2407.6	86.0	8.66	0.9	2.4	2.0	1.21	0.02	23.6

Table 2. Elemental analyses of Canning Basin kerogens.

cent, it seems probable from the reflectance data in Table 1 that immature material is present in Meda 1 (<2000 m), Blackstone 1 (<2500 m), Barlee 1 (<1300 m), St George Range 1 (<1000 m), Matches Springs 1 (<2000 m), Wilson Cliffs (<1500 m), Sahara 1 (<2000 m), Kidson 1 (<2000 m), Thangoo 1A (<1000 m) and in most of the shallow BMR holes. Similarly, kerogen which is past the stage of oil generation, appears to be present in Great Range 1 (>3700 m), St George Range 1 (>2800 m), Lake Betty 1 (>2900 m), Wilson Cliffs 1 (>3000 m), Willara 1 (>2600 m), Kidson 1 (>4000 m) and Mimosa 1 (>4000 m). The varied history of the rocks of the basin is reflected in the fact that, in some wells, Permian, Carboniferous and Devonian organic matter is still immature, while in other wells only Permian material has not already passed through the zone of oil generation.

Another way of assessing the maturity and hydrocarbon potential of a core is through measurement of the elementary composition of isolated kerogens. Five samples were chosen and, after numerous treatments with HCL/HF, the resulting kerogens gave the data in Table 2. The Carboniferous samples from St George Range have the lowest H/C values (and the highest reflectance) and show little, if any, potential for further oil generation. Methane could continue to be formed until the H/C ratio drops to ~0.35 (Saxby, 1978). Two immature samples from the Permian Noonkanbah Formation (Meda and Point Moody) have low H/C values indicating that the type of organic matter present is unsuitable for oil generation regardless of its maturity. The Ordovician Matches Springs kerogen is particularly interesting because of its high hydrogen content. Exposure of such kerogen to temperatures higher than the maximum already experienced would result in significant oil generation.

Burne & Kanstler (1977) suggested, from known hydrocarbon shows, that the most suitable source rocks in the basin occur in the Middle Devonian to Lower Carboniferous rocks. Oil shows have been encountered in areas where these sediments are at present between 50 and 75°C. It was concluded from a comparison of indicators of organic metamorphism and present burial temperatures that these two temperature surfaces, in general, defined the Palaeozoic section of the onshore Canning Basin in which oil occurrence was a possibility.

The data on which this conclusion was based have now been augmented by several more vitrinite reflectance readings (Table 1). Comparison of this new data with the relevant diagrams in Burne & Kanstler (1977) generally confirms the earlier work, although the varied burial history in the Fitzroy Graben anticlines means that in this region the picture is more complex (Fig. 4).

From these analyses three possibilities for oil accumulations emerge as worth consideration, in that they combine potential source rocks with suitable levels of organic metamorphism:

- Ordovician prospects of the Broome Arch;
- Devonian and Carboniferous rocks at the margins of the Fitzroy Graben;
- Upper Carboniferous/Permian rocks in the Fitzroy Graben.

Ordovician prospects of the Broome Arch

Lower and Middle Ordovician rocks are preserved in the Canning Basin, and they represent the deposits of shallow-marine environments that seem to have covered most of the area of the present Basin. Oil shows have been recorded from Ordovician rocks in several of the wells drilled on the Broome Arch (Burne & Kanstler 1977), but, of the five wells in the area sampled in this study only two contain lithologies with good source potential (Lower Ordovician in Thangoo

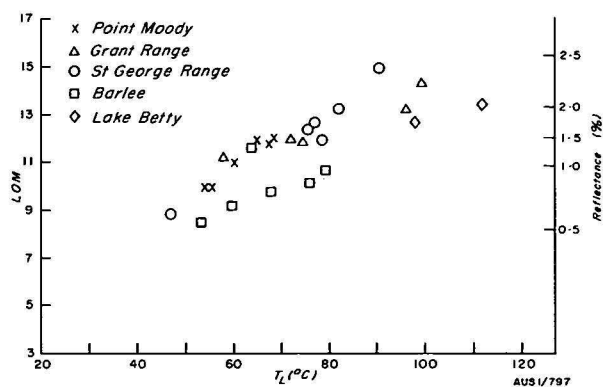


Figure 4. Relationship between levels of organic metamorphism (Hood & Castano, 1974) and ambient temperature for wells in the Fitzroy Graben.

1A and Matches Springs 1). Both these horizons are in or approaching the oil mature zone ($R_o = 0.78\%$). The high H/C ratio of the Matches Springs kerogen indicates good potential for hydrocarbon generation. The burial history of the area probably indicates relatively uncomplicated burial to shallow depths (Burne & Kanstler, 1977), and, given a uniform geothermal gradient with time, the section could not have attained any level of maturity prior to the Cretaceous. This is particularly promising as the area was emergent and subject to erosion during the Devonian and Early Carboniferous, and migrated early petroleum would possibly have been lost. Unfortunately, by the time the section had reached maturity much of the early

porosity of the Ordovician had been filled. Nevertheless, any preserved, sealed post-Ordovician structure could provide a suitable trap. Alternative interpretations of the burial history of this area suggest that at least 2000 to 3000 metres of Silurian, Devonian, and Lower Carboniferous rocks were stripped off this area during the late Carboniferous and early Permian. Since the present cover of post-Carboniferous sediments is only ~1000 m, the Ordovician sediments on the Broome Arch would in this case have reached their maximum depth, temperature, and hence maturity in the Early Carboniferous. Petroleum generated and migrating at this time would probably have been lost, although some pockets may remain. Generation since the Carboniferous would depend on local heating effects giving additional maturation within the oil generation range. Evidence for the migration of Ordovician-sourced oil into Permian reservoirs is provided by the occurrence of oil shows in the Permian of Thangoo 1, where these rocks directly overlie the Ordovician. Unfortunately, many of the known structures of the Broome Arch are open or breached, and intensive seismic exploration has revealed the presence of relatively few structures in the area (Fig. 5). This, together with the disappointing results of drilling, offers little promise of future exploration success.

Devonian prospects at the margins of the Fitzroy Graben

The Middle and Upper Devonian, as well as the Lower Carboniferous sediments, consist of a variety of lithologies formed in generally shallow marine environments, though with paralic and deeper water environ-

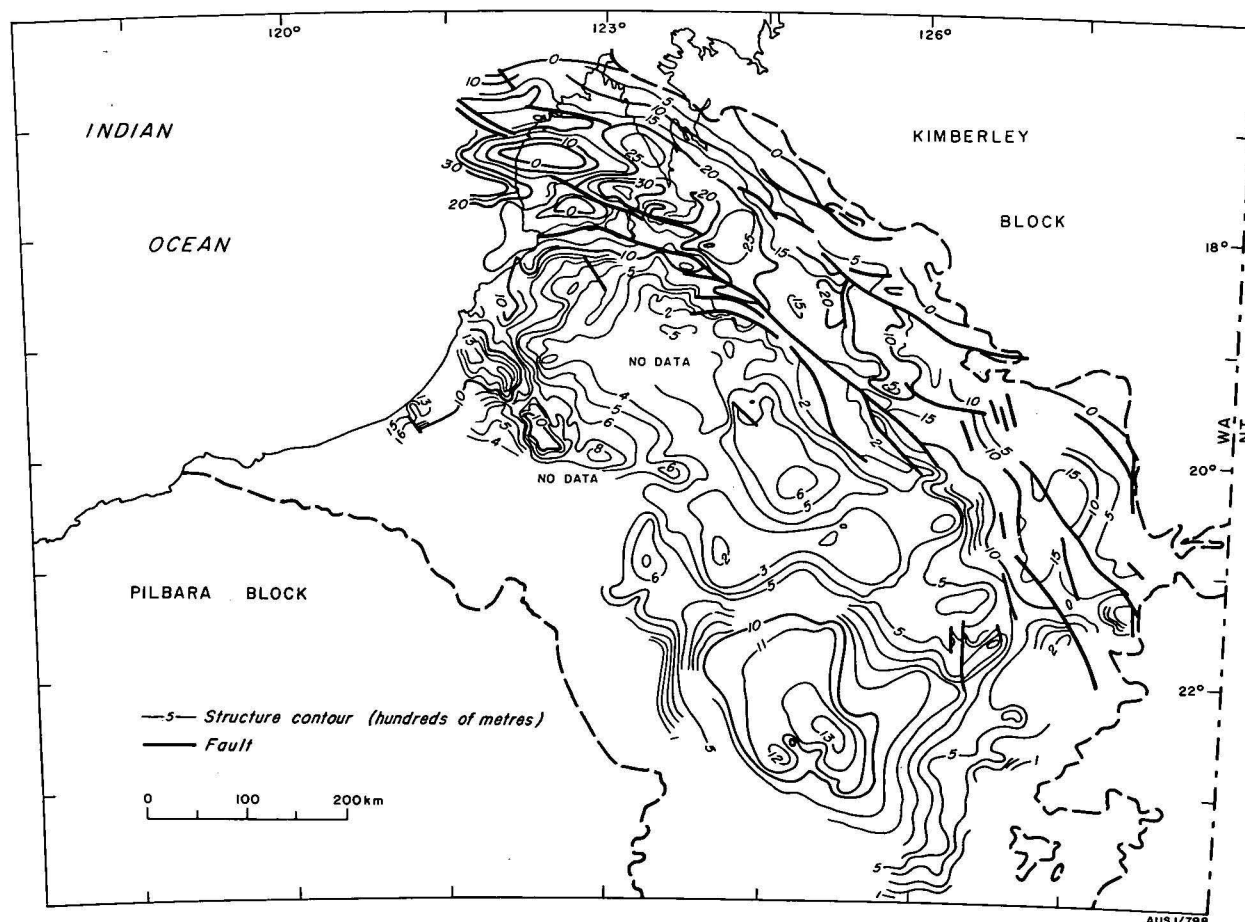


Figure 5. Structure contour map of the base of the Permo-Carboniferous Grant Formation (compiled by J. S. Rasidi).

ments also being represented. These sediments are localised in the northeastern half of the basin, occupying the area of the Broome Arch, Fitzroy Graben and adjacent terraces, and the Lennard Shelf.

The region provides some of the most remarkable exposures of Devonian carbonates in the world (Veivers & Wells, 1961; Playford, 1976); similarities between these rocks and the petroliferous Devonian reefs of Canada have been documented (Playford, 1969). Between 1959 and 1970 the search for petroleum in the Canning Basin concentrated almost exclusively on testing the hydrocarbon potential of Devonian reefs (Rasidi, 1978). Results were disappointing, for not only were no commercial or appreciable deposits of hydrocarbons discovered, but in several wells no carbonate bodies were encountered. Indeed, only two wells (Meda 1 and Hawkstone Peak 1) seem to have been sited in a position to test the hydrocarbon potential of a buried reef structure adequately, and subsequent seismic surveys have shown that even these were not sited on a structure. Data gathered during this exploration and during the concomitant scientific investigations of the carbonates (Playford & Lowry, 1966; Playford, 1969; Playford, 1976; Logan & Semeniuk, 1976), have pointed to several factors which make the Devonian reefs less promising prospects than their Canadian counterparts. The Canning Basin carbonates are not set in a thick sedimentary sequence, but rest directly on Precambrian basement or on thin sequences of continental sediments. Only in Tappers Inlet 1 is there evidence of carbonates overlying an older sequence of potential source rocks (in this well the thin cross-laminated organic-rich Poulton Sandstone has an organic carbon content of 0.8%).

There is evidence from some areas of erosion and uplift of the carbonates both during the period of their formation and after growth ceased in the Fammenian (Playford, 1976). This early exposure may have modified primary porosity and probably also reduced organic content. The carbonates of the Lennard Shelf have never been deeply buried, and have been subjected to gentle uplift since the Triassic. In some areas, for example the Napier area of the Lennard Shelf, the reefs have never been buried sufficiently deeply to attain a level of metamorphism appropriate for the generation of oil. Another limiting factor is the absence of continuous, permeable units in the formations so far encountered. The available porosity is generally late-formed solution porosity, and is patchily developed, mainly in the Nullara Limestone. The stratigraphical units of the carbonate complexes (Playford, 1976) are essentially facies controlled (Fig. 3). Samples from the Nullara Limestone, Napier Formation, and Luluigui Formation were analysed in this study. Only one sample, from the Pillara Formation in Matches Springs 1, had an encouraging content of organic material (0.4%). However, the recently described (but not drilled) reef structures on the Lennard Shelf (Rasidi, 1978) still represent an attractive target for exploration. Based on organic carbon analyses, the two best source lithologies in the Devonian and Lower Carboniferous sequence are the Frasnian Gogo Formation and the Fairfield Group (together with the overlying Anderson Formation), which range from the Fammenian to the early Carboniferous.

The Gogo Formation is described by Playford (1976) as a basinal facies. Sections of Gogo Formation onlapping a downfaulted Frasnian reef knoll at Wade

Knoll are considered by Playford to have been transported by turbidity currents. Examination of cores from the Gogo Formation in BMR Noonkanbah 4 and Mimosa 1 confirms the presence of thin, sharp-based turbidite units interbedded with black fine-grained sediments. Moderate organic carbon values were observed in this formation in two of the samples from Mimosa 1 (0.5 and 0.4%). The Gogo Formation is a widespread sequence, but is dominantly fine-grained, with thin interbeds of coarser material. Thick clastic units, such as fan-channel sands, have not been identified and so any hydrocarbons sourced by this formation would need to accumulate in onlapped carbonate bodies or by migration into younger carbonates, particularly near faults at the northern margin of the Fitzroy Graben. A widespread lower Fammenian unconformity truncates the formation in Mimosa 1 and elsewhere, and this may have acted as a barrier to upward-migrating hydrocarbons.

The Fairfield Group, and the overlying Anderson Formation, are a mixed sequence of sandstones, shales and carbonates. These sediments were formed in a variety of shallow marine, paralic, and fluvial environments formed during a series of small transgressive cycles after the cessation of carbonate formation in the Fammenian, and culminating in a major regression during the Lower Carboniferous (Druce & Radke, 1979). Overall, these sediments, and particularly the Laurel Formation, are the most consistently petroliferous in the basin. In areas of the Lennard Shelf the maturity is suitable for oil accumulation, but in many areas of the Graben this may not be the case. Our analyses (Table 1) show variable organic carbon content, although in places good potential source rocks are present. Unfortunately the prospectivity of these formations is limited by the generally low permeability of sandstones in the Laurel Formation on the one hand, and the absence of seals for the permeable sections of the Anderson Formation on the other.

The most encouraging recovery of oil from the Canning Basin was from the Fairfield Group in Meda 1. Stain and fluorescence were noted at 1562 m and on completion of drilling the show was tested and yielded 7 percent oil-cut salt water. Recovered oil was 38.6 API, gravity (Horstmann & others, 1976). Powell & McKirdy (1976) describe the oil as a highly paraffinic, high-wax oil which—despite a low pristane to phytane ratio—has other features which point to a non-marine source.

In 1976 WAPET kindly supplied a fresh sample of this oil recovered prior to sealing the well. This sample was separated into a high-boiling aliphatic fraction (65.9%), an aromatic fraction (3.2%), and a polar fraction (0.9%). Figure 6 shows the n-alkane distribution in the first of these fractions. The observed smoothly-decreasing n-alkane pattern is similar to that recorded for many crude oils. Unfortunately none of the Meda cores close to the oil-bearing interval give sufficient extract for a reliable chromatogram, but it seems possible that Meda oil may have formed from hydrogen-rich source material when temperatures were near the maximum values responsible for the observed reflectances. The Meda oil has apparently been protected from bacterial and other alteration processes during migration and within the sandstone reservoir. It is quite different from the immature extract from the Permian Noonkanbah Formation of core 2 in Meda 1, which lies higher in the sequence at 592–599 m (Fig. 6). The latter has an n-alkane distribution with a large hump

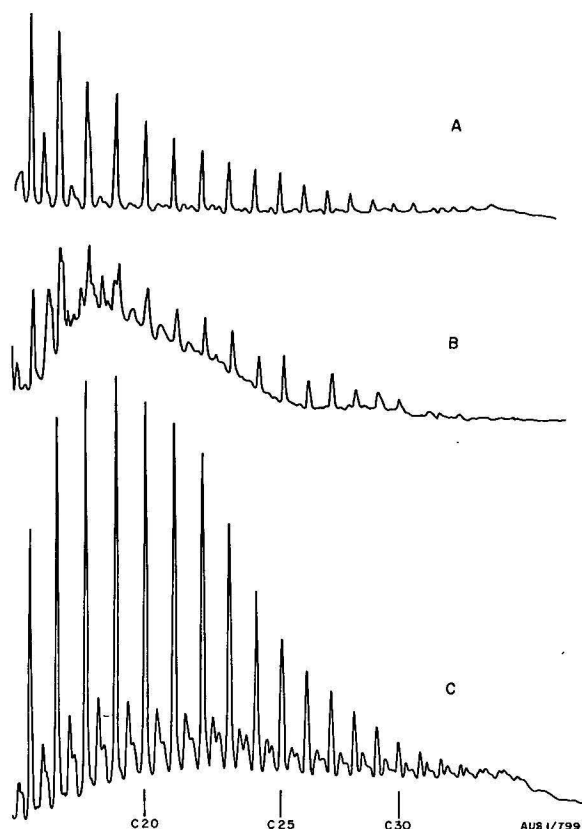


Figure 6. Gas chromatograms of n-alkane fractions, A—Meda 1, Crude Oil (1562 m). B—Meda 1, Core 2 (593.3 m). C—Grant Range 1, Core 56 (2432.5 m).

of unresolved branched and cyclic hydrocarbons comparable to that obtained when bacteria in flushing waters have in part preferentially removed n-alkanes from an oil or extract.

Upper Carboniferous/Permian prospects in the Fitzroy Graben

The Upper Carboniferous and Permian succession contains a variety of dominantly sandy clastic sediments deposited in paralic, fluvial and shallow-marine environments. Two main cycles of sedimentation may be distinguished. The first cycle was deposited from Stephanian or older times (Jones & others, 1973) to the Sakmarian. This coincided with the last episode of rapid subsidence in the Fitzroy Graben, and took place during a period of glaciation. Sprigg (1978) drew attention to the prolific production of organic source material during the warmer phases of the Permo-Carboniferous glacial succession throughout Australia, although he specifically excluded the Fitzroy Graben because of rapid downwarp. However the deposits of this first cycle of sedimentation, the Grant Formation, include a conspicuous dark shale and siltstone member. This member, the Winnifred Formation of Crowe & others (1978) is present throughout the Graben except in the region of Babrongan 1 and Myroodah I. It contains marine microfossils at the western end of the Graben (Crespin, 1958), and limestones in Sahara 1 area of the Kidson Sub-basin. This member is considered to have been deposited between two major glacial advances (Gorter, unpublished manuscript). Although no samples from it were analysed during this study, the presence of marine fossils and carbonaceous

material within it suggest that it may represent a potential source lithology.

The second cycle was deposited after a brief period of compressional tectonism (Crowe & others 1978); the cycle contains coals in the Poole Sandstone and Liveringa Group, abundant plant material in the Condron Sandstone, and limestone in the Noonkanbah Formation. It ranges in age from Sakmarian to Tatarian. High total organic carbon values are encountered in this sequence (Table 1), but are virtually confined to the Noonkanbah Formation. The Noonkanbah formation shows organic contents of up to 6 percent in the northern part of the Basin.

The vitrinite reflectance data of this study (Table 1) and the conclusions of Burne & Kanstler (1977) suggest that the Permian sequence is probably immature, except in parts of the Fitzroy Graben. In the graben varied development of anticlinal structures has resulted in complex burial histories for any given formation. Uplift in these structures provides one location where the present temperature is much less than the maximum temperature that the rocks have attained. The varying burial histories may be illustrated by comparing the present ambient temperatures and levels of organic metamorphism in wells from different structures (Fig. 3). Reflectance readings in the Noonkanbah Formation (e.g. .82% at 278 m in Point Moody 1) indicate the removal of at least 2000 m of sediment at this location. The indications are that the Noonkanbah Formation may be at a maturity level within the oil generation zone over much of the graben. The evidence from the reflectance data for an early attainment of maturity in the anticlines may mean that migration preceded the formation of the major anticlinal structures of the graben. This is considered unlikely, since these structures (Fig. 4) result from late Triassic compressional folding (Smith, 1968; Rixon 1978). Several wells have been drilled on such structures, but all have proved dry. This is not surprising since all the structures drilled seem to have been breached in the Jurassic and meteoric flushing of the potential Permian reservoirs has taken place. This applies to the Yulleroo, Barlee, St George Range, Grant Range, and Point Moody structures. However in parts of the southeast of the Graben, Triassic and Jurassic rocks overlie the Permian sequence (Yeates & others, 1975), and there exists the possibility of large unbreached unflushed structures sourced by the Noonkanbah Formation. The scant seismic evidence and the experimental model outlined by Rixon (1978) both suggest a continuation of the structural pattern of the western graben into the south-eastern part of the province.

Unfortunately, the best potential Permian reservoir lithologies underlie the Noonkanbah Formation and are found in the Poole Sandstone and sandstones of the Grant Group. Although down-sequence migration during the evolution of an anticlinal structure is possible, it is more likely that reservoirs to be fed from the Noonkanbah would be sandstones within or above the formation itself. The limited H/C data available for Noonkanbah Formation kerogen indicate that it is unlikely to be a source of liquid hydrocarbons (Table 2).

Conclusions

The Canning Basin has traditionally been considered to be one of Australia's most promising areas for petroleum exploration. Smith (1977) considers that the Canning Basin needs a more comprehensive seismic

coverage followed by several stratigraphic wells to enable a better assessment of its hydrocarbon potential. However, as pointed out by Burne & Kantsler (1977), despite apparently suitable levels of organic metamorphism, many of the apparently promising areas have already been unsuccessfully tested. The point has been made that because of the poor seismic data and the limited control available to early workers, many wells did not test valid objectives. However, a variety of wells have been drilled in the basin with the greatest success to date being the few gallons of oil recovered from the Fairfield Group in Meda 1.

Whilst the results of this study generally reinforce the conclusions of Burne and Kantsler (1977) and provide some explanation for the lack of exploration success, they do give some modest hope for the discovery of commercial hydrocarbons in the area. Although good source lithologies exist at suitable levels of organic metamorphism in the basin, they are not at optimum levels in the sequence to enable migration into the best reservoir lithologies. The slow rate of burial over much of the basin means that by the time maturation had occurred primary porosity had been lost in many potential reservoirs. Extensive periods of uplift, erosion, and groundwater flushing have adversely affected prospectivity, and, in the one area of rapid burial, the Fitzroy Graben, it is possible that oil migrated before the evolution of the Triassic structures.

The analyses show that some areas in the south of the Canning Basin have no petroleum potential. The best potential reservoir lithology in the basin is the Devonian Tandalgoo Red Beds of the Kidson Sub-Basin. This unit has porosities of up to 30 percent. However, both the aeolian Tandalgoo Red Beds and the underlying evaporitic Caribuddy Formation have no source potential. Similarly the Willara Sub-Basin samples show low organic carbon contents in the Ordovician succession, and there is an absence of suitable reservoir lithologies.

The source rock analyses provide evidence favouring oil accumulation in the Ordovician on the Broome Arch, but the most promising areas have already been adequately tested with no success, because of tight Ordovician formations and a lack of seal on overlying Permian formations. Similar Ordovician sourced prospects exist on the terraces adjacent to the Fitzroy Graben, and have been tested without success in the vicinity of Tappers Inlet 1.

The Upper Devonian Gogo Formation has moderate source potential, and the possibility of migration into porous carbonates at the margin of the Graben provides some attractive prospects. However, the deeper parts of the formation are likely to be supermature, and at this stage little can be said about the degree of porosity development in the buried part of the Lennard Shelf reef trend. Our data show that the Upper Devonian carbonates north of the graben seem to have little source potential, although minor areas of organic-rich sediments are implied by the analyses. South of the graben the lack of seal to the carbonates counterbalances their slightly more encouraging organic carbon content.

Source rock analyses and hydrocarbon shows confirm that the post-carbonate Upper Devonian and Lower Carboniferous sequence contains good source lithologies. However the prospectivity of this sequence is limited by the poor porosity and small size of potential Fairfield Group reservoirs, and by the lack of seal over much of the overlying Anderson Formation.

The Upper Carboniferous/Permian succession in the southeastern Fitzroy Graben appears to have favourable characteristics for the generation and retention of pooled hydrocarbons, sourced from the Noonkanbah Formation, in anticlinal structures. However the maturity of the kerogen in this formation may not always be adequate. Where erosion has caused the present temperature to be less than the past maximum, the possibility of hydrocarbon loss in poorly sealed traps is increased.

Since the source rocks stratigraphically overlie the best potential Permian reservoirs of the Poole Sandstone and the Grant Formation, it seems likely that sandstones within the Noonkanbah Formation itself would have to form the prospective reservoir in this area.

In areas of Triassic cover in the southeast it might be hoped that structures will not have suffered the breaching and flushing experienced by their counterparts in the northwestern part of the graben. Such accumulations might well be large, if the area of closure in anticlines in the northwest of the Graben is any indication, but the remoteness of the area would probably mean that only a large hydrocarbon deposit would be economic to develop. Available H/C data on kerogen indicate that liquid hydrocarbons are unlikely, and not even gas is a possibility unless sufficiently high maximum palaeotemperatures have been reached in post-Triassic time.

We conclude that there is modest hope for future hydrocarbon exploration in the Basin, although the generally poor quality of both source rocks and reservoir rocks encountered in the scattered drilling undertaken so far indicate that the Basin may never become a major hydrocarbon producing province.

Acknowledgements

We acknowledge the assistance of A. Bennett (reflection), L. Bruen (extraction and gas chromatography), and the members of the former Detailed Basin Study Group, BMR. The manuscript benefited from the comments of M. Johnstone, R. Towner, and K. Jackson. The figures were drawn by G. Clarke.

References

- BROWN & CAMPBELL, 1974—Contention Heights No. 1 Well, WA. Well Completion Report. *Australian Aquitaine Petroleum Pty Ltd, PSSA Report 73/230*.
- BURNE, R. V. & KANTSLER, A. J., 1977—Geothermal constraints on the hydrocarbon potential of the Canning Basin, Western Australia. *BMR Journal of Australian Geology & Geophysics*, 2, 271-88.
- CRISPIN, I., 1958—Permian foraminifera of Australia. *Bureau of Mineral Resources, Australia, Bulletin 48*.
- CROWE, R. W. A., TOWNER, R. R. & GIBSON, D. L., 1978—Permian and Mesozoic geology of the Derby and Mount Anderson 1:250 000 Sheet areas, Western Australia. *Bureau of Mineral Resources, Australia, Record 1978/8*.
- DICKEY, P. A., & HUNT, J. M., 1972—Geochemical and hydrogeologic methods of prospecting for stratigraphic traps. *American Association of Petroleum Geologists Memoir 16*, 136-67.
- DRUCE, E. C., & RADKE, B. M., 1979—The geology of the Fairfield Group, Western Australia. *Bureau of Mineral Resources, Australia, Bulletin 200*.
- HOOD, A., & CASTANO, J. R., 1974—Organic metamorphism; its relationship to petroleum generation and application to studies of authigenic minerals. *United Nations ESCAP, CCCP Technical Bulletin 8*, 85-118.

- HORSTMAN, E. L., LYONS, D. A., NOTT, S. A., & BROAD, D. S., 1976—Canning Basin, On-Shore. In LESLIE, R. B., EVANS, H. J., & KNIGHT, C. L. (Editors), ECONOMIC GEOLOGY OF AUSTRALIA AND PAPUA NEW GUINEA, 3. PETROLEUM. *Australasian Institute of Mining and Metallurgy, Melbourne*, 170-84.
- JONES, P. J., CAMPBELL, K. S. W., & ROBERTS, J., 1973—Correlation chart for the Carboniferous System of Australia. *Bureau of Mineral Resources, Australia, Bulletin 156A*.
- KOOP, W. J., 1966—Recent contributions to Palaeozoic geology in South Canning Basin, W.A. *APEA Journal* 6, 105-9.
- LOGAN, B. W., & SEMENIUK, V., 1976—Dynamic metamorphism; processes and products in Devonian carbonate rocks, Canning Basin, Western Australia. Edited by B. D. WEBBY. *Geological Society of Australia, Special Publication 6*.
- PLAYFORD, P. E., 1969—Devonian carbonate complexes of Alberta and Western Australia. *Geological Survey of Western Australia, Report 1*.
- PLAYFORD, P. E., 1976.—Devonian reef complexes of the Canning Basin, Western Australia. *25th International Geological Congress Guidebook, Excursion 38A*.
- PLAYFORD, P. E., & LOWRY, D. C., 1966—Devonian reef complexes of the Canning Basin, Western Australia. *Geological Survey of Western Australia, Bulletin 118*.
- POWELL, T. G., & MCKIRDY, D. M., 1976—Geochemical character of crude oils in Australia and Papua New Guinea. In LESLIE, R. B., EVANS, H. J., & KNIGHT, C. L. (Editors), ECONOMIC GEOLOGY OF AUSTRALIA AND PAPUA NEW GUINEA, 3. PETROLEUM. *Australasian Institute of Mining and Metallurgy, Melbourne*, 18-29.
- RASIDI, J. S., 1978—Buried reef structures in the Lennard Shelf, Canning Basin, Western Australia. *BMR Journal of Australian Geology & Geophysics*, 3, 80-3.
- RIXON, L. K., 1978—Clay modelling of the Fitzroy Graben. *BMR Journal of Australian Geology & Geophysics*, 3, 71-6.
- SAXBY, J. D., 1978—The organic geochemistry of oil and gas generation and its application to Bass Strait and the Northwest Shelf. *APEA Journal* 18, 137-42.
- SMITH, J. G., 1968—Tectonics of the Fitzroy wrench trough, Western Australia. *American Journal of Science*, 266, 766-76.
- SMITH, E. R., 1977—Australia's onshore basins: Their petroleum prospects and future exploration programmes. *APEA Journal*, 17, 17-23.
- SPRIGG, R. C., 1978—Proterozoic, Permo-Carboniferous and Pleistocene glacial cycles and cyclic sedimentation in relation to oil search. *APEA Journal*, 18, 83-92.
- VEEVERS, J. J., & WELLS, A. T., 1961—The geology of the Canning Basin, Western Australia. *Bureau of Mineral Resources, Australia, Bulletin 60*.
- YEATES, A. N., CROWE, R. W. A., TOWNER, R. R., WYBORN, L. A. I., & PASSMORE, V. L., 1975—Notes on the geology of the Gregory Sub-Basin and adjacent areas of the Canning Basin, Western Australia. *Bureau of Mineral Resources, Australia, Record 1975/77*.

The effects in Western Australia of a major earthquake in Indonesia on 19 August 1977

P. J. Gregson, E. P. Paull, & B. A. Gaull

The Indonesian earthquake of 19 August 1977, with a magnitude (M), 8 was felt in Western Australia up to distances of 2600 km. The maximum ground intensity felt was MM V in northwest towns up to 1100 km from the epicentre. The ground intensity in Perth, 2300 km from the epicentre, was MM III or less. Resonance of multi-storey buildings resulted in an eight-fold amplification of peak ground acceleration on the upper floors. Only minor damage occurred in Perth. Seismic sea waves up to six metres in height were reported several hours after the earthquake at towns along the northwest coast. There were no reports of damage associated with these waves. They arrived along the coast near low tide, otherwise there could have been some flooding. An examination of data from the Sunda arc region, for the period 1900-1977, suggests that about eight earthquakes of magnitude greater than 7.5 could occur in this region every hundred years. Of these, two or three may be felt in Western Australia. The 1977 earthquake was the largest and closest to Western Australia since 1900 and its effects are the maximum likely to be experienced from this region.

Consideration should be given to installing accelerographs in selected buildings in Perth.

Introduction

A large area of Western Australia was shaken by a major earthquake which occurred on 19 August 1977. The earthquake was located about 900 km northwest of Broome, in one of the world's most active seismic areas, the Sunda arc.

There were no casualties in Australia and only a few reports of minor damage. The most severe effects were felt in the northwest towns of Port Hedland, Broome, and Derby. Although the ground movement in Perth was less than for the Meckering earthquake, the duration was longer and resonance of the tall buildings produced easily detectable movement on the upper floors. Several high-rise buildings in Perth were evacuated. In Port Hedland, the town's power supply was cut and shoppers ran from shops.

Seismic sea waves occurred along the northern Western Australian coast with wave heights (crest to trough) up to six metres.

Instrumental data

The shock waves from the earthquake saturated all the seismographs, with the exception of the Wood Anderson seismograph at Mundaring.

Earthquake details given by the US Geological Survey are:

Latitude: 11.09°S
Longitude: 118.46°E
Depth: 33 km
Origin time: 06h 08m 55.2s U.T.
Magnitude: MB 7.0; MS 7.9-8.0

Data related to ground motion at Mundaring and Marble Bar are given below. Figures given for Marble Bar are estimations for the main shock based on data from aftershocks of magnitude (mB) = 5.

Isoseismals

Because of the large, relatively unpopulated areas in Western Australia, the available information is sporadic, but of sufficient value to give some idea of the extent of the MM II to IV intensities (see Fig. 1).

The maximum ground intensities observed in Western Australia was along the northwest coastline, where the

	Mundaring	Marble Bar (Vertical component)
Time of maximum	40s after S arrival	—
Maximum trace amplitude	0.3×10^{-3} m	0.15×10^{-3} m
Period	0.9s	0.5s
Ground acceleration	4×10^{-3} m/s ²	2.3×10^{-2} m/s ²
Duration of acceleration $\geq 1 \times 10^{-3}$ m/s ²	approx. 7 mins with periods 0.5s to 1.3s	—
Peak surface wave amplitude	10^{-2} to 10^{-3} m	—
Surface wave period	10s to 100s	—

value approached MM V. The earthquake was felt in Albany and Esperance (2600 km) with intensity MM II. One experienced observer felt the earthquake in Adelaide (3300 km). For comparison, the Alaskan earthquake (M 8.5) of 28 March 1964, was perceptible over a radius of the order of only 1000 km (Kachadoorian, 1964). Milne & Davenport (1969) suggest that transmission efficiency of seismic energy is enhanced with homogeneity of the crustal structure.

This factor could explain the unusually low attenuation of seismic energy in Western Australia following the Indonesian earthquake. It may also explain why the isoseismals were elongated in the southerly direction (Fig. 1), along the Precambrian shield of Western Australia.

In Figure 1 the mean isoseismal radii for intensities MM IV, MM III and MM II were about 1000 km, 1500 km, and 2000 km respectively. Comparisons of these values were made with those obtained by Milne & Davenport (1969) in the Canadian shield zone, and by Gaull (in prep.) in Papua New Guinea. Milne & Davenport (1969) results have been taken from a graphical presentation of their data for an M 8 earthquake. Gaull's values have been obtained from the following formula for an M 8 earthquake of depth 33 km.

$$I = 1.5M - 2.5 \log (d^2 + 3h^2/2) + 1.5 \log h + n$$

where I = MM intensity

M = magnitude; MS = 8.0

n = empirical constant = 4

d = isoseismal radius (km)

h = focal depth = 33 km

The data are summarised in the following table:

Intensity boundary	Observed mean radii km	Milne & Davenport (1969) km	Gaull (in prep.) km
IV	1000	1500	700
III	1500	1750	1150
II	2000	2050	1800

Effects on Perth buildings

Introduction

Data on the effects of the earthquake in Perth were obtained from personal interviews supplemented by information from questionnaires. Intensity estimates varied from MM II-III at ground level, to MM V-VI on the upper floors of multi-storey buildings. This amplification has been attributed to building resonance.

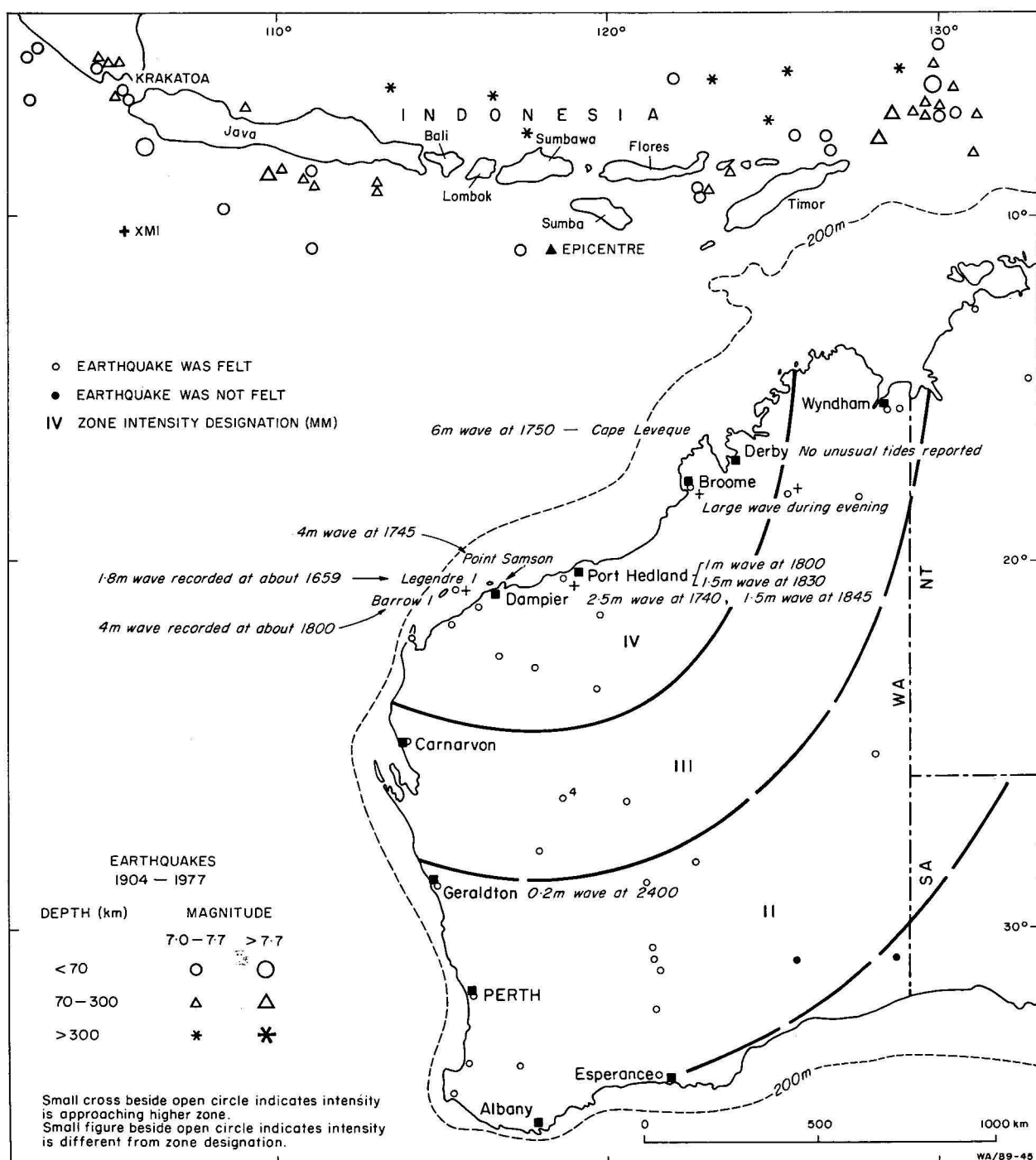
A summary of the intensity estimates at various levels in the buildings is presented in Gregson & others (1978).

Ground motion in Perth

An estimate of the peak ground acceleration (A) in Perth of $3 \times 10^{-2} \text{ m/s}^2$ was obtained from the ground intensity (I) of MM II-III using the empirical relation:

$$\log A = \frac{I}{3.1} - 2.3 \quad (\text{Gaull, in prep.})$$

This is about 7.5 times the peak acceleration recorded at Mundaring. A difference of acceleration of this order is to be expected between the Precambrian granite at Mundaring and the unconsolidated sediments of the Perth Basin. Gaull (1976) has previously reported similar amplifications in Papua New Guinea.



All conversions from intensity to peak acceleration and vice versa in the text have been calculated using the above relation.

Effects in the buildings

Buildings between 5 and 15 storeys registered the greatest average maximum intensity of MM V+. This is equivalent to a peak acceleration of 0.23 m/s^2 . Average maximum intensities in high-rise buildings (greater than 15 storeys) and low-rise buildings were MM V and MM III+ respectively (equivalent to peak accelerations of 0.15 m/s^2 and 0.06 m/s^2 respectively).

Confirmation of the order of the estimates of peak building acceleration stated above was provided by an observation of oscillating saline solution in the third floor of the 5-storey Red Cross Transfusion Centre. The peak amplitude and period of the wave motion of the solution inside the 20 cm trough was reported as about 2.5 cm and 0.5s respectively. By reproducing this wave motion in the laboratory it was determined that the peak acceleration of the bench supporting the trough was about 0.13 m/s^2 . This compares well with the estimated peak acceleration of 0.17 m/s^2 on the fifth floor.

No structural damage occurred in the buildings of Perth. The minor damage that did occur was confined to the middle-rise buildings and is listed in Gregson & others (1978). The main features of this damage is tabulated below.

Structural type	No. of storeys	Floor level of damage	Cracks, type and material	Other damage
Load-bearing brick	8	8	5 mm shear (in bricks), diagonal miscellaneous	Minor spalling from expansion joints
Reinforced concrete	12	9-12	Plaster cracks, one in gypsum wall	Ducting moved 2 mm
Reinforced concrete	13	11	Minor	—
Reinforced concrete	15	12	Corner	Ceiling tiles drooped; exterior stone chips flaked off

Note: Most of the cracks were reported as re-opened, enlarged or extensions of old cracks.

Building response

A suspended lamp of pendulum length 30 cm (natural period, $T = 1\text{s}$) on the 10th floor of a 12-storey building in Perth, was described as swinging with such a large amplitude that it almost touched the ceiling. A nearby lamp of pendulum length 60 cm ($T = 1.5\text{s}$) swung with about half the amplitude. Hence the natural period of the building must have been close to 1s. This fits in well with the formula $T = 0.1n$, where n is the number of storeys in the building (Standards Association of Australia, 1976).

All evidence presented suggests that the buildings with $n = 5$ to 15 were driven into greater resonance than those with $n < 5$ or $n > 15$, which means that the period of the driving signal must have been closer to the natural period of these middle-rise buildings. Thus the power spectrum of the seismic signal arriving at the base of the buildings in the city block must have been such that the greater part of the energy was within the period limits of 0.5 and 1.5s. These limits compare well with the ground periods at which the greatest amplitudes were recorded at Mundaring.

Other observations made during the survey were:

- In any one building, seismic intensities generally increased with floor level in all but the tallest buildings.
- There was no apparent correlation between amplification effects and structural type.

The tallest buildings in Perth were probably mainly resonating in the second mode of vibration. This is considered to be so because:

- The intensity in a 30-storey building in Perth did not necessarily increase with floor level—possibly owing to a nodal effect.
- The period of the second mode of vibration of a 30-storey building is close to 1s—the wave period at which most of the earthquake energy occurred.
- The average maximum intensity was lower on the 30-storey buildings than the middle-rise buildings, which were probably resonating in the first mode of vibration.

Peak acceleration at roof level of multi-storey buildings in Perth was about eight times greater than the ground acceleration. This was double the effect registered in the buildings of San Fernando during the earthquake of 1971 (Murphy, 1973). The probable reason for the relatively high amplification in Perth is that the period of ground motion matched the natural period of the middle-rise buildings for a much longer duration than in San Fernando. This would allow a greater resonance effect to take place.

Accelerographs

Had accelerographs been installed in some high-rise buildings in Perth, they would almost certainly have been triggered during the August 1977 earthquake. The resulting accelerograms would have been invaluable in quantifying building response. A recommendation is therefore made for the installation of three accelerographs in selected buildings in Perth. The accelerographs would be located somewhere on the top floor, about the middle floor, and on the ground floor in any one building. In the event of an earthquake, it is likely that the accelerograph at the top would be subjected to the greatest acceleration and therefore would be used as a 'master' to switch on the two 'slaves' located below. The buildings chosen for this purpose should provide as much variation in size, shape and type as possible.

Earthquake risk to Perth buildings

All other factors being equal, the risk of damage during an earthquake increases as the period of the ground motion approaches the natural period of structures.

This was demonstrated on 19 August 1977 when the large Indonesian earthquake generated greater amplification of ground acceleration in the Perth middle-rise buildings than any other type. However, the effects of this earthquake in Perth are not likely to be greatly exceeded by future earthquakes from this source, as this was one of the largest earthquakes recorded in the Sunda arc region. From earthquake frequency data in this region, the return period of such an event is estimated to be of the order of 100 years.

A greater threat to buildings in Perth come from the southwest seismic zone of Western Australia. For example, during the Meckering earthquake of October 1968, greater damage was incurred than in the Indonesian event. On this occasion the greatest damage was

confined almost exclusively to the low-rise buildings. It is proposed that this was owing to a close match between the natural period of these buildings and the ground period. Evidence to support this is supplied by Denham & others (1973), who showed that most of the seismic energy recorded at distances in the order of 100 km from moderate to large earthquakes in Papua New Guinea is at ground periods from 0.15 to 0.5 s. Most low-rise buildings have a natural period in this range.

It is suggested that during the Meckering earthquake the low-rise buildings in Perth amplified the estimated peak ground acceleration of 0.2 m/s^2 (MM V) to up to 0.9 m/s^2 (MM VII) at the top of the buildings. There are descriptive, photographic, and numerical examples to support this statement in Everingham (1968), and Everingham & Gregson (1970). Building resonance in the middle-rise and taller buildings of Perth could only have occurred during the passage of the surface waves. Only these waves could have had both period and amplitude characteristics to set up a significant resonance effect. By comparison with the San Fernando earthquake (Murphy, 1973), it is estimated that the middle-rise buildings would have amplified the surface waves by a factor of four. However, because the peak amplitude of the surface waves was estimated to have been only about one-half of the body waves (Everingham & Gregson, 1970) the resultant building acceleration is estimated to have been 0.4 m/s^2 (MM VI). High-rise buildings probably experienced less amplification than the middle-rise buildings. The return period of an equivalent Meckering earthquake in the southwest seismic zone is estimated to be about 100 years (Everingham & Gregson, 1970).

Earthquakes arising from other regional seismic zones of Australia occur so infrequently and are so distant from Perth that they do not represent a real threat to the buildings of Perth. A summary of earthquake risk in Perth buildings is presented below.

Source of earthquake	Estimated peak acceleration in Perth buildings (m/s^2)			Estimate return period (yrs)
	Low-rise	Middle-rise	High-rise	
Sunda arc	0.1	0.3	0.2	100
SW seismic zone	0.9	0.4	0.4	100

Note: Greater peak accelerations could possibly be experienced over much longer time spans, but owing to the limited planned life time of a building, these values are of less interest.

From the earlier discussion it is apparent that structures in Perth with natural periods in the range 0.15 to 0.5 s (e.g. low-rise buildings) are at the greatest risk of earthquake damage than any other and therefore aseismic design and building standards should not be relaxed for this type of structure. Also, providing tall buildings are constructed to the high standard set by the suggested code (Australian Standards Association, 1976) the occupants of such buildings are probably safer than those in the low-rise buildings. The wisdom of evacuating people from high-rise buildings is questionable. People standing in streets are in more danger from falling debris shaken from buildings than from being injured inside the building.

Effects in northwest towns

The maximum effects from the earthquake were experienced in the northwest towns of Port Hedland, Broome and Derby. The typical effects of rattling win-

dows, shifting or overturning of small objects and ornaments, and liquids being disturbed, indicate intensity MM V. The major ground movement reported was east-west which corresponds to the passage of the S wave.

The Marble Bar seismograms showed that the period of ground motion at which peak acceleration was reached, was about 0.5 s, which corresponds to the natural period of 5-storey buildings.

A report from the Port Hedland Control Tower (27 metres high) stated that there was a strong and rapid vibration increasing in intensity to such an extent that the observer left the building. Another report from the top floor of a 6-storey building indicated an intensity close to MM VI. These two reports show that the ground movement was amplified in the taller buildings.

The tsunami

The seismic sea wave generated by this earthquake wreaked havoc on the Indonesian Islands of Sumba, Sumbawa, and Lombok. Almost 150 people died or are missing, and losses amounted to one million dollars, including houses, boats, and fishing gear. An investigating team reported a maximum wave height of 5.5 m above MSL at Kuta on Lombok Island (ITIC, 1977). The tsunami arrived near low tide, so that the actual height of the wave above tide level at the time would have been greater.

Fortunately, the effects experienced along the Western Australian coastline were much less severe. As far as is known, the only damage or property loss was by rock fishermen on Barrow Island (see Figure 1). The fishermen were wet by a 4 m high wave at about 1800 WST; some of them lost fishing gear. Three more waves followed, decreasing in size. The report of the largest wave, 6 m high, at about 1750 WST, came from the lighthouse keeper at Cape Leveque. At Point Samson, six to eight 4.6 m high waves were observed at 1745 WST. In Dampier Harbour, four waves 2-2.5 m in height were observed at 1740 WST. No damage occurred, but a tug berthed at the seismic wharf broke mooring lines and a 165 000 tonnes DWT ore carrier berthed at East Intercourse Island ranged 12 m, controlled by her tension winches.

Two tide gauges located in Dampier Harbour recorded waves commencing at 1730 WST, with maximum height above sea level of 0.4 m and period between 15 and 34 minutes. Unusual activity was still evident the next day at 1400 WST. At the time of the tsunami, a wave rider buoy was being operated near Legendre Island, 34 km north of Dampier, by Woodside Petroleum Pty Ltd. This gave the earliest recorded wave arrival time of 1659 WST. Two more waves followed in the next 12 minutes. Maximum height was 1.2 m above sea level for the first wave, with a period of 30 seconds. This wave height must be regarded as conservative, as the buoy only responds to waves of periods less than one minute, whereas tsunami waves are long-period waves usually in the range 15 minutes to several hours. The wave rider buoy would thus only record any high frequency component in the wave, namely the crest of the wave. The travel time to Legendre Island of 2 hrs 50 mins gives an average velocity of 366 km/h.

Another tsunami report came from Port Hedland where at about 1800 WST, three waves 1 m high were observed from an incoming ship. At 1830 WST, a wave 1.5 m high was reported from another ship anchored

12 km north of the town. At Cable Beach, an exposed westerly-facing ocean beach near Broome, a large wave was reported during the evening causing people to flee from its path. Broome itself is situated in Roebuck Bay, the entrance to which faces south, so protecting the town from the tsunami. A tide gauge in the harbour recorded 12 minute-period waves with maximum amplitude of 2.5 cm commencing at 1742 WST. No unusual waves were reported from Derby. This is not surprising, as the town lies in the lee of Cape Leveque at the end of King Sound. The entrance to the south is shallow and cluttered with small islands, coral reefs, and shoals.

Coastal towns south of North West Cape lie in the lee of the Cape; they would only receive diffracted waves with, as a consequence, lesser effects. No tsunami effects could be expected along the south coast of Western Australia. A tide gauge at Geraldton recorded waves commencing at 2120 with periods between 22 and 38 minutes. The maximum wave height was 0.2 m at 2400. No unusual waves were noticed on tide gauge records from Wyndham, Fremantle, Albany or Esperance. Gauges at Port Hedland and Carnarvon were unserviceable. For more detailed information on tsunami effects and tide gauge recordings see Gregson & others, 1978.

Previous tsunamis

A tsunami was observed along the Western Australian coast after the Krakatoa eruption of 27 August 1883. The following reports were obtained from a record published by the Bureau of Meteorology (1929). The tide at Geraldton rose to eight feet (2.4 m) at 8 p.m., and again at 8.30 p.m. on 29 August. At Carnarvon on 28 August, a succession of tidal waves 3 to 4 feet (0.9 to 1.2 m) high occurred, causing a rise and fall of the tide three times in one and a half hours. On 30 August and the following two days, the tides were still irregular. At Cosack (near Point Samson) an extraordinary tide set in at 4.30 p.m. on 27 August and rose nearly 5 feet (1.5 m), then ebbed just as rapidly, all in 30 minutes. For some days afterwards, tides were erratic. A similar report was received from Ashburton, except that the tide occurred at midday. Noises were heard at Derby on the morning of 27 August, as if the banks of the Sound, some 3 miles (5 km) away, were falling in. Nothing extraordinary was noticed in the tide, however.

Another tsunami was experienced at Geraldton on 5 January 1885 (Everingham & Tilbury, 1971). The town was shaken by an earthquake at about 10.25 p.m. The intensity of shaking was quite severe, possibly MM IV. Shortly after the shock, the sea subsided about one metre, but there was no significant rush of tide; the water rising gradually.

Discussion

Western Australia is fortunate in having a wide, shallow continental shelf. For large tsunami wave heights to develop, the transition from deep sea floor to coastline must be sudden. It is therefore unlikely that severe tsunami effects will ever be experienced in Western Australia, either from a close offshore earthquake as in the case of Geraldton in 1885, or from more distant earthquakes. Further, the towns most at risk, i.e. those on the coast between North West Cape and Derby, are also those which have a sizeable range in tide (3 m at North West Cape to 11 m at Derby). It would be necessary for the largest tsunami wave to arrive near high tide for much damage to be done.

Had the tsunami from this recent earthquake coincided with high-water spring tide and not low tide, some coastal flooding might have resulted, with the possibility of damage, and loss of life. Those most at risk are rock fishermen or people on low-lying islands or low-lying coastal areas.

Considering the infrequency and probable moderate size of tsunamis on the Western Australian coastline, it would not seem justified for Western Australia to establish a costly tsunami warning system. Tsunamis are, however, notably unpredictable and there is no guarantee that damaging waves will never strike the Western Australian coast. Consideration should be given to collaborating with the existing Pacific Tsunami Warning Centre in Honolulu. This Centre routinely locates all earthquakes in the Pacific Ocean of sufficient magnitude to generate a tsunami (this includes the Sunda Arc region—the earthquake of 19 August was located by the Centre). If the epicentre is under or near the ocean a tsunami-watch warning is issued. When confirmation of a tsunami is received, the Centre issues a tsunami warning. An earthquake felt in coastal areas is of course a natural tsunami warning just as if the sea level suddenly falls or rises. Residents should keep clear of low-lying coastal areas and listen to the radio for the location of the earthquake and any tsunami information.

Seismicity and earthquake frequency

The Sunda arc region is among the most seismically active regions of the world. The region extends from the east through the lesser Sunda islands of Timor, Flores, Sunda, Sumbawa, Lombok, and Bali to the greater islands of Java and Sumatra, up to the Nicobar and Andaman islands.

The arc turns north at about longitude 105°E. Earthquakes north of this point have no significance with relation to effects in Western Australia as they are too far away. Fifty-one earthquakes of magnitude 7 or more have occurred in the eastern part of the region between 1900 and 1977 (see Fig. 1). Of these, only five had a magnitude greater than 7.5 (see below).

Year	Latitude °S	Longitude °E	Depth (km)	Magnitude (M)
1903	8	106	—	8.1
1917	7½	128	100	7½
1918	7.0	129.0	190	8.1
1943	8.6	109.9	90	7½
1950	6.5	129.5	60	8.1
1977	11.1	118.4	Shallow	8.0

The earthquake of 1917 is the only other reported as having been felt in Western Australia (Everingham, 1968). This was felt as a slight tremor at Wyndham lasting five seconds.

It would not be unreasonable to expect about eight earthquakes of magnitude greater than 7.5 to occur every hundred years in the Sunda arc region. Of these, two or three may be felt in Western Australia. Of the earthquakes listed above, the most recent is the largest and also the closest to Perth and northwest coastal towns. It is therefore unlikely that the effects, with perhaps the exception of tsunami effects, will ever be greater than those for the recent earthquake.

Conclusions

Large earthquakes in the Sunda arc region can be felt in Western Australia and cause minor damage in

some centres. Records show that of the eight or so major earthquakes expected to occur in the Sunda arc region every hundred years, two or three could be felt in Western Australia. The earthquake of 19 August 1977 was one of the largest and closest to Western Australia recorded from the region this century, with the possible exception of tsunami effects, and the effects are likely to be the maximum experienced in Western Australia.

Significant effects from this earthquake were:
(a) Maximum intensities and estimated peak accelerations at various localities were:

Place	Maximum MM intensity	Estimated peak acceleration
Mundaring (granite outcrop)	I	$4 \times 10^{-3} \text{ m/s}^2$
Perth (ground)	II+	3×10^{-2}
Perth (1-4-storey buildings)	III+	5×10^{-2}
Perth (5-15-storey buildings)	V+	2.5×10^{-1}
Perth (>15-storey buildings)	V-	1.5×10^{-1}
Northwest towns (ground)	V	2×10^{-1}
Northwest towns (5-storey buildings)	VI	4×10^{-1}

- (b) Damage reports in Perth, such as re-opening of old cracks, were confined to middle-rise buildings. This is probably because the period of the seismic waves matched the natural period of vibration of these buildings.
- (c) The high-rise buildings of Perth are considered to be relatively safe in terms of earthquake risk, compared with the low-rise buildings. It is considered that the dangers of evacuating high-rise buildings in Perth during earthquakes in the Sunda arc region are greater than remaining in the building.
- (d) Seismic sea waves up to 6 m in height occurred along the northwest coast between three and five hours after the earthquake. The waves arrived near low tide and no damage resulted. Had the waves arrived at high-water spring tide there could have been some coastal flooding.

Acknowledgements

The authors wish to thank the numerous observers and companies, particularly those who supplied information during interviews or completed questionnaires. Especial thanks are due to the State Public Works

Department and Pilbara Harbour Services for providing copies of tide gauge recordings, to Woodside Petroleum Development Pty Ltd, for a copy of the wave rider buoy recording, and to the State Geological Survey for reports of damage. The text figure was drawn by G. Clarke.

References

BUREAU OF METEOROLOGY, 1929—Results of rainfall observations made in Western Australia. *Government Printer, Melbourne*.

DENHAM, D., SMALL, G. R., & EVERINGHAM, I. B., 1973—Some strong motion seismic results from Papua New Guinea. *Bureau of Mineral Resources, Record 1973/13* (unpublished).

EVERINGHAM, I. B., 1968—The seismicity of Western Australia. *Bureau of Mineral Resources, Australia, Report 32*.

EVERINGHAM, I. B., & GREGSON, P. J., 1970—Meckering earthquake intensities and notes on earthquake risk for Western Australia. *Bureau of Mineral Resources, Australia, Record 1970/97* (unpublished).

EVERINGHAM, I. B., & TILBURY, L., 1971—Information on Western Australian earthquakes which occurred during the periods 1849-1900 and 1923-1960. *Bureau of Mineral Resources, Australia, Record 1971/40* (unpublished).

GAULL, B. A., 1976—Accelerograph recordings of the Musa earthquake, 16 September 1972. *Bulletin of the New Zealand Society of Earthquake Engineering*, **9**, 115-21.

GAULL, B. A., in prep.—Attenuation and amplification of seismic energy in Papua New Guinea. *Bureau of Mineral Resources, Australia, Record* (unpublished).

GREGSON, P. J., PAULL, E. P., & GAULL, B. A., 1978—The Indonesian earthquake of 19 August 1977: effects in Western Australia. *Bureau of Mineral Resources, Australia, Record 1978/19* (unpublished).

ITIC, 1977—Tsunami report No. 1977-12. *International Tsunami Information Center, Hawaii*.

KACHADOORIAN, R., 1964—Effects of Alaska's Good Friday earthquake on land. *Transactions of American Geophysical Union*, **45**, 634.

MILNE, W. G., & DAVENPORT, A. G., 1969—Distribution of earthquake risk in Canada. *Bulletin of the Seismological Society of America*, **59**, 729-54.

MURPHY, L. M., 1973—San Fernando, California earthquake of 9 February 1971. *US Government Printing Office, Washington*.

STANDARDS ASSOCIATION OF AUSTRALIA, 1976—Draft: Australian standard rules for the design of earthquake resistant buildings. *Standards Association of Australia Committee BD/12*.

Seismic refraction — a tool for studying coral reef growth

N. Harvey¹, Peter J. Davies, & John F. Marshall

Seismic refraction studies have been conducted in close proximity to shallow boreholes previously drilled at Bewick (Northern Great Barrier Reef), Hayman (Central Great Barrier Reef) and Heron Islands (Southern Great Barrier Reef). Results show a seismic discontinuity at depths similar to the unconformity separating Holocene and pre-Holocene carbonates in the boreholes.

Extensive seismic refraction studies have been conducted in the Capricorn/Bunker Reefs to assess the effects of substrate on modern reef growth, and the classification of modern reefs in the area. One hundred and twenty-four profiles were completed on six reefs. A marked seismic discontinuity, detected at depths ranging from 8-23 m, is equated with the Holocene/pre-Holocene unconformity identified in the boreholes. Results show that the pre-Holocene surface forms a central depression with a raised rim around the perimeter beneath those reefs which have lagoons. This also appears to be the case beneath those reefs which presently have small or no lagoons, the inference being that Holocene sedimentation and growth have infilled the original depressions.

The geophysical evidence does not support the claim that reefs of the southern Great Barrier Reef follow a latitudinal genetic sequence, but rather that the varied growth forms of the Holocene reefs have been determined to a considerable extent by the shape of the pre-Holocene surface.

Introduction

The principal source of data for studies of Pleistocene to Holocene reef development in the Great Barrier Reef has been the cores obtained from boreholes at Bewick and Stapleton Reefs (Thom & others, 1978), Hayman Island (Hopley & others, 1978), and Heron Island (Richards & Hill, 1942). Dated core material from the northern (Thom & others, 1978) and central (Hopley & others, 1978) Great Barrier Reef show that a Holocene/pre-Holocene boundary exists at depths of between 4 and 20 m. Radiocarbon dates recently obtained from the Heron Island borehole (Davies & Marshall, in press) indicate that at a depth of 15 to 21 m the sequence is Pleistocene. This confirms Davies' (1974) interpretation of a solution unconformity at this depth.

The unconformity between the Holocene and pre-Holocene seen in the boreholes is clearly a widespread subsurface feature, and should be possible to trace by quicker methods than drilling. We have applied the seismic-refraction technique to this problem, the rationale being that a seismic discontinuity exists at the interface between the Holocene reef and its pre-Holocene substrate. Such a velocity contrast was detected by Dobrin & Perkins (1954) at Bikini, at depths similar to the solution unconformity identified from drill core (Schlanger, 1963). Similar velocity contrasts have been detected beneath modern reefs in the Great Barrier Reef (Harvey, 1977a; Davies & others, 1977b), and are believed to be related to the mineralogical and textural alteration which has occurred below solution unconformities similar to that described in the Heron Island borehole (Davies, 1974). This makes the seismic refraction method a useful tool in determining the depth and shape of the unconformity and the thickness of the Holocene reef, i.e. without recourse to a costly drilling programme. Such data have important applica-

tion to problems of reef growth, and to the origin of the growth substrate.

The aims of this paper are to relate the seismic discontinuity to the solution unconformities recognised in the boreholes, and to present the results of extensive seismic refraction surveys on certain reefs of the Capricorn and Bunker Groups. Using these data the effects of substrate on modern reef growth are discussed, and comment is made on genetic classifications of reefs based on two-dimensional morphological/sedimentological analyses.

Instrumentation and methods

Shallow seismic-refraction profiles were conducted using a Huntec FS3 portable facsimile seismograph. This is a single channel time-distance plotting instrument, which permanently records an entire seismic event produced either by a hammer or explosive sound source. The record is produced on electro-sensitive paper in the form of short, two millisecond dashes representing the positive zero crossings of each cycle of shock waves initiated by the sound source. A variable gate correlator circuit provides a markedly improved signal-to-noise ratio, which is particularly important because of the high ambient noise levels encountered on windward reef margins.

The method of operating this equipment in the reef environment has been outlined by Harvey (1977b). The seismic lines were usually run at low tide when parts of the reef, such as algal rim and reef flat, were exposed. In such cases a hammer rigged with an inertia switch was used as the sound source and operated in conjunction with two waterproof geophones, orientated perpendicular to the traverse. In areas that were covered by water, even at low tide, seismic detonators were used in conjunction with a pressure-sensitive hydrophone. In the lagoon at One Tree, the seismic detonators were lowered to the lagoon floor from a dinghy.

The length of the traverses was limited to the length of the trigger cable (120 m); most seismic lines were

¹ Department of Geography, James Cook University, Townsville, Queensland 4811.

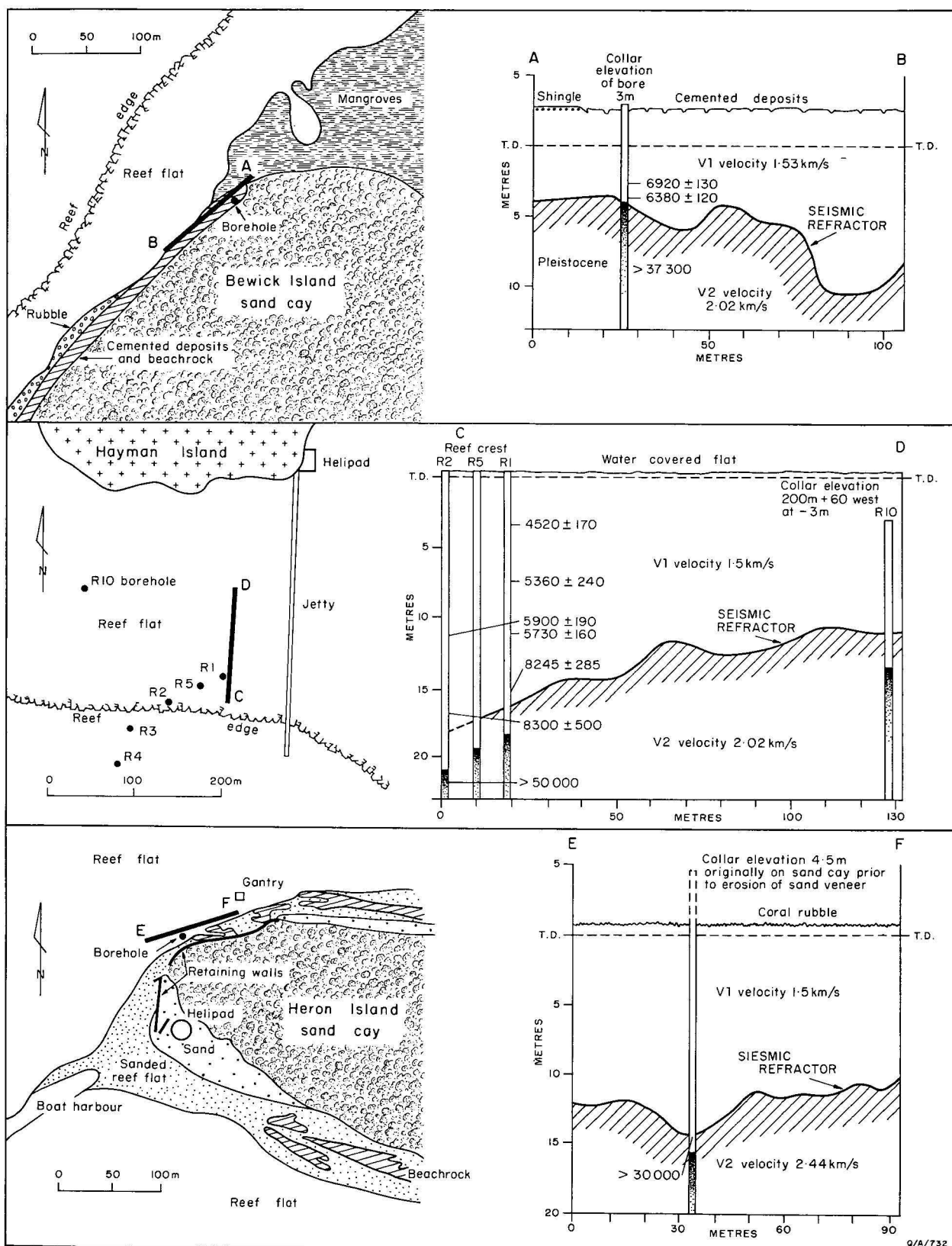


Figure 1. Relations of seismic refraction lines to drill holes at Bewick Island (northern Great Barrier Reef), Hayman Island (central Great Barrier Reef), and Heron Island (southern Great Barrier Reef). The radiocarbon dates shown on these boreholes are published in Thom & others (1978), Hobley & others (1978), and Davies & Marshall (in press).

run over this distance. In some cases adjoining traverses provided a longer section line. Shot spacing varied, depending on the sound source. With the hammer, closely spaced shot points (3 m) were used, whereas this spacing was doubled when using detonators. Most lines were reversed to obtain control on the attitude of the unconformity and the apparent velocities of the different layers.

In all cases a simple two-layer situation existed between the Holocene and the pre-Holocene materials. Seismic velocities were determined directly from the records, and these assumed velocities were converted to true velocities using published nomograms. In order to map the geometry and depth of the subsurface Hales' graphical method for interpreting seismic refraction lines was used (Hales, 1958), as it is particularly applicable to high-relief structures which might be expected from coral reefs. Hales' method involves the identification of two points of incidence at the surface of ray paths propagated from opposite directions from a point on the refractor. The distance between these points is used to calculate the radius and centre of a circle to which the refractor is tangential. Forward and reversed data are matched intrinsically so that the profile is automatically plotted. The method assumes that the cosine of the dip angle is equal to unity, which introduces only a negligible error, and has the advantage of being able to handle large dips, or rapid changes of dip, with little error. The procedure and the underlying theory of the method is outlined fully in Hales (1958).

Seismic refraction results from borehole sites

To test the validity of the assumption that the seismic discontinuity detected beneath the reefs is the Holocene/pre-Holocene boundary, refraction lines were run close to boreholes on Bewick Island (Lat. $14^{\circ}25'S$, Long. $144^{\circ}50'E$), Hayman Island (Lat. $20^{\circ}S$, Long. $149^{\circ}E$) and Heron Island (Lat. $23^{\circ}S$, Long. $152^{\circ}E$) where the boundary has been identified in drill core. Figure 1 shows the location of the refraction profiles in relation to the position of the boreholes, and interpreted seismic sections showing the depth and variation of the seismic discontinuity in relation to the stratigraphic position of the Holocene/pre-Holocene boundary.

The refraction line on the leeward side of Bewick Island (Fig. 1: profile AB) was run parallel to the beach along a coral shingle and beachrock surface 2.6 m above tidal datum. The transect is situated approximately 3-4 m to leeward of the borehole, which had a collar elevation 3 m above tidal datum. A seismic discontinuity between V_1 (1.53 km sec^{-1}) and V_2 (2.02 km sec^{-1}) was detected at depths of between 6.5 and 13.6 m below the surface. It is at a depth of about 7 m at the borehole site; this depth is almost exactly the same as the Holocene/pre-Holocene boundary identified in the borehole (Thom & others, 1978).

At Hayman Island a seismic line (Fig. 1: profile CD) was run north-south parallel to the jetty. Boreholes R1 and R5 are situated along the line of the profile near the reef crest, but a few metres to the west. R10 is on the reef flat almost 200 m to the west. Boreholes R2, R3 and R4 are all to seaward of the profile. A marked seismic discontinuity was noted between the upper layer ($v_1 = 1.50 \text{ km sec}^{-1}$) and a subsurface interval ($V_2 = 2.02 \text{ km sec}^{-1}$). This discontinuity varies in depth from 11.5 m below tidal datum near D to 17.5 m near the reef crest (Fig. 1). The seismic dis-

continuity at 17.5 m is very close to the position of the solution unconformity at 19-22 m in boreholes R1, R2 and R5 (Hopley & others 1978). The differences between the seismic results and the borehole interpretation is consistent with the relief expected over the substrate surface, and is near the estimated ten percent error inherent in refraction sounding. The cores were bagged at intervals ranging from 0.5 to 3.0 m, so that the precise depth of the solution unconformity is unknown. Although a difference of about 2 m exists for borehole R10 (Fig. 1), this can be largely discounted because the borehole is some 200 m west of the refraction line.

Profile EF on Heron Island (Fig. 1) was run along the reef flat immediately to the northwest of the present retaining wall on the northwestern side of the cay. The borehole, which is estimated to have had a collar elevation of 4.6 m above tidal datum, was originally positioned on the cay, but marked erosion has since removed the sand veneer reported in the original drilling log. A seismic discontinuity was detected between the surface layer ($V_1 = 1.50 \text{ km sec}^{-1}$) and the subsurface ($V_2 = 2.44 \text{ km sec}^{-1}$), at depths varying down to 15 m below tidal datum. In the vicinity of the boreholes, the refraction data indicated a depth of about 15 m below tidal datum, i.e. approximately 20 m below the top of the borehole. This is consistent with the detection of Pleistocene material within the interval 15.3 to 22.0 m below the top of the borehole (Davies & Marshall, in press).

Therefore, the results from seismic refraction profiles show that the depth of the seismic discontinuity can be correlated with the depth of the solution unconformity in the boreholes. Slight differences in depth between the two can be accounted for by errors inherent in the seismic refraction method, and errors in determining the actual depth of the solution unconformity by drilling methods. The good correlation between the two techniques substantiates claims that the seismic discontinuity represents the interface between the Holocene reef and its substrate (Harvey, 1977a; Davies & others, 1977b).

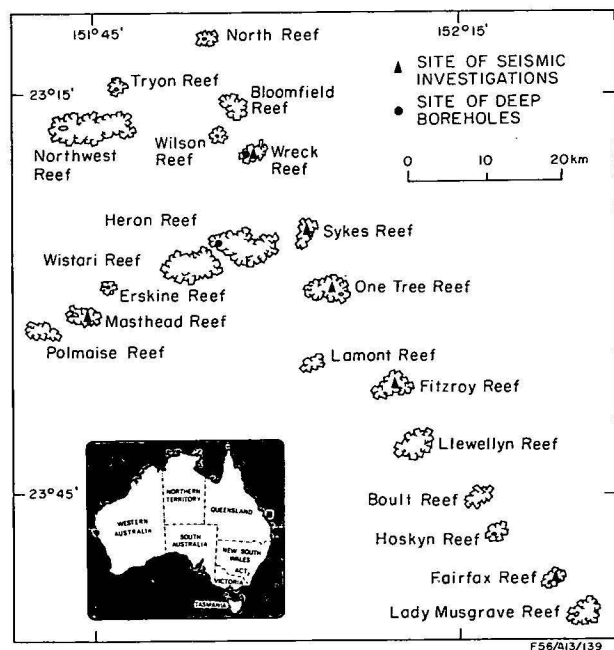


Figure 2. Location map showing the reefs investigated by seismic refraction techniques.

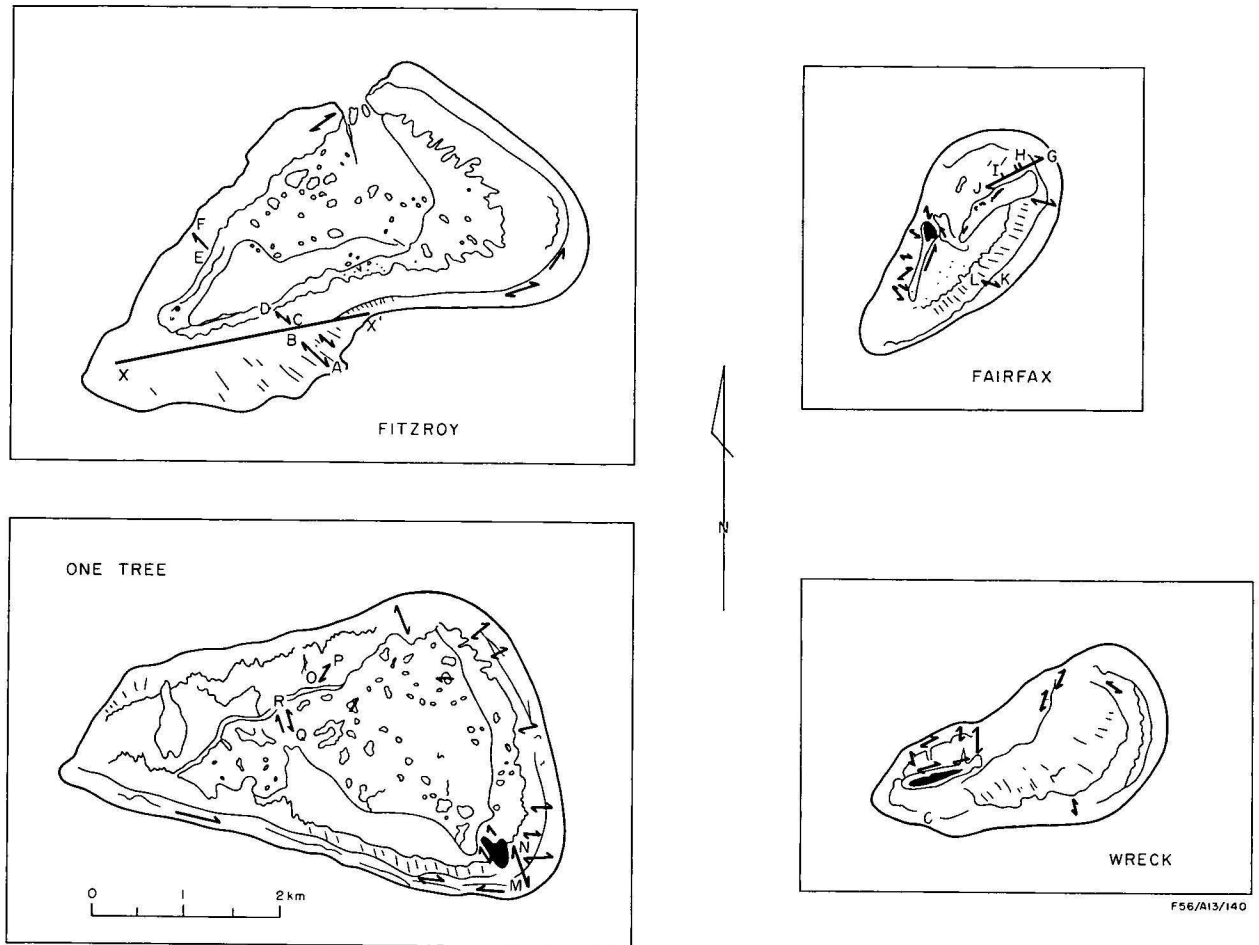


Figure 3. The location of seismic traverses conducted on Fitzroy, One Tree, Fairfax and Wreck Reefs. Lettered sections (A-Q) are shown in Figure 4.

Reef	Depth of seismic discontinuity	Depth range	Windward side	Leeward side	Lagoon	Patch reef
Wreck	8-17	9	10-14	8-17		
Fairfax	7-23	16	8-14	7-15	18-23	
One Tree	10-23	13	11-19	10-18	16-23	13-17
Fitzroy	9-21	12	11-21	9-18		

Table 1. Depth range and variation (in metres) of the seismic discontinuity of the four main reefs studied in the Capricorn and Bunker Groups.

Seismic refraction results from the Capricorn and Bunker groups

Seismic refraction data have been obtained from Fairfax, Fitzroy, One Tree, Wreck, Lady Musgrave, Sykes, and Masthead Reefs (Fig. 2). Profiles have been obtained from windward and leeward margins, in lagoons, and across patch reefs. A total of 124 traverses, each 120 m long, were completed, only eighteen of which were not reversed. The basic data from the reefs are given in Harvey & others (1979). The position of profiles on Fitzroy, Fairfax, One Tree, and Wreck Reef are shown in Figure 3, and selected examples of seismic sections are illustrated in Figure 4. Table 1 shows a marked variation in the depth of the Holocene/pre-Holocene unconformity, both on individual reefs and between one reef and another. Overall, the depth of the unconformity between One Tree and Fitzroy is greater than beneath Fairfax and

Wreck. This points to a relationship between the depth of the unconformity and modern reef morphology, because One Tree and Fitzroy are reefs with large lagoons, whereas Fairfax has only a small modern lagoon and Wreck none at all. Profiles run north-south across the windward and leeward sides of Fitzroy (Fig. 4: A-B, C-D, and E-F) illustrate the topographic variations at the margins of the reef. On the windward (southern) side Figure 3 shows the position of seismic profiles on either side of an east-west orientated, low ridge (X-X¹), which is a continuation of the algal rim a few hundred metres to the east. The modern reef surface slopes gently north and south away from the linear surface feature. That part of the reef to the south of it appears almost as an addition to the otherwise triangular-shaped reef. Profile A-B (Fig. 4) shows the Holocene/pre-Holocene unconformity at its shallowest (−12 m) below the surface lineation, sloping southwards towards the reef margin where it reaches −20.5 m. To the north of the surface lineation, profile C-D (Fig. 4) also shows the unconformity higher (−14.5 m) close to the lineation, sloping down beneath the edge of the lagoon, where it reaches a depth of at least 19 m. This depth is some 14 m deeper than the floor of the lagoon, immediately to the north of the end of the profile. On the leeward margin, profile E-F (Fig. 4) shows the unconformity at a depth of 12 m close to the edge of the lagoon, and sloping irregularly up to 9 m near the leeward reef margin. The unconformity is higher beneath the perimeter margins than beneath or close to the lagoon. Its

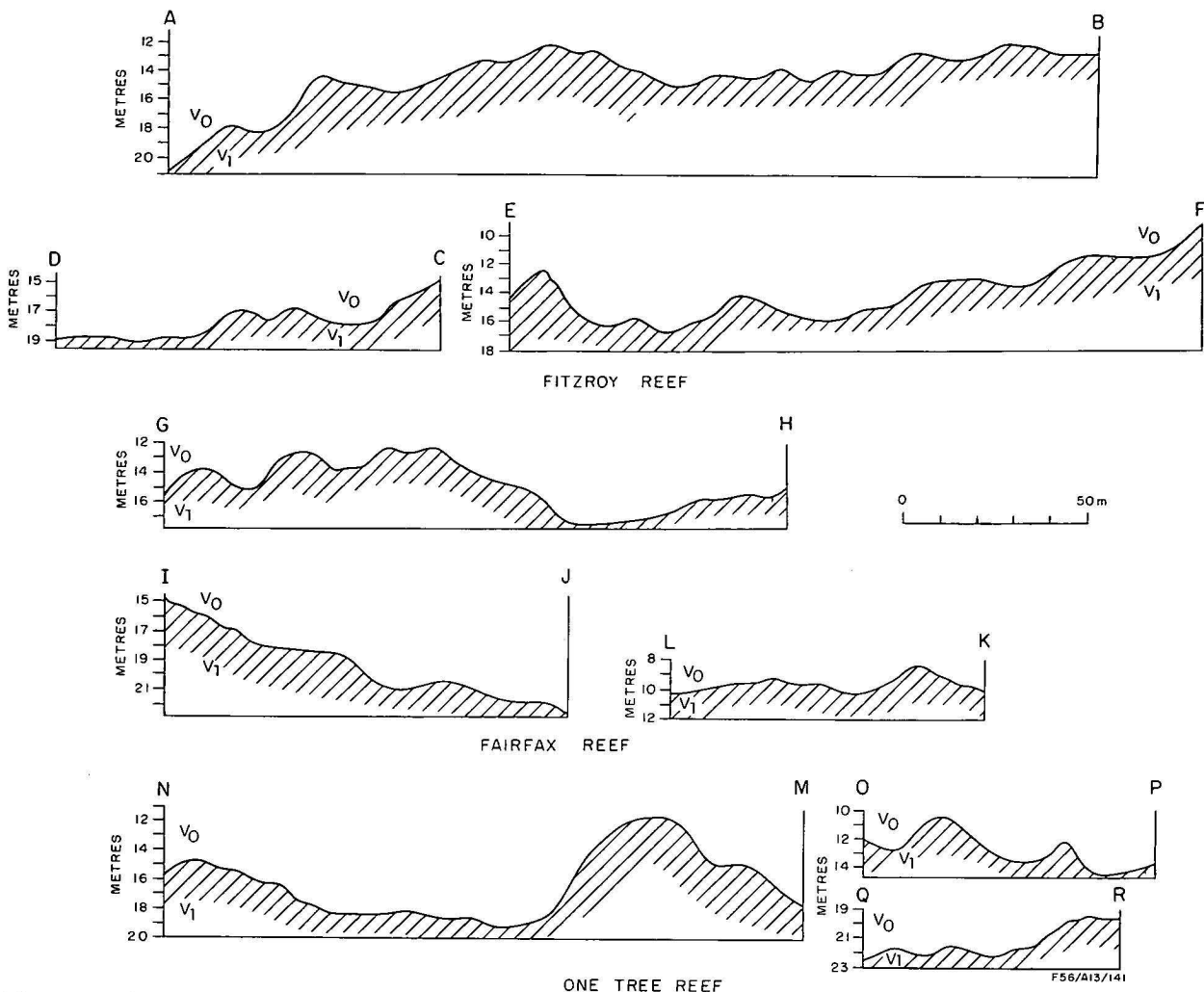


Figure 4. The results of selected seismic refraction profiles on reefs in the southern Great Barrier Reef. Profiles AB, CD, and EF are from Fitzroy Reef; Profiles GH, IJ, LK are from Fairfax; Profiles MN, OP and RQ are from One Tree. Location of these profiles are shown in Figure 3.

depth at the leeward margin (9 m) is in places higher than the present lagoon floor (10 m water depth). Assuming a reasonable thickness of Holocene sediment accumulation in the lagoon, it seems incontestable that the pre-Holocene surface forms a rim, elevated appreciably (5-10 m) above, and enclosing a central depression. This conclusion has more general application, as is seen in the data from other reefs.

At Fairfax Reef, profile G-H (Fig. 4) shows the Holocene/pre-Holocene unconformity at -12 m close to the northern windward margin, sloping both seaward and beneath the reef to leeward. Near the lagoon the unconformity slopes down to a depth of 23 m (Fig. 4: profile I-J). However, over most of the traverse the unconformity is relatively shallow (12-15 m). Profile L-K (Fig. 4) on the southeastern windward margin shows that the unconformity is relatively shallow (9-10 m), with gentle slopes to both windward and leeward. On the leeward margin the unconformity is also shallow (7-12 m).

At One Tree Reef, profile N-M (Fig. 4) shows the unconformity at a depth of 12 m close to the south-eastern windward margin, with a steep slope both seaward and towards the cay. On the leeward margin profile O-P (Fig. 4) shows the unconformity at a depth of 10.5 m close to the vertical wall at the edge of the

lagoon and sloping down beneath the leeward margin. The other section across the leeward margin shows a similar relationship, with the unconformity at a depth of 12 m near the lagoon sloping down to -18 m near the edge of the reef. Data from the lagoon (Fig. 4: profile R-Q), shows the unconformity at depths of 19 to 23 m; this is some 8-12 m deeper than that below the leeward edge of the lagoon.

At the other reef for which substantial data were obtained, Wreck Reef, the seismic results are similar to those already described. The unconformity beneath both windward and leeward margins is relatively shallow, and slopes both outwards and inwards beneath the centre of the reef.

The evidence obtained from the four reefs studied in detail indicates a pre-Holocene surface below the modern reef which has raised rims standing above a central depression. The height of the rims, the overall depth of the depression, and the asymmetry of the depression all vary. Two of these reefs—One Tree and Fitzroy—still have large depressions today, i.e. lagoons; the small remnant lagoon at Fairfax corresponds with a deep pre-Holocene substrate. This is proof that in terms of gross morphology the substrate has exerted a marked influence on present-day morphology. The less precise relationships at Wreck and Fairfax are believed

to be a result of sediment infill of a lagoon where the substrate is shallower overall. While this model is supported by the evidence, it is not suggested that the perimeter formed an unbroken rim around the central depression. Some sections at One Tree Reef indicate that there are breaches in the rim, and these are probably more numerous than the limited seismic data indicate.

Previous studies at One Tree Reef (Davies & Kinsey, 1977) had suggested that lagoonal patch reefs may have been located on prominences in the pre-Holocene substrate. Seismic profiles across two patch reefs (Table 1) show the unconformity at -13 to -17 m, some 3-10 m shallower than it is beneath the lagoon. The patch reefs have grown on substrate highs, as was previously suggested.

Discussion

The data and conclusions in the body of this paper support the previously published views (Davies, 1974; Davies & others, 1976, 1977a, 1977b; Davies & Kinsey, 1977) that substrate has a dominant influence on the growth of modern reefs in the Capricorn and Bunker Groups. The data from One Tree and Fitzroy show that their present overall shape appears to be inherited from an older surface. At both these reefs, the substrate beneath the modern lagoon is deep. The seismic data also suggest a similar conclusion for the early growth stages of Wreck and Fairfax, but the generally shallower overall depths have resulted in almost total infill of the lagoonal depressions. Smaller scale features such as patch reefs are also controlled by the substrate. However, the seismic-refraction technique provides no firm evidence which might explain the origin of the shape of the pre-Holocene surface. In recent years it has been suggested that karst processes have affected the shape of the pre-Holocene surface, which in turn has influenced the shape of the modern reef (Purdy, 1974). While it is tempting to conclude that the topographic variations shown by the seismic profiles has been caused by such processes, it is also possible that they may represent variations in an older reef surface. Answers to these problems will have to wait until extensive drilling has been carried out.

The variations in the thickness of Holocene growth on individual reefs, taken with the close relationship of morphology to substrate control, suggest that the reefs of the Capricorn and Bunker Groups have not grown according to the scheme of reef development envisaged by Maxwell (1968). The classification of reefs as platform reefs, lagoonal platform reefs, closed-ring and in-grown closed-ring reefs is not borne out by our geophysical evidence. All the reefs are platform reefs, because they are underlain at shallow, but varying depths by pre-Holocene platforms. Variations in the morphology of the modern reefs can be attributed to variations in the shape of the platforms, while the depths of the platforms ultimately determine how closely the modern reef resembles its original shape. Reefs growing off shallow platforms reached a stabilised sea level earlier than reefs growing off deeper platforms, and will have undergone greater surface modification.

The model of reef growth for the Capricorn and Bunker Groups (Flood & Orme, 1977; Jell & Flood, 1978) invoking a genetically related series of reef types varying latitudinally from south to north is unsupported by the geophysical evidence gathered by us in the same area. Wreck and Fairfax Reefs are the most similar in

size, shape and depth to the pre-Holocene surface, but occur at opposite ends of the reef chain. Additionally, we suggest that the only real difference between One Tree and Lady Musgrave Reefs is that the pre-Holocene substrate beneath the lagoon at Lady Musgrave did not possess as many prominences for promoting lagoonal patch reef development.

Acknowledgements

The authors wish to thank Doug Foulstone, Andy Short, Ken Martin and Bruce Thom for their help in the field; Mr and Mrs T. Chilvers for their assistance and hospitality at One Tree Reef, Mr Alex Frodsham and the crew of the M.V. *Escape*, and Mr Ron Isbel and crew of the M.V. *Sea Hunt*. We would like to thank A. L. Bloom and J. S. Jell for their comments on the manuscript. Acknowledgment is made to the Australian Research Grants Committee and the One Tree Island Research Board.

References

- DAVIES, P. J., 1974—Subsurface solution unconformities at Heron Island, Great Barrier Reef. *Proceedings Second International Symposium on Coral Reefs, Brisbane*, **2**, 573-78.
- DAVIES, P. J., & KINSEY, D., 1977—Holocene reef growth—One Tree Island, Great Barrier Reef. *Marine Geology*, **24**, M1-11.
- DAVIES, P. J., RADKE, B. M., & ROBISON, C. R., 1976—The evolution of One Tree Reef, southern Great Barrier Reef, Queensland. *BMR Journal of Australian Geology & Geophysics*, **1**, 231-40.
- DAVIES, P. J., MARSHALL, J. F., FOULSTONE, D., THOM, B. G., HARVEY, N., SHORT, A. D., & MARTIN, K., 1977a—Reef growth, southern Great Barrier Reef—preliminary results. *BMR Journal of Australian Geology & Geophysics*, **2**, 69-72.
- DAVIES, P. J., MARSHALL, J. F., THOM, B. G., HARVEY, N., SHORT, A. D., & MARTIN, K., 1977b—Reef development—Great Barrier Reef. *Proceedings Third International Symposium on Coral Reefs, Miami*, **2**, 331-7.
- DAVIES, P. J., & MARSHALL, J. F., in press—Aspects of Holocene reef growth—substrate age and accretion rate. *Search*.
- DOBRIN, M. B. & PERKINS, B., 1954—Seismic studies of Bikini Atoll, *United States Geological Survey Professional Papers*, **260-J**, 487-504.
- FLOOD, P. G., & ORME, G. R., 1977—A sedimentation model for platform reefs of the Great Barrier Reef, Australia. *Proceedings Third International Symposium on Coral Reefs, Miami*, **2**, 111-18.
- HALES, F. W., 1958—An accurate graphical method of interpreting seismic refraction lines. *Geophysical Prospecting*, **3**, 285-94.
- HARVEY, N., 1977a—The identification of subsurface solution unconformities on the Great Barrier Reef, Australia, between 14°S and 17°S, using shallow seismic refraction techniques. *Proceedings Third International Symposium on Coral Reefs, Miami*, **2**, 45-52.
- HARVEY, N., 1977b—The application of shallow seismic refraction techniques to coastal geomorphology: A coral reef example. *Catena*, **4**, 333-9.
- HARVEY, N., DAVIES, P. J., & MARSHALL, J. F., 1978—Shallow reef structure: southern Great Barrier Reef. *Bureau of Mineral Resources, Australia—Record* **1978/96**.
- HOPLEY, D., MCLEAN, R. F., MARSHALL, J., & SMITH, A. S., 1978—Holocene-Pleistocene boundary in a fringing reef: Hayman Island, north Queensland. *Search*, **9**, 323-25.

- JELL, J. S., & FLOOD, P. G., 1978—Guide to the geology of the reefs of the Capricorn and Bunker Groups, Great Barrier Reef Province, with special reference to Heron Reef. *Papers, Department of Geology, University of Queensland*, 8, 44.
- MAXWELL, W. G. H., 1968—ATLAS OF THE GREAT BARRIER REEF. *Elsevier, Amsterdam*.
- PURDY, E. G., 1974—Reef configurations: cause and effect. In LAPORTE, L. F. (Editor), REEFS IN TIME AND SPACE. *Society of Economic Palaeontologists Mineralogists, Special Publication* 18, 9-76.
- RICHARDS, H. S., & HILL, D., 1942—Great Barrier Reef bores, 1926 and 1937. Description, analysis and interpretations. *Reports of the Great Barrier Reef Committee*, 5, 1-122.
- SCHLANGER, S. O., 1963—Subsurface geology of Eniwetak Atoll. *United States Geological Survey Professional Papers*, 260-BB, 991-1006.
- THOM, B. G., ORME, G. R., & POLACH, H., 1978—Drilling investigations at Bewick and Stapleton Islands. *Philosophical Transactions of the Royal Society of London*, 291, 37-54.

A sabkha model for the deposition of part of the Proterozoic McArthur Group of the Northern Territory, and its implications for mineralisation

M. D. Muir

Abundant pseudomorphs and relicts of gypsum, anhydrite, and halite occur in the Mallapunyah Formation and Amelia Dolomite of the Proterozoic McArthur Group of the Northern Territory. The rocks have undergone a complex history, in which several stages can be detected. These are: (a) They were deposited in a regressive/transgressive cycle with frequent minor oscillations. The sedimentary sequence shows a striking resemblance to the Pleistocene and Holocene sediments of the Abu Dhabi sabkha. (b) The evaporites were emplaced diagenetically after formation of black chert and early dolomite. Deposits in the McArthur Group sections can be closely compared with the early diagenetic facies zones of Abu Dhabi. By analogy with the Holocene the positions of particular evaporite parageneses can be located within the palaeo-sabkha. (c) Textures indicating dehydration of gypsum to anhydrite and vice versa can be detected, but the sulphate evaporites, and some of the halite, have been replaced by ferroan carbonate during burial diagenesis, at a depth of burial estimated at over 1 km. Sulphate-rich brines which also contained high metal concentrations were released at this time, and made their way through a number of accessways to overlying formations. These brines provided, at least in part, a source of sulphate and of metals for mineralisation in the Emmerugga Dolomite and Barney Creek Formation. (d) Later vadose and phreatic activity resulted in minor copper mineralisation, and in cementation and recrystallisation of the carbonates. Silcrete and magnesite-rich crusts are common on beds of replaced evaporite minerals. (e) The presence of an arid Abu Dhabi-like sabkha indicated the prevalence of a particular climatic regime. If these same climatic conditions can be identified in northwest Queensland, there exists the possibility for climatic stratigraphic correlation at an intermediate level between radiometric, and micropalaeontological and magneto-stratigraphic correlation.

Introduction

The Carpentarian rocks of the McArthur Basin are subdivided into the mainly arenaceous and volcanic Tawallah Group, succeeded by the predominantly carbonate sediments of the McArthur Group, overlain by the arenaceous and argillaceous Roper Group (Smith, 1964). The rocks crop out in the Northern Territory from northern Arnhem Land to the Queensland border, and similar rocks of equivalent age continue through Paradise Creek to Mount Isa. The top of the Tawallah Group has been dated at 1600 m.y. (Webb, 1973: quoted in Plumb & Derrick, 1976), and it is overlain without apparent unconformity by the Mallapunyah Formation of the McArthur Group. The Amelia Dolomite is conformable with the Mallapunyah Formation (Fig. 1). West of the Tawallah Fault and south of the Abner Range, the Mallapunyah Formation and Amelia Dolomite crop out extensively (Fig. 2). Small inliers of both formations are exposed in the Batten Trough (Walker & others, 1978) near the Emu Fault, but much of the apparent outcrop of the Amelia Dolomite on the Bauhinia Downs 1:250 000 geological Sheet area was misidentified in early regional mapping (Smith, 1964), and has been reassigned to younger formations (Plumb & Brown, 1973). East of the Emu Fault, the Mallapunyah Formation and Amelia Dolomite occur in small inliers exposed by removal of the Cambrian Bukalara Sandstone.

The Mallapunyah Formation and Amelia Dolomite have been studied by mapping of selected areas, and sections have been measured in a number of places (Fig. 2). Other sections have been examined without detailed measuring. The Carpentaria Exploration Company Pty Ltd Tawallah Pocket No. 1 diamond drill hole penetrated the lowest part of the Amelia Dolomite and the uppermost part of the Mallapunyah Formation. Samples of various kinds of evaporite relict, both from outcrop and from subsurface, have been studied using

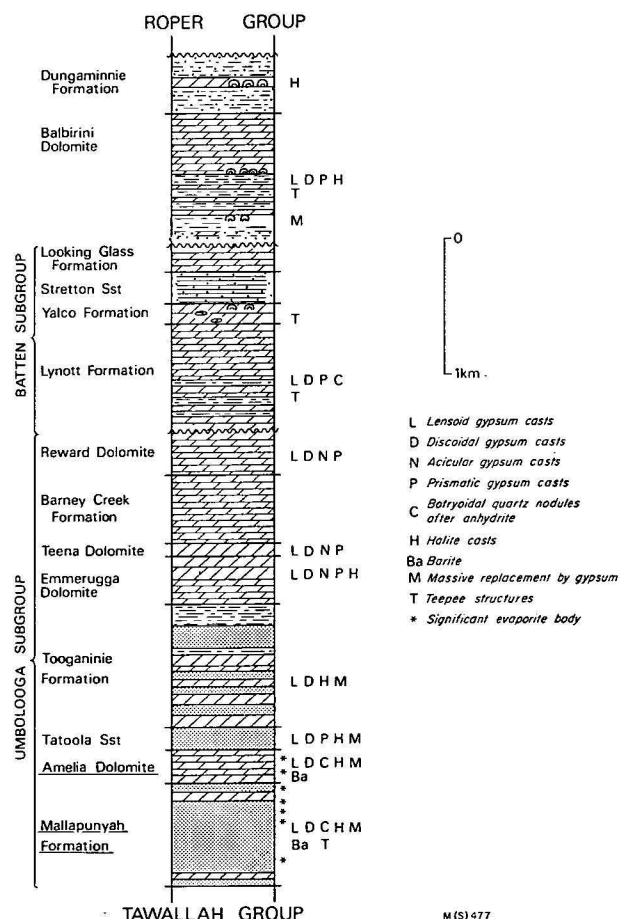


Figure 1. Stratigraphic section through the McArthur Group showing distribution of various types of evaporites and the levels in the Amelia Dolomite and Mallapunyah Formation which contain significant bodies of evaporite pseudomorphs.

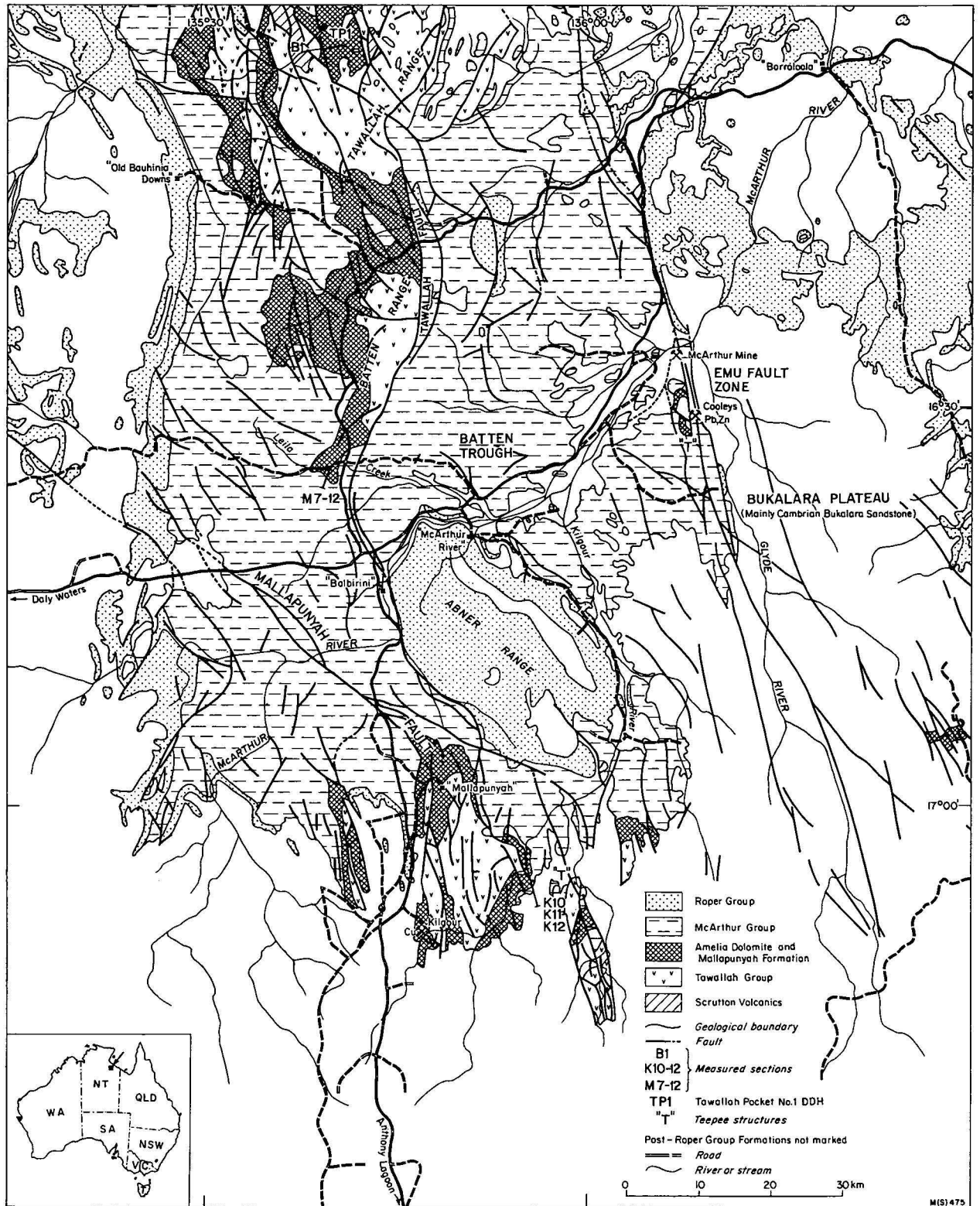


Figure 2. Locality map of the McArthur River area, Northern Territory, showing important localities and the outcrop of the Amelia Dolomite and Mallapunyah Formation.

light and scanning electron microscopy, and X-ray microanalysis techniques. Cut and polished slabs also provided valuable textural information.

The sedimentary rocks of the McArthur Group are characterised by structures indicating shallow-water, desiccating, and hypersaline environments of deposition. With the exception of two Formations (the Barney Creek Formation and Reward Dolomite), the sediments

of the group appear to have been deposited on an extensive, very stable shelf, which remained more or less at mean sea level for long periods of time. Depositional environments range from continental, lacustrine (Muir & others, 1979) to shallow marine.

The Amelia Dolomite and Mallapunyah Formation have many features in common. The Mallapunyah Formation is largely composed of red and purple, sandy

and silty mudstone, but up to 25 percent of the measured sections (Jackson & others, 1978) is dololite or dolarenite. The Amelia Dolomite is predominantly dolomitic, but red and green fine sandstone, siltstone, and shale are common in the lower parts of the section.

In both formations, features of shallow-water sedimentation include numerous localised breaks in sedimentation, cross-bedding, symmetrical ripple marks, beds of oolites, some of which are cross-bedded, stratiform, domal, and columnar stromatolites, oncrites, and cross-bedded intraclast horizons.

The evidence for shallow-water conditions is supported by frequent indications of emergence. Desiccation cracks are abundant, and occur in all rock types from lutite and quartz sandstone to dololite and dolarenite. Halite casts on upper bedding surfaces are common, and indicate evaporation to dryness of the water body. Small discoidal impressions of gypsum crystals, flattened parallel to bedding are occasionally found, and these, too, indicate emergence (observations made at Hutchinson's Embayment, Shark Bay, 1978). Teepee structures and polygons in the Mallapunyah Formation indicate a hydrological system operating under evaporation rates seasonally higher than local rainfall (Muir & others, 1979). Continual evaporation gives rise to hypersaline brines: evidence for their former presence is abundant in casts of lenticular and acicular gypsum crystals, blade-shaped and rhomboidal anhydrite crystals, hopper and solid halite crystals, and quartz replacements of anhydrite nodules.

In this paper, the primary and some of the early and burial diagenetic environments of deposition of the two formations are identified and described. A comparison is made with Pleistocene and Holocene sediments of the Persian Gulf. It is possible to identify evaporite mineral parageneses that are remarkably similar to those described (Butler, 1969) from distinct zones parallel to the coast from the supratidal sabkha and intertidal flats of Abu Dhabi. From the evidence of the primary sedimentary structures, a period of regression in the Mallapunyah Formation is followed by an overall transgression in the Amelia Dolomite. Minor oscillations can be detected in both regressive and transgressive sequences. The early diagenetic zones follow the same pattern as the primary phases in the Mallapunyah Formation, but not invariably in the Amelia Dolomite.

Most of the evaporite minerals have been silicified, or replaced by ferroan carbonates on burial. West's (1964) model for burial diagenesis in the English Purbeckian can be applied to many of the textures found in the evaporites. Their replacement by carbonate is readily understood in the light of Curtis' (1977) model of burial diagenesis zones. Use of these models permits prediction of the depth of burial at the time the evaporites were replaced, and the sulphate-rich brines released. The timing can be associated with mineralisation in overlying McArthur Group sedimentary rocks.

Evidence for the former presence of evaporites

Halite casts and their environmental significance

The commonest form of non-sulphate evaporite pseudomorph in the Mallapunyah Formation are halite casts, which are abundant throughout the section. These take the form of cubic casts, frequently hopper crystal casts, and range in size up to 6 cm. Moulds occur on

the tops of beds, while casts mark the undersurfaces. In this case, halite was formed from evaporation to dryness of brine in a mud or silt-bottomed pond or lake. Later influx of fresher water dissolved the halite, leaving behind moulds of the crystals. Deposition of the supervening sand, silt, or clay-grade bed filled the moulds and formed casts of the bottom part of the crystal only.

However, casts are sometimes observed on the upper surfaces. These are produced when the halite is not dissolved before deposition of the next layer. Rather less commonly, dolomite-filled casts may be found within beds of dolomite or dolomitic siltstone. These casts are generally outlined by a thin layer of ferruginous material and appear to have grown displacively in the sediment. Neev & Emery (1967) have described halite deposition in the Dead Sea, in the diagenetic pile, by precipitation from highly saline interstitial ('epigenetic') brines.

In the Amelia Dolomite, halite casts are much less common than in the Mallapunyah Formation, although occasional examples have been found. Almost all the Amelia Dolomite halite casts appear to have formed at the sediment surface: few of the epigenetic forms have been observed.

Sulphate evaporite minerals and their replacements

Sulphate evaporite minerals have been very common in the Mallapunyah Formation and Amelia Dolomite: their pseudomorphs take the form of discoidal, acicular, euhedral or subhedral crystals, replaced by ferroan carbonate. The sulphates appear to have formed at a number of times during deposition and diagenesis of the sediments.

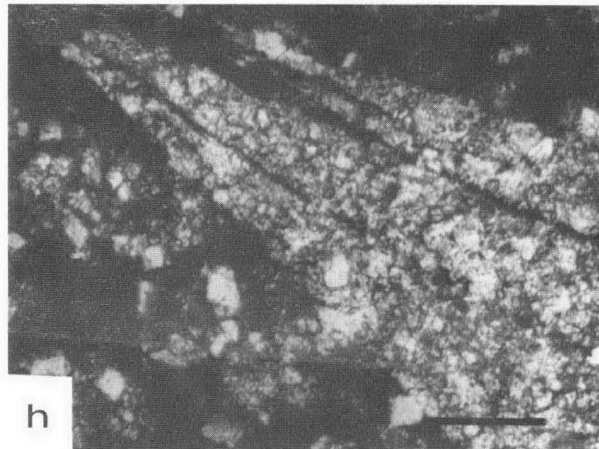
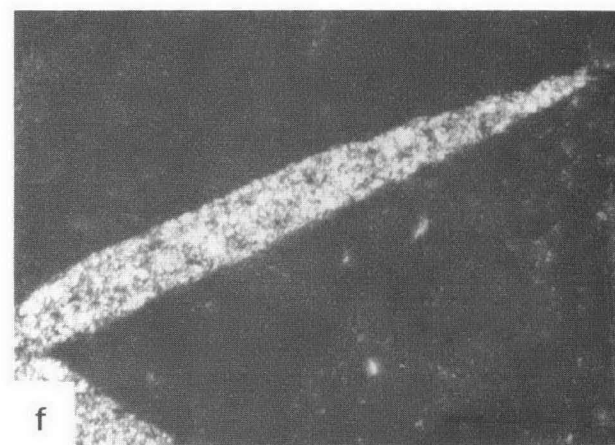
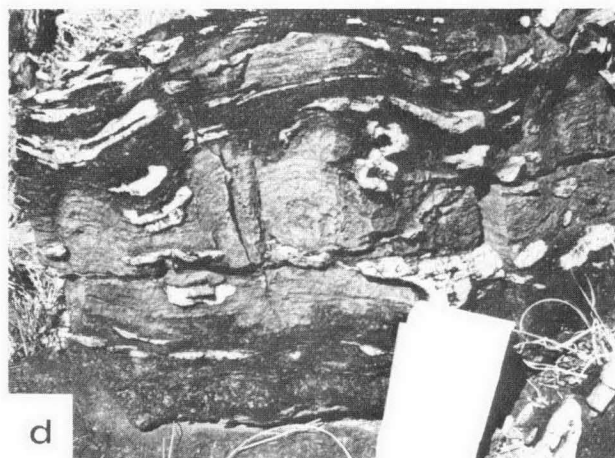
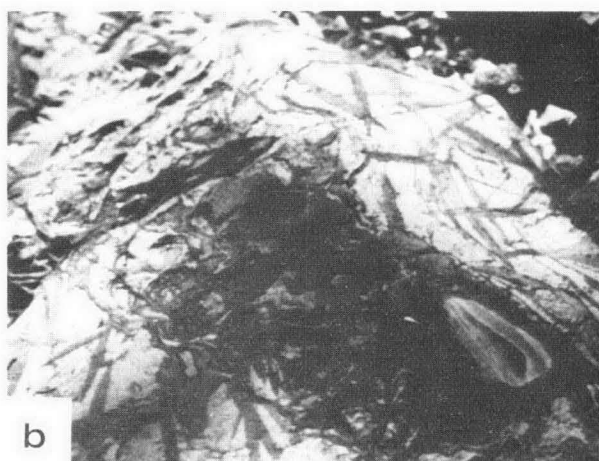
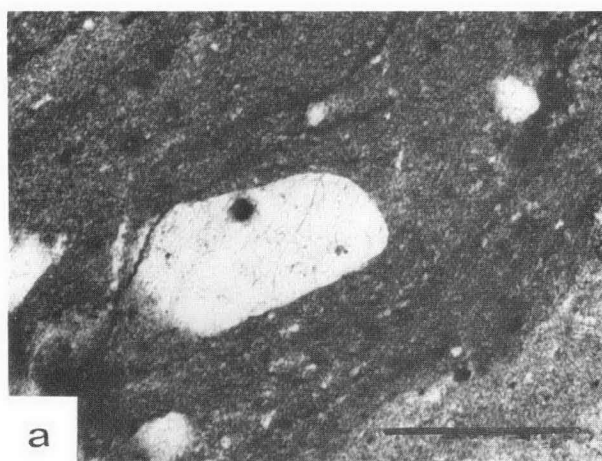
Syndepositional sulphates. In the McArthur Group as a whole, these take three forms: (a) microscopic euhedral and discoidal crystals, which occur in very early diagenetic chert containing abundant, well preserved microfossils, are common in the Amelia Dolomite. Neither the crystals nor the microfossils show any sign of compressional deformation. In some cases, the sulphates are still preserved in the cherts. They have been identified by their optical properties, and by energy dispersive X-ray microanalysis to determine their chemical composition.

(b) small nodules (up to 1 mm in diameter) of anhydrite have also been identified in the early diagenetic chert (Fig. 3a).

(c) hollow acicular crystals in radiating bundles, usually replaced by dolomite (Walker & others, 1977). These have only recently been found in the Amelia Dolomite, and will be described elsewhere (Walter, Krylov, & Muir, in prep.).

Post-depositional pseudomorphs. From their morphologies, the remainder of the sulphate crystal pseudomorphs appear to have grown displacively, by deposition from pore waters in the sedimentary pile (Shearman, 1966; Butler, 1969). The crystal pseudomorphs may be scattered through the sediment or may almost totally displace it.

(a) Scattered pseudomorphs. Scattered pseudomorphs are usually discoidal with elongate lenticular cross-sections; they occur in both the Mallapunyah Formation and Amelia Dolomite. In a single hand specimen, they tend to be relatively uniform in size, but at different stratigraphic levels the size varies. Pseudomorphs after single discoidal crystals reach 15 cm in length. They are usually randomly oriented in the sedimentary matrix, and are occasionally intergrown in



rosette-shaped clusters (Fig. 3b). Scattered pseudomorphs are usually found in non-stromatolitic, flat-bedded dololomite, sandstone, siltstone, and mudstone, but occasionally also in stromatolitic dololomite.

(b) Crystal felts. In other instances, scattered pseudomorphs which may be discoidal, acicular, or euhedral rhombohedra occur as crystal 'felts' or 'mushes' along or parallel to bedding, joints or cracks. These are usually rather small crystals, none bigger than 1 cm diameter. These crystal felts are confined to non-stromatolitic flat-bedded dololomite and are more common in the lower part of the Amelia Dolomite.

(c) Total replacement of primary non-stromatolitic carbonate. The almost total replacement of original carbonates is a common occurrence in the Amelia Dolomite. This takes the form of dark reddish brown ferroan dolomite or sideritic marble. The rock is now a mosaic of ferroan carbonate crystals which form pseudomorphs after subhedral (very rarely euhedral) crystals of gypsum or anhydrite. In some cases, crystal orientation is random and crystals are intergrown and mutually interfere (Fig. 3c). Bedding is indistinct, but appears to be flat laminated and non-stromatolitic. Stylolites are rare in this type of replacement.

(d) Total replacement of primary stromatolitic carbonate. Massive replacement of beds showing various types of stromatolitic lamination is common in the Amelia Dolomite. Different types of stromatolite can act as host to the sulphates, and their laminae can be detected at outcrop as discontinuous chert layers which had become silicified prior to emplacement of the sulphates (Fig. 3d). Stratiform stromatolites are most common as the sulphate host. These chert layers frequently contain the small primary gypsum crystals or anhydrite nodules described previously, and in many cases contain fine-grained pyrite and chalcopyrite, as well as abundant organic matter and microfossils.

In stromatolitic hosts, the sulphate minerals have grown more or less normal to bedding, although some crystals can always be found sub-parallel to bedding. Single crystals range up to 15 to 20 cm and may transgress several bedding plane laminations. Some of the crystals were initially precipitated as gypsum and some as anhydrite. Following Shearman (pers. comm., 1975), discoidal crystals were originally gypsum (Fig. 3e), whereas discoidal crystals with a flat face near one end were originally anhydrite (Fig. 3f). Crystals with pyramidal terminations were originally gypsum (Fig. 3g), while those with rhombohedral ends were originally anhydrite or anhydrite overgrowths on gypsum (Fig. 3g). Crystals with serrated ends were also originally anhydrite (Fig. 3h). In some samples, mosaic textures similar to those produced by the dehydration of gypsum to anhydrite are common (Fig. 4a). Stylolites are abundant in this type of replacement, and affect the host and sulphate equally. Many bedding planes are stylolitic (Fig. 4a), and oblique stylolites are common in some specimens (Fig. 4b). In weathered material, the stylolites are outlined in iron minerals, such as goethite, limonite, or hematite,

whereas in fresh material, pyrite is the most common stylolite mineral infilling. Sulphate mineral pseudomorphs are often abruptly truncated against stylolites, while at other times stylolites pass through the sulphates causing only minor fracturing and solution. There are often stylolitic margins between adjacent crystals, and between crystals and fragments of the original bedded carbonates (or silicified carbonates). Growth of the crystals has quite frequently markedly distorted the original sediments.

The density of the crystals in these laminae is variable. In some, replacement of the original carbonate has been almost complete, and in others there have been gaps between the crystals which may originally have contained halite, producing textures which are very reminiscent of the fabric of the calcitised evaporites from the Devonian Winnipegosis of Canada (Shearman & Fuller, 1969). Individual beds range up to 3 m in thickness, and internal laminations may vary in thickness from 1 mm to 1 cm. Sections consisting predominantly of massive evaporite replacements range up to 40 m in thickness at Leila Creek (Table 3).

In one case only does some of the sideritic marble probably represent replacement of primary gypsum. This occurs at the top of the upper evaporite unit south of Leila Creek, where there are stromatolites and oncolites up to 30 cm in diameter with a core of coarse-grained gypsum replacements, surrounded by 2-3 cm width of fine-grained laminated dololomite (Fig. 4c). They occur in a matrix of sideritic marble. Morphologically and in their lithological setting, the stromatolites are strikingly similar to those described from Holocene gypsum deposits of Marion Lake (Yorke Peninsula, South Australia) by von der Borch & others (1977).

(e) Botryoidal quartz nodules (Smith, 1964). These occur mainly in the Mallapunyah Formation, but small examples, less than a few centimetres in diameter, have been found in the Amelia Dolomite. The Mallapunyah Formation nodules are up to 3 m long and 1 m high, and have an outer rind of silica with a bladed texture, and a coarse-grained inner core composed of quartz and dolomite, sometimes with barite and/or fluorite. The nodules generally occur in a matrix of fine sand or siltstone, and are commonest near the top of the Mallapunyah Formation.

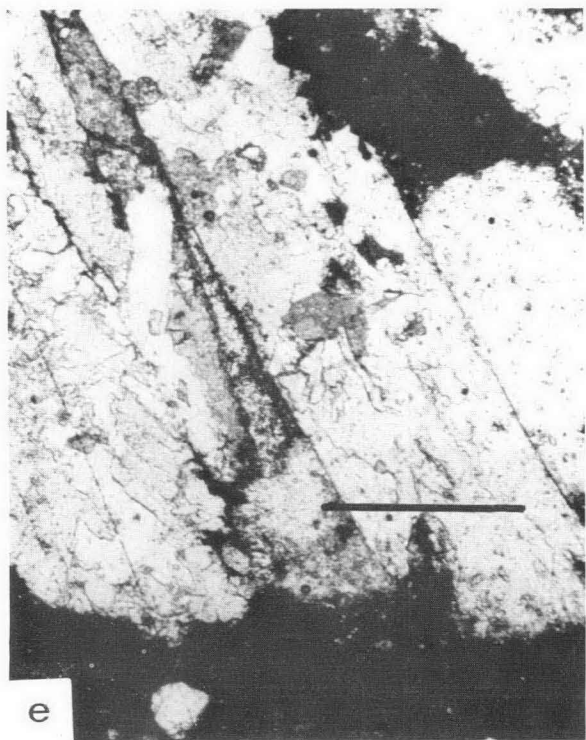
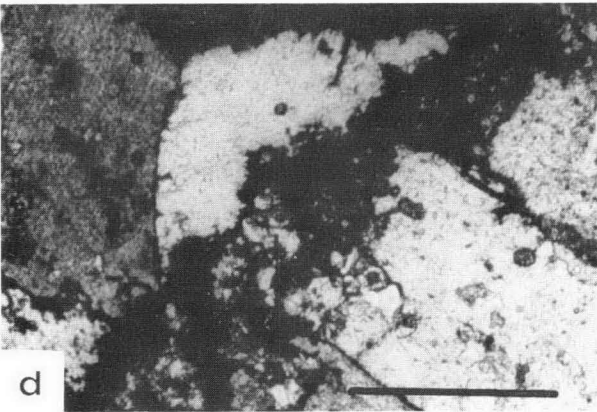
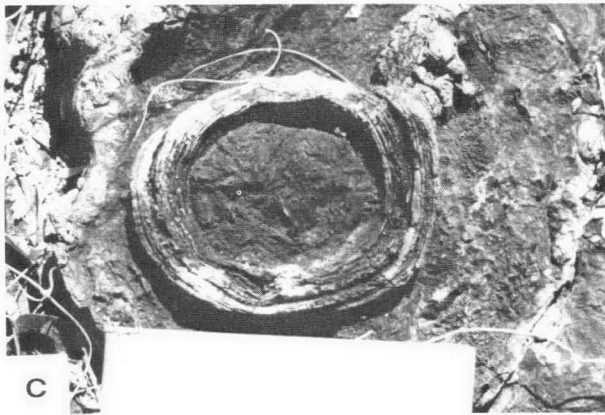
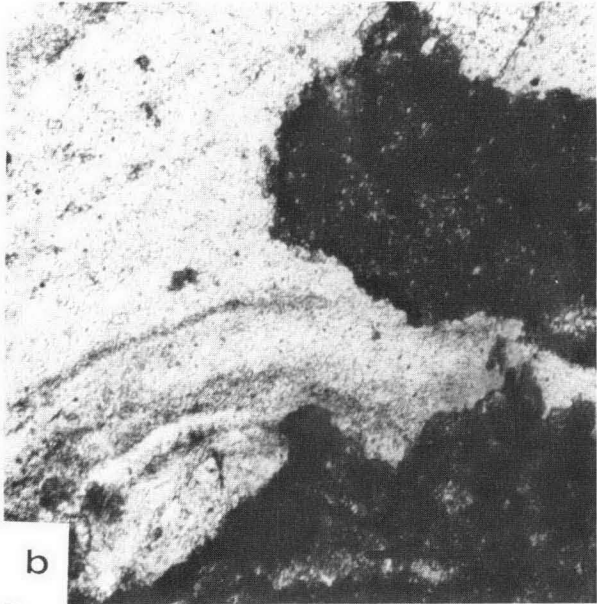
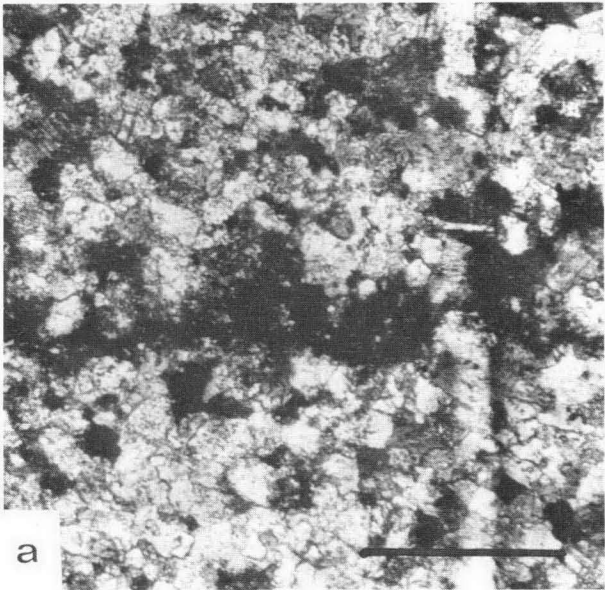
Primary depositional and early diagenetic environments

Mallapunyah Formation

A composite lithological section through the Mallapunyah Formation in the Kilgour area is shown in Figure 5. **Unit A**, at the bottom of the column, is an underlying cross-bedded quartz arenite of the Master-ton Formation. **Unit B** is a thin (2 m) completely silicified stromatolitic horizon. On a tributary of the Kilgour River, the stromatolites are *Conophyton*-like, but at Leila Creek and at the southern end of the Tawallah Range, stratiform stromatolites appear to predominate.

Figure 3. Scale bar = 10 mm, except where other scale is shown. Micrographs under crossed nicols.

(a) Small nodule, still anhydrite, in early diagenetic black chert. The black chert contains abundant microfossils. (b) Ferroan dolomite pseudomorphs after gypsum in dololomite matrix. The largest discoidal crystal is 15 cm long. (c) Randomly oriented mosaic of ferroan dolomite pseudomorphs after anhydrite. The abundant small inclusions have the optical properties of anhydrite and contain Ca and S. (d) Stratiform stromatolites preserved in sideritic marble. White-weathering laminae of black chert show the form of the stromatolites. (e) Small discoidal crystal pseudomorph after gypsum. The crystal is cross-cut by a stylolite, with little loss of material. (f) Discoidal crystal with straight edge on it, after anhydrite. (g) Pseudomorphs with an initial gypsum growth phase, overgrown by anhydrite rhombohedra. (h) Serrated crystal pseudomorphs after anhydrite.



These stromatolites occur about 3 m above the top of the Masterton Formation, and may represent a marginal marine or lagoonal phase of sedimentation. Stratiform stromatolites are fossilised examples of flat, wrinkled and crenulate mat types which at the present time grow in supratidal, upper intertidal and lacustrine environments—where water depth is too shallow to permit vertical differentiation of stromatolites into columnar forms. Modern equivalents of *Conophyton* require sub-aqueous, quiet conditions for their development (Walter, Bauld, & Brock, 1976; Walter, 1977). Some Precambrian examples may have grown in supratidal marshes (Hoffman, 1976) and others are believed to have occurred in marine subtidal environments (Donaldson, 1976). A supratidal marsh or lagoonal environment for the *Conophyton* is more compatible with the available lithological evidence, but non-marine lacustrine environments could provide the necessary conditions for contemporaneous growth of *Conophyton* and stratiform stromatolites (Siedlecka, 1978 illustrates a comparable environment for late Precambrian stromatolites). The overlying red-bed sequence contains halite casts on several bedding planes, so the water in the *Conophyton* lagoon was probably saline.

The red beds of Unit C have many features indicating that they were water-laid (ripple marks, cross-bedding and scour structures) but they also show signs of emergence and desiccation such as mud-cracks and halite casts.

The depositional environment, then, of this earliest part of the Mallapunyah Formation was extremely shallow water, saline or at least brackish. Wide flats developed, permitting the growth of stratiform stromatolites on the emergent and rarely wetted sediment surface. Locally small, more permanent pools (lagoons or lakes) developed in depressions on the surface (Siedlecka, 1978), where *Conophyton* was able to grow. The maximum relief on these is about 30 cm, so the pools may have been no deeper than that. At other times, the area emerged, and desiccation produced mud-

cracks and halite casts. There is no evidence at this stage for intertidal or subtidal marine conditions.

Unit D consists of a rather monotonous sequence of poorly sorted, slightly dolomitic siltstone, which is dark reddish brown in colour, although pale-green spots and joint fillings are common throughout the section. Some coarser, dolomite-cemented quartz sandstones are intercalated. Cross-bedding is small-scale and low-angle. Abundant small vuggy nodules, up to 8 cm in maximum diameter, occur throughout this part of the Mallapunyah Formation. The nodules are generally encased in thin films of dark green or dark red clay, and occur at discrete levels, parallel to bedding. They are filled with coarsely crystalline dolomite and/or barite, which is usually anhedral in form, but occasional euhedral crystal terminations occur where nodules have a central void. The siltstone laminae wrap around the nodules,

	Mallapunyah Formation	Abu Dhabi
Mineralogy	Quartz/chert/dolomite/barite/sulphides Traces of anhydrite	Anhydrite
Texture of outer surface	Bladed	Bladed
Shape of upper surface	'Cauliflower'-shaped	'Cauliflower'-shaped
Height	5 mm-40 cm	1-30 cm
Distribution	Parallel to bedding	Parallel to bedding
Surface coating	Fine clay films	Fine clay films
Surrounding sediment	Fine/medium sandstone, siltstone, dolomitic sandstone, dololutite	Pleistocene aeolianites

Table 1. Comparison of Mallapunyah Formation nodules with those from Abu Dhabi.

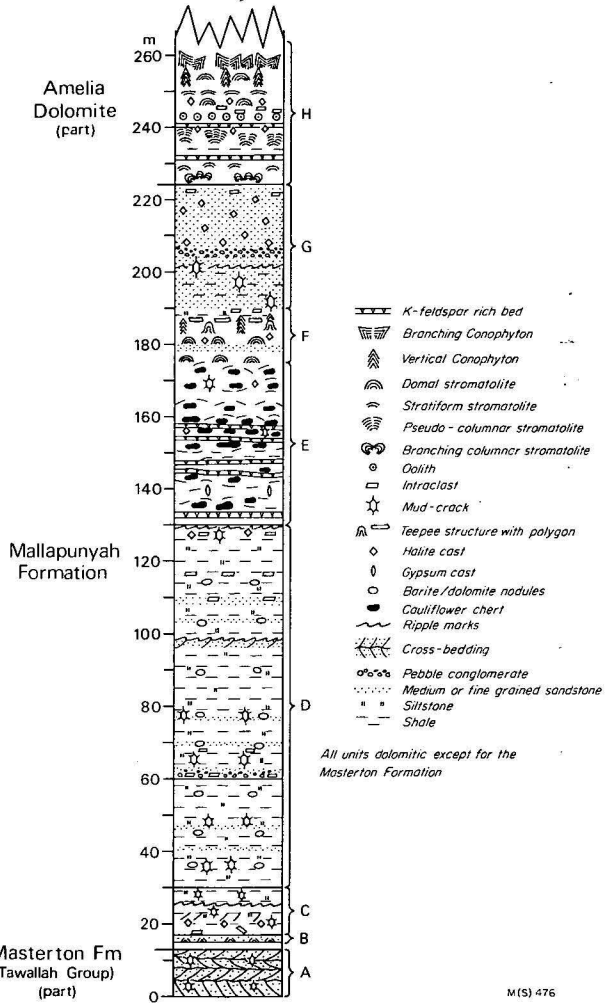


Figure 5. Composite section through the Mallapunyah Formation based on sections measured in the Kilgour River area (M.S. K10, 11 and 12 of Jackson & others).

Figure 4. Scale bar = 10 mm, except where other scale is shown. Micrographs with crossed nicols. (a) Fine mosaic texture in carbonate resembling the texture described by West (1964) from the Diagenetic Stage III (anhydrite). Note stylolite which actually represents a bedding plane. (b) Early diagenetic black chert with cross-cutting stylolite which brings the chert in contact with post-evaporite ferroan dolomite. (c) Small stromatolite with carbonate pseudomorphs after gypsum in the core, and fine dolomite laminae on the outside. The stromatolite is surrounded by ferroan carbonate pseudomorphs after gypsum. The core of the stromatolite must have contained gypsum (either as seeds or crystalline) before deposition of the dolomite laminae in a manner analogous to the gypsum-cored stromatolites at Marion Lake, South Australia. (d) Pseudomorphs after large anhydrite laths truncated by a stylolite. (e) Pseudomorphs after anhydrite or gypsum cross cut by a bedding plane stylolite with considerable loss of material. Bedding parallel to bottom edge of photomicrograph. (f) Pseudomorph after gypsum interpenetration twin.

		Environment			Environment		
Height in section (m)	Lithology	Primary	Diagenetic (early)	Lithology	Primary	Diagenetic (early)	Vadose and late diagenetic
Lagoon waters	Algal mat, primary gyp. arag. calc.	Subtidal to intertidal	Intertidal	Stratiform stromatolites Beach/splash travertine	Supratidal to high supratidal.	Dol./chert small gyp pseudo-morphs	Dol. recryst/ recemented
Sabkha surface		Supratidal sabkha	Inner flood recharge zone				
13	Algal mat, gyp. cement. Qtz. sand		Intermed. flood recharge zone				
12	Arag./cal. muds gypsum mush on surface. gy. cement.		Outer flood recharge zone				
11	Algal mat + gyp cement. anh. nodls.						
10							
HOLOCENE							
9		Terrestrial	High supratidal zone	Dol. shale/silt ?eolian Cauliflower chert, cubic casts, K-feldspar beds	Terrestrial/shallow	Gyp./anh. halite, anh. nodls. ?polyhalite, ?sylvite, high supratidal Dol./chert	Dol. recryst/ recemented High K in clay-stones gives K-feldspar-anh. nodls. silicified
8	Unconsolidated, uncemented aeolianites.						
7	Large anh. nodls. 3 x 1 m.						
6	Gyp. interstitial cement. Halite, sylvite, polyhalite, and detrital clay in lenses and beds						
5							
4							
3							
2							
1							
PLEISTOCENE							
AMELIA DOLOMITE							
MALLAPUNYAH FORMATION							

Table 2. Stratigraphy of the Abu Dhabi sabkha (after Butler, 1969), compared with that of the Amelia Dolomite and Mallapunyah Formation.

indicating that the nodules must have formed either contemporaneously with the siltstones, or early in diagenesis, i.e. before any appreciable compaction had taken place. The siltstones have a dolomitic cement, and the crystalline dolomite in the nodules can reasonably be explained as having a concretionary origin.

The source of the barite, however, is more difficult to determine. Some understanding of the origin of the barite may be obtained from an examination of the results of Hirst & Smith (1974), who studied barite mineralisation in the Permian Lower Magnesian Limestone of the north of England (Fig. 6 for stratigraphic column). The barite occurs in nodules and cavities associated with calcite in fine-grained dolomites. Groundwater in the Coal Measures (believed to be derived mainly from black carbonaceous shale), is rich in barium (more than 4000 ppm in some samples: Edmunds, 1975). Hirst & Smith postulate that these groundwaters have migrated into the Lower Magnesian Limestone. This latter formation is evaporitic, and contains anhydrite relicts and pseudomorphs, providing a source of the sulphate ions that precipitated barite from groundwater BaCl₂. Thus, the barium is of continental origin, whereas the sulphate ions are derived ultimately from marine waters.

A similar dual source can be invoked for the barite in this and other parts of the McArthur Group. The Tawallah Group Masterton Formation rests on the Wollgorang Formation, which consists typically of bituminous dolomites, shales and siltstones. Barite also occurs in the sandstones of the Masterton Formation,

particularly along joints. The Gold Creek Volcanic Member of the Masterton Formation might have provided an additional source for the barium.

The dolomite-barite nodules show no compelling evidence for an evaporitic origin, but gypsum casts are known at a similar level in the Batten Range, to provide a source of sulphate.

The most striking aspect of Unit E is the presence of abundant botryoidal quartz nodules (geodes, cauliflower cherts (Walker & others, 1977)) in 20 to 30 different beds. The nodules vary in thickness from 5 mm to 90 cm, and in length from 5 mm to 1.5 m, and may coalesce to form tabular beds up to 20 cm thick. There is a fine-grained, cherty outer rind (up to 2 cm thick) and a coarser grained, often drusy, centre. The outer surface of the nodules is characteristically bladed, reflecting a meshwork of interlocking lutecite crystals (Walker & others, 1977). The coarsening inner part of the nodule consists of anhedral to euhedral crystals of quartz, dolomite, barite, and fluorite, with minor sulphides such as chalcopyrite and pyrite. About 50 X-ray microanalyses of the coarse-grained material indicate the presence of gold, silver, copper, zinc, iron, and fluorine in small amounts. The outer rind contains numerous inclusions showing three cleavages at right angles. Microanalysis of these inclusions indicates the presence of calcium and sulphur, thus confirming the occurrence of either gypsum or anhydrite. The crystal habit indicates anhydrite.

Botryoidal quartz nodules (see, for example, Chowns & Elkins (1974), and Walker & others (1977)) repre-

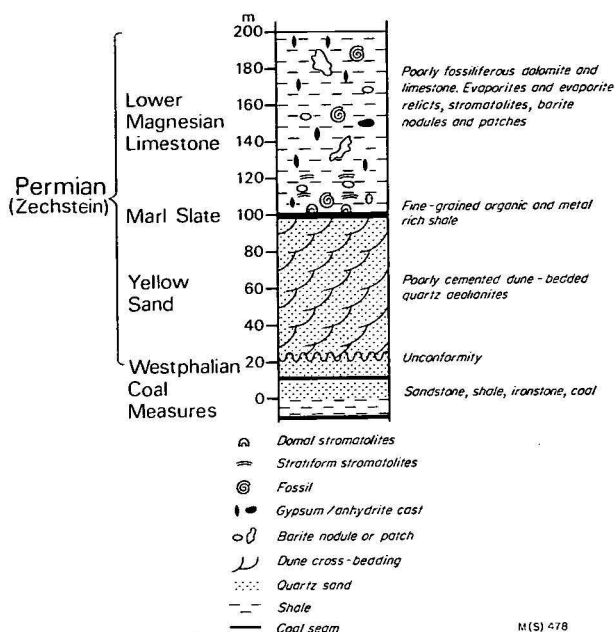


Figure 6. Schematic section through part of the Carboniferous and the Permian of the North of England. Thicknesses approximate based on data from a number of sources.

sent the silicified remains of anhydrite nodules like those which form displacively in the high supratidal zone of the modern sabkha at Abu Dhabi (Butler, 1969). The resemblance between the Mallapunyah Formation botryoidal quartz nodules and the Abu Dhabi nodules is remarkable (Table 1).

The high supratidal zone of the Abu Dhabi sabkha is never flooded by seawater, but concentrated brines derived from marine and continental groundwater precipitate sulphates and carbonates which grow interstitially in the uncompacted sediment. The concentrated marine and continental groundwaters are periodically subject to dilution by fresh waters derived from rainfall. This causes occasional hydration of anhydrite in the nodules to gypsum with partial destruction of the bladed texture (Butler, 1969). The environment of deposition of the upper part of the Mallapunyah Formation must have been a sabkha, very similar in climate and morphology to the modern sabkhas of the Persian Gulf, and in particular to Abu Dhabi. The Mallapunyah Formation sandstones show no signs of sub-aerial dune bedding, but could represent water reworked dune sands, as is the case with the Abu Dhabi aeolianites. The early diagenetic evaporites are so alike that they must indicate identical conditions during early diagenesis. Under these diagenetic conditions in the modern sabkha (Butler, 1969), precipitation of the anhydrite nodules is accompanied by deposition of small amounts of gypsum, halite, and larger amounts of polyhalite and sylvite, many of the elements of which were derived from terrestrial groundwaters. Much of the potassium is rapidly re-dissolved and reprecipitated in thin beds of illitic clays, which gives rise to authigenic potassium feldspar (Butler, 1969). Thin potassium feldspar-bearing siliceous claystones in the upper part of the Mallapunyah Formation have previously been identified as tuffites or tuffaceous shale (Muir & Diver, 1975). They could more plausibly be interpreted as potassium-enriched clays similar to those formed diagenetically at Abu Dhabi.

In Unit F, the silts and fine sands frequently have a dolomitic cement, grading into dololite, sometimes stromatolitic. Purple dololite, containing silicified ridge-shaped *Conophyton*-like stromatolites, with the ridges forming large teepee and polygon systems of up to 2 metres in diameter, occurs at this horizon in Kilgour River. These structures probably formed in supratidal seepage zones in a fashion analogous to the stromatolite-encrusted teepees and polygons described by von der Borch & others (1977) from the Holocene deposits of Marion Lake in South Australia.

Halite casts are extremely abundant in Unit G.

Sections comparing the upper part of the Mallapunyah Formation and the lower part of the Amelia Dolomite with the Pleistocene and Holocene of Abu Dhabi are shown in Table 2.

Amelia Dolomite

Depositional environments. There is no direct evidence as to the nature of the primary carbonates in the Amelia Dolomite. By analogy with the Holocene, they were most probably aragonite or magnesian calcite. The stromatolite morphologies imply supratidal to high intertidal conditions of deposition and the morphologies of the microfossils are similar to the morphologies of micro-organisms—mainly coccoid cyanobacteria, which at the present time are characteristic of supratidal algal mats in the modern Persian Gulf and Shark Bay, Western Australia (Golubic, 1976). In addition, the black cherts are brown in thin section, because of the presence of much more or less amorphous organic matter, which represents the fossilised remains of algal mucilage (Muir, 1976). This mucilage gives the modern Persian Gulf algal mats their characteristic rubbery texture.

The micro-organisms are morphologically very similar to those of the present time, and may have had very similar metabolic processes. Certainly, the three-dimensionally preserved mucilage sheaths (Muir, 1976) appear identical to those described from the Persian Gulf (Golubic, 1976). These are preserved in three dimensions because aragonite is precipitated in them as a by-product of the metabolic activity of the living algae, which then migrate upwards towards the light, leaving the sheaths already impregnated by aragonite before burial. Magnesium is preferentially absorbed by the organic matter, and released again on burial and diagenesis (mainly as a result of bacterial degradation of the organic matter: Krumbein, pers. comm., 1976). Small gypsum crystals (up to 1 mm) are sometimes found in thin sections of the algal mat. The microfossils cluster round the gypsum crystals, but apparently are not adversely affected by their presence. When incorporated into the sediment, the sea-water sulphate ions remaining interstitially provide a source for the activities of sulphate-reducing bacteria. In the Amelia Dolomite material, indirect evidence for the former presence of sulphate reducers can be adduced from the frequent presence of small grains of pyrite in the black chert. There are several possible sites for pyrite localisation: (a) along bedding-plane laminae marked out by mucilage. This pyrite is very fine-grained, one or two microns in diameter, and occasionally aggregates to form clusters or very irregular framboids (Muir, 1976, figure 7H). It may also be concentrated along bedding plane stylolites. (b) walls of cells which are partly decomposed often contain small cubes of pyrite (again 1-2 microns in diameter). Materials in the cell wall presumably acted as an organic nutrient medium for

KILGOUR RIVER		INFORMAL STRATIGRAPHIC UNITS		LEILA CREEK		
Lithology	Thickness (m)		Thickness (m)	Lithology	AMELIA DOLOMITE	
Conformable passage		Tatoola Sandstone		Local unconformity		
Mainly flake breccia with some oolites; dolarenite with stratiform, domal, and columnar stromatolites	56	Upper dolomite	60	Oolites, oncolites, abundant flake breccia; dolarenite with stratiform, domal, and columnar stromatolites		
Stratiform and domal stromatolites with <i>Conophyton</i>	27	Upper evaporite	30	Sideritic marble with stratiform and domal stromatolites. Some <i>Conophyton</i>		
Oolitic, oncolitic dolarenite and dololulite with stratiform stromatolites and flake breccia	30	Middle dolomite	60	Oolitic and oncolitic dolarenite with stratiform stromatolites and flake breccia		
Stratiform and domal stromatolites with abundant <i>Conophyton</i>	32	Lower evaporite	40	Sideritic marble with stratiform stromatolites and abundant <i>Conophyton</i>		
Shaley dolarenite and dololulite, purple, red and green shale and fine sandstone, stratiform and columnar stromatolites	16	Lower dolomite	30	Flaggy dololulite, flake breccia, green and purple mudstone and shale; stratiform stromatolites		
Conformable passage		Mallapunyah Formation		Conformable passage		

Table 3. Correlation of Amelia Dolomite: Kilgour River to Leila Creek (after Jackson & others, 1978).

the sulphate reducers and the cell contents or mucilage may have been the iron source (Oehler, 1978) causing precipitation of the pyrite precursors on or in the cell wall (Muir, 1976; figure 7J); (c) a third common site for pyrite precipitation is in the centre of spherical colonies (Muir, 1976, figure 7G). This pyrite is often coarse-grained, and the colonies have almost entirely decomposed, apart from an outer ring of uncrushed cells. The clear chert surrounding the pyrite crystals appear to pseudomorph a carbonate mineral (?calcite).

In some modern carbonate environments, too, early diagenetic dolomitisation takes place by bacterial release of magnesium from the organic matter trapped in the sediment (Krumbein, pers. comm., 1976). This early dolomite is very fine-grained and generally forms small (2-3 μm) rhombohedra. Similar rhombohedra are common in the Amelia Dolomite, although they have been subsequently replaced by chert. These rhombohedra postdate the incorporation into the sediment of the micro-organisms because rhombohedra are outlined in organic matter which has been pushed aside by the growth of the crystal (quite unlike the relationship between the growth of the small gypsum crystals and the microfossils and/or mucilage).

This early dolomitisation and the silicification which gives rise to the black cherts pre-date compaction of the sediment. The chert, however, postdates the dolomite, because it pseudomorphs it. Silica is a common constituent of groundwater in arid, hypersaline environments (von der Borch & Jones, 1976) and replaces earlier carbonates patchily as wisps, lenses and nodules, some of which may be sufficiently extensive to form discontinuous tabular beds. The distribution of the chert depends primarily on porosity and permeability of the original carbonates, but abundant organic matter appears to favour chert replacement of carbonates. Many of the microfossil assemblages described from Precambrian rocks occur in cherts such as these (Schopf, 1975).

Depositional history of the lower part of the Amelia Dolomite. The base of the Amelia Dolomite is taken at the base of the first conspicuous dolomite unit (Table

3). This may be up to 3 metres thick (e.g. Leila Creek, Tawallah Range) and consists of stratiform stromatolites containing numerous black cherts in which abundant microfossils are preserved. In addition, coniatolites (beach rock, splash travertine, cemented aragonite crusts) are commonly preserved, along with colloform textures.

Scattered small pseudomorphs after gypsum (ca 0.75 cm) occur throughout this unit. They are discoidal in shape and appear to have grown displacively in the sediment. They are similar to those described by Butler (1969) as having grown in the intermediate flood recharge zone.

The basal Amelia Dolomite bed is followed by a thin sequence of red, purple, and green siltstone and shale which contains occasional pseudomorphs after small gypsum crystals. The rock appears to be terrestrial in origin, although because of poor (or no) exposure, sedimentary structures have not been determined. The gypsum has grown displacively in a sabkha situation; this suggests a slight regression following the initial Amelia Dolomite transgression. In the southern part of the area, at Kilgour River, the lowest dolomite contains stratiform stromatolites at the base (just as in the north), but develops small branching columnar stromatolites (30 cm maximum height) at the top of the unit below the shaly and sandy interval. This indicates that the water depth may have been greater in the south, although this may have been a local, not regional trend. There are no gypsum crystal pseudomorphs in the lowest dolomite or overlying shale and siltstone in the Kilgour River sections (see Table 3).

In the Leila Creek area, this lowermost shaly sequence is followed by thin stratiform stromatolite beds and then by some 40 metres of sideritic marble. The marble is a distinctive dark reddish brown colour and forms beds up to 3 metres thick. The original lamination is difficult to detect but the early diagenetic black cherts remain in sufficient quantity to delineate stratiform stromatolites and, in places, *Conophyton*. Thin sections of the black cherts from the stratiform stromatolites in the sideritic marbles contain micro-

fossils, primary gypsum crystals, pyrite, and dolomite rhombohedra identical with those found in the lowermost bed of the Amelia Dolomite. Thin sections of the *Conophyton* black chert (from the sideritic marble) have not yet proved fossiliferous, but the other constituents are present. Lamination away from the black cherts is extremely difficult to detect, and in most cases is stylolitic. The contacts between the black cherts and the sideritic marble are also frequently stylolitic, although sharply cross-cutting relationships are also common (Fig. 4b). The sideritic marble clearly forms later in diagenesis than the black chert.

The marble is coarse-grained and consists of sub to anhedral pseudomorphs after gypsum and/or anhydrite (Walker & others, 1977), with frequent inclusions of small anhedral flakes of relict anhydrite. The crystals are most often normal (Fig. 4e), or nearly so to the bedding, but in some cases are completely intergrown, forming an interlocking random meshwork (Fig. 3c). Cruciform twinning is not uncommon (Fig. 4f). Stylolisation occurs throughout, with the stylolites usually formed parallel to the bedding, although almost any direction with respect to bedding is possible. In some cases, the passage of a stylolite through a crystal causes little disruption or loss of material, but in many cases, at least 30 percent of the crystal has been lost (Fig. 4d). The total loss of section is difficult to estimate but it could be as much as 30 percent in places, and may, perhaps, be assessed overall at a minimum of 10 percent. Collapse conglomerates occur above many of these beds.

Most of the sulphate crystals are now replaced by coarse-grained carbonate (iron-rich-ferroan dolomite, pistomesite, or siderite) mosaics (Fig. 4a), reminiscent in texture of West's (1964) Stage Va porphyroblastic gypsum. In other cases, fine-grained carbonate mosaics infill the crystal outlines (equivalent to the textures of West's Stage Vd), where more or less equigranular gypsum results from the hydration of anhydrite. These stages can be used to give us some indication of the depth of burial of the sediment before the sulphates were replaced by carbonates. This will be discussed in greater detail later.

The diagenetic emplacement of the sulphates is proved by the fact that they are demonstrably later than the black cherts which are themselves diagenetic. In fact, such displacive gypsum precipitation has been shown by Shearman (1966), Shearman & Fuller (1969), and Butler (1969) to result from precipitation from concentrated brines in the capillary zone of a sabkha. In the lower part of the Amelia Dolomite, several features or stages similar to stages in the development of the Abu Dhabi sabkha can be recognised (see Table 2 for an analysis of the environments of deposition of the top of the Mallapunyah Formation and lower part of the Amelia Dolomite).

Similar analyses can be carried out for all parts of the section. In some cases, diagenetic gypsum and anhydrite must have been precipitating in older sediments while new primary deposits were being formed to seawards. It should be possible by careful mapping of selected intervals to determine the position of the sabkha and the shoreline at any given time in the Amelia Dolomite. Some assessment of the width of the sabkha should also be possible by comparison with Butler's data. The width of the Abu Dhabi sabkha is approximately 12 km and the distance between the intertidal and intermediate flood recharge zone is

approximately half of this. Future mapping of primary and early diagenetic facies should permit the calculation of sabkha width. Using regional studies, it will be possible to make a very accurate reconstruction of palaeogeography and palaeoclimates in Mallapunyah Formation and Amelia Dolomite times. Recent work (Muir & others, 1979) has indicated that the Yalco Formation of the Batten Sub-group (Fig. 1) was deposited in climatic conditions that were seasonally more humid than the arid sabkha conditions of the Amelia Dolomite and Mallapunyah Formation. It may be eventually possible, after detailed studies have been carried out on other formations, to construct a series of climatic intervals throughout the McArthur Group. The climatic sequence thus produced may prove to be useful for regional correlations with the rocks of similar age in northwest Queensland, which have a similar stratigraphy. It should provide a level of accuracy of correlation intermediate between the large scale using radiometric dating, and the fine scale possible using micro-palaeontological and magnetostratigraphic correlation.

Metallic concentrations

Renfro (1974) postulated that the distribution of copper mineralisation in evaporitic provinces could be related to palaeoshore lines. It may be significant to note that anomalously high copper values occur in both the Amelia Dolomite and Mallapunyah Formation.

The Persian Gulf sabkha is a product of extreme climatic conditions of high temperature and almost total aridity. These give rise to extremely high evaporation rates, and the groundwaters, both marine and terrestrial, become concentrated. As a result of this concentration process, carbonates, including dolomite, sulphates, and silica are precipitated and may be redissolved and reprecipitated many times. The connate brines become enriched in heavy metals (mainly as chloride complexes, or sometimes in organic complexes) which will not precipitate until the brine reaches a suitable environment. Some relics of these metal-rich brines can be found in the centres of the botryoidal quartz nodules of the Mallapunyah Formation where gold, silver, copper, zinc, and fluorite occur. This last is an important indicator, since fluorine is very soluble and tends to precipitate late in an evaporitic sequence, after considerable concentration has taken place (Shearman, pers. comm., 1975).

Late diagenetic and burial diagenetic environments

Burial diagenesis of gypsum and anhydrite

West (1964) concluded that the conversion of gypsum to anhydrite (his Diagenetic Stage III) had taken place with an overburden of no less than 2000 feet (~600 m). The mosaic texture described by West from Purbeck evaporites occurs occasionally in the upper evaporite unit of the Amelia Dolomite (Table 3), which must also have formed at a minimum depth of burial of 600 m. However, most of the pseudomorphs show porphyroblastic textures similar to West's Stage V (some pseudomorphs retaining traces of (anhydrite) net-texture (Va), and others retaining little evidence for anhydrite (cf. West's Vb)). Stage V textures result from rehydration of anhydrite to gypsum after removal of overburden and thus we must conclude that the Amelia Dolomite evaporites have undergone a cycle of burial to at least 600 m, after which some of the overburden was removed by erosion processes.

During mapping in the Leila Creek area, a local unconformity could be traced between the Amelia Dolomite and the overlying Tootola Sandstone. However, this would not permit the accumulation or erosion of sufficient thickness of sediment to cause either the dehydration or the rehydration phases.

However, the Tootola Sandstone (ca 140 m) is overlain by the 800-900 m thick Tooganinie Formation. Approximately 600 m above the base of the Tooganinie Formation, the normal carbonate/silt and sand sequence is interrupted by the 140 m thick Leila Sandstone Member, which is a coarse, glauconitic, oolitic quartz sandstone, with abundant current structures indicating both fluvial and shallow-marine environments. It is possible that this influx of coarse, mainly detrital material may indicate a period of erosion or non-deposition, and may account for the rehydration of anhydrite to gypsum in the Amelia Dolomite evaporites.

The Leila Sandstone Member is host to a number of small Cu/Ba prospects. Most of these occur as disseminated fine-grained chalcopyrite (weathering to malachite) and barite in one of the sandstones. The occurrence of barite may indicate escape of sulphate-rich groundwaters from the underlying evaporite sequences (small botryoidal quartz nodules are found occasionally in the Leila Sandstone Member). If the Leila Sandstone Member does indeed overlie an unconformity, a land surface may have been exposed, and the barium source, as in the Permian of the north of England, could well be terrestrial.

Silicification

West (1964) finds that silicification affects only the dehydration stages I, II, and III of his diagenetic sequence. That is to say that silicification is somehow associated with dehydration and burial, perhaps because of pH changes consequent to the release of connate water from the gypsum. If these interpretations can be generalised, then it may be possible that the silicification of the anhydrite (now botryoidal quartz) nodules of the Mallapunyah Formation occurred during the maximum depth of burial of the evaporites and before later erosional phases. Unlike the gypsum/anhydrite reactions, the silicification appears to be irreversible. There is no evidence that the siliceous rinds on the outer surfaces of the botryoidal quartz nodules went through an intermediate carbonate stage between anhydrite and chert, but deposition of the inner, coarser grained material may either pre or postdate the silicification of the outer rind. The evidence is equivocal.

Replacement of evaporites by carbonates

On burial, sediments pass through a number of diagenetic facies or zones (Curtis, 1977). The zones may vary from as little as millimetres to kilometres in thickness, and are delineated by specific temperature and porosity ranges, and characteristic mineral assemblages which are produced in each zone. We have seen evidence previously (p. 157) of the zone of sulphate reduction, which, according to Curtis (1977), occurs in the uppermost millimetres of the sediment. Pyrite, calcite, and dolomite are precipitated in this zone. The carbonates are low in iron and enriched in ^{12}C .

In Curtis' model, below about 10 m, sulphate is exhausted from pore waters of organic-rich clays, thus putting an end to pyrite precipitation from a lack of sulphur source. The situation in the hypersaline environments in the Mallapunyah Formation and Amelia Dolomite does not essentially differ from this, although

the actual depth might be somewhat greater. By analogy with the Abu Dhabi sabkha, emplacement of solid evaporites is complete within a depth of about 10 m, and interstitial sea water would also have evaporated, leaving no more sulphate ions for bacterial reduction. The sediments would tend to be relatively dry at this stage, permitting access of oxygen, which also inhibits sulphate-reducing bacteria. Only on deeper burial into underlying aquifers could further diagenetic changes be initiated. Then, applying the Curtis model, anaerobic bacterial fermentation processes began, with the production of ^{12}C -enriched methane, which escapes from the sedimentary pile, and ^{13}C -enriched carbon dioxide, which causes the precipitation of ^{13}C -enriched carbonates. These heavy carbonates are ferroan calcite, ankerite, and siderite, because iron activity is high as a result of the very reducing conditions in the sedimentary pile, and because of the cessation of pyrite precipitation. At depths below 1 km, inorganic processes (decarboxylation) continue to generate CO_2 , and iron-rich carbonate precipitation continues.

Curtis' model may be applied to the replacement of the Amelia Dolomite evaporites by iron-rich carbonates. There is no direct evidence for bacteria capable of producing CH_4 or CO_2 by fermentation processes at that geological time, but the inorganic decarboxylation processes must have operated under suitable conditions. The depth of burial required for the replacement of sulphate minerals by ferroan carbonates must have been greater than 10 m, the top of the fermentation zone. However, from the evidence of the gypsum/anhydrite conversion stages, the sediments were buried as sulphates at least to ~600 m. This depth is well into the fermentation zone. The colour of the preserved organic matter is light brown, indicating that it has been heated to between 50-100°C (Sengupta, 1975), and the temperature boundary between fermentation and decarboxylation falls at only 28°C. Thus it seems reasonable to assume that replacement of the sulphates by the iron-rich carbonates must have taken place within the decarboxylation zone, at a depth of a kilometre or more.

Implications for mineralisation of the release of sulphate-rich waters

The Mara Dolomite Member of the Emmerugga Dolomite lies ~1 km stratigraphically above the Amelia Dolomite. The sulphate released from the evaporites would have moved into brines which would then have become available for sulphate reduction and ore deposition. The Mara Dolomite Member contains numerous small epigenetic sulphide deposits (i.e., Cooleys Pb/Zn) which could result from the release of these sulphates into the groundwater. The metals (Pb, Zn) could have been concentrated during the existence of the sabkha, directly from sea water, or indirectly from precipitated halite (Carpenter & others, 1976); or have been concentrated by processes such as dolomitisation, or during burial diagenesis. The Mara Dolomite Member occurs on the eastern side of the Emu Fault (as well as farther west) and is believed to have been exposed, at least during deposition of the McArthur ore body (Walker & others, 1978). It is possible that the Emu Fault acted as a channelway for the metal and sulphate-rich brines, which were moved through the fault zone by some mechanism such as seismic pumping (Sibson & others, 1976), and subsequently arrived in the depositional basin of the McArthur ore body. This mechanism does not preclude diagenetic emplacement of metals and sul-

phides. Williams (1979) has discussed the possibility of an evaporite source for at least some of the metal in the McArthur ore body.

Using Renfro's (1974) model, copper mineralisation can be expected on the landward side of a sabkha: both the Amelia Dolomite and Mallapunyah Formation are copper-enriched. Furthermore, any syngenetic or diagenetic mineralisation requires a source of brines, rich in metals or in sulphates—so formations geographically remote from the sabkha deposits, or connected with different groundwater systems, will have less chance of enrichment in metals such as Cu, Pb, Zn. The sedimentary sequence must have adequate accessways for the brine solutions, either through porosity (primary or secondary), permeability, aquifers in the sediments, or through faults and joints in the sequence. The accessways can operate at any stage, from earliest diagenesis, to late vadose and phreatic situations (as in karst-type deposits).

Secondary enrichment, in particular of copper ore, is known from a number of localities, related either to the present weathering profile, or to former surfaces. The karstic copper deposit at Kilgour (Fig. 2) lies underneath a covering of Cambrian Bukalara Sandstone (Jackson & others, 1978; Muir, 1979). Thus a brief consideration of the effects of vadose and phreatic alteration is relevant to this paper.

The dolomites of the Mallapunyah Formation and Amelia Dolomite have undergone extensive recementation and recrystallisation. The dating of this is uncertain, but it postdates the replacement of the sulphates, as shown by cross-cutting relationships. It does not, however, appear to be a superficial effect, because recrystallisation can be observed in drill-core material.

Superficial weathering takes the form of magnesite ('magcrete') or silcrete crusts which particularly affect the replaced evaporite beds. Silcrete forms along the tops of ridges, along joints and faults, and along certain beds, for no obvious reason. Magcrete tends to form on low ground or on dip-slopes. The silcrete is often iron-rich and may grade into pure hematite in places (presumably as a result of the release of iron from sideritic marble). In some sections, barite is common, especially in association with replaced evaporite sections (which nearly all contain barite). Senior (1977) points out that barite is a common constituent of silcrete, and can be abundant in some silcrete profiles (up to 6000 ppm in places).

Conclusions

The primary depositional environments of the Mallapunyah Formation and Amelia Dolomite range from terrestrial to shallow-marine. The Mallapunyah Formation is predominantly red and purple dolomitic silt and sand of sub-aqueous and possibly originally terrestrial origin. Minor lacustrine or lagoonal deposits formed in a high supratidal environment and these contain a stratiform stromatolite/*Conophyton* assemblage. The Mallapunyah Formation was deposited on a marginal marine plain, which has many of the diagenetic features of the reworked Pleistocene aeolianites of the present-day Persian Gulf sabkha. The overlying Amelia Dolomite ranges from supratidal to subtidal deposits, with a number of distinctive stromatolite and microfossil assemblages. A number of zones which correlate closely with the Holocene sabkha deposits of Abu Dhabi can be recognised by the distribution and nature of the evaporite mineral parageneses. The two forma-

tions constitute together a complex regressive/transgressive cycle, with a major progradation of the coastline during deposition of the Mallapunyah Formation.

Evaporite relicts after gypsum, anhydrite and halite are abundant. The remains of both primary gypsum and halite have been observed, but most of the evaporite minerals were emplaced diagenetically—and invariably so for anhydrite. The commonest form of anhydrite relict is the botryoidal quartz (cauliflower chert) nodule, found mainly in the Mallapunyah Formation. Modern analogues of these nodules are associated with potassium-rich brines which metasomatically alter illitic clay lenses. Potassium feldspar-rich fine-grained rocks are closely associated with the botryoidal quartz nodules of the Mallapunyah Formation. The barite which occurs in the botryoidal quartz and other small nodules in this same part of the section is not solely evaporitic in origin. The sulphate is evaporitic, but the barium is derived from continental groundwater.

Several stages of burial diagenesis may be recognised. The conversion of gypsum to anhydrite and its rehydration can be identified. On deeper burial, the sulphates were replaced by iron-rich carbonates, releasing sulphate-rich brines just after the time of deposition of the Mara Dolomite Member of the Emmerugga Dolomite. This contains numerous small epigenetic Pb/Zn deposits which may have been derived from the newly released sulphates. The metal-rich brines may also have contributed to the mineralisation in the McArthur ore body.

Detailed mapping of the Mallapunyah Formation and Amelia Dolomite should permit an assessment of the geography of the sabkha to be made with some accuracy. Correlations between diagenetic phases will enable an accurate time-limited palaeogeography to be determined.

Because other formations in the McArthur Group (e.g. the Yalco Formation) contain indications of climatic regimes which are different from the arid sabkhas of the Mallapunyah Formation and Amelia Dolomite, it should be possible to develop a sequence of climates for the group as a whole. It will then be possible to attempt to correlate these climatic sequences with those from northwest Queensland, where Carpentarian rocks of similar lithologies are exposed. Correlation at this level of precision is a useful step between the coarse, but universal, scale of radiometric correlation, and the fine, but local, scale of micropalaeontological and magnetostratigraphic correlation.

Acknowledgements

The fieldwork on which this paper is based was mainly completed in 1975, when M.D.M. and W. L. Diver (Imperial College, London) measured sections B1 and M7-12, and mapped selected areas. Extensive sampling was undertaken at that time, and laboratory work was carried out at Imperial College, London, as part of a Natural Environment Research Council Programme. Sections K10-12 were measured in 1977 as part of the BMR McArthur Basin Project, and some of the information from this work is incorporated in this paper. Thanks are particularly due to M. J. Jackson, M. C. Brown, and D. E. Large, for stimulus and discussion during this part of the fieldwork. The diamond drill hole Tawallah No. 1 was drilled by the Carpentaria Exploration Co. Pty Ltd in 1972, and the core was presented to the BMR for study. K. J. Armstrong,

R. V. Burne, W. E. Krumbein, K. A. Plumb, M. R. Walter, and I. M. West have also contributed to this paper in numerous ways, and I am particularly grateful to C. D. Curtis, B. C. Schreiber, D. J. Shearman, and R. N. Walker for their unstinting help and encouragement.

References

- BUTLER, G. P., 1969—Modern evaporite deposition and geochemistry of coexisting brines, the sabkha, Trucial Coast, Arabian Gulf. *Journal of Sedimentary Petrology*, **39**, 70-89.
- CAR/ENTER, A. B., TROUT, M. L., & PICKETT, E. E., 1974—Preliminary report on the origin and chemical evolution of lead- and zinc-rich oil field brines in Central Mississippi. *Economic Geology*, **69**, 1191-206.
- CHOWNS, T. M., & ELKINS, J. E., 1974—The origin of quartz geodes and cauliflower cherts through the silicification of anhydrite nodules: *Journal of Sedimentary Petrology*, **44**, 884-1003.
- CURTIS, C. D., 1978—Sedimentary geochemistry: environments and processes dominated by involvement of an aqueous phase. *Philosophical Transactions of the Royal Society of London*, **A286**, 353-72.
- DONALDSON, J. A., 1976—Palaeoecology of Conophyton and associated stromatolites of the Precambrian Dismal Lakes and Rae Groups, Canada. In WALTER, M. R. (Editor). STROMATOLITES. Elsevier, Amsterdam, 523-34.
- EDMUNDS, W. M., 1975—Geochemistry of brines in the coal measures of northeast England. *Transactions of the Institute of Mining and Metallurgy. (Applied Earth Sciences)* **B84**, 39-52.
- GOLUBIC, S., 1976—Organisms that build stromatolites. In WALTER, M. R. (Editor), STROMATOLITES. Elsevier, Amsterdam, 113-26.
- GOLUBIC, S., & HOFMANN, H. J., 1976—Comparison of Holocene and Mid-Precambrian Entophysalidaceae (cyanophyton) in Stromatolitic algal mats: cell division and degradation. *Journal of Paleontology*, **50**, 1074-82.
- HIRST, D. M., & SMITH, F. W., 1974—Controls of barite mineralisation in the Lower Magnesian Limestone of the Ferryhill area, County Durham. *Transactions of the Institute of Mining and Metallurgy. (Applied Earth Sciences)* **B83**, 49-55.
- HOFFMAN, P. F., 1976—Environmental diversity of Middle Precambrian Stromatolites. In WALTER, M. R. (Editor), STROMATOLITES. Elsevier, Amsterdam, 599-611.
- JACKSON, M. J., MUIR, J. D., PLUMB, K. A., LARGE, D. E., BROWN, M. C., & ARMSTRONG, K. J., 1978—Field work report, McArthur Basin Project 1977. *Bureau of Mineral Resources, Australia, Record* **1978/54** (unpublished).
- KINSMAN, D. J. J., 1969—Modes of formation, sedimentary associations, and diagnostic features of shallow water and supratidal evaporites. *Bulletin American Association Petroleum Geologists*, **53**, 830-40.
- MUIR, M. D., 1976—Proterozoic microfossils from the Amelia Dolomite, McArthur Basin, Northern Territory. *Alcheringa*, **1**, 143-58.
- MUIR, M. D., 1979—Mineralisation. In PLUMB, K. A. (Coordinator) McArthur Basin research project progress report, December quarter, 1978. *Bureau of Mineral Resources, Australia, Record* **1979/16** (unpublished).
- MUIR, M. D., & DIVER, W. L., 1975—Report on a field trip in Australia, April 23-September 7, 1975. *Research report submitted to the National Environment Research Council, U.K.* (Unpublished).
- MUIR, M. D., LOCK, D. E., & VON DER BORCH, C. C., in press—The Coorong—model for penecontemporaneous dolomite formation in the Middle Proterozoic McArthur Group, Northern Territory, Australia. In ZENGER, D. H. (Editor). CONCEPTS AND MODELS OF DOLOMITIZATION—THEIR INTRICACIES AND SIGNIFICANCE. *Proceedings 1979 SEPM Research Symposium*.
- NEEV, D., & EMERY, K. O., 1967—The Dead Sea. *Israel Geological Survey Bulletin*, **41**, 1-144.
- OEHLER, D. Z., 1978—Microflora of the middle Proterozoic Balbirini Dolomite (McArthur Group) of Australia. *Alcheringa*, **2**, 269-309.
- PLUMB, K. A., & BROWN, M. C., 1973—Revised correlation and stratigraphic nomenclature in the Proterozoic carbonate complex of the McArthur Group, Northern Territory. *Bureau of Mineral Resources, Australia, Bulletin* **139**, 103-15.
- PLUMB, K. A., & DERRICK, G. M., 1976—Geology of the Proterozoic rocks of the Kimberley to Mount Isa region. In KNIGHT, C. L. (Editor), ECONOMIC GEOLOGY OF AUSTRALIA AND PAPUA NEW GUINEA. 1. METALS. *Australasian Institute of Mining & Metallurgy, Melbourne*, 217-52.
- RENFRO, A. R., 1974—Genesis of evaporite-associated stratiform metalliferous deposits—a sabkha process. *Economic Geology*, **69**, 33-45.
- SCHOFF, 1975—Precambrian paleobiology: problems and perspectives. *Annual Review of Earth & Planetary Sciences*, **3**, 213-49.
- SENGUPTA, S., 1975—Experimental alterations of the spores of *Lycopodium clavatum* as related to diagenesis. *Review of Palaeobotany Palynology*, **19**, 173-92.
- SENIOR, B. R., 1977—Landform development, weathered profiles and Cainozoic tectonics in southwest Queensland. *Ph.D. Thesis*, University of New South Wales (Unpublished).
- SHEARMAN, D. J., 1966—Origin of marine evaporites by diagenesis. *Transactions of the Institute of Mining and Metallurgy (Applied Earth Sciences)*, **B75**, 208-15.
- SHEARMAN, D. J., & FULLER, J. G., 1969—Anhydrite diagenesis, calcitization and organic laminites, Winnipegosis Formation, Middle Devonian, Saskatchewan. *Bulletin of Canadian Petroleum Geology*, **17**, 469-525.
- SIEDLECKA, A., 1978. Late Precambrian tidal-flat deposits and algal stromatolites in the Batsford Formation, East Finnmark, North Norway. *Sedimentary Geology*, **21**, 277-310.
- SIBSON, R. H., MOORE, J., McM., & RANKIN, A. H., 1975—Seismic pumping—a hydrothermal fluid transport mechanism. *Journal of the Geological Society of London*, **131**, 653-59.
- SMITH, J. W., 1964—Bauhinia Downs, N.T.—1:250 000 Geological Series. *Bureau of Mineral Resources, Australia, Explanatory Notes*, **SE/53-3**.
- VON DER BORCH, C. C., BOLTON, B., & WARREN, J. K., 1977—Environmental setting and microstructure of subfossil lithified stromatolites associated with evaporites, Marion Lake, South Australia. *Sedimentology*, **24**, 693-708.
- VON DER BORCH, C. C., & JONES, J. B., in press—Spherular modern dolomite from the Coorong area, South Australia. *Sedimentology*, **23**.
- WALKER, R. N., LOGAN, R. G., & BINNEKAMP, J. G., 1978—Recent geological advances concerning the H.Y.C. and associated deposits, McArthur River, N.T. *Journal of the Geological Society of Australia*, **25**, 365-80.
- WALKER, R. N., MUIR, M. D., DIVER, W. L., WILLIAMS, N., WILKINS, N., 1977—Evidence of major sulfate evaporite deposits in the Proterozoic McArthur Group, Northern Territory, Australia: *Nature*, **265**(5594), 526-9.
- WALTER, M. R., BAULD, J., & BROCK, T. D., 1972—Siliceous algal and bacterial stromatolites in hot spring and geyser effluents, Yellowstone National Park, Wyoming. *Science*, **178**, 402-5.
- WALTER, M. R., 1977—Interpreting stromatolites. *American Scientist*, **65**, 563-71.
- WEST, I. M., 1964—Evaporite diagenesis in the Lower Purbeck Beds of Dorset. *Proceedings of the Yorkshire Geological Society*, **34**, 315-30.
- WILLIAMS, N., in press—The timing and mechanisms of formation of the Proterozoic stratiform Pb-Zn and related Mississippi valley-type deposits at McArthur River, N.T. Australia. *Proceedings of the Society of Economic Geologists* (in press).

Stream-sediment sampling near two porphyry copper prospects, Georgetown area, Queensland

Allan G. Rossiter

Introduction

The Phyllis May prospect is about 29 km west of Georgetown, north Queensland (Fig. 1). It was discovered in 1970 during geological prospecting by Central Coast Exploration NL, and it was soon established that the deposit was of the porphyry-copper type (O'Rourke, 1971). In 1975 evidence of similar mineralisation was recognised at Mount Turner, 11 km west-northwest of Georgetown (Fig. 1), by officers of the Bureau of Mineral Resources and the Geological Survey of Queensland. Stream-sediment sampling was carried out in the two areas during 1976 to test the applicability of this technique for detecting similar deposits in other parts of the region.

The Georgetown area has a sub-humid tropical climate. Temperatures are moderate to high all year, and the mean daily maximum is about 32°C. Rain is almost entirely confined to the period November-April; the annual average is about 700 mm. Two consequences of the seasonal rainfall are that all but a few streams are dry during the winter, and that a sparse savannah woodland covers the region. The Phyllis May area is fairly flat, although a well-defined stream pattern exists; at Mount Turner relief approaches 100 m.

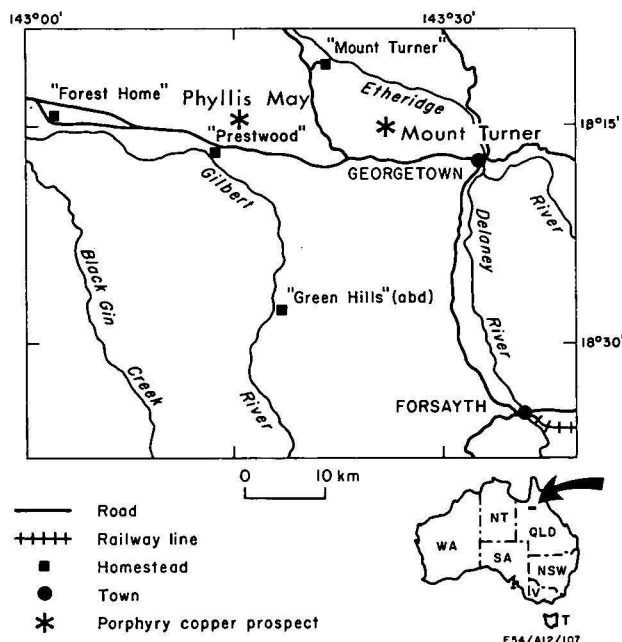
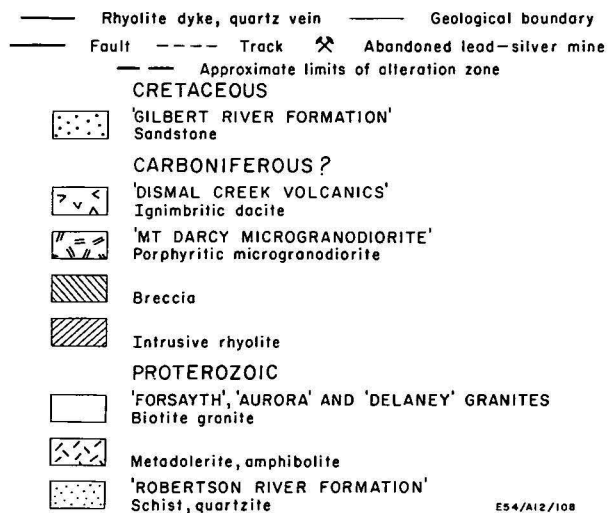
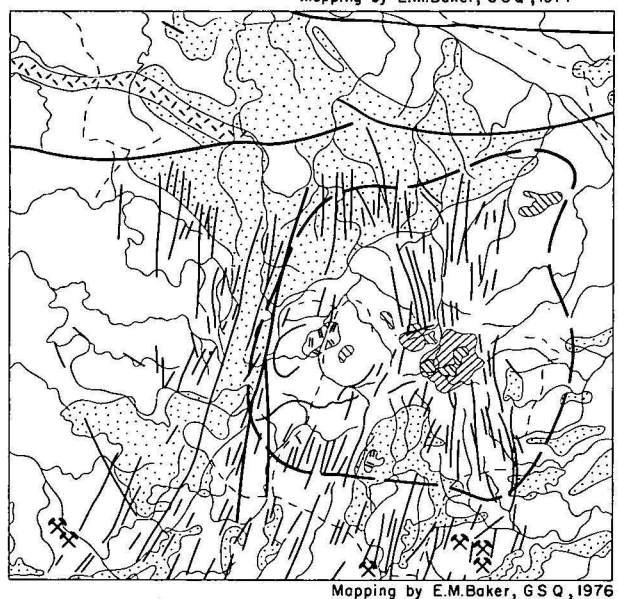


Figure 1. Location map.

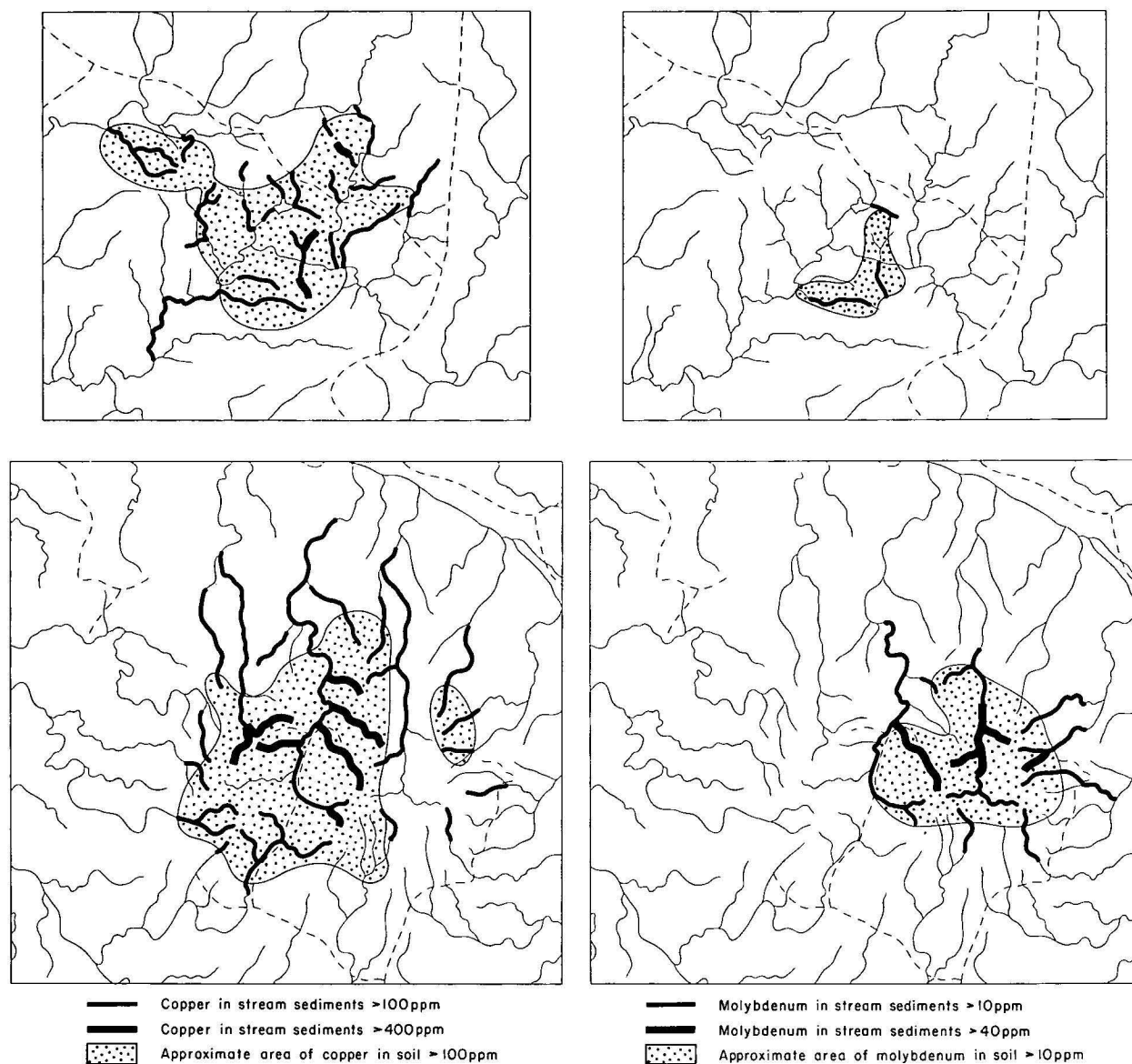
Geology

The Phyllis May and Mount Turner prospects have been described by O'Rourke (1971) and Baker (1978). Geologically, the two are strikingly similar—in both areas a complex series of Palaeozoic rocks intrudes Proterozoic granite and metasediments (Fig. 2). The

Figure 2. Geology of the Phyllis May (top) and Mount Turner prospects.



E54/A12/108



ES4/A12/109

Figure 3. Copper and molybdenum anomalies at the Phyllis May (top) and Mount Turner prospects.

younger rocks comprise stocks and dykes of porphyritic microgranodiorite and rhyolite, and small bodies of granitic and rhyolitic breccia. Numerous silicified fracture zones and quartz veins also occur. Potassic, phyllic, argillic, and propylitic alteration, pervasive as well as fracture-controlled, are present in both prospects. Pervasive alteration has taken place over about 12 km² at Mount Turner, but its extent at Phyllis May is less well established.

Pyrite-chalcopyrite mineralisation in the inner alteration zone is largely fracture-controlled at Mount Turner, but apparently mainly disseminated at Phyllis May. Molybdenite is present at both prospects, usually in silicified zones and quartz veins. At Mount Turner small galena-sphalerite deposits lie in and near silicified fractures radiating from the main alteration centre; several of these have been mined, mainly for their silver content.

Neither area has been fully evaluated by drilling. At Phyllis May, 29 percussion holes totalling 1106 m have been drilled; the deepest of these was 65.5 m. The best intersections reported by O'Rourke (1971) were 22.6 m of 0.41 percent copper, 1.5 m of 0.26 percent molybdenum, and 4.6 m of 1.13 percent zinc (in three different holes). At Mount Turner, a total of 1339 m of

diamond drilling has been carried out. Of the 15 holes drilled, only four penetrated deeper than 100 m; the greatest vertical depth attained was 266 m. As only small amounts of sulphide were intersected, splitting and analysis of the entire core were not considered justified (Baker, 1978). The small amount of analytical work was carried out and gave values of up to 0.35 percent copper and 0.13 percent molybdenum were encountered (in different holes), but these grades were maintained over only very short intervals.

Geochemistry

A total of 196 stream-sediment and 120 soil samples were collected over the two prospects—roughly equal numbers in each area. The reconnaissance soil sampling was undertaken to better delineate the main zones of bedrock mineral concentration, so that the stream-sediment results could be related to them. All samples were sieved to minus 180 μ m, and analysed for copper, lead, silver, and zinc by atomic absorption spectrophotometry, following a hydrofluoric/perchloric acid digestion, and for molybdenum by X-ray fluorescence spectrometry.

The sampling at Phyllis May revealed a zone of about 6 km² within which copper ranges from 101-651

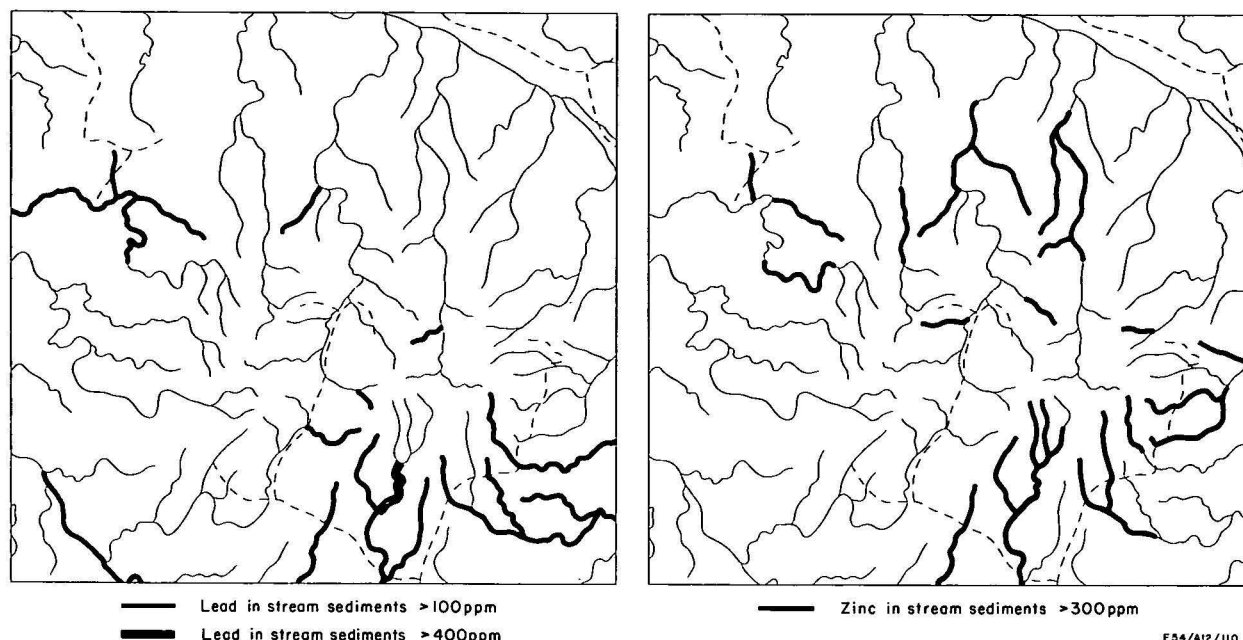


Figure 4. Lead and zinc in stream sediments at Mount Turner prospect.

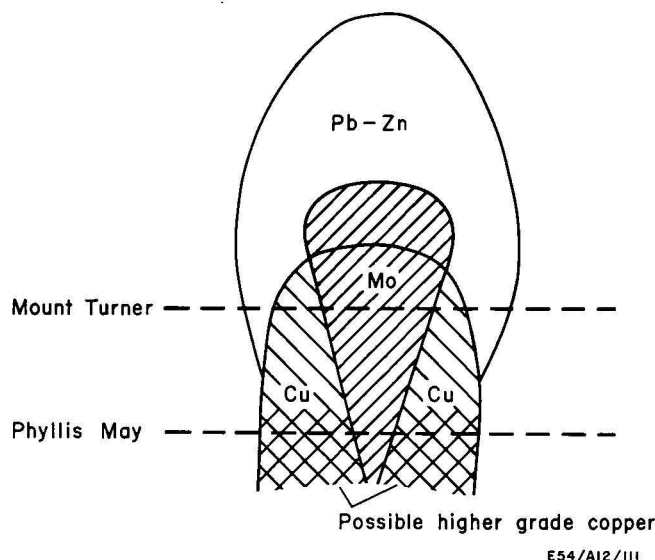


Figure 5. Geochemical differences between the Phyllis May and Mount Turner prospects in terms of different erosion levels for each hydrothermal system.

ppm in stream sediments (Fig. 3). A molybdenum anomaly with a maximum of 17 ppm is much less extensive (Fig. 3). A few high zinc values (up to 587 ppm) are scattered through the area, but lead and silver are not anomalous. The relationship between mineralisation and geology is obscure, and high copper and molybdenum concentrations are associated with a number of rock types.

At Mount Turner, stream-sediment copper values exceeding 100 ppm occupy an area of at least 12 km² (Fig. 3); a dispersion train in one stream extends for over 5 km. A molybdenum anomaly covering about 6 km² is also present (Fig. 3). The main molybdenum and copper anomalies do not coincide. Molybdenum values peak (at 78 ppm), on the eastern slopes of Mount Turner, where rhyolite plugs and breccia pipes crop out, whereas the highest copper values (to 958 ppm) occur to the north and northwest of Mount Turner, and appear to centre on a small body of porphyritic microgranodiorite. Discontinuous lead and zinc haloes

ring the prospect (Fig. 4); peak values are 813 ppm and 871 ppm, respectively. There is no appreciable concentration of silver in the stream sediments.

Conclusions

Stream-sediment sampling at Phyllis May and Mount Turner has revealed extensive copper anomalies in both areas, and the value of this technique in prospecting for porphyry copper deposits in other parts of the region is clearly demonstrated. The work has also highlighted some interesting geochemical differences between the two prospects. At Phyllis May there is only a poorly-developed molybdenum anomaly, and no appreciable lead-zinc halo. At Mount Turner, molybdenum values are considerably higher, and anomalous concentrations of the element occur over a much more extensive area; there is also a conspicuous lead-zinc halo. Perhaps genetic factors caused these dissimilarities, but the present-day geochemistry can also be explained in terms of erosion to different levels within originally similar hydrothermal systems (Fig. 5). The suggestion that Phyllis May is more deeply eroded than Mount Turner is supported by the lower topographic level, the larger size of the porphyritic microgranodiorite intrusions, the absence of ring dykes and rhyolite stocks, and the less intense style of fracturing at the former. Because of the apparently better copper grades at Phyllis May, the possibility that higher copper values will be found in deeper drilling at Mount Turner cannot be completely discounted.

Acknowledgements

Sampling in the two study areas was carried out by K. Armstrong, M. Baker, and N. Holzapfel, and the analytical work was done by B. Cruickshank, K. Ellingsen, J. Fitzsimmons, C. Madden, J. Pyke, T. Slezak, and J. Weekes. J. Bain, John Ferguson, D. Haldane, D. MacKenzie, and P. Scott assisted with preparation of the manuscript, and L. Hollands drafted the figures.

References

- BAKER, E. M., 1978—Mount Turner copper-molybdenum prospect, Departmental Area 71D. *Queensland Government Mining Journal*, **79**, 85-94.
- O'ROURKE, P. J., 1971—Phyllis May prospect. Report of investigations to 6/12/71. *Central Coast Exploration NL* (unpublished).

New microform publications

The reports whose titles and abstracts appear below have recently been issued as microfiche.

- | | |
|------------------------------|--|
| Report 184
Microform MF10 | An analysis of strong-motion accelerograms from Yonki, Papua New Guinea, 1967-1972. |
| | by <i>D. Denham</i> |
| ISBN 0 642 03707 8 | 55 pp., 41 figs., 1978. 1 fiche, \$0.50 |

In the period 1967-1972 an MO2 accelerograph at a soft-rock site at Yonki, in Papua New Guinea, was triggered 22 times, including once by the magnitude 7.0 (MS) Madang earthquake of October 1970, which took place about 165 km from Yonki, where a maximum acceleration of 93 cm/s² and velocity of 4.0 cm/s were recorded. The highest ground acceleration (187 cm/s²) and velocity (10.2 cm/s) were recorded in February 1971 from an earthquake which occurred about 130 km from the recording site. Least-squares analyses relating maximum ground motion to earthquake magnitude and focal distance gave the best results when ML magnitudes were used. The preferred formulas are: $\log Y_a = 2.65 + (0.47 \pm 0.20)ML - (1.80 \pm 0.64) \log R$; and $\log Y_v = 0.48 + (0.30 \pm 0.15)ML - (0.87 \pm 0.53) \log R$, where Y_a and Y_v are the maximum

acceleration and velocity, ML is the Richter magnitude, and R is the distance in km. The standard errors in the regression coefficients are large and preclude the accurate prediction of maximum expected ground motions. Most of the energy recorded at Yonki was contained in the 2-8 Hz band, and there seemed to be no correlation between the spectral peaks within this range and the magnitude or distance of the earthquakes. Good correlation was found between Modified Mercalli intensity and the maximum acceleration and velocity. The least-squares formulas for these parameters are: $\log Y_a = -(0.41 \pm 0.18) + (0.44 \pm 0.04)I$; and $\log Y_v = -(0.72 \pm 0.20) + (0.25 \pm 0.50)I$, where I is the estimated Modified Mercalli intensity at Yonki.

- | | |
|------------------------------|---|
| Report 186
Microform MF73 | Acquisition, processing, and interpretation of airborne gamma-ray spectrometry data. |
| | by <i>P. G. Wilkes</i> |
| ISBN 0 642 04158 X | 116 pp., 25 figs., 1979. 2 fiche, \$1.00 |

The 'Gamma-ray spectrometry project' was initiated in 1974 to study the state of the art in acquisition, processing, and interpretation of airborne radiometric data and related ground and laboratory measurements. The theoretical and experimental backgrounds to acquisition and processing of radiometric data are presented first in this report, followed by details of computer programs written to process digital airborne radiometric data acquired by BMR. Information is given on different types of data presentation, geological applications, and interpretation of airborne spectrometry.

Height correction coefficients depend on geology as well as on the areal extent of the sources of radioactivity in the ground, and should be determined by test flying in each survey area. Stripping ratios are functions of detector volume, detector configuration, ground clearance, and channel limits. Their accurate measurement requires calibration pads and a number of test areas to be established.

Background measurements needed for data processing should either be recorded at survey altitude over water or at about 915 m above ground. Measurements made at 610 m are likely to include some ground component of radiation and over-estimate the background levels recorded by up to 25 percent. Ground gamma-ray spectrometry can produce approximate quantitative estimates of radioelement concentrations in situ, provided the instrument is properly calibrated and survey procedures are carefully designed. The accuracy is inadequate for in situ geochemical measurement. If higher accuracy is required, a differential scanner should be used with the spectrometer. Laboratory techniques which produce satisfactory results are XRF for uranium and thorium, and atomic absorption analysis for potassium. If higher accuracy or independent checks are required for uranium measurements, delayed neutron analysis is recommended.

- | | |
|------------------------------|--|
| Report 193
Microform MF61 | Stratigraphic tables, Papua New Guinea. |
| | by <i>S. K. Skwarko</i> (compiler) |
| ISBN 0 642 03709 4 | 137 pp., 1 fig., 1978. 3 fiche, \$1.50 |

The major stratigraphic units on the 1:1 000 000 map of Papua New Guinea published by BMR in 1972 are divided into their constituent units mapped at the 1:250 000 scale. Age, thickness, 1:250 000 Sheet area distribution, lithology, and additional data of each of the constituent units are tabulated for the nine regional subdivisions defined on the 1:1 000 000 map. The stratigraphy for most Sheet areas in

Papua New Guinea has been finalized, but data for some are lacking or incomplete—especially in the southwest mainland, in one Sheet area on the Papuan peninsula, and on islands northwest of the Admiralty Islands and northwest and east of New Ireland—and for others are subject to revision.

- Report 200 **Isotopic ages of rocks from the Georgetown/Mount
Microform MF28 Garnet/Herberton area, north Queensland.**
by *L. P. Black*
ISBN 0 642 03712 4 87 pp., 22 figs., 1978. 2 fiche, \$1.00

New isotopic ages indicate that Late Palaeozoic magmatism in the Georgetown/Mt Garnet/Herberton area extended over roughly 60 m.y. During this time there was at least an approximate correlation of volcanic with plutonic activity. Amongst the earliest dates are those determined for the Newcastle Range and Featherbed Volcanics (about 320 m.y.), the Nymbool Granite, and some areas of Elizabeth Creek Granite. A later period, between 314 and 300 m.y., saw the development of relatively basic magmatism (granodiorite to gabbro) in the area. Intrusion of the Mareeba Granite took place about 290 m.y. ago. The final stages of Late Palaeozoic magmatic activity were emplacement of the Trevethan and Finlayson Granites, near Cooktown, and some bodies of Mareeba Granite, and the extru-

sion of the northwestern segment of the Featherbed Volcanics.

Isotopic data for the Gurrumba Ring Complex show that the total-rock regression represents a mixing line rather than a true isochron. Those for the Featherbed Volcanics reveal a more complex geochronological history than previous isotopic data had suggested. Several analyses on the Hodgkinson Formation indicate possible derivation of these sediments from the Precambrian inlier. However, the initial ratios of the Upper Palaeozoic igneous rocks (mostly 0.707 to 0.717) are generally too low to allow their derivation from either the Hodgkinson Formation or rocks of the Precambrian inlier; a deeper source appears necessary.

- Report 201 **The Great Australian Bight: a regional interpretation of gravity, magnetic,
Microform MF25 and seismic data from the continental margin survey.**
by *J. B. Willcox*
ISBN 0 642 03736 1 111 pp., 18 figs., 6 pls., 1978. 2 fiche, \$1.00

The Great Australian Bight is underlain by four main Mesozoic and Tertiary sedimentary basins: these are the intracratonic Eucla Basin which underlies the western part of the continental shelf, and the Bremer, Great Australian Bight, and Otway Basins which underlie the continental slope (including the Eyre, Ceduna, and Beachport Terraces). The 'slope basins' are associated with the rifting apart of Australia and Antarctica and commencement of seafloor spreading in the late Paleocene. Their structures are characterized by numerous normal faults which trend parallel to the continental margin. Sediment thicknesses range from 2 to 6 km or more, and are 2 to 3 km under the continental rise which reaches its maximum width of 250 km south of the Eyre Terrace. Basement probably consists mainly of Proterozoic crystalline and sedimentary rocks. The Early Cretaceous to early Paleocene pre-breakup sequence probably consists largely of continental sediment,

and the post-breakup sequence of shallow marine clastic sediment and prograded carbonates. A section with similar acoustic characteristics underlies the continental rise.

Gravity and magnetic data indicate that a band of ultrabasic rocks may flank the Precambrian Gawler Block. A magnetic trough, and in places an associated gravity ridge, correspond with a major fault along the continental margin. The 'magnetic quiet zone' which occurs over the continental rise appears to be caused by deep-seated continental crust.

The 'slope basins' extend for almost 3000 km along the southern margin and contain thick sections largely untested by drilling. The Upper Cretaceous sequence has the greatest petroleum potential, and has yielded a short-lived gas/condensate flow in the offshore Otway Basin. Although structural traps are apparent the lack of anticlinal folds downgrades its prospectivity.

- Report 204 **Catalogue of airborne magnetic and radiometric
Microform MF78 surveys up to December 1977.**
by *W. J. Gerula* (compiler)
ISBN 0 642 04193 8 126 pp., 1979. 2 fiche + 2 1:5 million index maps, \$7.00

- Report 205 **Combined ground geophysical survey, Alligator Rivers area, NT.**
Microform MF29 by *B. R. Spies*
ISBN 0 642 04013 3 18 pp., 5 pls., 1978. 1 fiche, \$0.50

Transient electromagnetic (TEM), Slingram (EM gun), VLF, magnetic, and resistivity methods were used to assist 1:100 000-scale geological mapping in an area of poor out-

crop in the Kapalga 1:100 000 Sheet area. Regional TEM results indicate carbonaceous units are wide and continuous within the Koolpin Formation.

- Report 206 **Ground geophysical surveys, Mary River area, NT, 1973.**
Microform MF30 by *I. G. Hone & J. A. Major*
ISBN 0 642 04015 X 24 pp., 14 pls., 1978, 1 fiche, \$0.50

From July to October 1973 a field party of the Bureau of Mineral Resources made a series of ground geophysical surveys to determine the geology and to search for mineralisation in a region of sparse outcrop west of the Mary River, Northern Territory. Lead-zinc mineralisation in a small quartz-filled fracture zone had previously been discovered nearby. Surveys were also made in areas of interest established by previous surveys. At the Mary River West grid there appears to be good correlation between geophysical responses and rock type; zones defined by characteristic geophysical responses were differentiated. Electromagnetic anomalies can be attributed to carbonaceous shales; sharp magnetic anomalies occur in the zone of intense metamor-

phism around the Cullen Granite, which itself has flat geophysical responses. The resistive zone of the Gubberah gossan, which overlies the mineralised fracture zone, was closely defined using the transient electromagnetic method (TEM). The efficacy of gravity surveying in this area was reduced by the effects of rugged topography. Areas north and south of the gossan were also investigated. A conductive zone at Minglo 2, detected in 1972, was defined more precisely. Drilling revealed carbonaceous pyrrhotitic shales as the source of the anomaly. Further work in some areas of the Mary River West grid is required before drilling targets can be selected to determine if any of the anomalies are related to mineralisation.

- Report 207 **Australian gravity network adjustment, 1975.**
 Microform MF68 by *H. M. McCracken*
 ISBN 0 642 03879 1 99 pp., 3 figs., 1978. 2 fiche, \$1.00

The Australian National Gravity Network has been adjusted according to new values established for the Australian Calibration Line in 1974. Intervals between base stations observed during surveys in 1964-65 and 1967, corrected for earth tides and meter drift, are listed. These intervals are converted to intervals consistent with the 1973 gravity scale, and gravity values are determined for all Isogal stations by adjusting these intervals to remove loop misclosures. These values and their estimated accuracies

are listed with the latitudes, longitudes, elevations, and informal station names. The Isogal-74 values have estimated uncertainties of the order of 0.1 mGal, while May 1965 Isogal values were estimated to have uncertainties of the order of 0.2 mGal. Isogal-74 values are compared with values computed by linear adjustment of the May 1965 Isogal values for the change of datum and scale. The largest differences are between 0.2 and 0.3 mGal, and are found near Darwin, in Tasmania, and near Perth.

- Report 209 **Chemical analyses of rocks from the late Cainozoic volcanoes of north-central New Britain and the Witu Islands, Papua New Guinea.**
 Microform MF76 by *R. W. Johnson & B. W. Chappell*
 ISBN 0 642 04035 4 47 pp., 1 fig., 1979. 1 fiche, \$0.50

Major and trace-element analyses for 210 island-arc rocks from volcanoes on New Britain and the Witu Islands are compiled in 21 tables. Modal analyses (phenocryst abundances) and locality descriptions, including grid references, are also listed. Each sample is assigned an alpha-numeric

identification code that enables its chemical analysis to be found readily. The coding system is based on the grouping of New Britain and Witu Islands volcanoes in five zones, E to H, which overlie successively deeper parts of the New Britain Benioff zone.

- Report 211 **Annotated bibliography of the Georgina Basin, Northern Territory and Queensland.**
 Microform MF77 by *E. C. Druce & J. H. Shergold*
 ISBN 0 642 04091 5 94 pp., 1978. 1 fiche, \$0.50

This annotated bibliography includes all known references to the Georgina Basin up to December 1976. The limits of the Basin used to compile this bibliography are the 1:250 000 Geological Series Sheets covering the Brunette Downs, Lawn Hill, Glenormiston, Huckitta, Wallhallow, Beetaloo, Helen Springs, Barrow Creek, Alcoota, Hay River, Mount Whelan, Bedourie, Boulia, and Duchess areas

(or parts thereof). The depositional limits are the latest Proterozoic and the ?Triassic (Tarlton Formation). Some company reports are not available and are not listed because of their confidential nature; other company reports and some early BMR records have not been included because they are no longer available.

- Report 212 **Geological Branch summary of activities, 1978.**
 Microform MF81
 ISBN 0 642 04197 0 311 pp., 40 figs., 1979. 4 fiche, \$2.00



26^e CONGRÈS GÉOLOGIQUE INTERNATIONAL

26th INTERNATIONAL GEOLOGICAL CONGRESS

Chairman: Jean Aubouin

Secretary General: Paul Sangnier

The International Geological Congress first met in 1878 in Paris. In 1980 in Paris, under the auspices of the International Union of Geological Sciences, the 26th session of the Congress will celebrate its Centenary.

26 June to 5 July—Pre-Congress scientific excursions

7 July to 17 July—26th session of Congress

18 July to 27 July—Post-Congress scientific excursions

Scientific Program

Opening Scientific Meeting: Leading specialists will survey five main themes concerning the current state of scientific progress.

Sections: The proposed program covers almost the entire field of the Earth Sciences and is divided into 20 sections. The Organization Committee has also planned to have the work of the various international scientific organizations affiliated with the International Union of Geological Sciences integrated into the program of the Congress. Authors are free to choose their own subjects for communications and these should be sent to the Secretary General before 1 October 1979 for the publication of abstracts.

Colloquia: The program for the colloquia was chosen so as to illustrate the main themes of current scientific and economic interest. There will be seven in all and they will be chaired by leading scientific figures. Communications to the Colloquia are made by invitation only.

Excursions

The Organization Committee in association with the National Committees for Geology of 18 European countries has organized an attractive program of geological excursions. The chosen themes make it possible to offer Congress participants a survey of all aspects of Western Europe. 85 different excursions each lasting for 9 days are planned from 26 June to 6 July 1980 or from 19 July to 26 July 1980. Since only a limited number of persons can participate in the excursions the places will be reserved by the Organizing Committee in October 1979 in the order in which the reservation forms were received.

Exhibition

An exhibition to be called "GEOEXPO 80" will be held in the same premises as the Congress from 7 to 11 July 1980. It will be open to all international institutions and will make it possible for exchanges of ideas and contacts to take place with scientists from all over the world.

Social Program

Since the Congress is taking place in Paris the organizers will be able to plan a very attractive program for the participants and a special program for persons accompanying them.

State of Advancement of Congress Preparation

80,000 copies of the first circular were sent out in October 1977. By 1 December 1978 the Organization Committee had received 5,800 answers from 114 different countries and 4,000 persons had asked to take part in the excursions.

The second circular is now available and contains the final registration form. Those interested in participating in the Congress and wishing to receive the second circular should request it from the:

Secrétariat Général du 26ème Congrès Géologique International
Maison de la Géologie
77-79, rue Claude Bernard
75005 PARIS — FRANCE

CONTENTS

	Page
J. B. Colwell	
Heavy minerals in the late Cainozoic sediments of southeastern South Australia and western Victoria	83
D. G. Backshall, J. Barnett, P. J. Davies, D. C. Duncan, N. Harvey, D. Hopley, P. J. Isdale, J. N. Jennings, and R. Moss	
Drowned dolines—the blue holes of the Pompey Reefs, Great Barrier Reef	99
B. R. Senior	
Mineralogy and chemistry of weathered and parent sedimentary rocks in southwest Queensland	111
R. V. Burne, J. D. Gorter, and J. D. Saxby	
Source rocks and hydrocarbon potential of the Palaeozoic in the onshore Canning Basin, Western Australia	125
P. J. Gregson, E. P. Paull, and B. A. Gaull	
The effects in Western Australia of a major earthquake in Indonesia on 19 August 1977	135
N. Harvey, P. J. Davies, and J. F. Marshall	
Seismic refraction—a tool for studying coral reef growth	141
M. D. Muir	
A sabkha model for the deposition of part of the Proterozoic McArthur Group, and its implications for mineralisation	149

Notes

A. G. Rossiter	
Stream-sediment sampling near two porphyry copper prospects, Georgetown area, Queensland	163
New microform publications	166